OXIDATION OF ORTHOXYLENE IN A TRANSPORTED BED REACTOR

OXIDATION OF ORTHOXYLENE IN A TRANSPORTED BED REACTOR

by

MARK SEBASTIAN WAINWRIGHT, M. App.Sc.

A Thesis

Submitted to the Faculty of Graduate Studies

in Partial Fulfilment of the Requirements

for the Degree

Doctor of Philosophy

McMaster University

February, 1974

Doctor of Philosophy (1974) McMaster University,
(Chemical Engineering) Hamilton, Ontario.

TITLE: Oxidation of Orthoxylene in a Transported Bed Reactor

AUTHOR: Mark Sebastian Wainwright, M.App.Sc.
(University of Adelaide)

SUPERVISOR: Dr. T. W. Hoffman

NUMBER OF PAGES: xvi, 327.

SCOPE AND CONTENTS:

The objective of this research program was to evaluate a gas-solid contacting reactor (called a transported bed reactor) in which the solid catalyst is conveyed upward in a vertical pipe by the gaseous reactants/products; at the top of the reactor the solids are separated from the gas stream and recirculated through the system. The reaction employed in this evaluation was the oxidation of orthoxylene on a vanadia on silica gel catalyst.

This oxidation reaction was studied separately on the same catalyst in a bench-scale fixed bed reactor over a range of temperatures, oxygen and orthoxylene concentrations and flow rates to provide conversions from 1 to 100% and considerable variation in selectivity. Reaction products were analyzed at short on-stream times and after considerable reaction times. These results indicated that reaction rates on freshly oxidized catalyst are much higher than those observed after steady-state has been achieved; selectivity to organic oxidation products is also improved significantly. Reaction studies are also carried out with other catalysts, notably a titania based

one, and these results are similar in general behaviour but differ in some important details. Kinetic parameters in the Redox or steady-state adsorption models are evaluated.

This reaction was carried out in a pilot-scale transported bed reactor, 3/4 in. O.D. by 27 ft. long. Solid hold-up was measured by activating quick shut-off valves. It was demonstrated that stable operation could be achieved at very high solids loadings (solid/gas ratios up to 250 and voidages from 0.60 to 0.86). It is demonstrated that the high reaction rates and selectivities can be exploited in such reactors. Suggestions for further research on such reactor systems are included.

ACKNOWLEDGEMENT

The author wishes to express his gratitude to those who in various ways have contributed to the work embodied in this thesis. He is particularly indebted to:

His research director, Dr. T. W. Hoffman, for his guidance, encouragement and friendship throughout this study.

Mr. R. W. Dunn and Mr. J. Newton for their assistance in designing and fabricating the experimental equipment.

His fellow students Jeet Khosla and Pieter Groeneweg for many helpful discussions.

Dr. P. Reilly of the University of Waterloo and Dr. J. F. MacGregor for their advice on statistical methods.

Dr. R. B. Anderson and Dr. C. M. Crowe for helpful discussions concerning reaction kinetics.

Ms. BettyAnne Bedell, for her patience and care in her excellent typing of the manuscript.

His wife, Adrienne, for her encouragement and understanding. This thesis is dedicated to her.

CONTENTS

TABLES

FIGURES

NOTATION

Notation for Rate Equations

C	Concentration of reactant or product, gm.-moles/litre
C_a	Concentration of oxygen, gm.-moles/litre
E	Activation energy, calories/gm.-mole
E_{as}	Active site parameter, calories/gm.-mole
F_{ao}	Feed rate of o-xylene, gm.-moles/hr.
k	Reaction rate constant, litres/gm. catalyst hr.
k_6	Rate Constant for tar formation, gm.-moles/gm. catalyst hr.
k_a	Rate constant for oxygen up take by catalyst by reaction or adsorption, litres/gm. catalyst hr.
K	Pre-exponential factor for reaction rate constant
n	Stoichiometric coefficient, gm.-moles of oxygen consumed/gm.-mole of hydrocarbon reacted
R	Gas constant, calories/gm.-mole ^oK
r	Rate of reaction, gm.-moles/gm. catalyst hr.
r_a	Rate of oxygen up take by catalyst by reaction or adsorption, gm.-moles/gm. catalyst hr.
T	Temperature, ^oK
W	Mass of catalyst, grams
θ	Fraction of catalyst surface sites in fully oxidized state at steady state

Superscript:

$*$	Denotes transformation of parameter by Hunter-Atkinson method

Subscripts:

o	Denotes inlet condition
r	Denotes hydrocarbon reactant

Notation for Fluid Mechanics

ΔP_T	Total pressure drop per foot of reactor, psi/ft.
ΔP_S	Pressure drop due to head of solids, psi/ft.
ΔP_F	Frictional pressure drop, psi/ft.
U	Superficial velocity, ft./sec.
W	Mass flow rate, lb./min.
ϵ	Void fraction
ρ	Density, lb./ft.^{3}

Subscripts:

G	Denotes gas
S	Denotes solids

Notation for Statistical Methods

n	Number of experiments
p	Number of parameters
s^2	Variance estimate
$\|S\|$	Determinant criterion of Box and Draper
y	Measured response
z	Normalized transformation of y
η	Expected value of response
θ	Parameter in a model
λ	Transformation according to Box-Cox method
ν	Degrees of freedom
ξ	Independent variable (experimental condition)
σ^2	Variance

Superscripts:

T	Denotes transformed variable
.	Denotes geometric mean.
'	Denotes transpose of matrix
^	Denotes estimated value
λ	Denotes transformation according to Box-Cox method

Subscript:

—	Denotes matrix or vector

CHAPTER 1

INTRODUCTION

In general, gas-phase reactions catalyzed by solids are carried out in fixed or fluidized beds. The major advantage of the former is that the gas approaches slug flow and hence close to 100% theoretical conversion can be achieved. Fixed beds have very inefficient heat exchange and this leads to the formation of hotspots which can adversely affect reaction selectivities. In addition they can only be used for very slow or non deactivating catalysts. Fluid beds overcome these disadvantages of packed beds. In particular, circulation of catalyst between two fluid beds can be used for catalyst regeneration and heat removal. The major disadvantage of this type of reactor is that there are large deviations from plug flow of gas. Bypassing of solids by gas bubbles leads to very inefficient contacting and for high conversions staging is frequently necessary.

Cocurrent pneumatic transport, in which reactant and product gases pneumatically convey the particles used to catalyze the reaction, in a vertical tube, overcomes the disadvantages of the two contacting methods described above, whilst exploiting the advantages of both. The advantages of this form of contacting are: nearly plug flow behaviour of the gas and solid and hence better control of residence times of the reacting and

product gases, essentially isothermal operation even at high reaction rates because of the good heat transfer rates from solid particles-to-gas and solid/gas slurry-to-wall and the heat sink provided by the mass of solid entrained in the gas, continuous use of reactivated catalyst since the solids are continually added and withdrawn. The main disadvantages are: possibly the dilute concentrations of solids in the pneumatically conveyed systems and hence the need for high specific reactivity of the catalyst, the possible high attrition of the catalyst and erosion of the reactor internals, and the complicated equipment, especially the catalyst recovery system.

Industrially, the advantages of transported bed reactors are exploited primarily in catalytic cracking operations (B1). The development of highly active cracking catalysts has enabled transported beds to replace continuous fluidized beds in this application. Another important industrial application is in the synthesis of gasoline from coal via the Synthol process (G1). This process, based on the Fischer-Tropsch synthesis reactions, has been in commercial operation in South Africa since late 1954. The current fuel crisis will no doubt renew interest in synthetic fuel production from coal. The gasification and combustion of coal are two other processes that have been conducted in transported beds. The use of these processes will probably increase during the next decade.

Objectives, Scope and Contents

The object of this study was to evaluate the performance of this unique contacting reactor for aromatic hydrocarbon

oxidations of the orthoxylene type. This reaction is an excellent one for this system since reaction rates are high enough and intermediate products in the reaction sequence are desired; moreover, the reaction is highly exothermic and there is the suggestion that short-term, reversible catalyst decay may occur.

The use of a transported bed reactor to study the oxidation of orthoxylene on a vanadia catalyst has further interest. Phthalic anhydride is produced industrially by the oxidation of naphthalene or orthoxylene on vanadium pentoxide catalysts. Although naphthalene can be oxidized equally well in fixed or fluidized beds, phthalic anhydride has not been successfully produced from orthoxylene in fluidized beds. In fact, a multi-million dollar process employing fluidized bed oxidation of orthoxylene was scrapped soon after coming on stream. Data presented in this and another study (K1) show that it is the catalyst composition which is responsible for the low phthalic anhydride yields from orthoxylene in fluidized beds. However, the significant backmixing in fluid beds may also be responsible for considerable over-oxidation.

Any attempt to evaluate the performance of a particular type of catalyst-gas contacting requires that the behaviour of the catalyst be determined under well-defined reaction conditions. This normally requires experimentation in an isothermal packed-bed reactor. The performance of vanadium pentoxide catalysts in hydrocarbon oxidations is not well understood. In addition, short-term deactivation effects, although alluded to in the

literature, have not been investigated experimentally. Therefore, a comprehensive study of orthoxylene oxidation on various catalysts under a number of reaction conditions was undertaken prior to carrying out experiments in the transported bed reactor.

This thesis contains a detailed review of the literature on the oxidation of orthoxylene on vanadia catalysts. In particular four Japanese papers (K1, K4, M3, S3), representing probably the major contribution in the field, are reviewed in depth. The experimental program has involved the development of novel reactor and chemical analysis procedures. A detailed study of the performance of several different vanadia catalysts in both unsteady-state and steady-state operation is reported. The problem of catalyst deactivation is described in some depth on the basis of the results obtained in this and other studies. Finally, the performance of the transported bed reactor for oxidizing oxylene is reported. Both the fluid mechanics and reaction results provide an excellent background for conducting other reactions in transported bed reactors. This study has also indicated a number of areas both in the field of solid-gas flow and reaction kinetics where knowledge is lacking and further research is required.

CHAPTER 2

PROBLEM DEFINITION AND LITERATURE REVIEW

Whereas the academic literature abounds with studies of solid-catalyzed, gas-phase reactions conducted in fixed and fluidized beds, relatively few studies (M1, P1, E1) in transported beds had been reported at the time this project was commenced. This is somewhat surprising, since the patent and industrial literature has been quite extensive.

The relatively high voidages encountered in pneumatic transport effectively limit the use of these reactors to very fast chemical reactions (K2). An attempt to thoroughly investigate the excellent heat transfer properties of a transported bed reactor requires that a highly exothermic reaction be studied. In order to take advantage of the plug flows of solids and gas one should study a complex chemical reaction in which the yield of an intermediate product is to be maximized. Furthermore, the continuous withdrawal of catalyst from the reactor enables the regeneration of spent catalyst in a separate stage. This advantage is exploited industrially in fluid catalytic cracking units (B1) in which the activity half-life of the catalyst is in the order of 0.1 to 1.0 seconds (L1).

The partial oxidations of aromatic hydrocarbons on vanadium pentoxide catalysts appear to have all the reaction characteristics required to adequately evaluate the performance

of a pilot-plant scale transported bed reactor. This chapter describes the relevant literature in the fields of transported bed reactors, the fluid mechanics of pneumatic transport and the kinetics of the oxidation of orthoxylene on vanadia catalysts.

2.1. Transported Bed Reactor Studies

Most of the literature on transported beds has been in the form of patents. Zenz and Othmer (Z1) present an excellent summary of such studies made prior to 1960. In general those patents are concerned with catalytic cracking of hydrocarbons, and the production of synthetic hydrocarbon fuels by the Fisher-Tropsch process. Klar (K3) has patented a transported bed for the oxidation of benzene and naphthalene. A spiral member in the reactor is used to centrifuge the catalyst to the walls of the reactor to improve heat transfer in the system. No studies have been reported on the oxidation of orthoxylene in transported bed reactors. However, several academic studies have been made of systems other than those involved in petroleum production. These studies will now be reviewed.

Merten (M1), in 1950, reported studies of the hydrogenation of benzene and oxidation of sulphur dioxide by what he described as "fluidized heterogeneous catalysis by the method of currents". The rate of hydrogenation of benzene on a $Ni-Al_2O_3$ catalyst at 200°C was twelve times greater in the transported bed than in a fixed bed. The results of the oxidation of sulphur dioxide on 150μ particles of a $Pt-SiO_2$ catalyst

were inconclusive. The rather crude apparatus and the extremely low solids to gas flows (99.7 voids) employed, limit the value of the study. It is reported here for historical purposes.

In 1964 Paetkau (P1) undertook a study of the oxidation of ortho-xylene on a silica-supported, vanadia catalyst in a transported-bed reactor. Mechanical problems with the apparatus and inadequacies in the method of chemical analysis limited the accuracy of the study. However, it was apparent from the limited data obtained, that the method of catalyst-gas contacting produced extremely high rates of reaction. No attempt was made to measure solids-hold-up in the reactor. A simple homogeneous, two-phase flow model was assumed. High slip velocities (gas minus particle velocity) with the accompanying build-up of solids in the reactor would make calculated rates of reaction much higher than the actual rates. However, it appears highly unlikely that the extremely high reaction rates could be entirely attributed to this factor.

Perhaps the major weakness of the study was the lack of understanding of the mechanism of ortho-xylene oxidation on vanadium pentoxide catalysts. It was intended that a concurrent study (B2) in a fixed-bed would provide an insight into the reaction mechanisms, and would also provide comparative rates of reaction in fixed and transported beds of the same catalyst. Such experiments would have given much more insight into the underlying mechanism accounting for the high reaction rates for this reaction system in this contacting equipment. Unfortunately, the packed-bed programme did not achieve any of

goals; however, it did provide evidence that the extent of uncatalyzed reaction in the transported bed would be small. It will be shown in section 2.3. that a fundamental understanding of the catalytic process would have indicated the need to reoxidize spent catalyst from the transported bed in a separate regeneration step. It is possible that partial regeneration did occur unintentionally in Paetkau's work.

Another weakness of the study was introduced by continually withdrawing a small fraction of the exit stream from the reactor outlet through a gas sample valve. Without some averaging procedure in the analysis samples, with such complicated equipment, any small perturbation to the reactor operation could lead to considerable variations in the outlet analysis and hence require more samples to achieve meaningful average performance.

Despite the weaknesses described above, the study accomplished its goal in that it demonstrated that hydrocarbon oxidations could be carried out in transported bed reactors.

Recently a Japanese group (E1) has reported the catalytic decomposition of cumene on a silica-alumina catalyst in a gas-solid transport reactor. The catalyst (SiO_2: 87%: Al_2O_3: 13%) - 100 to 150 mesh) was transported through the stainless steel reaction tube (1.0 metre long and 1.1 cm inside diameter) by hydrogen with a maximum velocity of 2.5 metres/sec. Since the catalyst was deactivated by reaction, it was continuously withdrawn and only activated catalyst was used for reaction. Pulse testing was carried out, and it was found that

the gas flow approximated plug flow. They assumed that the solid-gas slurry flowed at the same velocity (homogeneous model), first order kinetics for the reaction, and that the catalyst was of uniform concentration of the entire length of the reactor. In particular, this latter assumption is questioned since some length of tube is required to accelerate the particles. However, a non-uniform solids concentration would not change the integral conversions calculated for the reaction provided isothermal conditions prevailed. Due to the highly endothermic (22 K cal/mole) nature of the reaction, and the high mole ratios of cumene employed (up to 10% cumene in hydrogen), the temperature at the outlet was observed to be between 4 and 15°C lower than the inlet. Another weakness of the study was the low solids loading employed, the highest loading corresponding to a void fraction of .997.

In addition to the transported bed reaction and residence time studies, cracking was carried out in a pulse micro-reactor. Experiments using unreacted catalyst and catalyst which had undergone a single pass through the transported bed were found to have identical activities. This indicated that initial rates were measured in the transported bed.

The results for the study were quite predictable, since it has long been established that cumene cracking obeys first order kinetics. Furthermore, one would expect plug flow of gas in a reactor of such high (90:1) length to diameter ratio. No continuous measurement of catalyst flow rate was made, although the catalyst hold up was determined by stopping the flow and

weighing the settled catalyst in the reactor.

Pulse testing of fresh and reacted catalyst in a separate packed bed reactor in order to determine the activity change across the reactor, is a useful technique that should be applied to other studies of transported beds involving decaying catalysts.

The most recent study of chemical reaction in a transported bed (D1) has been the decomposition of ozone on a silica-gel-supported ferric oxide catalyst. The study was made in a glass tube 3 metres high and 2 cm. inside diameter at relatively low gas flows (less than 30 feet per second) and at high solids loadings (the maximum value being less than 20 volume percent solids).

The authors refer to a previous study (S9) by Solar Baeza who has defined the flow characteristics of the apparatus in this flow regime. It was found that under these dense phase conveying conditions, catalyst "aggregates" are rapidly forming and dispersing. It is probable that the authors are referring to the formation of aggregates or particle "clouds" which has been discussed elsewhere by Zenz (Z1) and Boothroyd (B3).

The authors have attempted to characterize the effect of these "aggregates" by comparing the first order rate constant obtained for the decomposition of ozone in a transported bed with that obtained from fixed bed experiments using the same catalyst at the same temperature. They have also conducted adsorption experiments in both fixed and transported beds, using silica-gel which had not been impregnated with ferric oxide.

The results of both the decomposition and adsorption rate experiments confirmed the authors' view that, although solid aggregates were visually apparent in the transported bed, the gas flow through the reactor closely approximated plug flow. This behaviour has been attributed to the high (150:1) length to diameter ratio of the reactor.

The study employed various techniques which permitted measurement of the following column parameters:

(i) the mean solids concentration in the reactor, by trapping the catalyst in a section of the reactor above the acceleration zone by the rapid closing of two slide valves.

(ii) the solids feed rate, by diverting the catalyst in the return line from the cyclone to a weighing vessel.

(iii) the concentration of ozone in the gas-phase, by sampling at a number of points along the reactor.

In both the reaction and adsorption experiments the ozone was introduced to the reactor at a level above the acceleration zone. The authors have assumed that the solid particles have a constant mean velocity in this region. The validity of this assumption is difficult to assess, since no pressure drop or other corroborating data were given. In addition, no evidence was given to suggest that they measured that acceleration was completed in this zone. It is probable that they have assumed that this condition exists.

This study is the first to be reported on a pilot-plant scale transported bed reactor in which a reaction was carried out in reasonably defined conditions of dense-phase

conveying. In particular, by adsorbing ozone on silica gel under reaction conditions and measuring the gas-phase ozone concentration at a number of axial locations, it was found that there are two distinguishable operating regions for the reactor:

(i) the entrance region, where adsorption on the support is most important and where, as a consequence, it is the internal diffusion within the particle which is rate determining.

(ii) a second region where adsorption equilibrium is established, and where chemical reaction controls the overall rate of ozone decomposition.

The authors have discussed, at some length, the importance of conducting both adsorption and reaction in a fixed bed, as well as the transported bed when studying such systems. In the case of reaction, such studies are essential. However, whilst conceding that adsorption effects are always present in transported bed reactors, it appears that too much significance has been placed in the results obtained in their study. The rate at which adsorption equilibrium is attained is a function of the effective diffusivity of the adsorbate within the catalyst particle and the concentration driving force from the entrance of the pore to the active sites within the pore. It is easily shown that with these small particles the mass transfer rate is usually sufficiently high to make the concentration at the particle surface essentially the same as that in the bulk gas. In their study, however, the gas phase concentration of ozone is 0.07 percent, far below reactant concentrations normally

encountered in industrial reactors. One might expect that the length required to reach equilibrium adsorption would be considerably reduced when concentrations in excess of 1% are used. The adsorption length under these conditions would be expected to be of the order of inches rather than feet.

The study of ozone decomposition had the advantage that flow visualization was possible under reaction conditions since the reaction was conducted in a glass tube at room temperature. However, this caused the disadvantage that reaction was conducted at only one temperature level. Industrially these reactors would normally be used at temperatures above 200°C. Ozone decomposition is usually used as a tracer reaction in reactor studies for measuring flow characteristics in various types of gas-solids contacting.

Jasimuzzaman (J1) has studied the vapour-phase oxidation of n-butane in homogeneous and transported-bed reactors in which the solid particles were inert to the reaction, being only there to provide a heat sink for the strongly exothermic reaction. The reactor was a 9 foot length of 5/8 inch inside diameter stainless steel tube. The reactor was operated with or without solid particles. Low loadings of 150 mesh solid particles were employed, the highest loading being 5.0 pounds per pound of gas. Despite the low loadings, the presence of the particles considerably improved the temperature profile in the reactor and improved selectivities were obtained. If dense-phase pneumatic conveying had been employed, more spectacular results would probably have been obtained by operating

at near isothermal conditions at higher temperatures. Nevertheless, the study was very useful, in demonstrating the advantages of the excellent heat transfer properties of transported bed reactors for conducting series reactions, such as hydrocarbon oxidations.

2.2. Pneumatic Conveying of Fine Particles

Most of the literature in this field has been concerned with dilute-phase pneumatic conveying. In general, previous investigations have been concerned with the development of correlations that predict pressure drops, slip velocities, and the conditions which produce choking in such systems. Most of the work has been done with particles which have narrow size distributions, and which are generally larger than fluidized catalysts. Loading ratios commonly used in these studies have been as low as 0.02, and have rarely exceeded 5 pounds of solid per pound of gas; corresponding voidages range from 0.999 to 0.970. Such low loadings would not be effective in pneumatic transport reactors.

This review is mainly confined to the fluid mechanical properties of dense-phase, vertical pneumatic conveying. In addition, the various techniques available for measuring the relevant system parameters, such as solids hold-up, and measurement and control of solids flow rate, will be discussed.

Dense Phase Pneumatic Transport

The main advantages of the use of dense-phase over dilute-phase conveying in transported bed reactors, resulting

from the higher solids loadings are:

1. Smaller reactor size for the same production.
2. Better heat transfer between the suspension and the reactor wall.

The main disadvantages, which generally result from slugging are:

1. Poor contacting of gas and solids due to erratic nature of the flow.
2. High pressure drops and fluctuations causing increased power requirements and major pipeline vibrations.

In dilute-phase vertical pneumatic conveying, the particles are transported up the tube as an evenly dispersed suspension having a low volumetric solids concentration (typically less than 5%). It is generally believed that if the air velocity is gradually decreased whilst maintaining a constant mass flow rate of solids, the solids hold-up in the conveyor increases until a point is reached where the air velocity is not sufficient to support the particles as a uniform suspension. At the point of choking, the suspension collapses and is transported up the tube in slug flow. It is generally believed that by decreasing the gas flow rate still further, a point is reached where the bubbles cannot extend sufficiently across the tube to restrict the downflow of solid emulsion, that is the bubble phase can move up through the emulsion phase thus giving rise to aggregative fluidization. If solids are

continually added to the system the entire tube fills with solids and they flow out of the system with the bubbles. If the gas flow rate is increased again the same behaviour is noted, that is the behaviour is reversible.

On the basis of limited experimental evidence, Zenz (Z2) suggests limits of dilute and dense phase slugging depend on the particle size and the ratio of particle-to-fluid density. He further suggests that at low ratios of solid-to-fluid density, particles of a given size may not exhibit this slugging phenomena. This means that the solids-gas system exists as a completely homogeneous flowing suspension over the entire voidage range from a packed bed ($\varepsilon \gtrsim 0.4$) to that of a single particle ($\varepsilon = 1.0$), whereas systems having higher density ratios will exhibit slugging over some of that range. This behaviour also depends on particle diameter. Zenz points out that slugging may occur with a particular solid material; however, the same material made up of particles with smaller diameters may exhibit only homogeneous flow. This behaviour is summarized in Figure 2.1, taken from reference (Z2). It must be emphasized that no systematic study of the slugging phenomena in solid-gas conveying systems has been reported and hence there is no way to calculate the slugging limits in these systems.

Recent studies in transparent tubes (S9, S11) have shown that this type of dense phase conveying is not completely homogeneous. It has been observed that aggregates of solid particles are constantly being formed and broken up during the

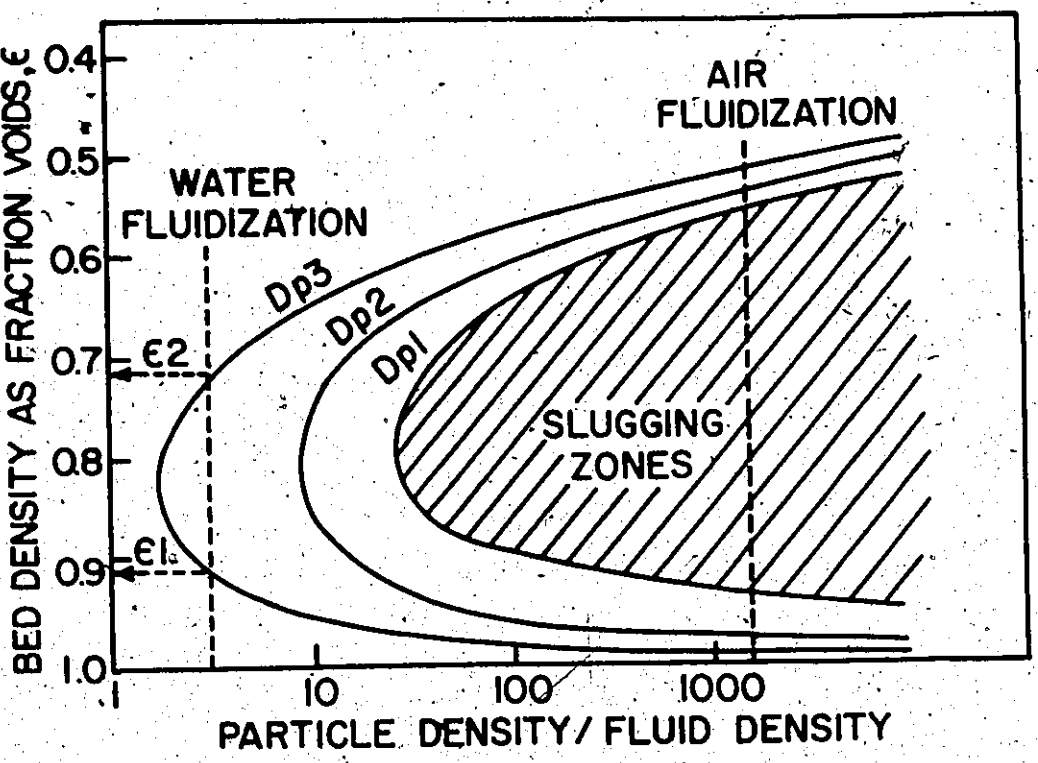

Figure 2.1. Slugging Limits in Fluidized System (from Z2)).

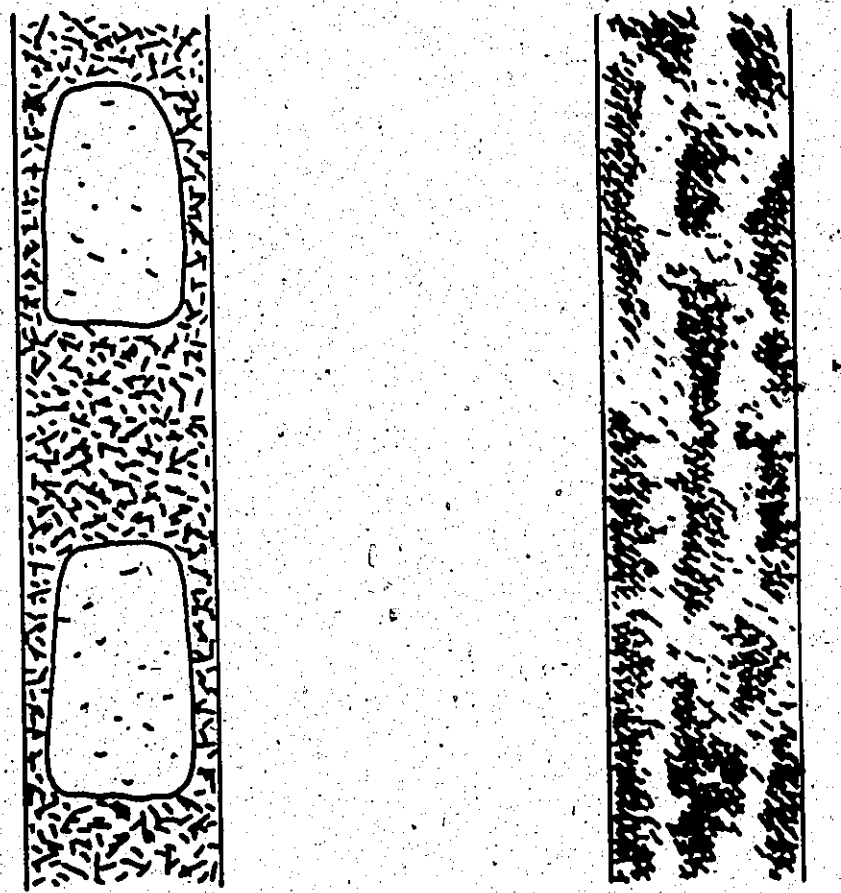

Figure 2.2. Representation of Slug Flow and Aggregative Flow.

passage of the gas-solid mixture through the tube. Boothroyd, (B3) through analogy to hindered settling, has described these aggregates as particle "clouds". However, Squires (S11) has observed that they exist as long strands or rivulets.

From the foregoing discussion, it is apparent that these are two types of dense phase conveying, namely slugging, two-phase, gas-solid flow and aggregative, two-phase gas-solid flow. The two types of flow are illustrated in Figure 2.2. Slug flow is characterized by two distinct phases, the bubble phase which contains very little solid and which extends over almost the entire cross-section of the tube and the solid-gas emulsion phase in which the particles are suspended in the gas at a voidage corresponding to that at minimum fluidization. The emulsion phase exists between the bubbles; each phase moves up the tube together, since the solids cannot move down around the bubble. This phenomenon is described in greater detail in Zenz and Othmer (Z1).

In aggregative flow, the particle aggregates are probably formed by a wake mechanism (Z1) in which successive particles are drawn into the wake of their immediate downstream neighbour. In this manner the long strands are built up, until the effective terminal settling velocity of the aggregate becomes excessive and the strand can no longer be supported. The aggregate then breaks up to be reformed again. The effective terminal velocity is based on the dispersed solids density in the aggregate and on effective diameter of the aggregate. In addition to the breakup mechanism described above, the

aggregates are continually being eroded by the faster moving dilute phase which flows around them. The breakup-reforming process occurs many times during the passage through the tube, thereby providing excellent gas-solid contacting which has been shown to have an effectiveness equal to that in a completely homogeneous slurry. In the case of aggregative flow, the aggregates have high solids concentrations ($\varepsilon \approx 0.6$) whereas the surrounding slurry has concentrations similar to those encountered in dilute-phase conveying ($\varepsilon \approx 0.97$). On the overall scale, the gas/solid slurry can be considered to be effectively homogeneous. Pressure fluctuations are accordingly small.

It is apparent from the above discussion that all the advantages of dense-phase conveying can be had without the disadvantages caused by slugging, if a judicious selection of particle size and particle-to-gas velocity is made. However, it is not always possible to obtain these conditions. Therefore it is necessary to provide some additional means of preventing slugging. The methods of Capes (C1) and Berg (B4) will now be reviewed.

Capes (C1) has studied dense-phase conveying in both empty tubes and tubes packed with cylindrical screen packing. The conveyor was a 3 inch internal diameter polymethyl methacrylate pipe, 19 feet in length. The packing was 3/4 inch by 3/4 inch cylinders made from 6 mesh wire gauze and the particles were glass beads, having a mean diameter of 470 microns. The experiments were carried out in the slugging region, the minimum voidage being 0.85. Pressure measurements were made at

a number of axial locations using manometers. A differential pressure transducer was used to record pressure fluctuations across the 4 to 10 foot levels of the pipe. The presence of screen packing eliminated the wide fluctuations in pressure gradients, this being an indication of a more uniform solids concentration throughout the conveyor. The use of screens produced smooth pneumatic conveying, even at voidages in the range 0.95 to 0.98 where choking normally occurred in this tube containing no internals.

The presence of packings may well offer an excellent alternative to the "moving fixed bed" of Berg, which is described below. It provides stable operation from the dilute conveying region, down through the dense-phase conveying region, through to the fluidization region. This is accomplished without the use of restrictions in the exit of the reactor (B4) and without the need for mechanical power in the form of screw pumps (T1) which are normally required to produce stable dense-phase conveying.

The "moving fixed bed" process, which was developed by Berg (B4) and adapted by Union Oil in several processes, involves dense-phase co-current upflow in an unfluidized state. The expansion of the vertical column of fluids is restricted at the discharge end of the pipe, so that bubbles of gas cannot form. The restriction can be provided by a valve, an orifice, or an expanded section containing unfluidized solids.

Heat Transfer in Vertical Pneumatic Transport

Heating and cooling of tubular reactors is generally accomplished by circulating a heat transfer fluid around the tube. The effectiveness of the heat transfer process is greatly enhanced in the case of pneumatic transport by two means. There is the advantage of the high heat capacity of the suspended particles, and also the improved heat transfer due to the internal film resistance being lowered by the numerous collisions of particles with the tube wall.

Data on heat transfer in dense phase conveying is very limited (Z1). However, data obtained in dilute-phase conveying (F4, M9, L2) for solids loadings up to 5 volume percent, indicate that heat transfer rates of up to 100 times the empty tube rate can be achieved. It has also been observed that, at low solids concentrations, considerable improvement in heat transfer can be obtained by replacing larger diameter tubes with a bundle of small diameter tubes, even taking the increased area into account. The heat transfer is enhanced more significantly with slurries having a lower average particle size.

Solids Feeding

The feeding of solids in dense-phase conveying causes certain experimental difficulties. Capes (C1) has been limited to a 0.85 void fraction in his study, since he relied on the gravity head of packed solids in the feed stand pipe to maintain the flow of solids. He was unable to operate the conveyor at

flows much less than 6 feet per second, since the pressure in the conveying line caused the feed rate of solids from the stand pipe to drop off seriously at lower velocities.

Paetkau (P1) used a rotary solids feeder to introduce catalyst particles into the gas stream. Operation at temperatures around 400°C produced differential expansion in parts of the rotary star valve, causing it to jam. Increased clearances within the valve prevented the jamming, but permitted gas to pass through the valve and solids feed tank, thereby bypassing the reactor. Difficulties were also encountered through catalyst particles agglomerating and sticking in the vanes of the feed valve.

The problem of feeding so-called "sticky" powders from bins has been studied by Bulsara (B5). Two approaches have been used to render such powders free-flowing. The first of these, the addition of coarse inert particles in amounts large enough to make up the bulk of the mixture, is not appropriate to this study. However, the forced feeding of solids by the application of a pressure differential across a feed orifice, is relevant. Forced feeding has been recommended elsewhere (T2). The method relies on maintaining a constant level in a feed tank and a constant pressure differential across an orifice at the bottom of the tank. The solids efflux through the orifice is given in pounds per minute by

$$W_s = 31.4\ C_s\ \rho_B^{1/2}\ (P_2-P_1)^{1/2}\ (D_o-1.5\ D_p)^2 \qquad (2.1)$$

and the rate of gas flow in cubic feet per minute is given by

$$V_G = 0.327\ \varepsilon\ D_o^2\ [(96.5\ C_g\ ((P_2-P_1)/\rho_g)^{1/2} + \frac{W_s}{\rho_G})] \qquad (2.2)$$

where ρ_G is the orifice coefficient for gas efflux.

C_s is the orifice coefficient for solids efflux.

D_o is the orifice diameter in inches.

D_P is the particle diameter in inches.

P_2-P_1 is the pressure differential across the orifice in p.s.i.

ρ_B is the solids bulk density in lb./cu.ft.

and ε is the fractional voids in the effluxing solids.

The tank pressure needed to produce a certain mass flow of solids is determined by calculating P_2 from Equation (2.1) and substituting into Equation (2.2) to find the volumetric gas flow rate. The pressure drop through the fixed-bed of solids in the tank is then calculated by the usual expressions, and this added to P_2 gives the required tank pressure. The bridging at the orifice, which normally occurs with gravity feed, is prevented by the gas flowing along with the particles.

Hold-up and Pressure Drop Measurements

In any catalytic reactor it is important to know the distribution of catalyst throughout the reactor length. This is particularly true when reaction gases are to be sampled at various axial locations. In the case of transported bed reactors, the solids hold up (or reactor voidage) will vary considerably along the reactor length. The solids concentration

at the reactor inlet is very high since the particles are being accelerated in this region. In fact, the particles will be accelerating throughout the whole tube. However, it is generally assumed (C1, D1, P1) that homogeneous two-phase flow occurs in the upper sections of the conveyor. The condition of homogeneous two-phase flow implies that the particle velocity is constant above the initial acceleration zone. This simple model may be true for dilute suspensions but probably does not apply in dense phase conveying.

The gas pressure is the most commonly made measurement in two-phase, gas-solids flow. The pressure drop along a pipe can sometimes be used as a measure of the solids flow rate, provided the gas flow is known. When the solids are sufficiently coarse, the extra pressure drop caused by the presence of solids varies linearly with solids loading (R1). However, in the case of fine particles, the relationship can become non-linear (S2). For design purposes the assumption of a linear relationship between pressure drop and solids loading may be a reasonable approximation. Therefore pressure taps located at a number of axial positions would provide useful information on solids loading as a function of conveyor height. Goldberg (G2) has discussed the problem of pressure measurements in gas-solids flows.

The pressure drop in dense-phase conveying has two main components. These are the pressure drops due to the weight of solids in the line, and the frictional losses. As the void fraction is reduced, the former becomes the major effect. The pressure drop in moving fixed beds corresponds to

the pressure drop observed for an equivalent static bed. The pressure drop in slug flow is extremely difficult to predict, since it depends on the slugging characteristics of the particular system.

Capes (C1) has correlated pressure drop measurements for tubes with and without screen inclusions. The pressure drop due to the weight of solids in the line is given by p_g (ft. of water per ft. of pipe).

$$p_g = \frac{\rho_s}{62.4} \cdot (1-\varepsilon) \qquad (2.3)$$

He employed a model, which has been found useful in liquid-solid flow, to suggest an equation form for correlating gas-solid frictional pressure drop. His experiments provide the parameters, viz.:

$$p_w = 2.8 \times 10^{-6} \left(1 + 48.6 \frac{S}{A}\right)\left(\frac{F}{\varepsilon A}\right)^{1.91} \qquad (2.4)$$

where A is the cross sectional area of line ($ft.^2$).

F is the volume flow rate of fluid ($ft.^3/sec.$).

S is the volume flow rate of solid ($ft.^3/sec.$).

Using Equations (2.3) and (2.4) and pressure drop measurements gave poor predictions of solids hold-up, i.e., $(1-\varepsilon)$, for both the empty and packed tubes; therefore the usefulness of the correlation, Equation (2.4), is limited, since information on solids hold-up is essential to its use.

There are three parameters which characterize the flow of particles in a pneumatic conveyor. These are the mass

flow rate of solids, W_s, in pounds per second, the linear velocity of the particles, u_s, in feet per second and the solids loading per unit length of conveyor, w_s, in pounds per foot. Assuming a steady-state situation, where W_s, w_s and u_s are time invariant, the three are related by

$$W_s = u_s w_s \tag{2.5}$$

for homogeneous two-phase flow. However, generally u_s and w_s vary along the length of the reactor. Therefore the mass of solids, N, in pounds, present in a length, L feet, of tube is given by

$$N = W_s \times L = \int_{Z=0}^{Z=L} u_s(z)\, w_s(z)\, dZ \tag{2.6}$$

Therefore a complete characterization of the two-phase flow throughout the conveyor requires the accurate measurement of any two of the variables, W_s, $w_s(z)$ and $u_s(z)$.

The continuous measurement of solids concentrations in pneumatic conveying has received considerable attention in the past decade. The widespread use of pulverized coal as a fuel in electricity generation, in some countries, has required the development of instrumentation and control. Goldberg (G2, G3) has given a complete review of these and other measuremonts made in flowing gas-solids suspensions. The review covers literature up to 1969. Those methods that are relevant to the study of pneumatic transport reactors will be reviewed here, along with more recent advances.

The simplest method of measuring solids dispersed density involves trapping the material in a given section of tube by simultaneously closing two quick-shutting valves. This method suffers the disadvantages of only providing an average density over a given length of pipe, and from not being continuous.

Electrical capacity measurements may be made at points in the transfer line by inserting a parallel plate capacitor into the flow (V1). This method is applicable only to conveyors having large diameters, since plates of about one square inch are required. The introduction of such a large probe into a small tube would cause considerable disruption to the flow. Furthermore, the method is not very sensitive and its use is more obvious in fluidized bed studies where there are high solids loadings in the emulsion phase and low loading in the bubble phase.

More recently Beck (B6, B7, B8) has developed a capacitance method for measuring the linear velocity of solid particles in pneumatic conveying. The method has the advantage that it involves no obstruction to the flow of material. It is based on the observation that there are local variations in particle concentrations which are transmitted through the conveyor in a coherent manner. Two capacitance probes, located at axial positions along the tube, detect these variations as changes in capacitance. The linear velocity of the particles is determined by cross-correlating the noisy signals from the two capacitors. The capacitor plates take the form of short

lengths of half sections of the tube, which are insulated from the main tube and each other. The method requires the use of a small computer, or correlator, to cross-correlate e.m.f. signals that are generated by capacitance-to-e.m.f. transducers.

The method was developed in order to measure the mass flow of powders in pneumatic conveyors. Therefore some method of determining the local particle concentration is necessary to estimate W_s from Equation (2.5). The method is both expensive and complex. It could be used to calculate local particle concentrations by having capacitance plates at a number of axial locations.

Several disadvantages of the method are apparent. Firstly, it relies on the transmission of the concentration fluctuations over a finite length of conveyor. One can envisage that this length will be extremely small in cases where the particles have a wide size distribution. The fluctuations are likely to be quickly damped out in cases of high solids loadings where particle-to-particle interactions are frequent and complex.

Nuclear radiation attenuation has been used to measure solids dispersed density in pneumatic conveying (B7). Generally this has been achieved by attenuating β particles (I1). X-rays have also been used (B7) but they tend to penetrate the dilute suspensions in small tubes too easily. Their main application is in studying fluidized beds. Attenuation of a beam of light has also been used (S1) for dilute suspensions. All of these methods require the inclusion of windows in the walls of the conveyor. This is not always

possible in pneumatic transport reactors where high temperatures are used. Neutron beam attenuation (M2) does not require windows. However, the high cost of portable neutron sources and the associated counting equipment limit the application of the method.

Temperature Measurements

Themelis and Gauvin (T6) have made detailed experimental and theoretical analyses of heat transfer to clouds of particles. In studying the reduction of iron oxide particles by the Atomized Suspension Technique they found that for 76 micron particles there was no considerable lag between particle and gas temperatures due to the fact that the rate of convection is very much greater than the corresponding rates of radiation and chemical reaction. Therefore a dynamic temperature balance between gas and solid is established in the system. The effect was found to be more pronounced for smaller particles. Their analysis indicates that even for highly exothermic reactions the reacting particle (or catalyst particle) cannot reach a temperature significantly greater than the gas, unless the reaction is considerably faster than that of iron oxide reduction.

Goldberg and Boothroyd (G3) note that it is often observed that a thermocouple, when inserted in a gas-solid flow, will record a very high temperature due to frictional particles. However, it is unlikely that temperature errors of this type would be encountered except for extremely high particle velocities.

2.3. The Oxidation of Orthoxylene on Vanadia Catalysts

The oxidations of orthoxylene and other hydrocarbons on vanadium pentoxide catalysts have been studied extensively. An excellent review of the literature to 1959 is given by Dixon (D2). Most studies have been concerned with yield optimization and elucidation of the reaction network. Despite this large volume of work, a reaction mechanism that completely describes reaction rates and product distribution, has yet to be published. This is due to the lack of understanding of the influence of catalyst-support materials and catalyst promotors on reaction rates and selectivities, and the complex nature of the hydrocrabon-catalyst interaction.

This section is divided into two parts. The first deals with the properties of vanadium pentoxide catalysts. The importance of catalyst selection is reflected in the length of this review. Four Japanese articles (K1, K4, M3, S3) which have until now been neglected in the Western literature are discussed. These papers are the most comprehensive reports on the influence of catalyst promotors and supports yet published. The second section discusses attempts made to establish kinetic mechanisms for orthoxylene oxidation on vanadia catalysts.

2.3.1. Catalyst Properties

There are two broad classes of catalysts for the oxidation of aromatic hydrocarbons. The conventional catalyst is about 10 percent V_2O_5, on an inert support such as pumice or alundum which must be free from alkali metal oxides. A typical "German-type" catalyst contains about 10% V_2O_5 and 20-30% K_2SO_4 on a silica-gel or titanium dioxide support. The "German" catalyst is almost exclusively used now for orthoxylene oxidation. Since catalysts of this type were used in the current study, this review will be restricted to them.

Simard (S4) has suggested that the best catalyst for orthoxylene oxidation is one of small surface area and relatively low sensitivity to promotor addition. A highly porous catalyst is considered undesirable since it leads to over-oxidation, possibly because the intermediate oxidation products are caught in the pores and are further oxidized before they can diffuse out of the catalyst. It has been suggested that the role of potassium sulphate is to reduce the activity of the catalyst and hence reduce this tendency to overoxidize in spite of the high porosity of the silica gel support.

Perhaps the most important contributions in the field of catalyst properties have been made by the Japanese group (K1, K4, M3, S3). The first of these papers (K1) describes the preparation of V_2O_5-K_2SO_4 catalysts on silica-gel, gypsum, and titanium dioxide supports. The effects of K_2SO_4 and SO_3 content were studied by oxidizing naphthalene on the various catalysts. They also showed that the addition of a sulphur compound, notably sulphur dioxide, was necessary to maintain

some unknown SO_3 level within the catalyst. Catalysts were prepared by so-called wet and dry methods. A discussion of these methods is not warranted here.

The results of their initial study showed the following trends. The nature of the support material was found to be most important in determining catalyst activity and selectivity. The optimum yields of phthalic anhydride on silica gel, gypsum, and anastase titanium dioxide, supported catalysts were approximately 105 weight percent (91 mole %). Titanium dioxide in the form of rutile gave a maximum yield of 90 percent.

The effects of the potassium sulphate level in catalysts, on all three effective support materials, were examined. It was found that K_2SO_4 to V_2O_5 mole ratios of 2.0, 0.5 and 0.5 were optimal for the silica gel, gypsum, and anastase, supported catalysts respectively. The V_2O_5-K_2SO_4 mole ratio of 2 to 1 corresponds to the composition $V_2O_5 + 3\ V_2O_5.2K_2SO_4$ according to Kiyoura's phase diagram for the V_2O_5-K_2SO_4 system. The phase diagram is presented in reference (K1). The authors conclude that in the case of the silica-gel-supported catalyst, most of the K_2SO_4 becomes associated with the support, and only a minor portion is actively involved in the catalyst performance. They further conclude that a support with lesser surface area is to be preferred to a highly porous material since the latter allows longer contact between the hydrocarbon and the catalyst. The excellent yield of phthalic anhydride obtained on a silica-supported catalyst is thought to be due to the large amount of K_2SO_4 within the gel which, together

with the gel itself, creates a support structure that is similar to anastase titanium dioxide. The gypsum-supported catalysts produced considerable cracking of naphthalene when these catalysts contained large amounts of potassium sulphate.

The importance of sulphur trioxide as a catalyst addition was determined by preparing catalysts that were treated with oleum. Catalysts that had the SO_3 treatment gave phthalic anhydride yields in excess of 90%. Untreated catalysts gave yields around 40%. Furthermore, the treated catalysts were reacted with pure and "hot press" naphthalene feedstocks. A gradual decrease in catalyst activity was noted when pure feed was used. The yield from "hot press" naphthalene which contained sulphur as an impurity did not show any decrease in yield. It was concluded that the sulphur level in the feed was important to the catalyst activity. Experiments were conducted on oleum-treated catalysts using pure naphthalene feed. The decay phenomenon described above, was permitted to occur for an on-stream life of about 100 days. At this time the yield had dropped from 105 percent to less than 80 percent, depending on the reaction temperature. At this time sulphur dioxide was added to the feed stream and the original activity was restored within 48 hours.

In summary, the authors have concluded that the active catalyst component has a composition of $V_2O_5 + 3V_2O_5 \cdot 2K_2SO_4 + N\ SO_3$. They note that it has been claimed (F1, T4) that the K_2SO_4 takes the form of $K_2S_2O_7$ (potassium pyrosulphate) in these catalysts. A likely composition is therefore

$V_2O_5 + 3V_2O_5.2K_2S_2O_7 + NSO_3$.

The second of these articles (S3) is concerned with the oxidation of orthoxylene on silica and titania-supported catalysts of the type described above (K1). Whereas both catalysts gave the same optimum phthalic anhydride yields of about 105 weight percent when naphthalene was used as feed-stock, only the titanium dioxide-supported catalyst gave comparable yields for orthoxylene oxidation. The maximum yield using the silica-supported catalyst was of the order of 47 weight percent. The authors have proposed that the difference in yields may be attributed to either the cracking of the orthoxylene on the surface of the catalyst, or, to the occurrence of a mechanism that is different from that for naphthalene oxidation.

Experiments were conducted in which no oxygen was present in the feed stream. The different gases were analyzed for carbon dioxide, sulphur dioxide and hydrogen sulphide content. The carbon dioxide concentration was initially the same for both catalysts. However, the carbon dioxide level dropped rapidly in the case of the silica-supported catalyst. This catalyst also produced much higher levels of sulphur dioxide and hydrogen sulphide. During the first few minutes on stream, both catalysts deposited solid products in a cold-trap at the reactor exit. In the case of the titania-supported catalyst these were found to be mainly phthalic anhydride and maleic acid. The silica-supported catalyst produced mainly toluic acid, toluic alcohol and toluic aldehyde.

Catalyst samples were obtained at different reaction times and were analyzed for vanadium tetroxide and sulphur trioxide content. The silica-supported catalyst exhibited a much faster depletion of sulphur trioxide. The equilibrium level of V_2O_4 was reached much more rapidly in the case of the titania-supported catalyst. The authors have concluded that the vanadium pentoxide in the titania-supported catalyst is much more accessible to the orthoxylene in the reaction gas.

After reacting a sample of the titania-supported catalyst for about 16 hours, air was substituted for nitrogen. The loss of sulphur trioxide during the nitrogen cycle was shown to have produced a catalyst with lower activity. An attempt to restore the activity was made by passing an air-oleum mixture through the catalyst at room temperature. After three hours very little sulphur trioxide had become associated with the catalyst. The catalyst was then placed in the reactor and orthoxylene was oxidized in an air-oleum stream. During this treatment the sulphur trioxide level in the catalyst increased. However, no increase in the yield of phthalic anhydride was noted during the SO_3 treatment. Analysis of the catalyst bed showed that most of the SO_3 was concentrated at the reactor entrance. Subsequently, the SO_3 flow was stopped and the yield of phthalic anhydride increased to the value obtained on a fresh catalyst for the oxidation of orthoxylene in air. The catalyst bed was again analyzed and it was found that the SO_3 had become distributed evenly within the bed.

On the basis of the experimental results described

above, the authors have drawn the following general conclusions regarding the partial oxidation of orthoxylene on V_2O_5-K_2SO_4 catalysts.

(i) $V_2O_5.SO_3$ is responsible for the catalytic activity, whilst K_2SO_4 acts as a carrier of SO_3. Although potassium sulphate has long been considered to be an oxidation retarder or promoter of the intermediate reactions, it was found in their study that changing the K_2SO_4 level had little or no effect on catalyst activity. However, changes in sulphur trioxide level did cause great changes in catalyst activity.

(ii) The following changes occur when orthoxylene reacts with the catalyst in the presence of air.

a. $V_2O_5.SO_3 \rightarrow V_2O_4 + SO_2 + 20$ (used in oxidizing orthoxylene)

b. $SO_2 + V_2O_5 \rightarrow V_2O_4 + SO_3$

c. $V_2O_4 + O_2$ (air) $\rightarrow V_2O_5$

(iii) Orthoxylene oxidation occurs by two simultaneous reactions: phthalic anhydride formation and toluic acid formation. The difference between the yields of phthalic anhydride on titania and silica-supported catalysts is attributed to the greater ease with which toluic acid oxidizes to carbon dioxide on the latter.

Several aspects of their results and theories will now be discussed.

(i) No attempt was made to explain why SO_3 was

not adsorbed at room temperature. A possible reason is that a higher temperature is needed for the SO_3 to react with K_2SO_4 to form pyrosulphate.

(ii) It is difficult to understand why SO_3 accumulated at the entrance of the catalyst bed since SO_3 was being passed through the entire bed continuously.

(iii) If a catalyst bed had been packed at the entrance with catalyst containing high concentrations of SO_3 whilst the rest of the bed was low in SO_3, one could see supporting evidence for their oxidation mechanism involving SO_3.

(iv) They have noted that an increase in V_2O_4 with time of reaction is accompanied by a corresponding decrease in SO_3. They have based their reaction mechanism on this observation and the fact that reaction in the presence of orthoxylene distributes SO_3 evenly throughout the bed. However, it is more than likely, as will be shown in Chapter 4 that the change in oxidation state and loss of SO_3 may not be directly related; the former being due to the unsteady-state performance of a highly oxidized catalyst and the latter being caused by thermal desorption of SO_3.

It should be noted that Wonderlein (W1) has proposed an entirely different role for SO_3 in which

a) Sulphur compounds, generally in the form of SO_2, are oxidized to SO_3.

b) The SO_3 oxidizes the V_2O_4 in the catalyst to V_2O_5.

Thus the action of SO_3 is considered to be that of continuously carrying oxygen to the catalyst surface to overcome deoxidation of the catalyst. This mechanism appears highly unlikely since it is generally believed that V_2O_5 is responsible for the oxidation of SO_2 to SO_3 as well as for the oxidation of hydrocarbons. In addition, the concentration of SO_2 required would be much greater than those of the hydrocarbons unless V_2O_5 played only a secondary role in oxidizing the hydrocarbon, the bulk of the active oxygen being chemisorbed.

The differences in product distributions obtained for silica and titania-supported catalysts led to a further study (K4) in which the oxidation selectivity was found to depend on the amount of oxygen adsorbed by the different catalysts. Four types of catalyst support, namely, silica-gel, gypsum, titanium dioxide and carborundum were investigated. Selectivities for the formations of phthalic anhydride, carbon dioxide and carbon monoxide were measured at temperatures from 320° to 430°C. Surface area measurements were made on all catalysts using the B.E.T. method. In addition, Langmuir-type isotherms were obtained for the adsorption of oxygen on all catalysts at 400°C.

The selectivities for the formation of phthalic anhydride and carbon oxides formations were compared with the adsorption of oxygen expressed as the equilibrium volume of oxygen adsorbed per unit area of catalyst. The titanium dioxide-supported catalyst had the highest selectivity for

phthalic anhydride formation and the highest oxygen adsorption. Silica gel had the lowest selectivity and lowest adsorption. The other catalysts exhibited intermediate adsorptions and selectivities.

The final paper (M3) is concerned with the relation between the selectivity of the oxidation reactions and the level of free sulphur trioxide in the catalyst. For this study a number of catalysts supported on anastase titanium dioxide were prepared. The oxidations of both orthoxylene and naphthalene were studied on catalysts having a wide range of potassium sulphate and free sulphur trioxide levels. It was found that a catalyst containing 0.5 moles of K_2SO_4 per mole of V_2O_5 was optimal over a wide temperature range.

The effect of heat treatment on the free sulphur trioxide content of the catalysts was investigated by placing samples of a catalyst, containing 0.5 moles of K_2SO_4 per mole of V_2O_5 and a large amount of sulphur trioxide, in a reactor immersed in a salt bath and passing air through the catalyst bed. By varying the bath temperature and the time of treatment, nine catalysts containing different free sulphur trioxide levels were obtained. The nine catalyst samples were then reacted with naphthalene and orthoxylene feedstocks for a period of five hours during which time no sulphur dioxide was added. It was found that the free sulphur trioxide content of the catalyst had a great effect on the product yields and selectivities for both feedstocks. A free sulphur trioxide level of 5.0 weight percent was found to be optimal for both naphthalene

and orthoxylene. High sulphur trioxide levels produced catalysts that were highly active for total oxidation whereas lower levels produced less active catalysts which also had poor selectivities for phthalic anhydride formation. A further discussion of this aspect of their work is given in Chapter 4.

A catalyst that contained no potassium sulphate was prepared. By the addition of free sulphur dioxide to the feed air, a catalyst that had a free sulphur trioxide level near to the optimum value, was produced. This catalyst gave yields and selectivities comparable to those of the sulphate-promoted catalyst. This provided experimental evidence to support their earlier claims (K1) that a V_2O_5-SO_3 complex is responsible for orthoxylene oxidation and that the action of potassium sulphate is merely to stabilize the free sulphur trioxide content, thereby maintaining a constant V_2O_5-SO_3 complex.

The four articles discussed above represent major contributions to the knowledge of the performance of the so-called "German" catalysts. However, the studies suffered from the major drawback that they used a reactor that was essentially infinite in length. The yields and selectivities were generally obtained at 100 percent conversion of orthoxylene and naphthalene. Hence it is difficult to make positive quantitative claims regarding activity changes following changes in reaction conditions. Most of the claims made by the authors would tend to be conservative. Another weakness of the study was the use of a non-isothermal reactor. Hotspot temperatures of 60°C

above the bath temperature were common in the studies. No attempt has been made to evaluate the kinetics of the oxidation of either naphthalene or orthoxylene. These studies provide an excellent background knowledge of catalyst properties for future kinetic studies that can be made under more closely controlled reaction conditions, using more accurate analytical techniques.

A recent patent (M4) describes a new catalyst for orthoxylene oxidation in fixed beds. The catalyst has the following typical composition.

		Weight percent
Vanadium pentoxide	V_2O_5	6.0
Antimony oxide	Sb_2O_3	6.0
Potassium oxide	K_2O	2.0
Sulphur trioxide	SO_3	2.0
Titanium oxide (support)	TiO_2	84.0

The surface area of such a catalyst is typically 5 square metres per gram. Selectivities for phthalic anhydride formation are claimed to be as high as .874 moles per mole of orthoxylene at 100 percent conversion. It is suggested that certain other oxides can be substituted for antimony oxide. The patent covers Sb_2O_3, Nb_2O_5, UO_2, SnO_2, PbO_2, MnO_2, GeO_2, TaO_2 and CoO_2. The importance of antimony trioxide to the catalyst performance is shown by an increase in selectivity from 65.5 to 76.3 percent phthalic anhydride, when 6.0 percent Sb_2O_3 is added to the catalyst.

An important aspect of the use of "German-type" catalysts is the addition of sulphur dioxide to the air-hydrocarbon mixture. The amount of sulphur dioxide that should be added is somewhat vague. The Grace patent (M2) claims that a sulphur dioxide level between 0.2 and 1.5 weight percent, based on the orthoxylene fed, can be used. Froment (F2) suggests that approximately 0.4 percent sulphur dioxide, based on the weight of orthoxylene fed, should be used. Duckworth (D3) notes that the quantity required, calculated as sulphur, is 0.1 to 0.2 percent based on the weight of xylene fed. This agrees with Froment's figure of 0.4 percent sulphur dioxide. Duckworth further notes that coal-tar naphthalene, with a sulphur content as high as 1 percent, can be successfully oxidized on these catalysts. However, there is some reduction in phthalic anhydride yield. He also reports that the sulphur oxides formed are known to promote the formation of tars.

2.3.2. Reaction Mechanisms and Kinetics

In 1954 Mars and van Krevelen (M5) published a comprehensive study of a member of oxidation reactions carried out on vanadium pentoxide catalysts. Benzene, toluene, naphthalene and anthracene were oxidized in a fluidized bed of 200-300 micron catalyst particles. The catalyst contained 9 weight percent vanadium pentoxide and 21 weight percent potassium sulphate on silica gel. The results were interpreted by a mechanism which has since become known as the "Redox" mechanism. A steady-state is assumed to be reached in the

catalyst when the rate of reaction between the hydrocarbon and the oxygen of the catalyst is equal to the rate of reoxidation of the catalyst by the oxygen in the air carrying the hydrocarbon feed.

Shortly after the Redox model had been proposed, Shelstad, Downie and Graydon (S5) proposed a Steady State Adsorption Model (S.S.A.M.). This model assumes that the reaction takes place between the hydrocarbon molecule and chemisorbed oxygen molecules. The resultant rate expression for the overall rate of reaction is identical to that for the "Redox" model. Therefore the mechanisms cannot be distinguished simply by kinetic measurements.

The fact that the oxygen in the catalyst contributes, at least in part, to the oxidation of the hydrocarbon has been established by the oxidation of xylene and naphthalene (S3) and ortho-tolualdehyde (V2) when mixtures of these hydrocarbons in nitrogen have been passed over vanadia catalysts. Although no rates of oxidation have been determined, these studies do provide supporting evidence for the Redox mechanism. The amounts of oxygen contained within the reaction products were in excess of those which could be obtained from chemisorbed oxygen.

The basic rate equations for the oxidation of ortho-xylene to a single product, say ortho-tolualdehyde, will now be presented. It should be noted that this approach can be extended to more complex reactions involving parallel and series reaction steps. A typical analysis for a complex reaction

sequence is presented in Appendix F. The case for the formation of a single product is as follows:

Oxidized catalyst + hydrocarbon $\xrightarrow{k_r}$ reduced catalyst + product

Reduced catalyst + oxygen $\xrightarrow{k_a}$ oxidized catalyst.

If both reactions are considered to be first order with respect to hydrocarbon and oxygen, we can write the rate expressions for the individual steps.

$$r_r = k_r C_r \theta \tag{2.7}$$

and

$$r_a = k_a C_a (1-\theta) \tag{2.8}$$

where θ is the fraction of oxygen sites available for oxidation of the hydrocarbon.

In the steady-state we have

$$r_a = n\, r_r \tag{2.9}$$

where n is the number of oxygen molecules used per mole of hydrocarbon oxidized.

Equations (2.7), (2.8) and (2.9) yield the fraction of active sites available for reaction:

$$\theta = \frac{k_a C_a}{k_a C_a + n k_r C_r} = \frac{1}{1 + \left(\frac{n k_r C_r}{k_a C_a}\right)} \tag{2.10}$$

and hence the overall rate of hydrocarbon oxidation:

$$r_r = \frac{k_a k_r C_a C_r}{k_a C_a + n k_r C_r} \qquad (2.11)$$

It is well-known that several postulated mechanisms, yielding Langmuir-Hinshelwood-type rate expressions, can often fit experimental data equally well. Therefore the fact that Equation (2.11) provides a reasonable fit to the data for orthoxylene oxidation would not be sufficient evidence of the correctness of the postulated mechanism. One research group (S5, D4, H1, M6, J2, J3) has claimed additional support for the S.S.A.M. by oxidizing a number of different hydrocarbons on samples of the same catalyst. They have endeavoured to validate the mechanism by estimating the parameters k_r and k_a for the oxidation of benzene (J2), toluene (D4), xylene (M6, J3) and naphthalene (S5). They postulate that, since the reoxidation of the catalyst (Equation (2.8)) should be independent of the particular hydrocarbon being oxidized, the value of k_a, and its related activation energy, should be the same for all studies. The results of their studies have been far from conclusive. In particular, the values for k_a obtained for benzene oxidation differ greatly from those obtained for the oxidation of the other hydrocarbons. Such poor agreement is not surprising since a number of experimental weaknesses were apparent in their studies. Moreover, considerable non-catalytic reaction was found to occur in most of the investigations. In addition, no sulphur dioxide was added to the reactant gases. This caused unstable catalyst activities and an overall catalyst

decay with time. These points will be discussed later in the text.

The research has been conducted on the premise that the chemisorption of oxygen on a given catalyst is independent of the aromatic hydrocarbon being reacted. The observations (K1, S3) that different selectivities are obtained for the oxidation of orthoxylene on catalysts supported on different materials whereas naphthalene gives a constancy of selectivity on all supports, suggests that this may not be correct. Therefore, the studies may have been more successful, had they been carried out on an industrial catalyst which is capable of handling orthoxylene and naphthalene feedstocks equally well. Such catalysts do exist (S6).

An examination of Equations (2.7) and (2.8) suggests that more conclusive evidence, in support of the Redox and S.S.A.M. mechanisms, may be provided by studying the initial rate of oxidation of the hydrocarbon. Under these conditions θ can be assumed to be unity, provided the time of reaction is sufficiently small. These initial rates should be first order with respect to hydrocarbon concentration and independent of oxygen level. Therefore reaction in air and nitrogen streams should yield the same initial rates of reaction on a freshly oxidized catalyst. Initial rate studies using oxygen 18 in the catalyst or in the air would be of value in distinguishing between the Redox and S.S.A.M. mechanisms. However, a major difficulty may be that of removing chemisorbed oxygen from the catalyst surface prior to reaction.

Initial rate studies of the type described above would require the development of a method of chemical analysis that would completely analyze reaction gases from a single sample. They would also require the development of a reactor capable of producing actual contact times from a fraction of a second to several minutes. The development of such methods is described later in the text.

The oxidation of orthoxylene produces a wide range of products. Any complete rate expression for the formation of phthalic anhydride should incorporate the rates of the individual steps in the reaction scheme. Therefore a brief review of some of the more recently proposed routes to phthalic anhydride will now be discussed.

Herten (H2) has made a comprehensive study of the oxidation of orthoxylene in a quasi-isothermal fixed bed of a French Synoxy catalyst. He has inferred that this catalyst is supported on silica gel; however, the product distributions indicate that the support material was most likely titanium dioxide. Product distributions and the rates of overall conversion of orthoxylene were obtained over a wide range of experimental conditions. The overall rate of conversion of orthoxylene was found to be described equally well by both the Redox mechanism and a power-law type expression. The main reaction products obtained were phthalic anhydride, carbon monoxide, carbon dioxide, ortho tolualdehyde and phthalide. The maximum selectivity to phthalic anhydride at 100 percent conversion of orthoxylene was obtained at the lowest temperature

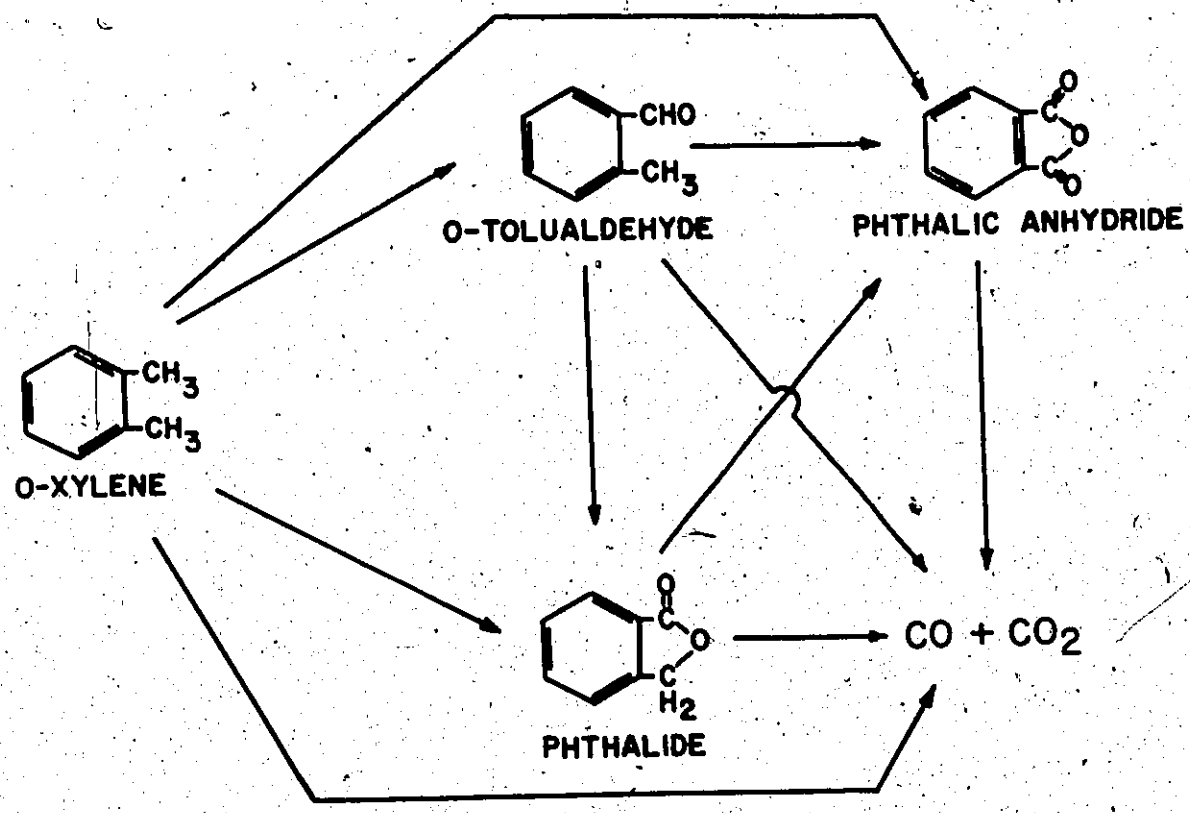

Figure 2.3. Reaction Scheme of Herten (H2).

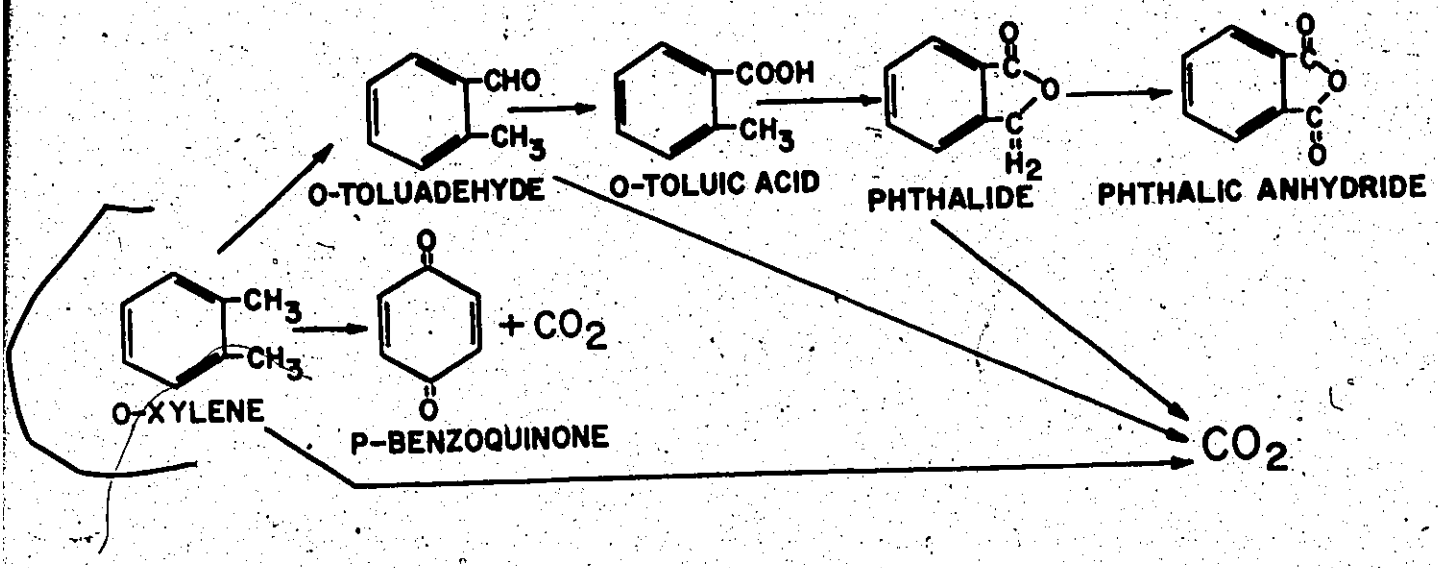

Figure 2.4. Reaction Scheme of Juusola (J4).

studied, 325°C. This would indicate that the steps leading to total oxidation are more highly activated than the partial oxidation steps.

On the basis of a number of selectivity plots obtained at different temperatures in the range 325°C to 402°C, Herten has postulated the following reaction scheme shown in Figure 2.3. Such a reaction scheme would lead to a series of rate expressions of the form of Equation (2.11). Each equation would contain eleven rate constants and their eleven associated activation energies. Obviously, estimation of such a large number of parameters is not desirable. However, judicious selection of the more important steps in the reaction sequence could significantly reduce the number of parameters needed to accurately describe the rate of phthalic anhydride formation.

Figure 2.4 shows the reaction network proposed by Juusola from observations of the oxidation of orthoxylene and ortho tolualdehyde on a silica-gel-supported catalyst. The presence of p-benzoquinone has been reported in the work of both Mann (M7) and Juusola (J4). One would generally not expect such a great structural rearrangement to occur when easier oxidation steps are possible.

The reaction network presented in Figures 2.3 and 2.4 are but two of the many schemes that have been postulated. Every study of product distributions from orthoxylene oxidation produces a slight modification of the general network. An excellent review of many of these studies is given by Juusola (J4).

It was established in section 2.3.1. that the product distribution, for orthoxylene oxidation, depends upon the nature of the catalyst support. Silica-supported catalysts produce large amounts of ortho tolualdehyde and carbon oxides. Titania-supported catalysts produce high yields of phthalic anhydride. Such observations do not preclude the possibility of the same reaction network applying to both types of catalysts. The different product distributions obtained in the studies by Herten and Juusola may be attributed to different rates of reaction for the individual steps in the reaction sequence. This point will be discussed in more depth later in the thesis.

The two reaction networks differ in that Herten has assumed carbon dioxide formation from phthalic anhydride and phthalide. Juusola has shown no such oxidation. It has been well established (H3) that phthalic anhydride is oxidized on vanadium pentoxide catalysts, to yield carbon dioxide, carbon monoxide and maleic anhydride. However, the rate of oxidation of phthalic anhydride below 400°C is almost negligible. Therefore, that step in the reaction network can be neglected. However, in industrial reactors, where excessive contact times are used, and large hot spots exist, this step cannot be neglected.

The oxidation state of the catalyst has a significant effect on product distributions. It has been established (S4, U1) that the average oxidation state of the catalyst is between 4 and 5 during reaction. A higher oxidized state favours partial oxidation, whereas a more reduced catalyst

produces considerable total oxidation. The active oxides for partial oxidation are thought to be V_2O_5 and $V_2O_{4.34}$ (S4). Catalysts in a low oxidation state have also been shown (H3) to readily oxidize phthalic anhydride to maleic anhydride and carbon oxides whilst the rates on highly oxidized catalysts are considerably lower.

Low oxidation states are produced in catalysts when high throughputs of hydrocarbon and low oxygen levels are used. Such conditions exist in industrial reactors where the highest concentrations of xylene, which are only governed by the explosive limits, are used. These higher concentrations result in reduced costs in supplying air, and in product recovery, since it is more convenient to recover a product from a more concentrated stream.

The extent of homogeneous oxidation of orthoxylene is important in that it can influence the results of catalytic reaction experiments. Bhalla (B2) and Satterfield and Loftus (S10) have made comprehensive studies of the homogeneous oxidation of orthoxylene in stainless steel and borosilicate-glass flow reactors. The results of these studies indicate that negligible homogeneous oxidation will take place at temperatures below 400°C even at residence times in excess of several seconds. Those findings differ from those of Mann and Juusola who found significant levels of homogeneous oxidation in aluminium and stainless steel tubes at temperatures below 350°.

2.4. Aims and Objectives

The overall aim of the project was to investigate the performance of a pilot-plant-scale transported bed reactor. In section 2.1 it has been shown that the advantages of such a reactor are best exploited by carrying out a highly exothermic reaction in which the valuable product is an intermediate in a series reaction network. In addition, it would be advantageous if a catalyst that undergoes rapid decay were used. This would permit the regeneration of the catalyst in a separate stage. The section on pneumatic conveying has shown that the level of knowledge of dense-phase pneumatic conveying is meagre. Any study of chemical reaction will require some measurement of solids hold-ups and flow rates. Although, as we have seen in section 2.3, there are a lot of unanswered questions regarding the mechanism of orthoxylene on vanadia catalysts, it is apparent that this is an excellent reaction for a transported bed study. In addition to it being highly exothermic (360 K calories per gram mole), partial oxidation products are formed as intermediates in a complex reaction scheme. The literature on both the "Redox" mechanism and the importance of the oxidation state of the catalyst in determining product distribution, tempt one to suggest that a catalyst decay problem might exist. However, no studies have been made of such a phenomenon, so that the rate of decay is unknown.

Before conducting reaction in the transported bed, it is necessary to investigate the performance of the catalyst in an isothermal packed bed. Under these conditions the fluid

mechanics are well-established and definitive statements regarding catalyst behaviour and reaction mechanisms can be made. Such a study will involve the steady-state performance of the catalyst, in order to determine the rates of reaction that would be obtained in a packed-bed reactor. A study of the unsteady-state performance of the catalyst, by making initial rate experiments on a highly oxidized catalyst, would provide some evidence of the relative rate of catalyst deactivation, should it occur. This would also give support to the "Redox" mechanism. Initial rate studies of the oxidation of orthoxylene in a nitrogen stream would also provide more evidence as to the validity of the two-step reaction model. In order to conduct initial rate studies, it is necessary to determine complete product compositions from a single gas sample. Such an analytical procedure must also be used in transported bed studies where contact times are generally less than one second. Steady-state studies have not required this type of analysis, since liquid and solid products can be condensed and collected over a finite period of time, thereby giving a time averaged product composition. Calderbank (C 3) has experienced some difficulty with condensing all the products in the exit line from his reactor.

The study of the transported bed reactor should include an evaluation of its industrial potential when compared with conventional methods of gas-solids contacting. Similarly, the factors that affect the performance of reactors currently in industrial usage, should be closely examined in the steady-state experiments.

CHAPTER 3

PACKED BED EXPERIMENTATION

Many of the kinetic studies reviewed in the previous chapter have suffered because of inadequate mass balances, non-isothermal reactor behaviour, and inaccurate methods of chemical analysis. This chapter describes the development of a packed bed reactor and gas chromatographic techniques that overcome many of the shortcomings of previous studies. In addition, there is evidence (S3, M4) to suggest that the catalyst support has a marked effect on reaction rates and selectivities. Kinetic measurements on silica-gel and titanium dioxide-supported catalysts have been made under steady-state and unsteady-state conditions.

3.1. Reaction Product Analysis

Background

All the studies of the partial oxidation of ortho-xylene, conducted during the past decade, have used gas chromatographic analysis to some extent. All have involved the trapping of condensable products and some have included on-line analysis of carbon monoxide and carbon dioxide. Incomplete trapping of condensable materials has been a major source of error in some of these studies. The use of separate analyses for the condensables (time-averaged) and fixed gases (instantaneous) is another possible source of mass balance deficiencies.

The complexity of the analysis of the reaction products can be determined by reviewing the wide range of products formed by this reaction on vanadium pentoxide. The most common products are phthalic anhydride, carbon dioxide, carbon monoxide, maleic anhydride, orthotolualdehyde and phthalide. Some studies have also reported the presence of benzoic acid, orthotoluic acid, orthoxylene oxide, orthophthalaldehyde, benzene, toluene, parabenzquinone, benzaldehyde, and methyl-benzyl alcohol in small quantities. Due to their small concentrations these trace components are generally not important in kinetic studies. However, they must be determined accurately for quality control purposes in the plant. In addition to the products, the reactor effluent contains unreacted orthoxylene and oxygen, as well as nitrogen.

There have been a number of separations of oxygen, nitrogen, carbon monoxide and carbon dioxide reported in the literature. They have involved either the use of several columns (M10) or subambient temperatures (H4) to separate the fixed gases. One analysis that completely separates the four gases involves the programming of a 2 foot by 1/4 inch molecular sieve, 5A column, from 35°C to 250°C, at a helium flow of 50 c.c. per minute giving a total analysis time of 15 minutes.

Mann (M7) has used a 6 foot by 1/4 inch column of 10% GE SE 52 (silicone gum rubber) on 60-80 mesh Diataport S packing to separate the condensable products of orthoxylene oxidation. The column was programmed from 75°C to 300°C at 10°C/minute.

A technique that analyzes most of the products of

toluene oxidation has been reported recently (J5). The method uses a temperature programmed Porapak R column to separate carbon dioxide and the condensable products. An isothermal molecular sieve column is used to separate oxygen, nitrogen and carbon monoxide. The authors claim that the technique may be applied to the analysis of the reaction products from the oxidation of other hydrocarbons. This claim is valid only for the oxidation of toluene and lower molecular weight hydrocarbons. Higher molecular weight hydrocarbons will be retained for unreasonably long times on the Porapak column at the upper column temperature limit (250^{o}C).

Apparatus

The selection of columns, switching procedures, and programming rates had to be made in such a way to effect the separation in the shortest possible time, whilst eluting the components with a minimum of peak overlap. The method is based on temperature programming a 5A molecular sieve column and an Se 52 silicone gum rubber column at the same rate. The column configuration and switching procedures finally adopted differed quite markedly from the methods tried initially.

A Varian Aerograph series 1520 gas chromatograph, with a thermal conductivity detector and matrix temperature programmer, was used for the analysis. Figure 3.1 is the chromatograph flow system. The valves used for gas sampling and column switching are Carle micro volume switching valves (Catalogue Number 2014).

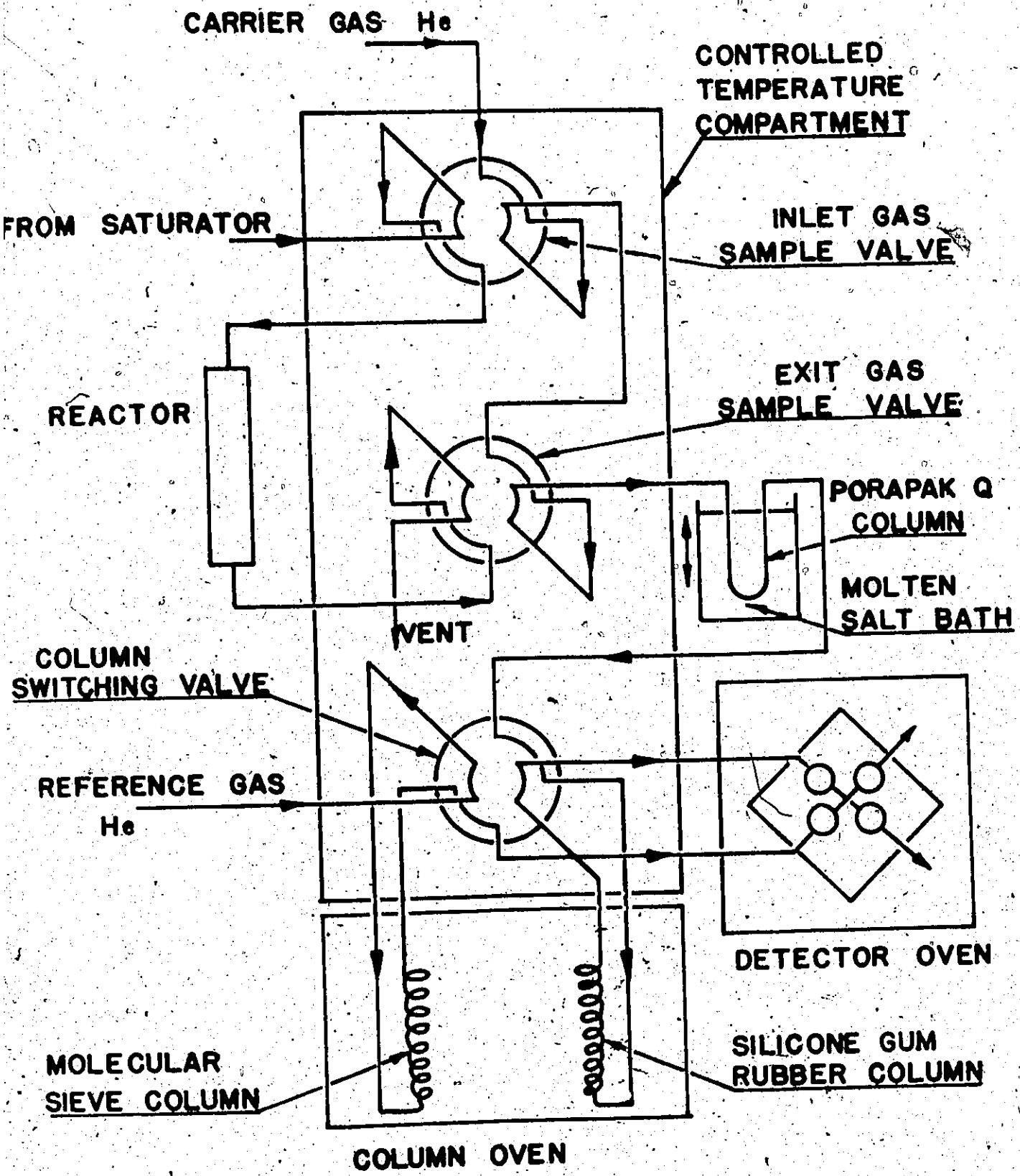

Figure 3.1. Flow Diagram of Gas Chromatograph.

The sample (approximately 5 c.c. at standard temperature and pressure) first passes to a 1 inch by 1/8 inch outside diameter stainless steel column packed with 50/80 mesh Porapak Q particles. A Carle sampling valve is used to switch the sample either to a 1/4 inch outside diameter stainless steel column containing 8 feet of 40/60 mesh 5A molecular sieves or to a similar 1/4 inch outside diameter column containing 16 feet of silicone gum rubber packing (10% Se-52 on chromosorb W, H.P., 80/100 mesh).

Figure 3.2 shows the chromatograms obtained for a typical product stream for the oxidation of orthoxylene on titania and silica gel-supported catalysts. The figure also shows the temperature programme used.

The operating procedure is as follows:

1. The column switching valve is in the position such that the carrier gas stream passes through the molecular sieve column and the reference stream passes through the silicone gum rubber column. The sample is introduced and passes to the short Porapak column which is at room temperature. This column traps all the condensable materials except water whilst the fixed gases and water travel virtually unimpeded to the molecular sieve column. The oxygen, nitrogen and carbon monoxide are eluted rapidly from the molecular sieve column. The retention times are given in Table 3.1.

2. When the carbon monoxide has been eluted (approximately 8 minutes) the carrier gas is switched to the silicone gum rubber column and the molten salt bath (at 220°C)

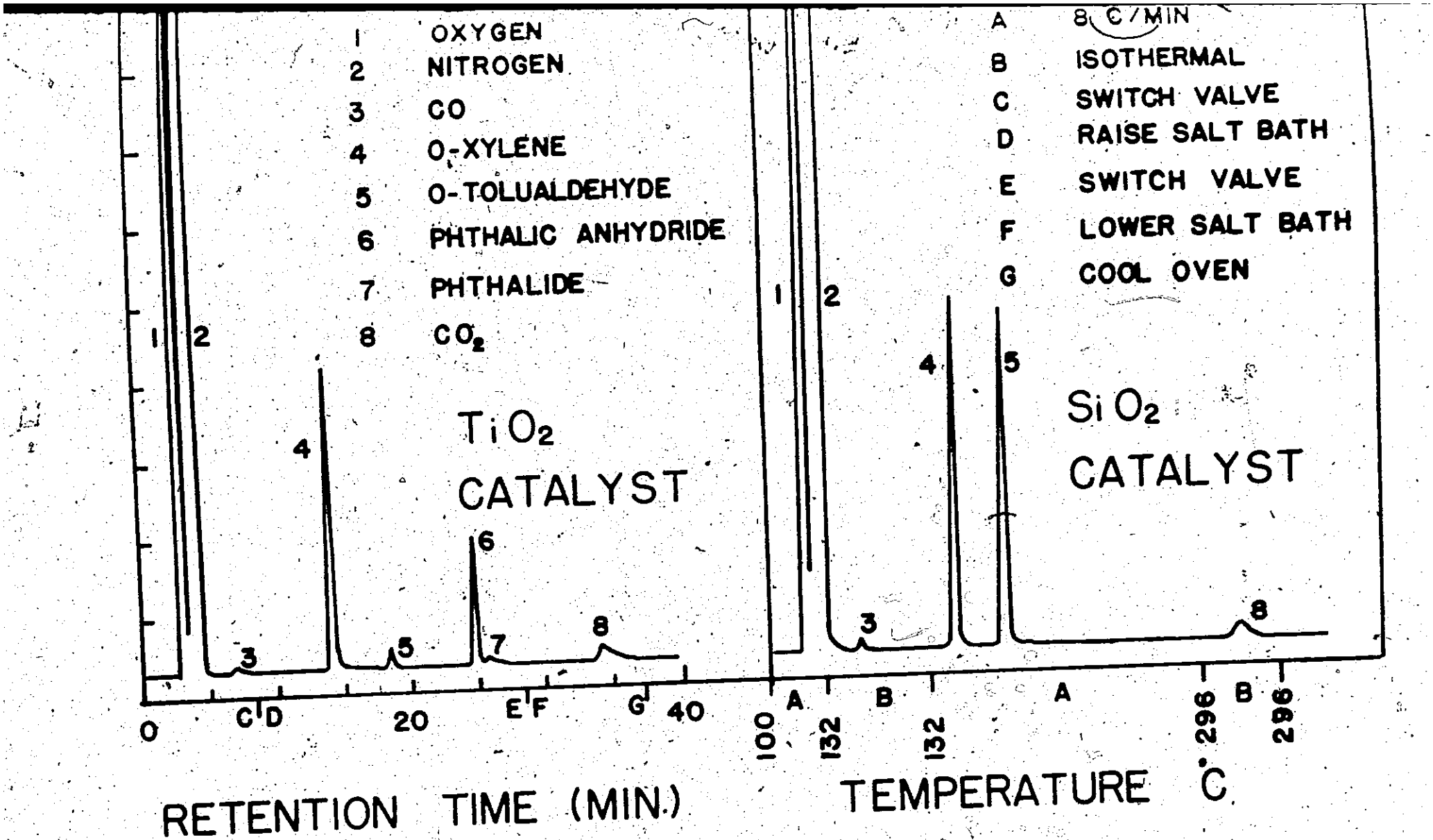

Figure 3.2. Typical Chromatographs.

Table 3.1

Component	Retention Time (Mins.)	Elution Temp. (°C)	Relative Molar Response
Oxygen	2.4	119	0.97
Nitrogen	3.3	126	1.00
Carbon Monoxide	6.7	132	1.06
Maleic Anhydride	13.7	146	2.20
Ortho-xylene	14.1	147	3.04
Orthotolualdehyde	17.4	175	3.19
Phthalic Anhydride	24.5	264	3.28
Phthalide	25.4	271	3.34
Carbon Dioxide	35.0	292	1.20

is raised so that the condensable products are driven from the Porapak column. The maleic anhydride, orthoxylene, ortho-tolualdehyde, phthalic anhydride and phthalide are eluted in that order. Following the elution of phthalide the carrier gas flow is returned to the molecular sieve column and the salt bath is lowered.

3. The elution of carbon dioxide (after 36 minutes) from the molecular sieve column marks the completion of the analysis. Then the oven is cooled from 292° to 100°C to repeat the procedure. The overall analysis time is less than 45 minutes.

The temperature programme used was as follows:

1. 100°C to 132°C at 8°C/minutes for 4 minutes.
2. Isothermal at 132°C for 8 minutes.

3. 132°C to 292°C at 8°C/minute for 20 minutes.

4. Isothermal at 292°C for 6 minutes.

The helium flow used was 80 c.c./minute; the filament current was 250 milliamps. The injection port was maintained at 200°C and the detector temperature was 225°C. The sample valves and column switching valve were housed in an oven that was maintained at 200°C by a supply of hot air from a Master heat gun. Care was taken to maintain all gas lines in the system at 200°C to prevent condensation of phthalic anhydride or phthalide.

Calibration

The detector was calibrated for the fixed gases by making up mixtures from cylinders of oxygen, nitrogen, and a mixture of carbon dioxide and carbon monoxide in nitrogen. The calibration apparatus is shown in Figure 3.3. The standard gas mixture was supplied by Matheson, and contained 5.06 carbon dioxide and 1.00 percent carbon monoxide with the balance being nitrogen. Molar responses, relative to a nitrogen response of unity, were obtained. Calibrations for liquid and solid components were made by injecting mixtures of all species in dioxane solvent. Responses for these components were obtained relative to orthoxylene. Absolute calibrations were then made for orthoxylene and nitrogen by injecting known quantities of these compounds. The response of xylene relative to nitrogen was then obtained, permitting the calculation of molar response of all components relative to

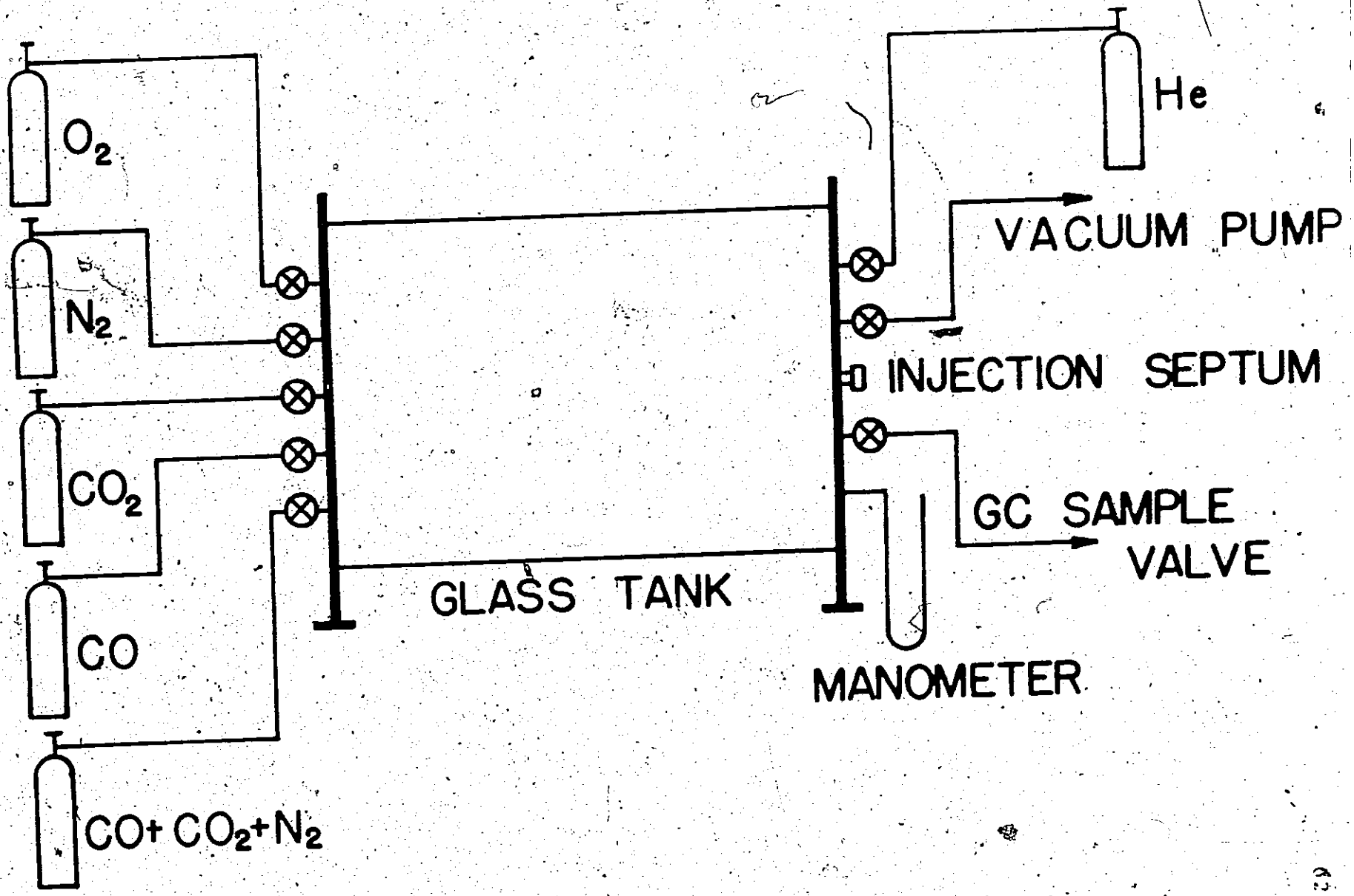

Figure 3.3. Apparatus used to Calibrate Chromatograph.

nitrogen. Table 3.1 presents the relative molar responses and retention times of all components.

Peak areas were obtained using a Hewlett Packard 3370 B electronic integrator. Since oxygen and nitrogen constitute more than 95 percent of the product stream, it is essential to use an electronic integrator to measure the peak areas of some of the lesser components. When incomplete resolution of peaks occurred, it was always such that the overlap was less than 20 percent. Drop-line analysis of the unresolved peaks was therefore used. The errors in the actual areas using this method are less than 4 percent (M11).

Discussion

The use of nitrogen as the "tie component" enables a direct comparison of inlet and exit stream compositions to be made. The accuracy of the analytical procedure was tested over a range of conversions of orthoxylene from 1 to 100 percent and for selectivities of phthalic anhydride from 30 to 85 percent. In general carbon balances ranged from 96 to 104 percent. Consistently low mass balances were obtained only when considerable tar formation occurred due to cracking of orthoxylene.

The need for the Porapak precolumn became apparent when low carbon balances were obtained during some of the earlier kinetic experiments. At that time, the analytical procedure was such that all components passed to the silicone gum rubber column. This enabled water to be eluted along with the hydrocarbons. The water appeared as a broad, flat peak that

was first interpreted as a drifting baseline. The elution of water took plage throughout the period of elution of all the hydrocarbon products. The presence of water was found to reduce the response of phthalic anhydride. Since phthalic anhydride constitutes a major proportion of the reaction products, around 70 percent, this was found to be the source of the carbon balance error. The effect of water on the phthalic anhydride response was determined by making up mixtures of phthalic anhydride and water in acetone. The results are shown in Table 3.2.

Table 3.2

Effect of Water on Phthalic Anhydride Response

Moles Water/Mole PAA	Relative Molar Response for PAA
0	3.34
2.01	3.07
3.08	2.89
4.42	2.77

It can be seen that a water content of 4 moles per mole of phthalic anhydride, a typical level in a reaction product stream, is sufficient to reduce the response by almost 20 percent. No attempt was made to determine if the responses of the other products, O-tolualdehyde and phthalide, were similarly reduced. Once the influence of water had been established it was considered necessary only to overcome the problem and not to investigate the phenomenon further.

It is difficult to suggest a reason for the effect of water on the response. Keulemans (K5) notes that "the presence of water introduces complications in many cases" (separations). However, he does not expand this point. He merely suggests that some form of water removal should be used. He also notes that "these complications appear to be less serious when employing radiological detection and other ionization methods, particularly the flame ionization detector (with which they are virtually absent)." By inference, one concludes that the complications to which he refers, occur mainly with conductivity-type detectors.

It was noted that when water was present in the sample, a small negative peak immediately preceded the phthalic anhydride peak. Anomalous thermal conductivity detector response of this type has been discussed in detail by Purnell (P2). Generally this condition, known as inverse W peaking, exists when low conductivity gases such as nitrogen replace helium or hydrogen as the carrier gas. The conductivity difference between the carrier gas and the component being analyzed is small. The possibility that the presence of water in the gas stream causes a reduction in the effective thermal conductivity of the carrier gas appears unlikely since the water levels are very small. Another possible explanation is that some bonding between the anhydride and water occurs, producing a species which has a higher conductivity than pure phthalic anhydride. This increase in conductivity would be attributable to the water molecule. Neither of the explanations given above should be considered to be more than speculation.

As stated above, the presence of water in samples often causes problems in gas chromatographic analyses, due to tailing of the water peak, and in some cases, due to chemical reaction occurring on the column. Water removal is generally accomplished by chemical reaction, adsorption or freezing. However, in many analyses none of these methods may be applicable since removal of water causes the simultaneous removal of one or more other components present in the sample. In the method described above, hydrocarbons are adsorbed whilst water is not. This unique method of water removal may therefore be beneficial in a number of separations.

An additional benefit of the short Porapak column is its excellent ability to trap hydrocarbon molecules. The method of trapping by adsorption and then desorbing by temperature activation may be superior to convontional trapping in dry ice baths. One can see an immediate application in conducting pulsed-micro reactor experiments.

Recommendations

The major weakness of the analytical method was the use of a molecular sieve 5A column to separate the fixed gases. In particular, the elution of carbon dioxide was slow. The carbon dioxide peak was very diffuse thereby reducing the accuracy of its determination at low concentrations. A more effective analysis requires that carbon dioxide be separated on a different column.

The separation of the hydrocarbons from the gases and water provides a means of separating the gas/water mixture on a single column. In this method the 5A molecular sieve column is replaced by a Porapak Q column (see Figure 3.1). Initially the Porapak column would be immersed in a dry ice/ethylene trichloride slurry and the nitrogen-oxygen-carbon monoxide separation would be effected. The column temperature would then be raised to room temperature, or a little above and carbon dioxide and water would be eluted. The gas flow would then be switched to the silicone gum rubber column and the salt bath raised, in order to separate the hydrocarbons. In addition to the advantage that carbon dioxide is eluted as a well-defined peak, there is also the possibility of obtaining a hydrogen balance from the water analysis. The method would have general applicability to the analyses of the reaction products of most hydrocarbon oxidations since the gases and water are common to all such reactions. The only modification to the procedure that would be necessary when different hydrocarbons are oxidized would be to employ a column that gives optimum separation of the hydrocarbon compounds. The modifications, described above, will be undertaken shortly.

3.2. Experimental Programme in Packed-Bed Reactor

Background

The oxidation of orthoxylene is a highly exothermic reaction. In order to make kinetic measurements, a number of methods have been tried to achieve near isothermal reactor

behaviour. By using a 304 stainless steel differential reactor Juusola (J4) has been able to make near isothermal measurements. Conversions measured, were typically less than 5 percent. The reactor was 8 inches long by 5/8 inch internal diameter, and was packed to a depth of 1 cm. with catalyst particles in the 14/16 mesh size range. Mann (M7) has used a reactor of similar dimensions constructed from aluminium, and has observed considerable "blank" reaction. Juusola found that above 315°C the stainless steel reactor also gave significant "blank" reaction. He therefore confined his kinetic measurements to the temperature range from 290°C to 310°C. The blank reaction evident in his work may have been caused by homogeneous reaction occurring due to the long residence time of the gas mixture in the relatively large void volume of his reactor. The very shallow beds of catalysts, typically 6 particles deep, which were used in these studies may have introduced errors to the results. Heating was achieved in both cases by cartridge heaters inserted in a metal block that encased the reactor.

Herten (H2) has used catalyst dilution to achieve near isothermal conditions. He has used relatively large particles (0.1 inch mean diameter) in a 1 inch internal diameter stainless steel reactor. Temperatures were measured in a central thermowell. He has claimed quasi-isothermal operation of the reactor. Considering the reactor and particle dimensions, it is possible that he had axial and radial gradients of the order of several degrees centigrade.

Calderbank (C2) has used a spinning-basket type reactor to study the oxidation of orthoxylene on a silicon carbide-supported catalyst. A mean particle size of 0.6 cm. diameter was used. The excessive residence times inherent in this type of reactor produce considerable overoxidation that limits its usefulness for studying hydrocarbon oxidations. Calderbank (C4) has also carried out the reaction in large fixed and fluidized beds. No kinetic measurements were made since the reactors were effectively infinite in length. The low activity found in the fluidized bed was probably due to the type of catalyst employed. The American-type catalysts generally have an impervious core coated with vanadium pentoxide. Crushing these catalysts produces excessive fine material from the vanadium-rich outer layer. The catalyst used in the fluidized bed therefore may not be truly representative of the catalyst used in the spinning-basket reactor study.

The ideal plug flow assumption made by Mars and van Krevelen (M5) for a fluidized bed used in making kinetic measurements, has been questioned elsewhere (J3).

When designing a reactor to study the kinetics of orthoxylene oxidation, the following considerations must be taken into account:

1. The reactor must be operated isothermally.

2. The temperature range of operation should be approximately that used industrially for a given catalyst.

3. The range of conversion should have an upper limit near 100 percent so that the catalyst is investigated at yields near those obtained industrially.

4. Both steady-state and transient measurements should be possible.

5. The amount of homogeneous or "blank" reaction should not be significant.

6. The catalyst activity should remain constant throughout the series of experiments.

7. Catalyst dilution should be avoided, if possible, in order to prevent any catalytic action of the diluent.

Zahner (Z3) has set down certain guidelines for the design of laboratory reactors for studying the kinetics of highly exothermic chemical reactions. In this study we have used a reactor and catalyst particle with dimensions similar to his recommendations.

In general, experimental conditions were chosen to cover the range of industrial operating conditions. Temperatures were chosen in the range 330°C to 390°C. Oxygen and xylene levels ranged from 10 to 30 percent and from 1 to 2 percent respectively. The mass of catalyst used was generally 1.0 grams, and the W/F_{ao} values ranged from 50 to 400 grams of catalyst per gram mole of orthoxylene fed per hour. This is the range of operation that is expected to be achieved in a transported bed reactor.

Apparatus

A diagramatic sketch of the apparatus is shown in Figure 3.4. Flows of oxygen and nitrogen from high pressure cylinders (Canadian Liquid Air) were controlled by needle valves

Figure 3.4. Flowsheet of Packed Bed Apparatus

B	Backpressure regulator
E	Electrical heating
F	Capillary flow meter
Ge	Gas sample valve to gas chromotograph
He	Heating elements
M	Manometer
Ms	Agitator
N	Needle valve
NR	Non-return valve
P	Preheating coil
R	Reactor
S	Xylene saturator
SB	Molten salt bath
T	Three way valve
TC	Thermocouple
W	From constant temperature water bath
V	Vent

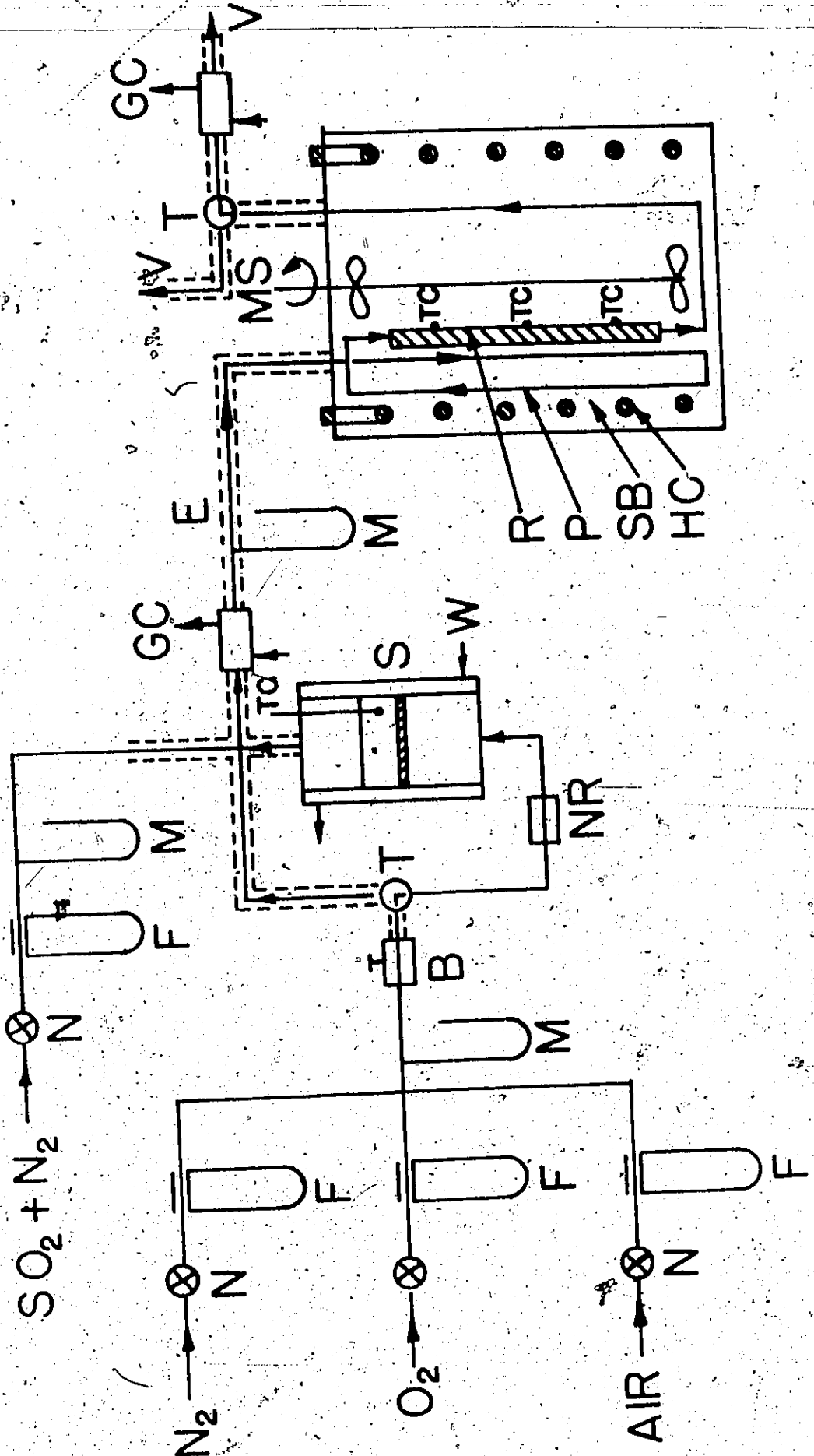
V
GC
T
V
MS
TC
TC
TC
E
M
R
P
SB
HC
GC
W
S
TC
M
NR
T
F
B
N
M
$SO_2 + N_2$
F
F
F
N
N
N
N_2
O_2
AIR

and measured by capillary flowmeters. The pressure in the measurement section was maintained at 80 cm. mercury by a back pressure regulator and was measured by a U-tube monometer. The oxygen-nitrogen mixture flowed to a three-way ball valve, which directed the gas flow either through the saturator when reaction took place, or bypassed the saturator to regenerate the catalyst. The saturator was a jacketed glass vessel, containing a coarse, porous frit. Water from a constant temperature bath circulated through the jacket to maintain the vapour pressure of orthoxylene at the desired level. A manometer was used to measure the pressure at the exit of the reactor, so that the required partial pressure or concentration of orthoxylene in the feed could be obtained by raising or lowering the vapour pressure.

The reactor was constructed from 316 stainless steel tube, 14 cms. long and 0.475 cms. internal diameter. The temperature of the reactor was measured by 3 chromel-alumel thermocouples that were welded at three axial locations on the reactor wall. The temperature was indicated by a digital voltmeter and was controlled to within $\pm$ 0.5°C by a proportional-integral electronic controller. The reactor was fitted with a preheater tube, constructed from 2 feet of 1/8 inch outside diameter stainless steel tube. The catalyst (mean particle diameter 250μ) was packed to a depth of approximately 11 cms. between wads of glass wool. The reactor was immersed in a vigorously stirred, molten salt bath which was a stainless steel pot 12 inches in diameter by 12 inches high and was fitted with a coiled electrical heater. The composition of the eutectic

salt mixture was 53 percent potassium nitrate, 40 percent sodium nitrite and 7 percent sodium nitrite.

The pressure in the reactor was measured by a U tube manometer. The gas stream leaving the reactor passed to the gas chromatograph sample valve, via a three-way vent valve. In order to prevent condensation of reactants and products, all lines after the saturator through to the reactor exit were maintained at approximately 200°C by a hot air gun.

Initially a reactor was built with thermocouples at 0.5 inch centres along the length and at several radial locations. A number of thermocouples were also attached to the reactor wall. It was found that the maximum temperature variation between all thermocouples was less than 2°C at 100 percent orthoxylene conversion. The wall thermocouples indicated the same temperatures as those in the catalyst bed. At the same time, it was found that the silver solder, used to fix the thermocouples in the reactor, had considerable catalytic activity. Since the reactor was found to be essentially isothermal even at 100 percent conversion, it was considered appropriate to use a reactor with thermocouples at three axial locations on the tube wall. The removal of the thermocouples from the bed overcame the problem of the blank reaction and improved the flow characteristics of the packed bed. The considerable "blank" reaction found by Mann (M7) was not apparent in this study, even at temperatures near 400°C. This is consistent with the findings of Herten (H2). No measureable amounts of homogeneous reaction were found in the

range of operating conditions studied.

In order to maintain a constant activity of the catalyst, it was necessary to introduce a small amount of sulphur dioxide to the gas stream. Industrially the quantity of sulphur dioxide required, expressed as sulphur, is 0.1 to 0.2% of the weight of orthoxylene fed (D3). Froment (F2) has suggested that this value is not too critical. The patent specifications (M4) for one of the catalysts used in this study claim the use of 0.2 to 1.5 weight percent sulphur dioxide based on the orthoxylene in the feed. The specification of an amount of sulphur dioxide, based on the weight of orthoxylene fed, is probably a convenient industrial expression that has little significant since the orthoxylene concentration is normally maintained constant at around 1 percent by volume. It is more likely that it is the amount of sulphur dioxide that is required to establish an equilibrium between free sulphur trioxide in the catalyst and the sulphur trioxide in the gas stream. For this reason the amount used should not be critical.

In this study, 0.01 volume percent sulphur dioxide in the gas stream was used, this fell within the range of industrially recommended values. Since the sulphur dioxide flows were of the order of 0.01 c.c. per minute, a calibrated mixture (Matheson) containing 0.502 percent sulphur dioxide in nitrogen was used. This enabled accurate control and measurement of the sulphur dioxide flow to the reactor. The sulphur dioxide stream was mixed with the main gas stream after

the saturator and before the inlet gas sample valve. The flow of sulphur dioxide was maintained throughout the series of experiments.

When the breaks between experiments exceeded one day, low pressure air was substituted for oxygen-nitrogen mixtures to maintain the highly oxidized state of the catalyst.

Experimental Procedure

The packed bed reactor, described above, was used to make both transient and steady-state kinetic measurements on 8 catalyst samples. A description of experimental procedures follows.

A catalyst sample, generally 1.0 grams, was placed in the reactor for conditioning prior to use. Air containing 0.01 volume percent sulphur dioxide was passed over the catalyst for a period of several days. The temperature level used for conditioning varied for the different catalyst samples. In general, the temperature was 20° higher than the maximum level contemplated in the experimental design.

An oxygen/nitrogen mixture containing the desired oxygen concentration was passed through the reactor. The saturator had been flushed with an oxygen/nitrogen mixture of this composition at the completion of the previous run to ensure that when the gas was first switched to the reactor it was at the desired composition. O-xylene was then introduced to the gas stream. In order to study the unsteady state performance of the catalyst, the reaction gases were sampled at

various on-stream times until steady-state behaviour had been achieved. It was assumed that steady-state was reached when three samples, taken at 45 minute intervals, had compositions that differed by less than 5 percent. The time required to reach steady-state was from one half to twenty four hours, depending upon the catalyst being studied. The initial rate was generally measured after 30 seconds on stream. However, in some cases many measurements of reaction rates were made in the period from 3 to 300 seconds. In these cases, the xylene flow was ceased immediately after sampling the reaction gases, in order to reoxidize the catalyst. That is, hydrocarbon oxidation took place for several seconds, followed by at least 45 minutes of reoxidation of the catalyst. Following the steady-state experiments, the gas composition was changed to that required for the next experiment. At this time the orthoxylene flow was stopped and reoxidation of the catalyst took place. The period of reoxidation following steady-state operation, was generally in excess of 12 hours.

Experimental Programme

A comprehensive investigation of a large number of catalysts was undertaken. This was required as a result of the lack of knowledge of the performance of different types of oxidation catalysts.

It was originally intended that only one catalyst, Aero PAA fluid bed catalyst from American Cyanamid, would be studied. However, after experiments had been conducted over

a wide range of operating conditions, at temperatures from 320 to 500°C, it was concluded that the catalyst had extremely poor selectivity for phthalic anhydride formation. In addition, considerable overoxidation and tar formation occurred. It was therefore decided that several other industrial catalysts should be investigated.

In all, 8 catalysts were studied. In some cases the investigation was limited to two or three experimental conditions since the catalysts showed adverse characteristics, such as considerable formation of tars, and these fouled the reactor and gas chromatograph.

In the case of catalysts which did not produce significant amounts of tars or overoxidized products, basic experimental designs were used to plan the experiments. In general, a one half fraction of the 2^4 factorial design (B10, B11) was used. This design was chosen so that the operating variables, temperature, orthoxylene concentration, oxygen concentration, and contact time, could be studied in an efficient manner. In addition, at least four centre point replicates were made in order to investigate the stability of catalyst activity. All experiments were randomized.

In the case of the 902 fluidization catalyst, finally chosen for use in the transported bed, a complete 2 level factorial design (B10) was conducted. Eight centre point experiments were also made to monitor catalyst activity. In addition, replication of another four operating conditions was conducted so that variance estimates could be made over a wide range of conversions.

Chapter 4 describes the results of unsteady-state experiments conducted according to the procedures described above. In addition, the importance of sulphur dioxide addition to the feedstream is discussed in some detail. In Chapter 5 the steady-state performance of several oxidation catalysts is reported.

CHAPTER 4

CHANGES IN CATALYST ACTIVITY

Mann (M7), in a comprehensive literature review of hydrocarbon oxidations on vanadia catalysts, cites a number of studies in which catalyst activity changes have occurred. Two types of decay have been reported. One is a short-term effect covering the initial unsteady-state operation of the catalyst and generally continues for a period of 1/2 to 2 hours after start-up. The other is a long-term deactivation which is characterized by a decrease in activity over the first 100 to 200 days of operation.

The significance of the unsteady-state operation of these catalysts has not been understood in other studies. This chapter provides experimental evidence that suggests that the initial activity of a highly oxidized vanadia catalyst is up to 50 times greater than the steady-state activity. These results support the concepts embodied in the Redox and S.S.A.M. mechanisms described in Chapter 2.

Long-term decay is generally considered to be caused by a loss of sulphur trioxide from the catalyst. However, no adequate explanation has been given to describe the part SO_3 plays in affecting catalyst activity. Section 4.2 discusses the theories put forward by a Japanese group that has made a comprehensive study (K1, M3) of the effect of

sulphur trioxide in the catalyst on the catalyst activity and selectivity of the O-xylene oxidation reaction. Experimental evidence of catalyst decay is presented to aid these discussions.

4.1. Initial Deactivation - Approach of Catalyst to Steady-State Behaviour

4.1.1 Background

The basic premise of the steady-state mechanisms, that hydrocarbon oxidations take place using oxygen contained within the catalyst, suggests that high initial rates of reaction should be possible on freshly oxidized catalysts. The oxidation is considered to be first order with respect to hydrocarbon concentration and is given by

$$r_r = k_r C_r \theta \qquad 2.7.$$

where θ is the number of active sites available for steady-state hydrocarbon oxidation, and is given by

$$\theta = \frac{1}{1 + \left(\frac{n\, k_r C_r}{k_a C_a}\right)} \qquad 2.10$$

A freshly oxidized catalyst can be considered to have a value of θ close to unity. The value of θ in the steady state will depend on the relative values of k_r and k_a. The data of Mann (M7) and Juusola (J4) suggest that θ takes a value of the order of 0.1 or 0.2. Therefore, a tenfold increase in rate may be attainable in initial operation of the catalyst.

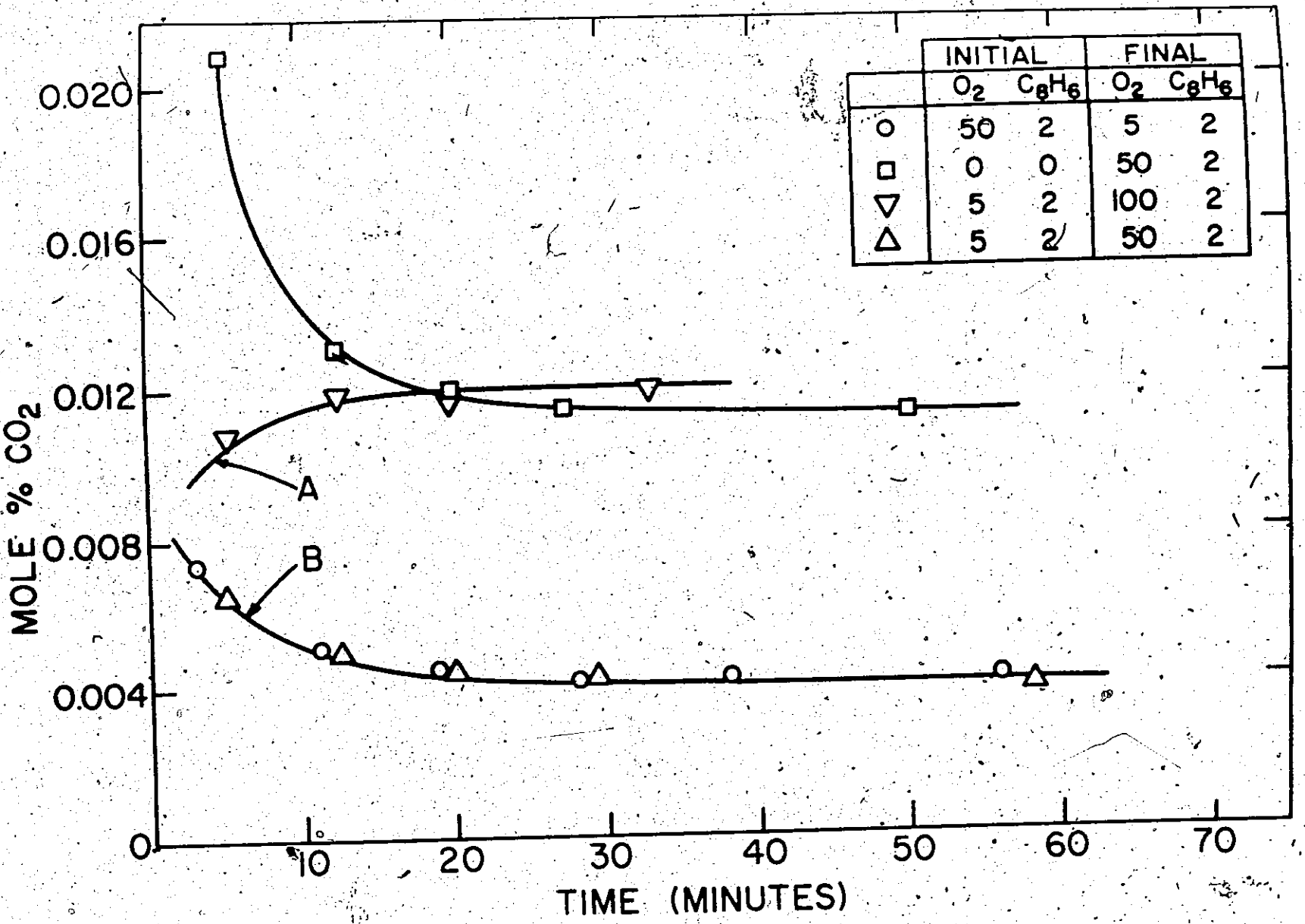

Figure 4.1. Approach to Steady-State Operation of Packed Bed (from (J4)).

Juusola (J4) has indicated that, after changes in operating conditions, there is a change in catalyst activity. Figure 4.1 has been extracted from his thesis to aid the discussion. He has monitored the CO_2 level in the exit stream at 7 minute intervals, in order to determine steady-state operation. It is obvious from his data that a catalyst which has not been previously reacted has high initial activity. The data also show that a change from a high oxygen level in the feed gas to a lower value produces a similar decay. When the oxygen concentration is changed from a lower to high value (curve A), the rate increases to a steady-state value. Curve B contradicts the result shown in A. However, the overall trend is apparent.

Froment (F2) found similar unsteady-state behaviour. In his studies a period of several hours was necessary to establish steady-state operation of the catalyst following changes in reaction conditions.

Ross (R2) has observed similar deactivation in a study of naphthalene oxidation on vanadia. He attributed high initial rates of reaction to reoxidation which resulted from his shut down procedure in which he allowed the catalyst to cool slowly in air with no naphthalene present.

4.1.2. Results and Discussion

High initial rates of reaction have been found for all catalysts used in this research. The data presented in this section are for only two types of catalyst, namely the 902

silica-gel supported catalyst and the titania-supported catalyst. The differences between the selectivities and other properties of these catalysts will be described in Chapter 5 when the influence of catalyst support is discussed.

The data presented in this section are typical of the results obtained for a large number of experiments. The approach of the catalyst to steady-state operation was monitored during all experiments. In many this was done simply by measuring the product composition after the catalyst had been on-stream for a period of 30 seconds.

The procedure for the packed bed experimentation has been described in Chapter 3. The selectivity and conversion data presented in this section were generated by the following procedures:

1. An orthoxylene/oxygen/nitrogen/SO_2 mixture was fed to a catalyst which had been oxidized overnight with a gas mixture of the same composition but which contained no O-xylene.

2. At a given time the product gases were sampled, the on-stream time (order of seconds) was noted, and the orthoxylene flow was discontinued.

3. During the analysis period, the catalyst was reoxidized. This oxidation was continued for a period of approximately 1 hour and procedures 1. and 2. were repeated for a different on-stream time.

4. Data were generally gathered in the above manner for times-on-stream up to 2 to 5 minutes; after this period the orthoxylene feed was continuous and steady-state measurements

were made.

The 902 catalyst is the one which was chosen for use in the transported bed reactor. It was found to achieve steady-state operation after approximately 30 minutes on-stream. This is in agreement with the work of Juusola for a similar catalyst. In the present case, the approach to steady-state operation was monitored at several times in the period from 10 to 600 seconds. Figure 4.2 shows the change in conversion during that period. It can be seen that a 40 fold decrease in rate occurred during that period.

It was not possible to obtain data for contact times below 10 seconds on this catalyst. At shorter times carbon balances were less than 90 percent and this was considered to result from some of the hydrocarbon being retained by adsorption on the catalyst, that is, equilibrium adsorption of xylene on the catalyst surface was not achieved with these short on-stream times. It is likely that this highly porous catalyst would cause a chromatographic-type adsorption process to occur in the bed of particles. The time on-stream was considered to be the time interval between introduction of xylene to the gas stream and sampling the exit gases at the chromatograph. The dead volume in the system was of the order of several cubic centimetres so that assuming the reaction gases were in plug flow, the actual contact times may have been from one to four seconds less than those indicated, depending on the gas flows used. This would serve to move the curves in Figure 4.2 slightly towards the ordinate. It does not, however, affect

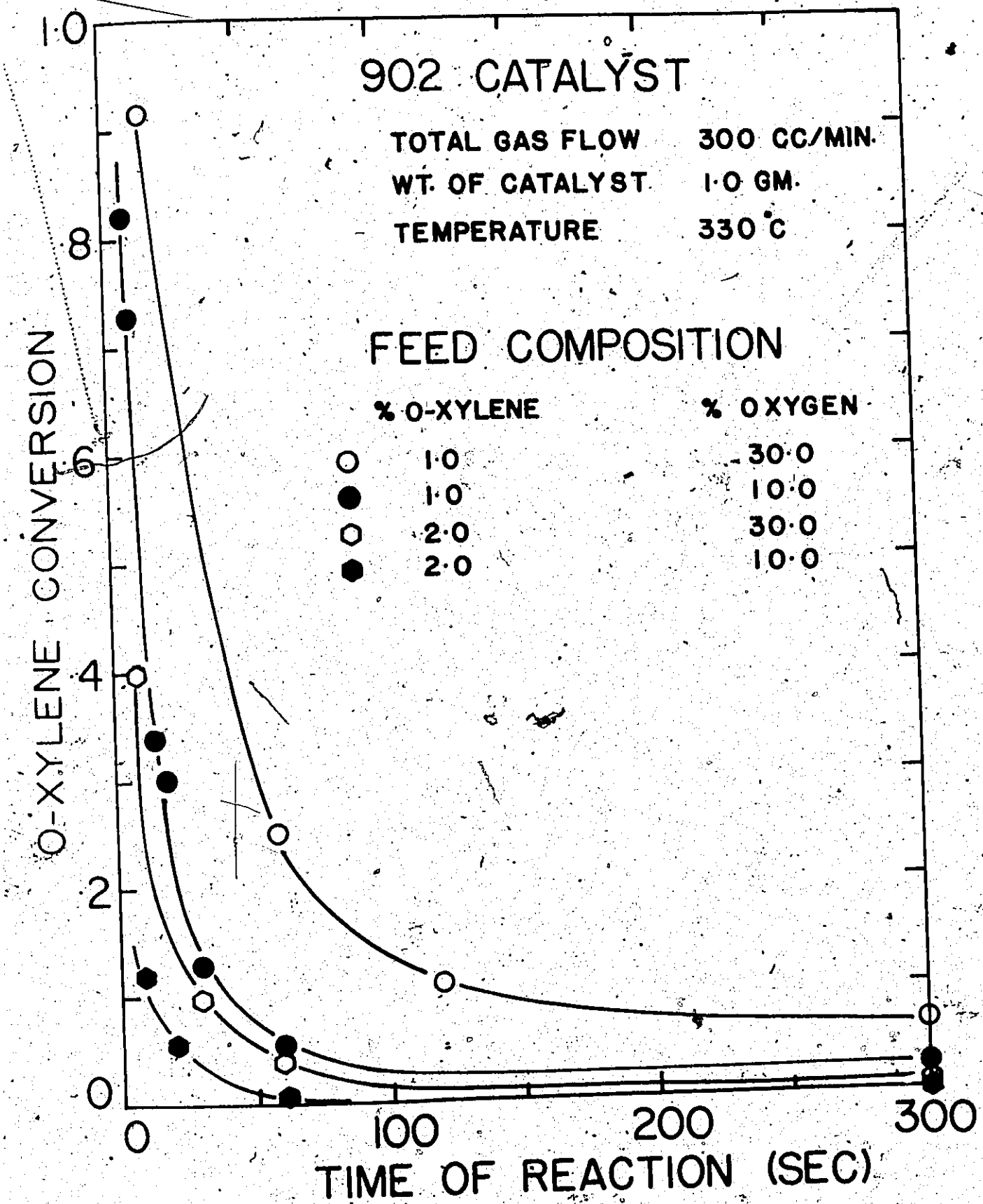

Figure 4.2. Approach to Steady-State Operation of Packed Bed.

the overall trend in the results.

One of the main difficulties in the experimental programme was caused by trying to obtain both unsteady-state and steady-state data from the same experiment. It was necessary to have at least 2 or 3 percent conversion in the steady-state in order to accurately determine the gas composition. Therefore, the conversions shown in Figure 4.2 would extrapolate to values greater than 100 percent at zero time. This, of course, is not possible. Despite this problem, Figure 4.2 shows that 40 fold changes in activity occur between 8 and 300 seconds. One might therefore envisage rates at 1 second contact that are of the order of 100 times greater than those at 5 minutes contact. The catalyst is characterized by high initial rates of reaction and a fast approach to steady-state operation.

The result for the titania-supported catalyst is shown in Figure 4.3. This catalyst shows a slower approach to steady-state operation. This condition was obtained only after almost 24 hours on-stream time. Froment (F2) has found that a similar catalyst required several hours to achieve stable operation following changes in operating conditions.

The titania-supported catalyst differed from the 902 catalyst in that adequate carbon balances were obtained after between 3 and 5 seconds on-stream. The low surface area of this catalyst (5 m^2/gm.) compared with the value of 40 m^2/gm. for the 902 catalyst suggests that adsorption equilibrium is quickly established. The data also show that the

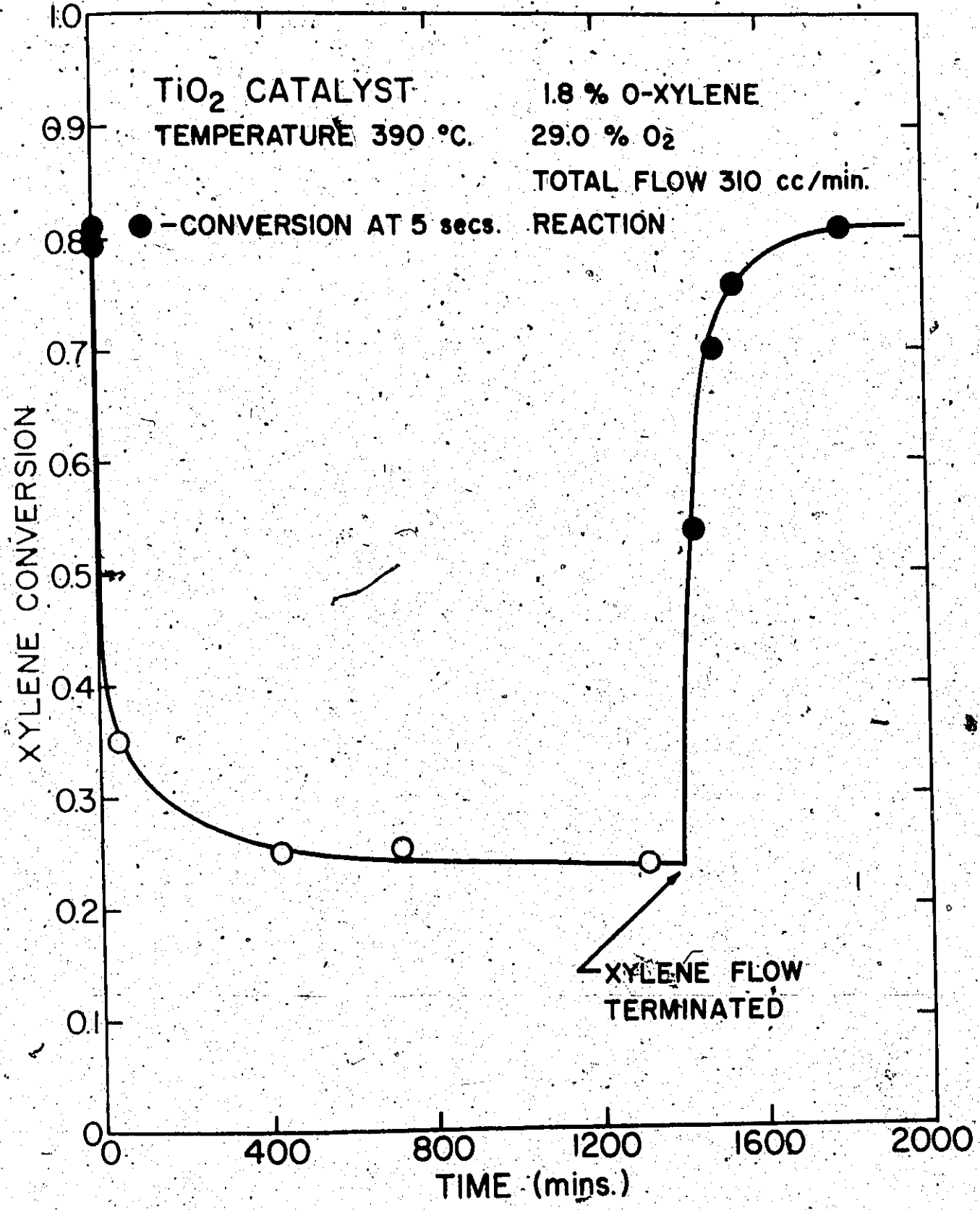

Figure 4.3. Reoxidation of Reduced Catalyst.

initial conversions are only 3 or 4 times greater than the steady-state values. It is obvious that another basic difference exists between the two types of catalyst in unsteady-state operations. These differences will be discussed in Chapter 5 when the effect of catalyst support material is further discussed.

Figure 4.3 shows the TiO_2 catalyst performance in the approach to the steady-state. When this condition had been reached, the xylene feed was discontinued and the catalyst was able to be reoxidized without the competition of hydrocarbon oxidation. The reactivity of the catalyst was measured at various times during this reoxidation process by determining the conversion at 5 second contact times. The catalyst was therefore subjected to orthoxylene oxidation for only a few seconds in the reoxidation period of about 7 hours. Figure 4.3 shows that the initial activity was restored after 6 hours operation. Therefore, for the same set of operating conditions, reduction of the oxidation state of the catalyst can be completely reversed.

The early literature contained two conflicting points of view concerning the action of oxygen contained within the catalyst. More recently, it is generally agreed that the catalyst oxygen is used to oxidize the hydrocarbon. Vrbaski (V2) has studied the oxidation of O-tolualdehyde in a nitrogen stream and has monitored carbon dioxide in the exit gases. He has shown that oxidation of the hydrocarbon does occur under such conditions. However, the study did not determine if

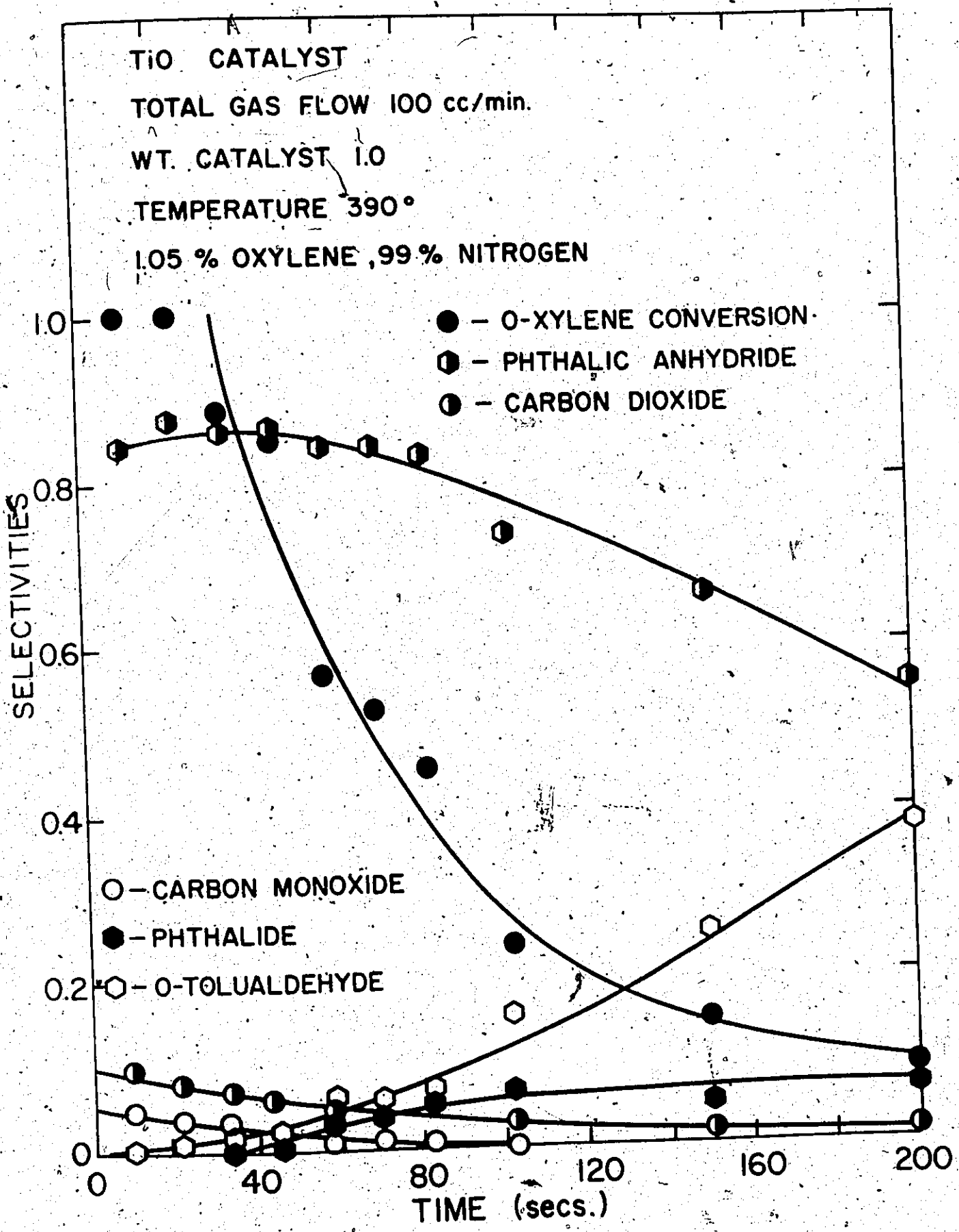

Figure 4.4. Reaction without Oxygen in the Feed.

normal selectivities could be obtained under such conditions.

The development of the chromatographic technique described in Chapter 3, enables the determination of conversions and selectivities of all components from a single gas sample. Therefore, in this study, it was possible to obtain a complete analysis of catalyst behaviour when orthoxylene was oxidized in a nitrogen stream. The results are shown in Figure 4.4. The experiments were conducted by using a catalyst sample which had been oxidized in air for several days. The system was purged with nitrogen for several hours to remove oxygen from the system. The gas leaving the reactor was monitored by the gas chromatograph to ensure that nitrogen was the only significant component present. Orthoxylene was then introduced to the nitrogen stream. The xylene flow was continued for 12 seconds. The exit gases were then sampled and nitrogen was passed over the catalyst sample until the process was repeated 45 minutes later.

The results in Figure 4.4 show that the catalyst has high initial activity and selectivity. Selectivities to phthalic anhydride were initially 85 mole percent. This is identical with the value obtained when oxygen is present in the reaction gases. The actual activity of the catalyst cannot be compared with that for the similar conditions when oxygen is present because in both cases the initial conversions were one hundred percent. However, the high activity does suggest that initial rates may be the same regardless of the oxygen level in the reaction gases. Reference to Figure 4.2 further supports

this view. The curves for 10 and 30 percent oxygen in the feed stream tend to be converging at very short contact times. Unfortunately shorter contact would have produced one hundred percent conversion under the conditions studied.

4.1.3. Conclusions and Recommendations

The data presented above are typical of the results obtained for initial rate studies on all catalysts used. Keeping in mind that the major objective of this research was to study orthoxylene in a transported bed reactor, it was not possible to develop these ideas further. However, the results have provided considerable support for the S.S.A.M. and Redox mechanisms. The high initial rates and the approach to steady-state operation agree with the concept of θ changing from unity to a steady-state θ value. The theory that oxygen from the catalyst takes place in the hydrocarbon oxidation has been confirmed by the fact that standard initial rates and selectivities obtained when xylene is fed with nitrogen are similar to those obtained when oxygen is present in the feed. The concept of a competing reoxidation of the reduced catalyst has been verified by reoxidizing the catalyst under conditions such that there is no competition from hydrocarbon oxidation.

The results have shown that reaction rates at different oxygen levels may converge to the same value at zero contact time. Further experiments should be conducted under conditions where such a phenomenon can be more fully investigated. Reference to Figure 4.3 suggests that this can be readily

accomplished. In this way it should be possible to evaluate rates of reaction at zero time when θ assumes a value of unity. The values of the rate constants for the various oxidation steps could then be evaluated independent of the evaluation of the rate constant for the oxidation of the reduced catalyst. Steady-state data should then provide an evaluation of k_a and hence the steady-state θ values. This would reduce the high degree of correlation which exists between reaction rate constants and k_a which are evaluated by parameter estimation from steady-state data.

The above discussion assumes that each catalyst site has the same activity irrespective of the activity of its nearest neighbour and further that if the catalyst is deoxidized to say V_2O_4 that this site will have no effect on the oxidation process. The observation in other studies that selectivities change significantly with oxidation state indicates that these points may be important. Another point to be considered is the possibility that different types of chemisorbed oxygen may exist depending on the oxidation state of the catalyst and also depending on whether or not hydrocarbon molecules are adsorbed to the catalyst surface.

It is further suggested in Figure 4.3 that, by running a catalyst to steady-state and then reoxidizing the catalyst, the rate of reoxidation of a reduced catalyst can be determined. By conducting such a series of experiments as well as the initial rate studies described above, it should be possible to have independent estimates of the rate constants of both steps

in the Redox and S.S.A.M. mechanisms.

4.2. Long Term Deactivation - The Role of SO_3 in K_2SO_4 Promoted Catalysts

4.2.1. Background

It should be noted that translations of the 4 Japanese papers (K1, K4, M3, S3) were obtained late in the research programme. The information on catalyst performance derived from these papers would have been invaluable for planning our research. In particular, a better understanding of the role sulphur trioxide plays in these catalysts, would have circumvented some of the long-term catalyst deactivation apparent in our work. Because of the fundamental importance of this aspect of the work, this section includes some of the data of the Japanese workers along with those of Juusola (J4), in order that a better understanding of the phenomenon can be achieved.

Long-term decay effects have been apparent in a number of studies in hydrocarbon oxidations (J2, J4, M7). Juusola (J4), at the completion of his research programme, realised the importance of SO_3 to catalyst performance. He analyzed a sample of catalyst that had been used to oxidize O-tolualdehyde. By comparing the result with that obtained for an unused sample of the same catalyst, he found a 20 percent loss of SO_3 in the reacted catalyst. He therefore concluded that the changes in catalyst activity and selectivity were attributable to this source.

In evaluating the effect of different support materials in the oxidation of naphthalene on vanadia catalysts, Kakinoki (K1) found remarkable differences between the rates and selectivities obtained using pure naphthalene or hot-press naphthalene containing significant amounts of sulphur impurities. The activity changes with time were similar for silica-gel, titania and gypsum-supported catalysts. The discussion which follows describes the results obtained for the silica-supported catalyst since it is most relevant to the current study.

When hot press naphthalene was employed as feedstock, there was no change in activity after 180 days on stream at a reactor temperature of 385°C. However, when pure naphthalene was fed to a sample of the same catalyst under the same reaction conditions, the phthalic anhydride yield gradually decreased. From 80 days to 160 days the decrease was from 98 to 83 percent. Having noted this difference in product distribution, the authors concluded that the sulphur content of the feedstock was important to the catalyst performance.

In order to determine if this deactivation is reversible, the authors introduced sulphur dioxide to the feed stream such that the SO_2 level was 25 percent based on the weight of naphthalene fed. Under these conditions the original activity was restored in 5 hours. The SO_2 flow was discontinued and the recovered activity was maintained for 3 days, after which the decay occurred again.

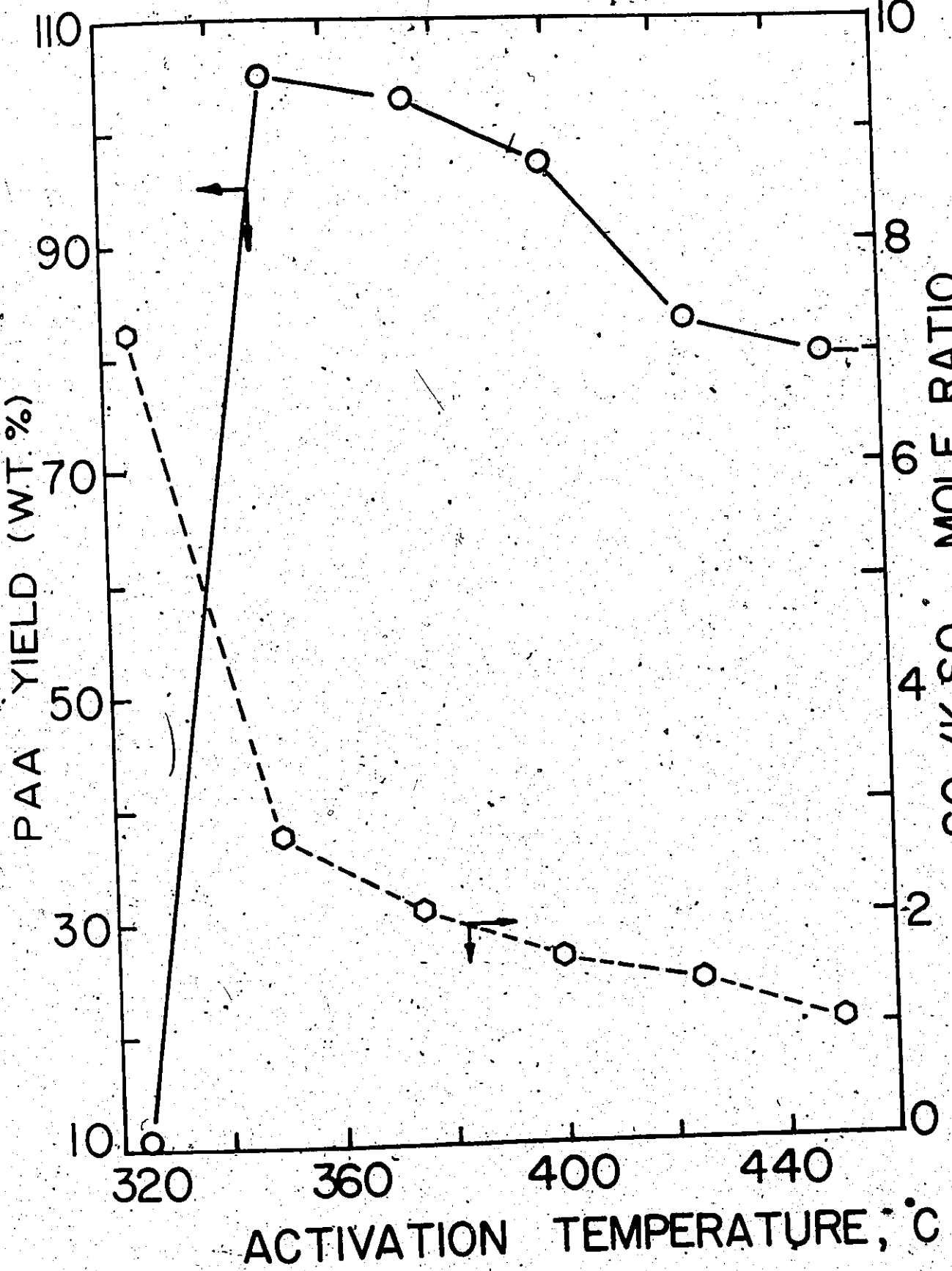

Figure 4.5. Influence of Activation Temperature on Catalyst Activity (from (K1)).

At bed temperatures of 410 and 435°C under hot press naphthalene feedstock, deactivation similar to that obtained with pure naphthalene at 385°, was noted. The rate of decay was much greater at 435°C then at 410°C. After 100 days on-stream, yields of phthalic anhydride had dropped from 105 weight percent to 87 and 74 percent for operation at 410°C and 435°C respectively. At this stage the SO_2 treatment, described above, was found to restore the activities so that phthalic anhydride yields of 98 percent were obtained.

The differences in activities obtained when hot press naphthalene was oxidized at different temperatures, led the authors to the conclusion that SO_2 contained within the catalyst is "evaporated" when the temperature was increased. It is apparent that the sulphur contained in the impure feed-stock was insufficient to provide enough SO_3 to replace that lost by evaporation. In order to investigate this effect more fully, they subjected a TiO_2-supported catalyst to heat treatment at different temperatures for a period of 10 hours. Following this pretreatment the catalysts were used to oxidize purified naphthalene in air. The results are summarized in Figure 4.5. Catalyst samples were analyzed for their free SO_3 content. Figure 4.5 shows that a low pretreatment temperature produces a catalyst of high SO_3 content and low activity. Higher heat treatment temperatures reduced the SO_3 levels in the catalyst by decomposition. The phthalic anhydride yield went through a maximum for heat treatment temperatures around 350°C, corresponding to a mole ratio of SO_3/K_2SO_4 of 2.77. It is

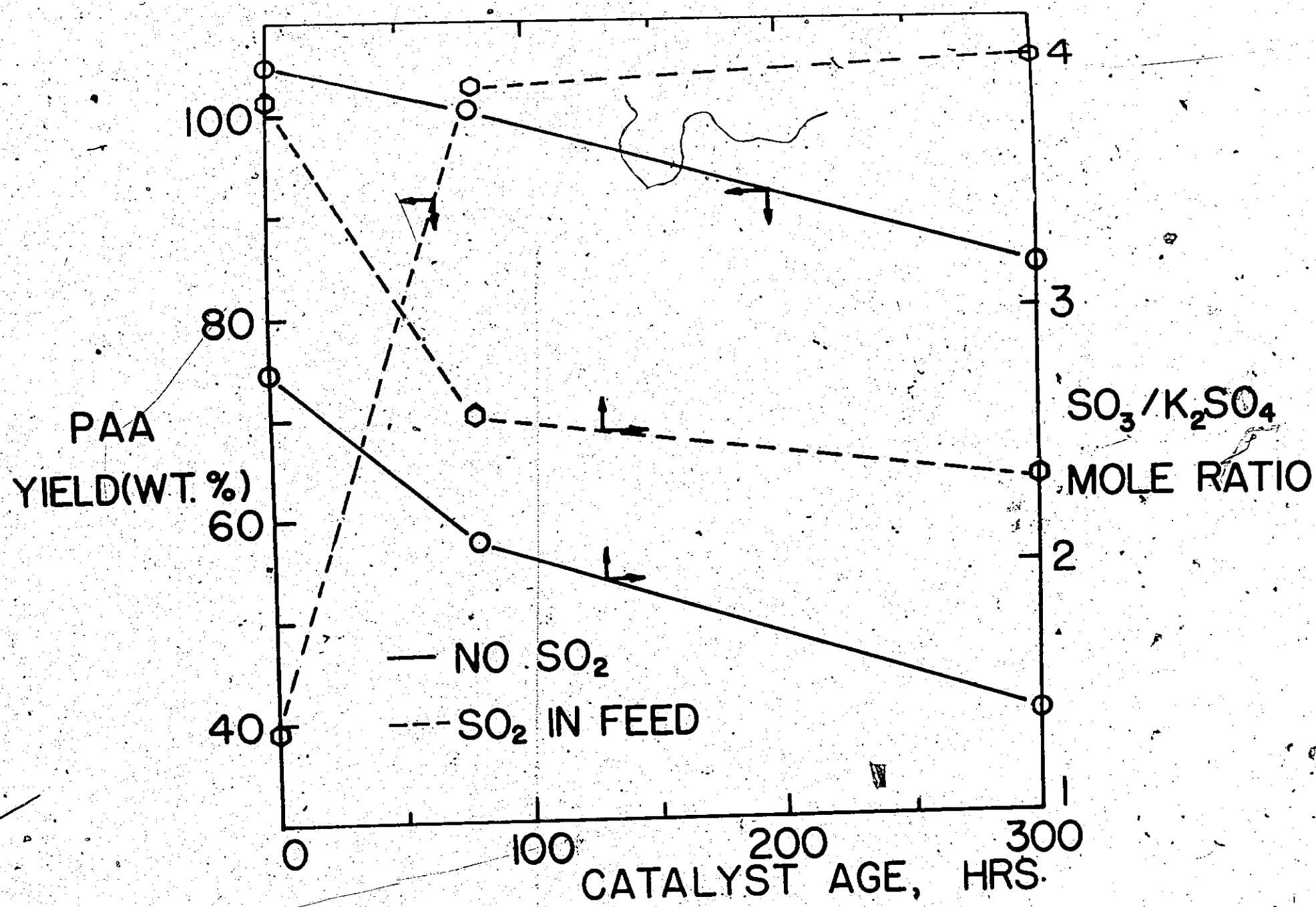

Figure 4.6. Effect of Treating Catalysts with SO_2 (from (K1)).

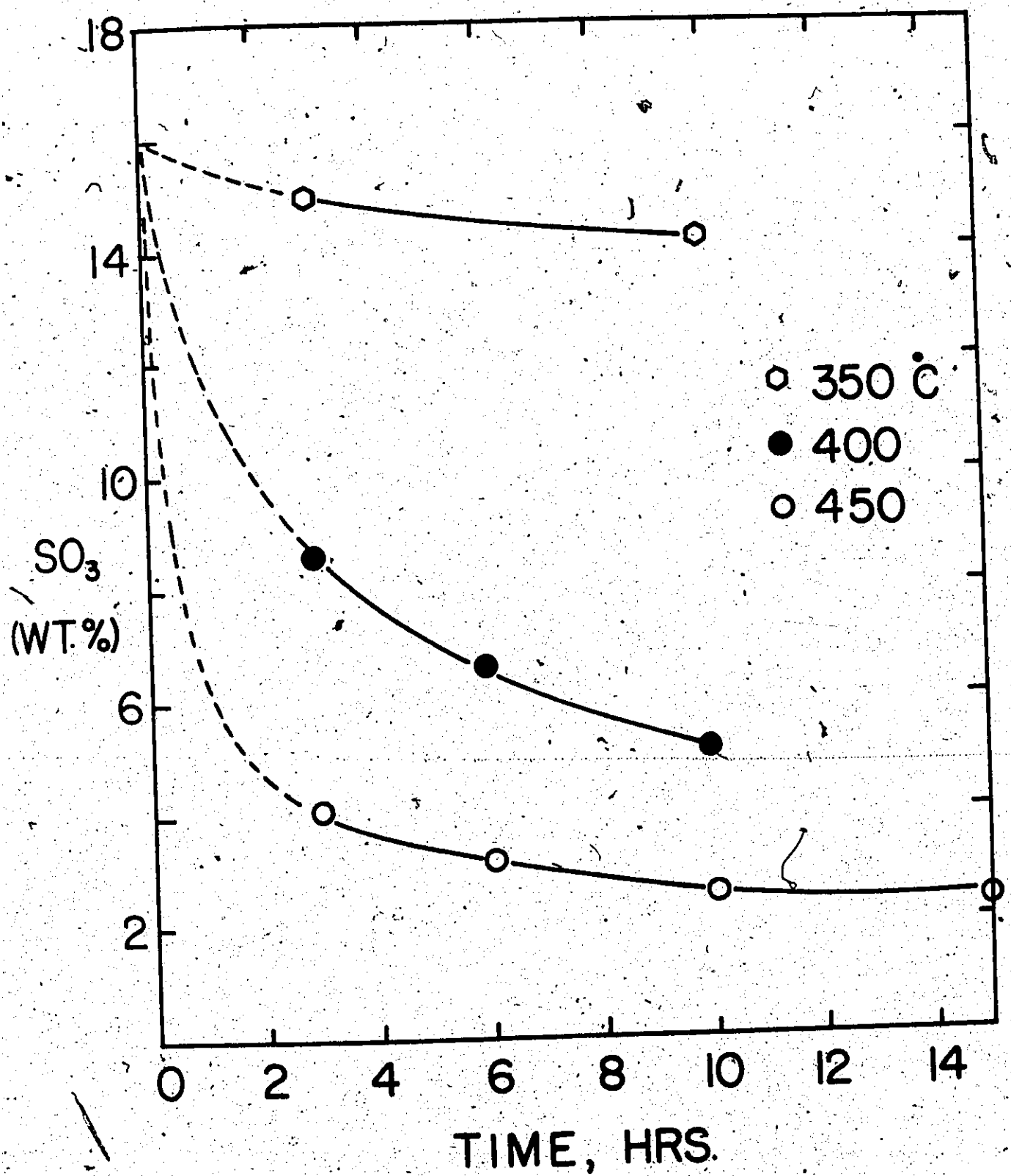

Figure 4.7. Effect of Heat Treatment on SO_3 Content of Catalysts (from (M3)).

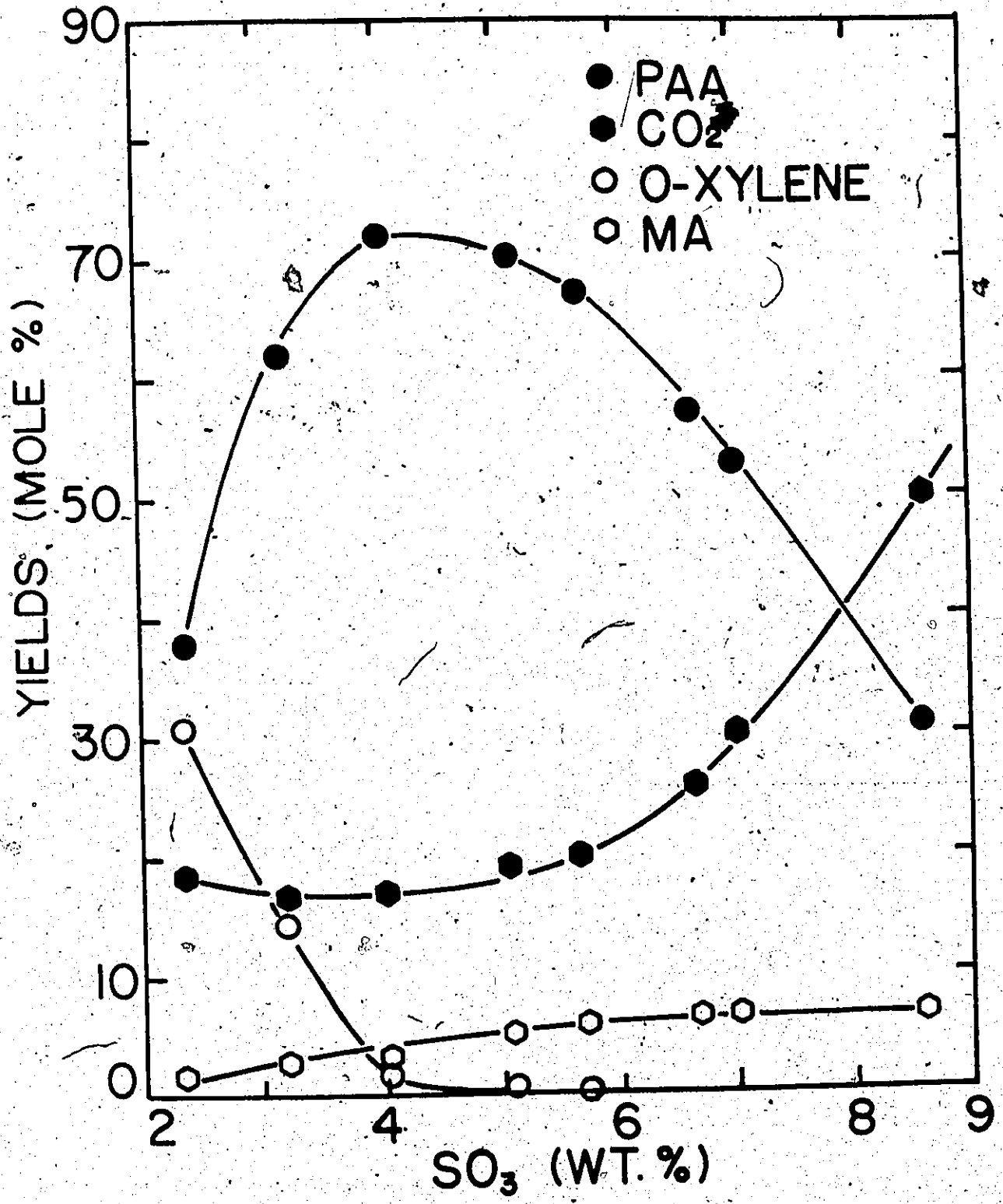

Figure 4.8. Influence of SO_3 Content on Reaction Yields, (from (M3)).

apparent from their data that there is an optimal SO_3 level for the catalyst.

The effect of SO_2 treatment on the SO_3 level in the catalyst was investigated by treating catalyst samples having on-stream times of 0, 80 and 300 hours, with SO_2/air mixtures for 5 hours. The SO_2 level was approximately 0.5 volume percent, the same as that used when naphthalene was oxidized. Samples of catalyst with and without SO_2 treatment were analyzed for SO_3 content. They were then used to oxidize naphthalene. The results, presented in Tables 1 and 2 in their paper, are summarized in Figure 4.6. It is apparent that treatment with SO_2 causes an increase in SO_3 level in the catalyst. This may or may not be beneficial depending on the SO_3 level.

In a further study (M3), the Japanese group have investigated the role that free SO_3 plays in the oxidation of orthoxylene on titania-supported catalysts. In particular, they have investigated the effect of potassium sulphate and free SO_3 levels on reaction selectivity. It was found that a catalyst containing 0.5 moles of K_2SO_4 per mole of V_2O_5 was optimal. The effect of free SO_3 level was determined for catalyst having this composition. Different SO_3 levels were achieved by heat treatment of the catalyst. Figure 4.7 summarizes the data presented in table 2 in the paper. Catalysts having SO_3 levels from approximately 2 to 9 weight percent were used to oxidize orthoxylene. No SO_2 was added to the reaction gases. Figure 4.8 shows the effect of SO_3 content on catalyst performance. Low SO_3 levels produced a catalyst of low

activity whereas high levels produced a highly active catalyst that produced significant amounts of overoxidation.

4.2.2. Results and Discussion

It is apparent from the research described in the preceding section, that catalyst deactivation is closely related to both the temperature and time of heat treatment. This section describes how these conditions influenced the results of this investigation. Centre-point experiments were carried out randomly throughout this entire investigation in order to monitor catalyst activity. The data presented represent the centre point experiments for some of these catalysts. It should be noted that, unlike in the Japanese studies, sulphur dioxide was fed to the catalysts at all times during their use.

Figure 4.9 represents the centre-point data for three of the catalysts investigated in this study. The data for the 902 catalyst show a gradual decay similar to that reported by other workers. The high activity noted at 19 days does not appear to be part of the general trend. A slight decay is apparent for the TiO_2 catalyst over a period of 20 days. In the case of the original 902 catalyst, there appears to be no trend towards deactivation in that period.

Two different 902 catalysts were used in the current study. The differences in reactivities of these catalysts will be discussed in Chapter 5. The catalyst referred to as the original 902 catalyst was used for preliminary testing before a large quantity was purchased for use in the transported bed reactor. Apart from the difference in reaction temperature

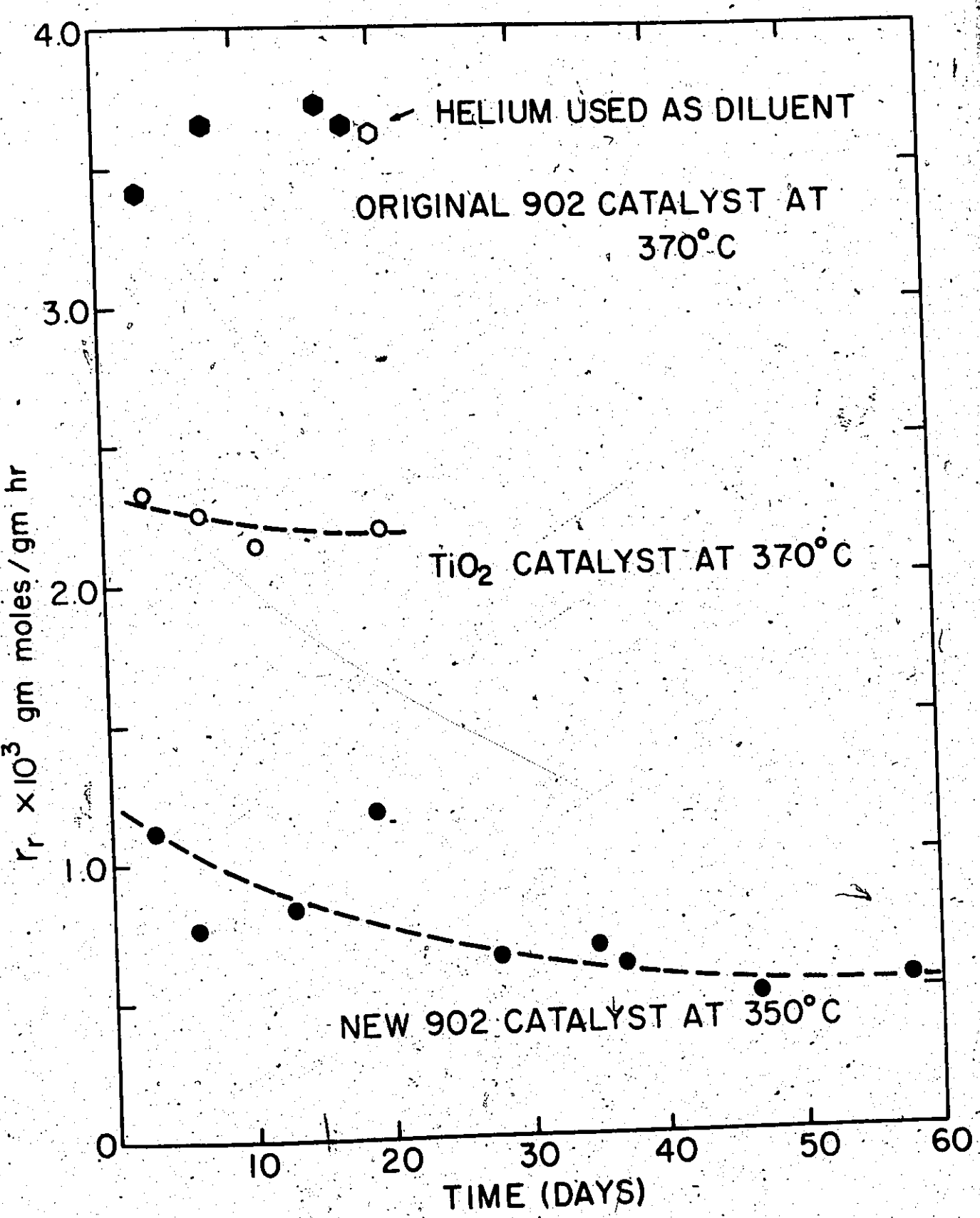

Figure 4.9. Catalyst Decay Phenomena.

used in the two 902 catalyst studies, there were differences in heat treatment procedures. In the case of the original catalyst, heat treatment was conducted at 410°C for a period of 3 days. A temperature of 390°C was maintained for approximately 36 hours for the new catalyst.

In order to obtain the temperature dependency of reaction on the TiO_2 catalyst, several experiments were conducted after the basic experimental design had been completed. These experiments were conducted in an increasing temperature sequence as shown in Figure 4.10. The reactor was held at each temperature level for a 24 hour period before the product composition was determined. Following an experiment at 400°C the temperature was lowered to 380°C. As can be seen from Figure 4.10, there appears to be no temperature dependency at 370, 390 and 400°C. The rate at 380°C is less than 60% of the value at 370°C.

A von Heyden WO catalyst (believed to be supported on TiO_2) was used to oxidize orthoxylene in the temperature range 350 to 460°C following the completion of a partial factorial design. The main reason for this higher temperature study was to investigate selectivity changes on a commercial phthalic anhydride producing catalyst at conditions similar to those for an industrial reactor. The experiments were conducted in an increasing temperature sequence to 460°C. The period of operation at each temperature level was determined by the analysis. Therefore, the temperature range 370-460°C was covered in less than 10 hours. When the centre point of the original experimental design was repeated, it was found that the

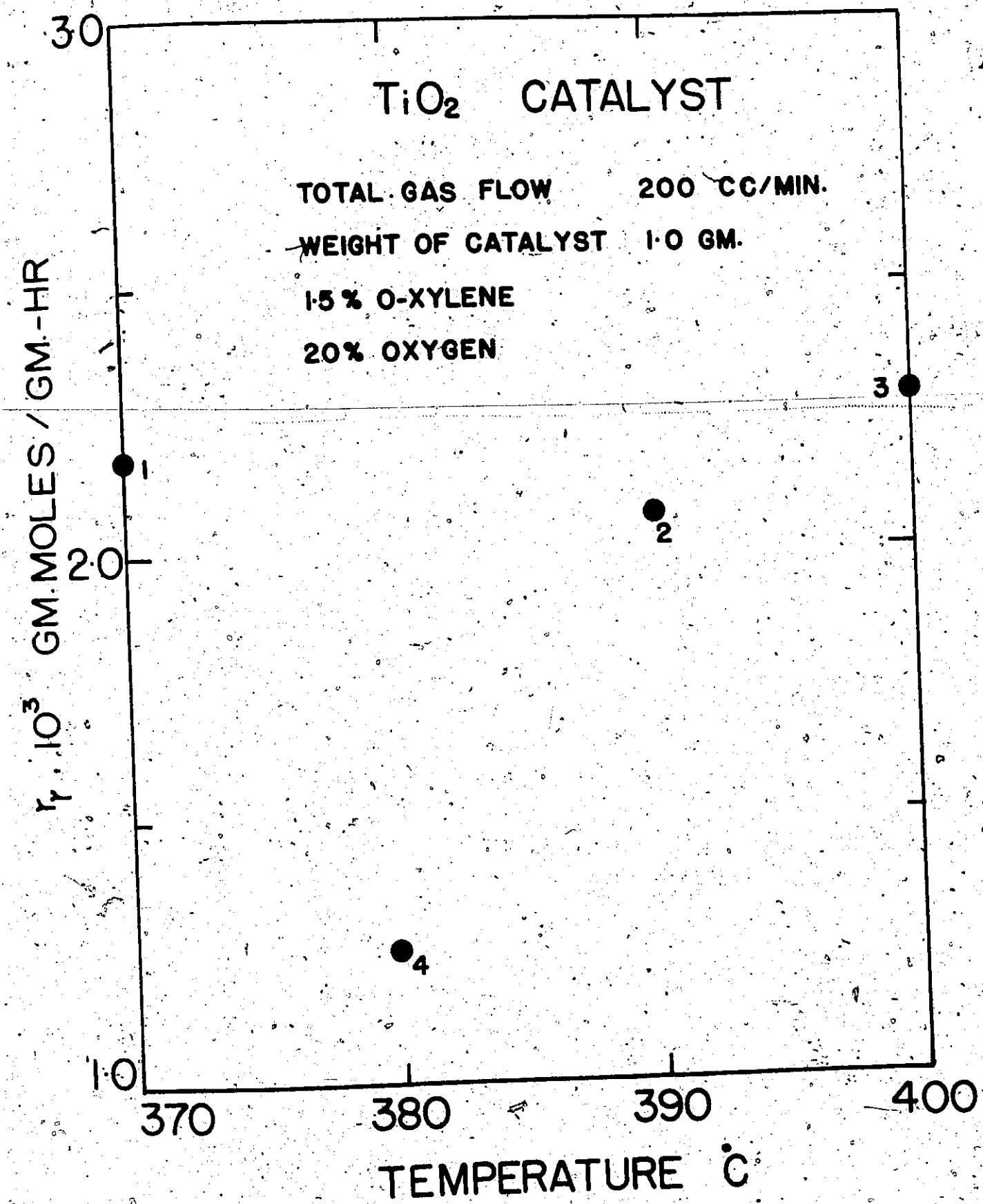

Figure 4.10. Thermal Deactivation of Catalyst.

catalyst activity had been reduced by 50%. This activity was not restored by oxidation of the catalyst with air containing 0.01 volume percent SO_2 over a period of several days.

Herten (H2) has found a decreased activity when oxidizing orthoxylene near 400°C. He has considered the departure from the Arrhenius dependency to be due to mass transfer effects. It is more likely that he has deactivated his catalyst by reacting at this higher temperature.

No specific experiments were conducted to determine the cause of long-term catalyst deactivation. The data described above were obtained from experiments designed solely to monitor activity. However, it is important that these results along with those of other workers are discussed here in order that future studies will take steps to remove or minimize this effect.

The importance of SO_3 level in determining catalyst activity has been demonstrated by Kakinoki (K1). It is seen in Figure 4.8 that the yield of phthalic anhydride passes through a maximum with SO_3 level in the catalyst. However, these results are a little misleading and reveal a major weakness in the Japanese studies. It is noted in Figure 4.8 that at the time that the maximum phthalic anhydride yield is achieved, the orthoxylene conversion is approximately 100 percent. At higher SO_3 levels the o-xylene conversion is always 100 percent and the phthalic anhydride yield is reduced. It is possible that SO_3 levels higher than the optimum value of

figure 4.8. have produced more active catalysts which completely oxidize the orthoxylene near the entrance of the bed and then oxidize phthalic anhydride in the rest of the bed. Considering the dramatic change in o-xylene conversion obtained with catalysts containing 2.3, 3.2 and 4% SO_3, such an explanation seems most reasonable. The use of reactors giving 100 percent conversion of o-xylene has similarly weakened a number of other postulates put forward by these researchers. Nevertheless, they have provided evidence to suggest that an increased SO_3 level does produce an increased activity.

The major difficulty in conducting research on these catalysts would appear to be the ability to maintain the SO_3 level in the catalyst at a constant value. The changes in activity in our studies do not appear to be as great as those of many other workers. This is probably because we have endeavoured to replenish the SO_3 by feeding SO_2 to the reactor at all times. The SO_2 level was always maintained near 0.01 volume percent on the recommendation of Froment (F2). However, it is highly likely that his advice, that the amount of SO_2 fed is not too critical, is not correct. One only has to consider the processes involved in restoring the SO_3 to the catalyst, to realize this fact. Firstly, SO_2 oxidation on vanadia catalysts is very slow below 400°C. In addition, the rate of oxidation is dependent upon the SO_2 concentration in the feed stream. There is also the fact that each SO_2 molecule is competing with 100 o-xylene molecules for oxidation by the vanadia. Therefore the likelihood that a single SO_2 level is

adequate for all reaction conditions is highly unlikely. One is further led to speculate that a particular industrial practice (F2) in which much higher SO_2 levels are fed to the reactor periodically, may be more effective than the use of low concentrations fed continuously. The ability to restore lost activity by treatment with 0.5 volume % SO_2 (K1), whereas 0.01% was found ineffectual in this study, also suggests that the SO_2 level is most important.

Further evidence that the SO_2 concentration required to maintain activity changes with reaction conditions is evident from the work of Kakinoki (K1). Hot press naphthalene, which typically contains 0.3 - 0.7 weight percent sulphur (S7), was oxidized without decay at bed temperature of 385°C. However, operation at higher temperatures produced decay which was reversed by treatment with 0.5 weight percent SO_2. It is apparent that the sulphur present in the crude naphthalene was not adequate to restore the SO_3 lost by thermal decomposition. The relative rates of decomposition and SO_3 production appear to determine the catalyst activity.

The role of K_2SO_4 in these catalysts appears to be as a carrier of SO_3. Various patents suggest that an optimum SO_3 to K_2O molar ratio is approximately 2. The SO_3 and K_2SO_4 are thought to exist in the form of potassium pyrosulphate. No data on the decomposition of potassium pyrosulphate was found in standard treatises of inorganic chemistry. However, it has been noted that elevated temperatures do result in a decomposition to potassium sulphate and SO_3. Mellor (M8) notes

that various workers have determined the melting point to be 210, 300 and 414°C. In addition, a melt of this system $K_2S_2O_7 \cdot H_2O$-$K_2S_2O_7$ has been found to undergo phase changes at 315, 225 and 214°C. Such changes could markedly affect the performance of K_2SO_4 doped catalysts. The lack of precise data on the melting point and decomposition of $K_2S_2O_7$ adds further confusion to the role of both K_2SO_4 and SO_3 in these systems.

Riley (R3), in a review of the work of Saffer (S7) has stated that the $V_2O_5/K_2S_2O_7$ complex in certain phthalic anhydride catalysts is a glassy amorphous material. He gives the melting point of $K_2S_2O_7$ as 360 - 370°C compared with a value of 700°C for V_2O_5. He states that the melting points of the binary system of $K_2S_2O_7$- V_2O_5 show a sharp minimum at 260°C, that is, well below normal reaction temperatures. Furthermore, active catalysts based on silica gel containing $K_2S_2O_7$ and V_2O_5 in such ratios that the complex would be liquid at reaction temperatures. In the solid state, these V_2O_5-$K_2S_2O_7$ complexes were glasses. By replacing potassium in the complex by sodium, the melting point rose and the catalyst remained active until the melting point rose to above that of the reaction temperature, when the activity diminished.

The results of Riley somewhat differ from results embodied in the phase diagram of Kiysura presented in reference (K1). In this phase diagram for the K_2SO_4-V_2O_5 system, the mimimum temperature at which liquid is presented is 440°C. This is far above normal reaction temperature. The fact that the complex does in fact exist as a liquid at reaction temperatures

has been verified by experiments (K1) in which a bed of TiO_2 supported catalyst was diluted with pure silica gel particles of similar size. Following reaction the particles were separated and analyzed for K_2SO_4, SO_3, and V_2O_5 content. It was shown both visually and by chemical analysis that some of the V_2O_5-K_2SO_4 complex had been transferred to the silica gel support.

Ross (R2) has found that an American-type catalyst (containing no K_2SO_4 or SO_3) has shown deactivation when reacted at 422°C. It is possible that the higher temperature has caused some form of sintering. If such conditions occur on this catalyst, it may be possible to have similar deactivation on a K_2SO_4-doped catalyst. This would cause deactivation above that caused by SO_3 desorption.

4.2.3 Conclusions and Recommendations

Evidence suggests that a liquid-phase complex containing V_2O_5, K_2SO_4 and SO_3 exists in German-type catalysts under reaction conditions. Furthermore, SO_3 and K_2SO_4 are considered to be present in the form of $K_2S_2O_7$ although excess SO_3 may also be present. SO_3 lost by desorption can be replaced by including some sulphur compound, preferably SO_2, in the feed. The SO_2 level required may vary depending on reaction temperature.

It is obvious from the discussion given above, that the level of knowledge of catalyst behaviour is very low. Considerable experimentation of the type conducted by the Japanese group (K1) is necessary at lower conversions in order

to determine if there is a narrow optimum SO_3 level, or if increasing the SO_3 level does in fact increase activity. An accurate construction of the phase-diagram for the V_2O_5-K_2SO_4-SO_3 system would also aid in understanding the system. However, the catalyst support material may also be important in determining the phase equilibria.

In this study we have endeavoured to stabilize the catalyst by heat treatment to reduce the SO_3 level and then conducted experiments at temperatures at least 20°C below the heat treatment value. This coupled with SO_2 addition has enabled us to maintain a relatively stable activity. Similar heat treatment is apparent in the work of Juusola (J4) who found that his catalyst had almost stable activity after 140 hours of operation. He could have obtained similar stability by operating for several hours at 400°C and then conducting his experiments near 300°C. We therefore conclude that heat treatment can produce catalysts of different stability and activity. It is recommended that future studies on this type of catalyst should be heat-treated in this manner prior to conducting kinetic experiments.

It is probable, in industrial reactors having considerable hotspots, that the pretreatment described above, occurs in the first few hours on stream. A highly active catalyst will lead to high bed temperatures and hence a rapid loss of SO_3. When the catalyst is deactivated in this manner, the hotspots will be reduced and greater stability will be achieved. In addition, the hotspots that do exist in industrial

reactors, may be beneficial in permitting increased oxidation of SO_2 to SO_3 over that attainable in isothermal beds operated at lower temperatures.

CHAPTER 5

INFLUENCE OF CATALYST SUPPORT MATERIAL ON REACTION RATES AND SELECTIVITIES.

This chapter describes kinetic measurements made on a number of catalysts supported on different materials. Discussion of the differences in behaviour of these catalysts is necessarily speculative since only rates and selectivities were measured. However, it is felt that this chapter in revealing the differences in selectivities obtained using the various catalysts, will aid other researchers in their studies of orthoxylene oxidation. In particular, it should reduce the considerable wasted effort apparent in this and other studies, caused by the use of unsuitable catalysts for a particular application.

5.1. Background

When this research programme was undertaken it was assumed that the Aero PAA catalyst obtained from Cyanamid of Canada would be suitable for oxidizing orthoxylene to phthalic anhydride. This belief was based on the fact that Herten (H2) had obtained phthalic anhydride yields of the order of 70 mole percent on a silica-supported catalyst. It was later discovered (F3) that the catalyst had in fact been supported on titanium dioxide. Our belief was further influenced by the fact that probably the most active group in this research area (M7, J4) had used silica-supported catalysts in their studies. The low

yields of phthalic anhydride obtained in their work were considered to be due to the low conversions investigated. Since o-tolualdehyde is an intermediate in the formation of phthalic anhydride, one might expect high levels of orthotolualdehyde at conversions that were typically less than 5%. Paetkau (P1) had obtained only small amounts of phthalic anhydride when he oxidized orthoxylene on the Aero PAA catalyst in a transported bed reactor. However, he had obtained conversions that were less than 15 percent and a similar argument was applied to his results. It was thought that normal selectivities to phthalic anhydride would result from operating at higher temperatures and conversions. As will be seen in section 5.2. this did not result.

5.2. Results and Discussion

Results

Initial experimentation showed that the Aero PAA catalyst was not suitable for oxidizing orthoxylene to phthalic anhydride. The reason for the poor selectivity was not understood at that stage. Therefore a number of catalysts were obtained or manufactured and used to oxidize orthoxylene. In general this initial catalyst screening was done by conducting one half of a two level factorial design for the variables: temperature, orthoxylene concentration, oxygen concentration and flow rate. The centrepoint was replicated to monitor catalyst activity. In the case of several catalysts, the study

TABLE 5.1. General Properties of Catalysts Investigated in this Study.

Catalyst	Type	Support	Supplier	Performance
Aero PAA	German Fluid Bed	Silica Gel 220 m^2/gm	American Cyanamid	Produced large amounts of tars. Yield of PAA < 30% High activity.
902 (Original sample)	German Fluid Bed	Silica Gel 40 m^2/gm	W.R. Grace	Low tar formation. Yields of PAA to 50% (from initial rate data). Excellent selectivity to OTA in steady state. High activity.
902 (Sample used in TBR study)	German Fluid Bed	Silica Gel 40 m^2/gm	W.R. Grace	Significant tar formation. Yield of PAA < 30%. Excellent selectivity to OTA in steady state. High activity.
906	German Fluid Bed	200 m^2/g	W.R. Grace	High tar formation. Yield PAA < 30%. High activity.
Laboratory Preparation	V_2O_5 on SiO_2	Silica Gel	-	High tar formation. Yield of PAA < 30%. High activity.
V-0501 S	American	Alumina 1 m^2/gm	Harshaw Chemical Company	High tar formation. Yield of PAA < 20%. Low activity.
Von Heyden	German	TiO_2(?)	BASF (Canada)	No tars. Yields of PAA > 70%. High activity.
V_2O_5/Sb_2O_3	German	TiO_2 5 m^2/gm	W.R. Grace	No tars. Yields of PAA > 80%. High activity.

Figure 5.1. Reaction Rates on Various Catalysts at Conditions of Approximately 0.01 atm. O-xylene and 0.21 atm. oxygen pressure.

1. Original 902 Catalyst
2. W. R. Grace TiO_2-Sb_2O_3 Catalyst
3. Von Heyden WO Catalyst
4. 902 Catalyst used in Transported Bed Reactor

5-10. Obtained from Reference C4.

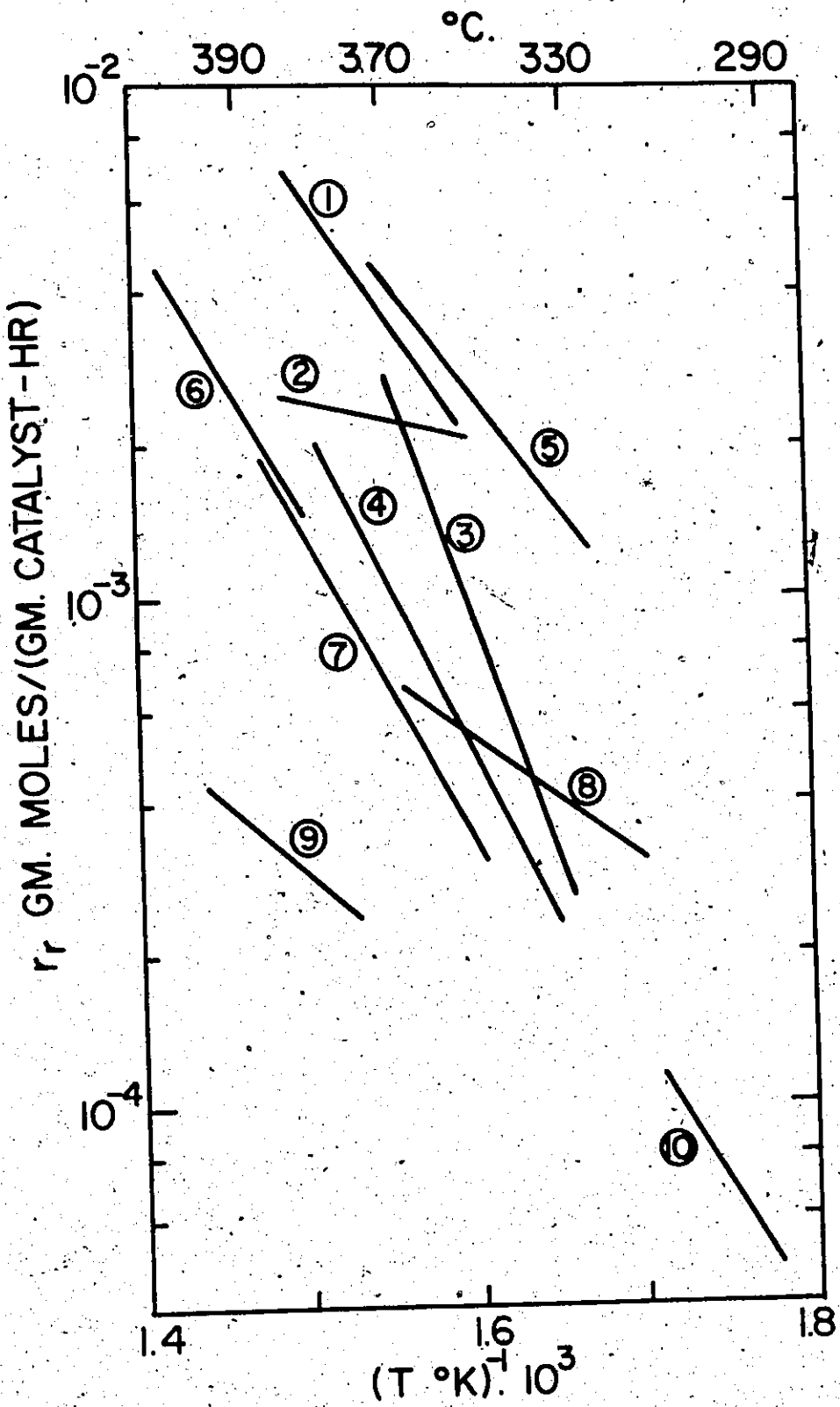
°C.
390
370
330
290
10^{-2}
10^{-3}
10^{-4}
r_r GM. MOLES/(GM. CATALYST-HR)
1.4
1.6
1.8
$(T\ °K)^{-1}\ 10^3$
①
②
③
④
⑤
⑥
⑦
⑧
⑨
⑩

terminated after conducting a few experiments because excessive tar formation caused blockages in the exit lines from the reactor. The general properties of the various catalysts are summarized in Table 5.1. In addition, the rates of ortho-xylene conversion on catalysts used in this and other studies are shown in Figure 5.1. The discussion that follows will describe the performance of the various catalysts in the chronological order in which they were investigated.

1. Acro PAA Catalyst

The catalyst was supplied by the American Cyanamid Company. The catalyst is reported by Thomas (T5) to have the following properties:

Composition: 62.0% SiO_2, 6.1% V_2O_5, 10.8% K_2O, and 17.0% SO_3, with a mole ratio of SO_3 to K_2O of 1.85.

Particle size: Supplied as a powder 95% finer than .149 mm.

Average Bulk Density: 0.55 gm./c.c.

Surface area: 220 m^2/gm.

This catalyst was originally used by Paetkau (P1) for an investigation of orthoxylene oxidation in a transported bed at 400°C. He conducted very few experiments and therefore some of the inadequacies of the catalyst were not revealed. In particular, the formation of tarry products was not detected. Paetkau obtained extremely high rates of reaction on this catalyst; however, almost no phthalic anhydride was produced,

the main reaction product being orthotolualdehyde. No analysis was made for carbon dioxide or carbon monoxide so that the extent of total oxidation could not be evaluated.

It was concluded at the commencement of this research project that low yields of phthalic anhydride obtained by Paetkau, were due to the low conversions which resulted from the extremely short contact times and low solids loadings inherent in his transported bed reactor. Since there is an upper limit to the value of W/Fa_o that can be achieved in a transported bed, it was decided to conduct packed bed experiments near to this condition. This upper value of W/Fa_o was considered to be that achieved when the solids loading in the reactor was 3 volume percent. This condition results in very low W/Fa_o values (typically less than 100 gm hr/gm mole). It was assumed that the reaction temperature could be raised to take the low solids-to-reactant ratio into account thereby producing high conversions. It was later found during the course of the packed bed experiments that the effect of operating in the temperature range 450 to 510°C was to produce considerable amounts of carbon monoxide and carbon dioxide whilst phthalic anhydride selectivities were typically less than 30%.

Having shown that an increase in temperature did not produce increased phthalic anhydride yields, it was decided to conduct experiments at conditions that were normally used for oxidizing naphthalene on this catalyst. Therefore experiments were conducted at temperatures in the range 330 to 390°C. In accordance with the long residence times that occur in fluidized

beds, which is the normal application for this catalyst, the experiments were performed at values of W/Fa_o that were many times greater than those expected to pertain in a transported bed. These experiments produced little change in the maximum phthalic anhydride yields. However, the extent of complete oxidation was reduced and this was accompanied by an increased conversion to orthotolualdhyde.

These steady-state experiments showed that the Aero PAA catalyst was unsatisfactory for phthalic anhydride production. However, the work on this catalyst did provide useful information on the behaviour of vanadia catalysts. During the high temperature experiments it was found that repeating a lower temperature experiment following reaction at an elevated temperature produced a loss in catalyst activity. In addition, it was found that for the first few seconds on-stream, a freshly oxidized catalyst produced considerable amounts of colourless crystals. After this initial period excessive tar formation occurred and an oily brown liquid was collected in the cold trap which was connected to the outlet of the gas sample valve. This was the first evidence that highly oxidized vanadium pentoxide catalysts would produce high rates of reaction in accordance with the "Redox" and S.S.A.M. mechanisms.

The results of some of the steady-state experiments are presented in Table 5.2. A comparison with other catalysts shows the Aero PAA to have high activity. However, it is apparent that the oxidation of orthotolualdehyde to phthalide and hence phthalic anhydride is an extremely slow step in the

Reaction Conditions					Reaction Rate	Xylene Conversion	Selectivities %				
Run	T(^{o}C)	% Xylene	% Oxygen	W/Fa$_{o}$	$r_r \times 10^3$	%	OTA	PI	PAA	CO_2	CO
1	382	.844	48.3	501	1.93	97.0	11.2	6.0	26.8	50.2	5.6
2	335	.750	50.0	564	1.16	65.6	74.0	5.5	1.8	18.7	0
3	338	.838	49.7	1010	.95	96.2	52.6	9.4	9.0	25.0	3.8
4	315	.605	48.7	1400	.43	59.7	73.9	4.7	.7	20.7	0
5	368	.554	49.3	573	1.64	93.8	18.5	12.3	29.1	35.0	4.8
6	340	.652	20.0	649	1.09	70.7	72.4	5.3	2.6	17.9	1.3
7	372	1.27	20.0	166	1.39	23.1	83.3	0.9	0	15.8	0
8	369	.506	20.0	418	1.30	54.5	82.8	3.9	1.2	12.2	0
9	370	.501	20.0	422	2.14	90.3	51.3	11.6	12.2	22.3	2.4
10	328	1.24	20.0	341	2.38	81.2	54.7	7.5	8.9	23.9	4.0
11	400	.948	20.7	231	4.24	97.9	36.4	7.7	19.4	30.2	6.2
12	399	1.12	23.0	360	2.74	98.6	17.6	6.4	28.6	38.1	9.2
13	400	1.12	15.0	377	2.62	98.6	33.6	8.0	19.2	31.4	7.7
14	380	1.08	15.0	391	2.22	86.8	55.4	7.4	10.5	23.6	2.7
15	352	1.05	15.0	404	1.12	45.2	83.6	0	0	16.4	0

TABLE 5.2. Rate Data for Aero PAA Catalyst.

reaction sequence.

Since this catalyst had poor selectivity to phthalic anhydride and resulted in considerable tar formation and since better performance with other catalysts had been reported in the recent literature, it was deemed necessary to investigate other catalysts that were readily available.

2. Catalyst Prepared in the Laboratory

Catalyst 2 was prepared in the laboratory by depositing 20 percent vanadium pentoxide by weight on silica gel. This high level of vanadium pentoxide was used in an effort to increase the surface area of vanadium pentoxide in order to achieve greater catalyst activity, and hopefully, increased selectivity to phthalic anhydride. The method of catalyst preparation is described in Appendix C. An analysis of the vanadium content by atomic absorption spectroscopy is described in Appendix .

Several experiments were conducted on this catalyst at temperatures around 350°C. The catalyst produced considerable tar formation and the investigation was terminated after several experiments had been conducted. In general, this catalyst had similar properties to the Aero PAA catalyst.

3. Harshaw V-0501 Catalyst

This catalyst was supplied by the Harshaw Chemical Company.

The catalyst is reported by Thomas (T5) to have the following properties.

10% V_2O_5 supported on inert alumina 1/4" spheres

Surface area: 1 m^2/gm

Average bulk density: 1.3 gm/c.c.

This was an American-type catalyst. When the spheres were split it was found that there was a much higher vanadium content at the surface than at the core. The spheres were crushed and screened to produce a catalyst of similar size to that which could be used in a transported bed reactor.

Experiments conducted at conditions similar to those for catalyst 2 showed that the Harshaw catalyst had low activity and produced phthalic anhydride yields that were less than 20 percent. In addition, tar formation was high. The low activity was not unexpected since American-type catalysts have high surface concentrations of vanadium pentoxide. Crushing and screening completely changes the catalyst characteristics. The fluidized bed experiments of Calderbank (C4) provided supporting evidence for this conjecture.

4. von Heyden "WO" Catalyst

Following the translation of the article by Suzuki et al. (S3), it was apparent that the catalyst support significantly influenced the selectivity of vanadium pentoxide catalysts in the oxidation of orthoxylene. The scarcity of information on the effect of the catalyst supported material led to brief investigations of two catalysts that have been successfully used to oxidize orthoxylene in packed beds. These studies were also intended to provide information on the performance of

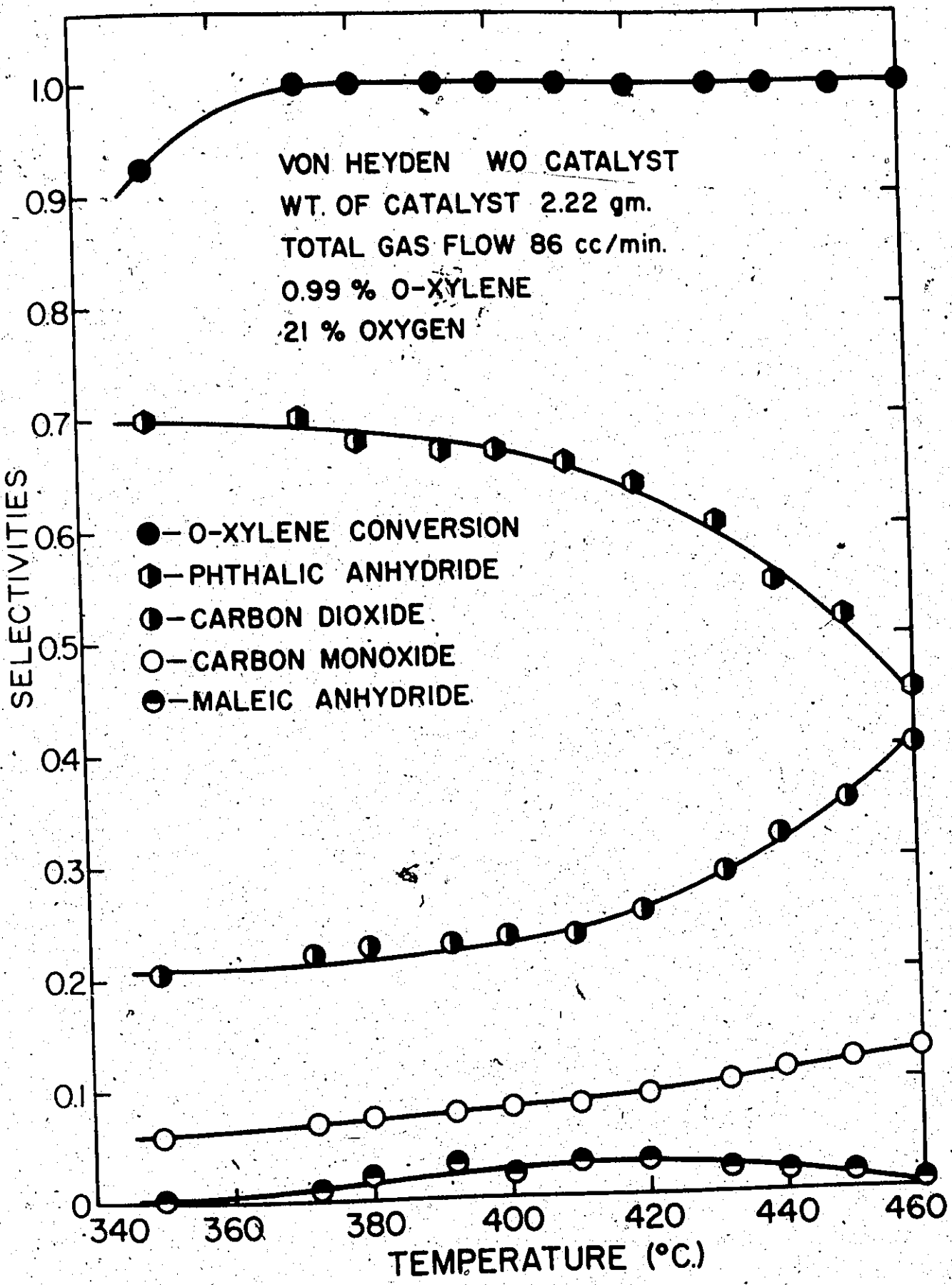

Figure 5.2. Selectivity Data for von Heyden Catalyst.

titania-supported catalysts should they be available for use in a transported bed reactor. The studies would also adequately test the method of chemical analysis over a wide range of product compositions.

The von Heyden WO catalyst was obtained in the form of 4 mm extruded pellets. These pellets were crushed and screened to give particles in the .15 to .3 mm size range. The catalyst had been used in an operating industrial reactor for three years at the BASF plant at Cornwall, Ontario. Since this catalyst, as supplied, was not in a form that could be used in a transported bed study, it was intended that the packed bed experimentation be limited to a few experiments that would provide selectivity and rate data for comparison with those of silica-supported catalysts.

Experiments were conducted in the temperature range 330° to 460°C. Complete experimental results are given in Appendix G. The overall rates of oxidation of orthoxylene for feeds containing approximately 21 percent oxygen and 1 percent xylene are shown in Figure 5.1. By obtaining the product composition for a reactor operating at 100 percent conversion, it was possible to determine the extent of phthalic anhydride oxidation. These results are shown in Figure 5.2. It can be seen that significant oxidation of phthalic anhydride takes place above 400°C. Below this temperature the yield of phthalic anhydride is fairly constant at around 70 percent. By comparison with other studies the catalyst appears to have high activity and selectivity. The loss in activity by operation at extremely

high temperatures has been described in the previous chapter. Since the catalyst sample used in this study had been employed in an industrial reactor for several years, it is probable that even higher activities would be obtained on a fresh WO catalyst sample.

5. W. R. Grace TiO_2 Catalyst

This catalyst was obtained from the research laboratories of W. R. Grace and Co., Baltimore, Maryland. It is covered by Canadian patent No. 873904 and has the following general properties:

Surface area: 5 m^2/gm

Bulk density: 1.2 gm/c.c.

Average particle size: 65 microns

Probable Composition (based on patent literature):

V_2O_5, 6.0 wt.%; Sb_2O_3, 6.0 wt.%; K_2O, 2.0 wt.%; SO_3, 2.0 wt.%, TiO_2, 84.0 wt.%.

The catalyst was supplied in the form of fine particles which are normally compressed into pellets for industrial use. It has been claimed that this catalyst has extremely high activity and selectivity for phthalic anhydride production.

Experiments were conducted according to a partial factorial design. The results are presented in Table 5.3. In addition, a detailed study of the unsteady-state performance of this catalyst was made. Complete results of these studies are presented in Appendix G.

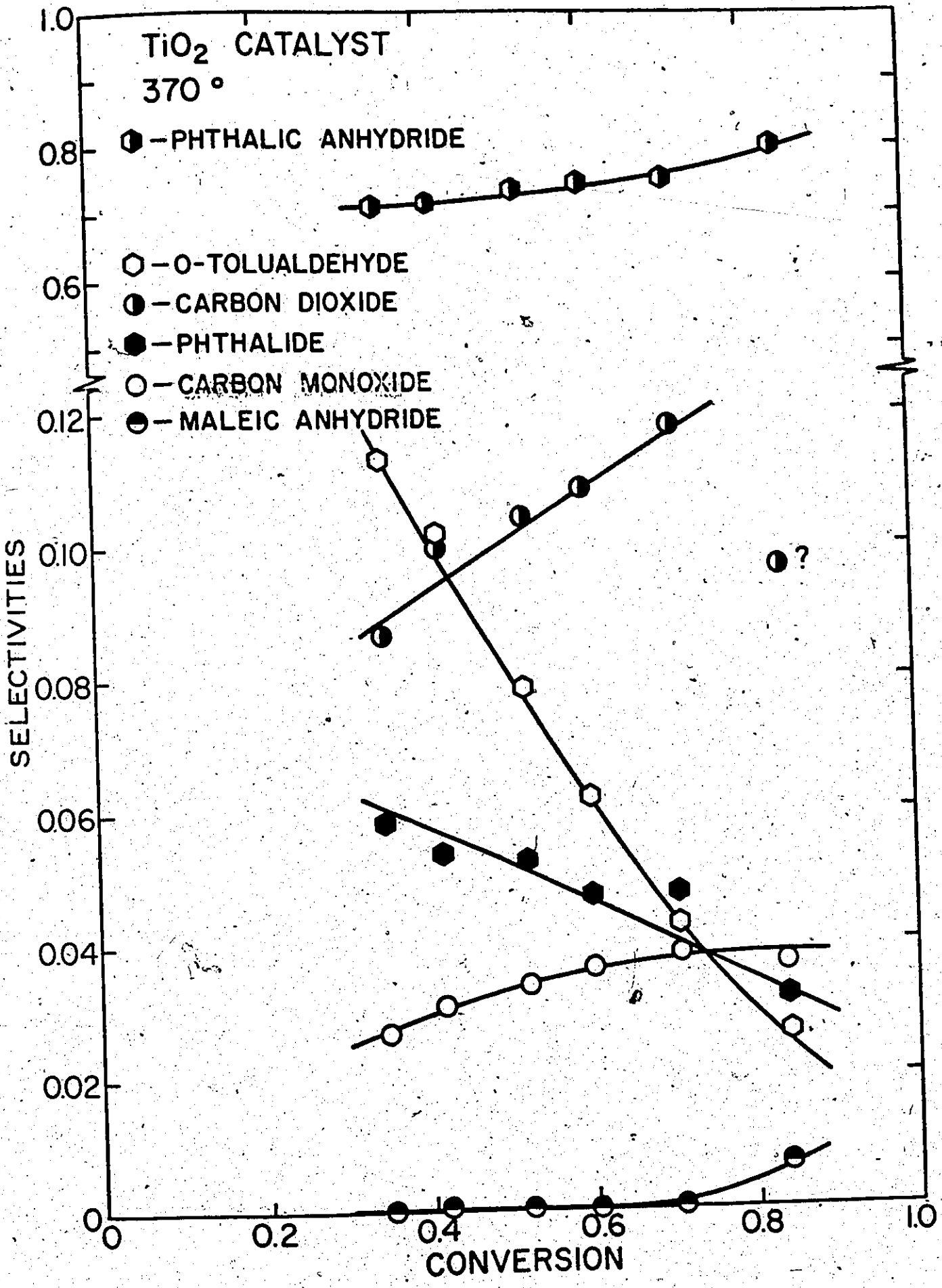

Figure 5.3. Selectivity Data for W.R. Grace TiO_2-Supported Catalyst.

The following general observations of catalyst behaviour were made:

1. The rate of oxidation was essentially independent in the temperature range 370° to 400°C. An explanation of this effect has been given in the previous chapter.

2. Steady-state operation following a change in operating conditions is achieved only after almost one day of reaction. This has been shown in Figure 4.3 . This is in accordance with the observations of Froment (F2) on a catalyst which is thought to be titania-supported. Juusola (J4) has observed that silica-supported catalysts achieve steady-state operation after less than one half hour. Our experience supports his observation.

3. The catalyst activity at low temperatures of operation seemed fairly stable. Figure 4.9 shows the rates of orthoxylene conversion obtained for replicated centre point experiments conducted over a period of 20 days.

4. The selectivity to phthalic anhydride was excellent. Figure 5.3 shows a typical selectivity versus conversion plot for experiments conducted at 370°C. Maximum yields around 85 mole percent phthalic anhydride were obtained at 100 percent orthoxylene conversion. This value has been claimed by the manufacturers (M4). Phthalic anhydride yields of 85 percent were obtained even when no oxygen was present in the feed stream (Figure 4.4).

5. The presence of maleic anhydride was detected in very few experiments. The maximum selectivity to maleic anydride was less than 1 percent and hence it could be effectively ignored.

6. Grace 906 Catalyst

This catalyst is used in the oxidation of naphthalene and is reported (T5) to have the following composition:

Composition: 4% V_2O_5, 14.9 % K_2SO_4, 6.7% SO_3, 73% SiO_2

Form: Powder

Average Bulk Density: 0.6 gm/c.c.

Surface Area: 200 m^2/gm

Average Pore Diameter: 35°A

In appearance this catalyst resembled the catalyst prepared in our laboratory. Several experiments confirmed that this catalyst produced excessive over-oxidation and considerable tar formation. Selectivity to phthalic anhydride was less than 30 percent. For this reason this catalyst was not considered for use in the transported bed study. In addition, it was a much coarser material than the Aero PAA catalyst and therefore its flow properties in the transported bed would probably have been inferior to other fluidizable catalysts that were available.

7. Grace 902 Catalyst (Original Sample)

This catalyst is reported (T5) to have the following general properties:

Composition: 9% V_2O_5, 29% K_2SO_4, 12% SO_3, 50% SiO_2

Form: Powder

Average Bulk Density: 0.6 gm/c.c.

Average Pore Diameter: 30°A

Surface Area: 40 m^2/gm.

It differed from the 906 catalyst by having lower surface area and higher vanadia content. Preliminary experiments revealed that this catalyst is superior to the other two fluid bed catalysts which had been investigated. Rates of reaction were high and tar formation was low. Unsteady-state experiments gave higher selectivities to phthalic anhydride and phthalide, than had been given by the previously tried silica-supported catalysts.

In order to more fully evaluate the catalyst prior to the purchase of the large quantity required for use in the transported bed study, experiments were conducted according to one half of a 2^4 design. The complete results of this study are given in Appendix G. Both steady-state and initial rate measurements were made, the unsteady-state measurements being made after 30 seconds on stream. The steady-state data are summarized in Table 5.3 to compare the performance of a typical silica-gel-supported catalyst with that of a TiO_2-supported catalyst.

Steady-state reaction rates are presented in Figure 5.1. It can be seen that this catalyst is highly active by comparison with those used in most other investigations. Catalyst activity, as shown by the reaction rates presented in Figure 4.9, was fairly stable over a period of 20 days. The initial rate data presented in Appendix G show that maximum phthalic anhydride yields were in excess of 40 percent. This was much higher than for either the 906 or Aero PAA catalysts. Throughout the entire program tar formation was negligible. It was therefore decided that this catalyst would be used in the transported bed study.

8. Grace 902 Catalyst (Sample used in Transported Bed)

The physical appearance of this catalyst differed slightly from that of the original sample. However, it was assumed that both catalysts would have similar properties. An extensive experimental program was conducted in the packed bed reactor and a complete 2^4 factorial design was completed. In addition, replicated centre points were conducted randomly throughout the experimental program to monitor catalyst activity. A further series of 22 experiments was conducted to determine the error structure over a wide range of conversions. Complete results of these experiments are presented in Appendix G Both steady-state and initial rate measurements were made.

The results of this study showed that the two 902 samples had different properties. The experimental program for this sample was hampered by the formation of considerable amounts of tarry material. This caused many shutdowns to remove tars that were blocking the exit line from the reactor. In addition, reference to Figure 5.1 shows that the rates of reaction, under similar conditions, were about half those for the original sample. The high initial yields of phthalic anhydride, obtained on the original sample, were not achieved in this study. Furthermore, it is apparent from Figure 4.9, that the catalyst underwent some loss of activity during the course of the experimental program.

A typical selectivity plot is presented in Figure 5.4. The selectivity for partial oxidation is excellent at conversions less than 50 percent. Typical yields of orthotolualdehyde are

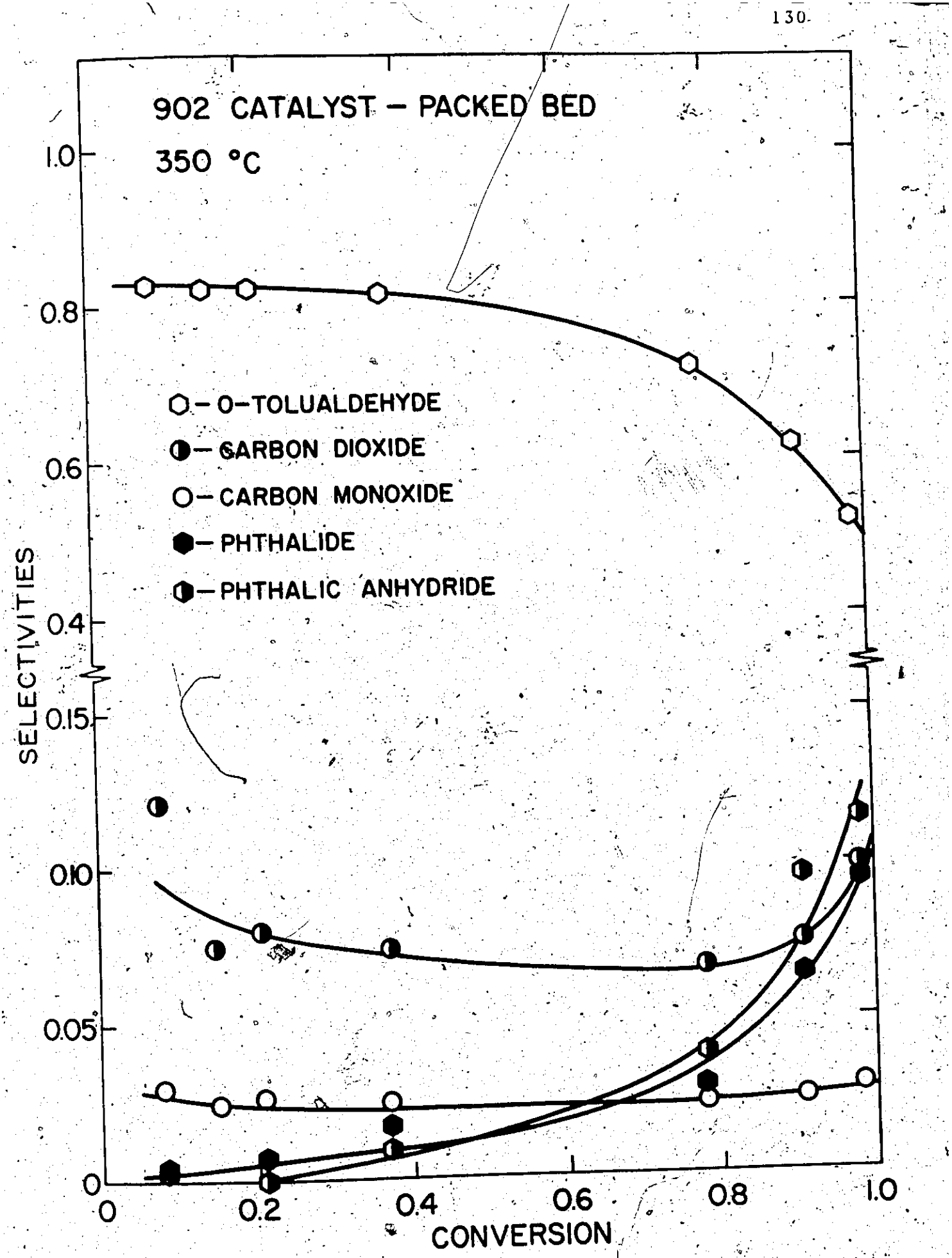

Figure 5.4. Selectivity Data for 902 Catalyst.

in excess of 80 percent. However, in common with all the silica-gel-supported catalysts used in this study, the rate-determining step appears to be the oxidation of orthotolualdehyde to phthalide and phthalic anhydride. More severe conditions, such as increased temperatures and contact times, produced considerable over-oxidation caused by orthotolualdehyde being totally oxidized to carbon oxides rather than partially oxidized to phthalic anhydride.

Initial rates of reaction on this catalyst were extremely high. This has been illustrated in Figure 4.2. The rapid loss of activity was one of the major difficulties in making measurements on the 902 catalysts. Steady-state conversions were low (less than 5 percent) at 330°C since an effort was made to keep initial conversions less than 100 percent.

Discussion

The differences in performance of the catalysts described above will now be discussed with reference to the results of other workers. To aid these discussions Table 5.3 has been included. The table summarizes the results of partial factorial design experiments on the original 902 and the TiO_2 catalysts supplied by W. R. Grace and Company. In these designs the following conditions were used:

Reaction Conditions				Reaction Rates X 10^3		Xylene Conversion %		Selectivities % PAA		OTA		CO_2		CO		Carbon Balance %	
T	F	X	O	902	TiO_2	902	TiO_2	902	TiO_2	902	TiO_2	902	TiO_2	902	TiO_2	902	TiO_2
+	+	+	+	11.43	3.37	62.3	23.9	9.0	56.9	64.1	20.8	15.4	10.7	5.5	3.0	101.0	99.2
+	+	-	-	3.88	1.49	43.4	20.8	13.4	62.7	69.7	20.6	13.1	5.9	4.5	1.8	95.7	96.1
+	-	+	-	2.19	0.96	49.8	21.1	7.3	63.0	50.0	18.5	21.6	9.1	7.2	2.0	102.0	97.3
+	-	-	+	2.14	1.68	90.6	68.8	45.0	76.5	2.8	3.8	38.4	11.6	13.7	4.0	104.0	101.0
-	-	-	-	0.74	1.37	33.2	47.5	8.7	78.8	69.3	5.5	11.7	8.9	3.7	2.7	98.2	103.0
-	-	+	+	2.09	2.25	46.9	46.2	7.2	74.2	70.2	6.5	13.0	12.4	4.1	3.4	98.5	103.0
-	+	-	+	3.07	2.28	33.8	32.2	4.5	67.6	82.1	13.1	7.6	10.2	2.5	3.5	98.7	97.5
-	+	+	-	1.21	1.86	6.33	12.8	3.8	59.7	82.1	24.4	11.2	5.7	2.3	1.6	99.5	100.0
0	0	0	0	3.44	2.16	40.4	31.5	6.1	70.9	73.8	12.3	11.4	9.3	3.7	2.5	98.6	100.0
0	0	0	0	3.67	2.18	42.8	27.2	6.6	69.1	74.2	13.6	10.6	8.5	3.6	2.7	97.0	98.5
0	0	0	0	3.73	-	42.1	-	6.4	-	73.0	-	11.3	-	3.8	-	96.7	
0	0	0	0	3.67	-	42.5	-	6.1	-	73.4	-	11.4	-	3.9	-	98.6	
0	0	0	0	3.50	-	40.5	-	6.1	-	74.3	-	11.0	-	3.7	-	96.7	

TABLE 5.3. Comparison of Performance of Silica-Gel and Titanium Oxide-Supported Catalysts.

Design Points	-1	0	+1
Temperature (^{o}C):	350	370	390
Xylene level (%):	1	1.5	3
Oxygen level (%):	10	20	30
Flow-SiO_2 (c.c./min.):	100	250	400
Flow-TiO_2 (c.c./min.):	100	200	300

The lower flow rates used in the case of the TiO_2 catalyst were necessary because higher pressure drops were encountered with this catalyst. 1 gm of catalyst was used in each study.

Table 5.3 shows that the silica-gel supported catalyst produces significantly less phthalic anhydride than the titania-supported catalyst. In addition, the degree of over-oxidation is much greater for the silica-supported catalyst. It was also noted that the titania-supported catalyst produced a product which was free from tarry impurities, unlike the silica-supported catalyst.

The effect of catalyst support material on the selectivity of orthoxylene oxidation has been neglected in all the reviews of both industrial and academic literature. In fact, the only academic study that the author is aware of, was published in an obscure Japanese journal (S3, K4). There has been considerable secrecy in both the academic and industrial literature. This has resulted in a large amount of wasted effort by a number of researchers.

On the basis of our experience and a review of the pertinent literature the main points to be noted in any discussion on the difference in behaviour on TiO_2 and SiO_2-supported catalysts are:

1. Naphthalene is equally well oxidized on both TiO_2 and SiO_2-supported catalysts.

2. The main product from the oxidation of orthoxylene depends on the support: For silica based catalysts it is ortho-tolualdehyde and for the titania based one it is phthalic anhydride.

3. Silica-gel-supported catalysts generally have high surface areas, typically 40-220 m^2/gm, whereas TiO_2-supported catalysts have surface areas from 5-10 m^2/gm.

4. It is possible that the V_2O_5-K_2SO_4 system exists as a melt under reaction conditions.

5. The selectivity to phthalic anhydride has been found to depend on the ability of a catalyst to adsorb oxygen (K4).

6. TiO_2 has been shown (A1) to have catalytic activity for oxidizing anthracene to anthraquinone.

7. Melts of V_2O_5-K_2SO_4 and V_2O_5-$K_2S_2O_7$ have been used to oxidize orthoxylene (S8). Selectivity to phthalic anhydride was poor. However, significant yields of ortho tolualdehyde were obtained.

8. Low surface area catalysts, both promoted and unpromoted, appear most successful for producing phthalic anhydride from orthoxylene.

This attempt to discuss the influence of the support material is purely speculative and is based on general catalytic

principles which may be supported by some of the points in the previous paragraph. The argument is an extension of the discussion of Vrbaski and Mathews (V2) who have noted a striking similarity between certain atomic distances in ortho tolualdehyde and in vanadium oxides. "The C-C distance between the methyl and carbonyl groups in ortho-tolualdehyde (2.8°A) and that between the C_1-C_4 (2.79°A) in benzene compare with the O-O distance in V_2O_5 (B9) along the trigonal base (2.8°A), whereas the C_1-C_3 distance in benzene (2.41 °A) agrees with the O-O distance of the two shorter bipyramid sides (2.39°A)." In the case of orthoxylene oxidation, ortho-tolualdehyde is the intermediate. If phthalic anhydride is to be produced, the ortho-tolualdehyde must have point-to-point adsorption of the methyl and carbonyl groups thereby forming phthalide and phthalic anhydride. Based on the interatomic distances quoted above, it would appear that this is only possible on the oxygen sites where the O-O distance is 2.8 °A. Adsorption on the closer oxygen atoms will result in oxidation of the benzene ring, forming carbon oxides. In the case of naphthalene oxidation, 1, 4 naphthaquinone is the intermediate. The distance between the 1, 4 carbon atoms is 2.79°A and naphthaquinone will be formed by point-to-point oxidation at oxygen atoms 2.8°A apart. Oxidation of naphthaquinone to phthalic anhydride takes place by completely oxidizing the 2, 3 carbon atoms which are 1.39°A apart. That is, point-to-point adsorption at oxygen atoms 2.8°A apart is necessary at all stages in the oxidation of xylene whereas it is necessary only for the formation of the

intermediate in the case of naphthalene oxidation. It is therefore possible that a lattice containing large concentrations of O-O (2.8°A) atoms is necessary for orthoxylene oxidation whereas only half this concentration is required for naphthalene oxidation.

If the postulate that the number of lattice oxygen atoms 2.8°A apart influences reaction selectivity for orthoxylene oxidation applies, the difference between performance of silica and titania-supported catalysts can be explained by a difference in the number of such oxygen pairs. The observation (K4) that the TiO_2-supported catalyst adsorbs more oxygen per unit surface area than the SiO_2-supported catalyst may cause a higher oxidation state to exist within the TiO_2-supported catalyst. In addition it can be noted in Figures 4.2 and 4.3 that the unsteady-state performance of the two catalyst types is quite different. The SiO_2-supported catalysts rapidly deoxidize and reach a steady-state whereas the process is very slow for the TiO_2 catalyst. This may be due to the fact that the relative rates of catalyst reoxidation/hydrocarbon oxidation are much higher for TiO_2 catalyst than the SiO_2 catalyst. This may be related to the fact that the TiO_2 catalyst adsorbs more oxygen. Possibly the TiO_2 itself acts as a source of oxygen for the vanadium oxides. Certainly trivalent titanium is more likely than trivalent silica since the latter forms a more stable oxide.

The difference may arise because the two catalyst supports stabilize different valence states in the vanadia catalyst. This has been known to occur in other catalyst systems (A2). This may explain the 20% higher selectivities to

phthalic anhydride that were obtained by incorporating 6% Sb_2O_3 in a TiO_2-supported catalyst.

In the previous chapter the possibility of melt formation has been discussed. If V_2O_5 exists as a melt this would somewhat weaken the arguments put forward above. The wide differences between the temperatures at which melts are thought to exist is another puzzle in this very complex catalyst system. Satterfield and Loftus (S8) have shown melts of V_2O_5-K_2SO_4 systems to have low reactivity for orthoxylene oxidation. The main reaction product was ortho-tolualdehyde. The conclusions are weakened by the fact that maximum conversions around 3% were obtained. They also worked at temperatures in the range 528 to 598°C which are far above those encountered in studies using supported catalyst. They state that the lowest temperature at which they could achieve a melt was 430°C. This was achieved using a vanadium pentoxide-potassium sulphate eutectic mixture containing 39% V_2O_5. They note that a "German patent (N1) describes the use of a mixture of vanadium pentoxide and alkali pyrosulphate which is liquid under reaction conditions, the preferred temperature of reaction being 270 to 350°C. A sulphur compound or sulphur dioxide is added to the feed stream to maintain the catalyst composition so that it remains in the form of a liquid". This would indicate that the role of SO_3 is thought to be one of maintaining the correct alkali pyrosulphate level in the catalyst.

Another interesting aspect of the effect of different support materials has been noted by Riley (R3). He has found that for the oxidation of naphthalene in fluidized beds, the

amorphous and liquid character of the V_2O_5:$K_2S_2O_7$ complexes and the nature of the silica gel were very important factors in determining catalyst efficiency. He has noted that substitution of alumina having similar specific surface area to the silica, produces an entirely different catalyst. When used for oxidation of naphthalene in fluid beds this catalyst caused the deposition of considerable carbonaceous material on the catalyst surface. Analysis of silica and alumina-supported catalysts showed a considerable difference in catalyst composition. A 1/4 inch silica gel particle which had been immersed in molten $V_2O_5/K_2S_2O_7$ for 30 minutes at 400°C was shown to have a uniform concentration of V_2O_5 throughout. However in the case of an activated alumina pellet of similar size, immersion in the same melt for a period of 48 hours, produced almost no penetration. Thus the two catalyst supports appear to have different wettabilities.

5.3 Conclusions and Recommendations

On the basis of this preliminary work and that of others and some speculation, the following conclusions and recommendations can be made.

1. Both silica-gel and titania-supported catalysts have similar activities and produce excellent selectivities for partial oxidation of orthoxylene. However, partial oxidation on SiO_2-supported catalysts is mainly terminated at the formation of ortho-tolualdehyde whereas the process continues through to phthalic anhydride via phthalide in the case of TiO_2-supported catalysts.

2. A high degree of cracking occurs on SiO_2-supported catalysts. This was evidenced by considerable tar formation and the large number of compounds (in small concentration) that appeared in the chromatograms. The extent of cracking appeared greater at higher temperatures. No such effects were observed for TiO_2-supported catalysts.

3. The silica-gel-supported catalysts achieved steady-state operation after a short time, order of minutes on-stream. Titania-supported catalysts required approximately 24 hours to stabilize.

The whole area of catalyst composition requires considerable research. In particular, fundamental studies are required on the effect of different support materials on catalyst structure in both the unsteady-state and steady state periods. The role of the various promoters and sulphur trioxide is still not clear. It is to be noted that almost all previous studies have been concerned with the measurements of rates and selectivities. Such investigations provide only limited insight into the understanding of catalyst behaviour.

CHAPTER 6

PARAMETER ESTIMATION IN STEADY-STATE REACTION MODELS

6.1 Introduction

Although the primary objective of this research programme was to evaluate the transported bed as a catalytic reactor by using the orthoxylene reaction on a vanadia catalyst as an example, the amount of reaction response data generated during the course of the packed-bed reactor programme has allowed considerable insight into the reaction mechanism and relative rates of reaction of the various steps. It was felt that those data would allow a test of the ability of the S.S.A.M. or the Redox model to describe this oxidation reaction, that is predict the conversion and product distribution over a wide range of operating conditions. Such a quantitative evaluation of the models might also uncover shortcomings of the model and suggest additional effects that should be included. In any event, the evaluation of parameters in the models would provide parameter estimates which will be useful in designing future experiments for model testing, parameter estimation or model discrimination.

Because of the wide differences in product compositions obtained when orthoxylene is oxidized on vanadia catalysts supported on different materials, it was decided that the reaction models should be tested using both the silica gel-supported catalyst (Grace 902 as used in the transported bed) and the titania-supported catalyst (Grace TiO_2-Sb_2O_3).

6.2. Reaction Models

Juusola (J6) has estimated pre-exponential factors and activation energies for adsorption and reaction rate constants in a model which lumps all reaction products. That is, he has considered the conversion of orthoxylene to products in a single reaction. He has shown the value of the use of sequential experimental design procedures for obtaining improved estimates of parameters in a given model with a minimum of experimentation. In addition, he has evaluated parameters for the oxidation of ortho-tolualdehyde and the oxidation of ortho-xylene by a parallel reaction scheme (J4).

Herten (H2) has indicated that a group led by Froment is working on a multiresponse model to describe the oxidation of orthoxylene over a wide range of experimental conditions. However, it appears that this goal has not been achieved in the 5 years since the publication and that the development is still far from complete (F3).

The reaction sequences adopted for the silica (902) and titania-supported catalysts are shown in Figures 6.1 and 6.2. These schemes are proposed after a qualitative evaluation of the selectivity data obtained on these catalysts as presented in Chapter 5. These schemes retain the main features of the more complex reaction networks proposed by Herten (H2) and Juusola (J4) as shown in Figures 2.3 and 2.4 respectively. In the case of the silica-supported catalyst the phthalic anhydride, phthalide and ortho-toluic acid have been lumped since they are all present in small amounts and are formed

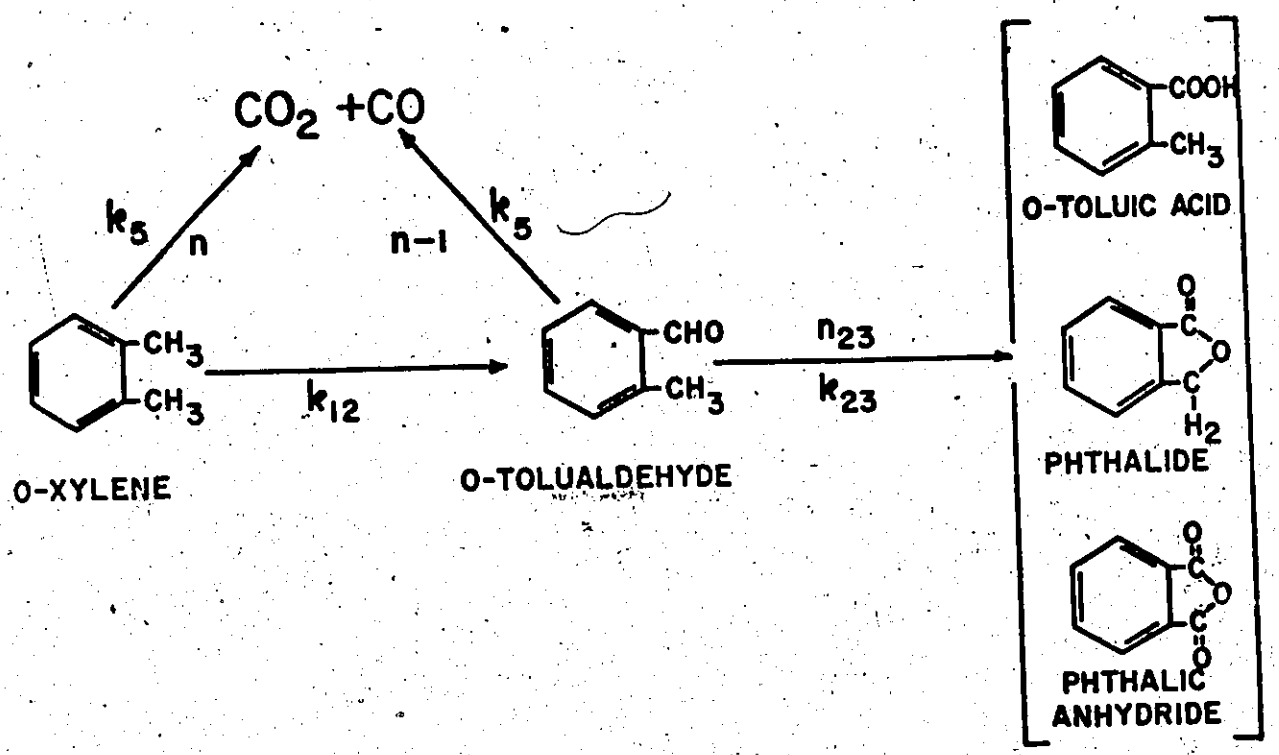

Figure 6.1. Reaction Scheme for Oxidation on 902 Catalyst.

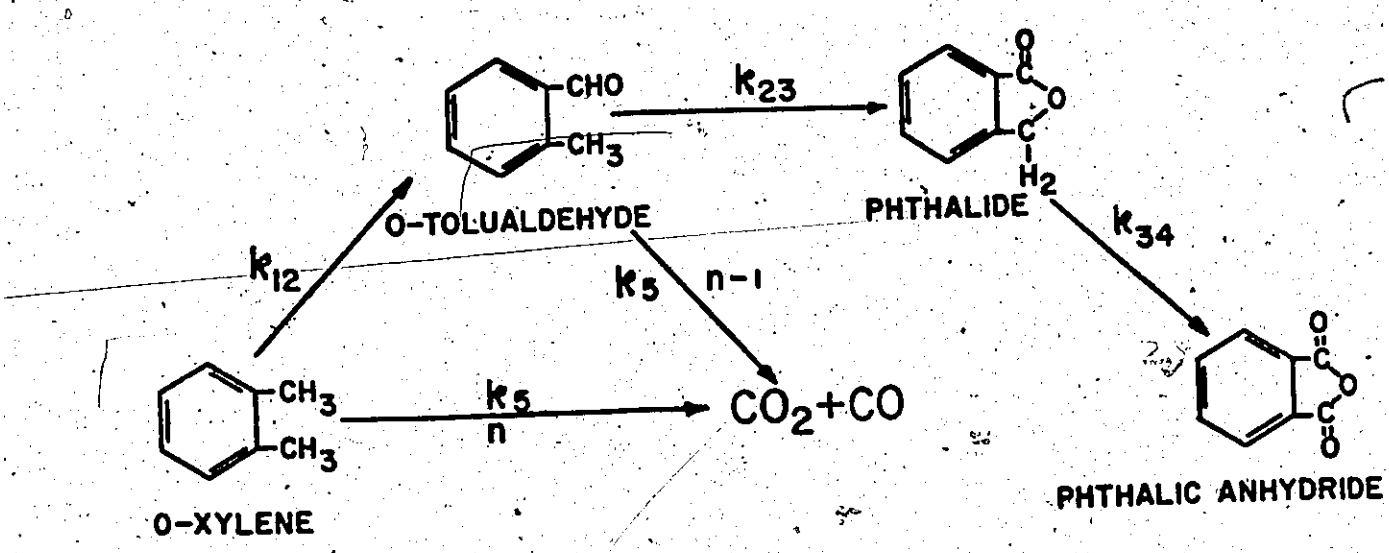

Figure 6.2. Reaction Scheme for Oxidation on TiO_2-Supported Catalyst.

sequentially from ortho-tolualdehyde. The titania-supported catalyst has been shown to produce considerable amounts of phthalic anhydride and so all three partial oxidation products, ortho-tolualdehyde, phthalide and phthalic anhydride have been included. The almost constant ratios of CO_2/CO found for both catalysts suggested that it would be appropriate to lump these two components so that they be considered together as "carbon oxides". In addition, it was decided that the rates of oxidation of orthoxylene and ortho-tolualdehyde to carbon oxides should be identical. That is, the activation energies and pre-exponential factors should be the same for these two steps. Juusola (J 4) has oxidized both orthoxylene and ortho-tolualdehyde on a silica-gel-supported catalyst which was similar to the 902 catalyst used in this study and observed that the overall rates of conversion and selectivities for CO_2 formation are of the same orders of magnitude for the two compounds. Moreover, it is likely that the rate of oxidation of the benzene ring should be nearly the same for both compounds since the ring should not be significantly stabilized by the aldehyde group replacing the methyl group. The formation of carbon oxides from phthalic anhydride and phthalide has been assumed to be negligible in comparison to that from orthoxylene and ortho-tolualdehyde. In the case of phthalide and phthalic anhydride it has been considered that the benzene ring is stabilized by the oxidized ring side structure.

Using these reaction schemes and the mechanism embodied in the S.S.A.M. and Redox mechanism it is possible to

develop the reaction equations describing the formation of the various oxidation products and the disappearance of orthoxylene. The equations describing the rates of the various steps for each catalyst are presented below. Their development is presented in Appendix F.

1. Reaction Equations for the Reaction Scheme in Figure 6.1 (902 Catalyst)

$$-\frac{dC_1}{dt} = k_a C_a (k_{12} + k_5) C_1/D \qquad (6.1)$$

$$\frac{dC_2}{dt} = k_a C_a (k_{12}C_1 - (k_5 + k_{23}) C_2)/D \qquad (6.2)$$

$$\frac{dC_3}{dt} = k_a C_a k_{23}C_2/D \qquad (6.3)$$

$$\frac{dC_5}{dt} = 8 k_a C_a k_5 (C_1 + C_2)/D \qquad (6.4)$$

where $$D = k_a C_a + k_{12} C_1 + n k_5 C_1 + n_{23} k_{23} C_2 + (n-1) k_5 C_2 \qquad (6.5)$$

n is the stoichiometric coefficient for the formation of CO_2 and CO from orthoxylene. It is calculated from the experimental selectivity data as follows:

$$n = (10.5 S_{CO_2} + 6.5 S_{CO})/(S_{CO_2} + S_{CO}) \qquad (6.6)$$

n_{23} is the stoichiometric coefficient for the formation of phthalic anhydride, phthalide and ortho-toluic acid from ortho-tolualdehyde. It is calculated from the experimental selectivity data as follows:

$$n_{23} = \left(\frac{1}{2} S_{OTAc} + S_{PI} + 2 S_{PAA}\right) / \left(S_{OTAc} + S_{PI} + S_{PAA}\right) \quad (6.7)$$

2. Reaction Equations for the Reaction Scheme in Figure 6.2 (TiO_2 Catalyst)

$$-\frac{dC_1}{dt} = k_a C_a (k_{12} + k_5) C_1 / D \quad (6.8)$$

$$\frac{dC_2}{dt} = k_a C_a (k_{12} C_1 - k_5 C_2 - k_{23} C_2) / D \quad (6.9)$$

$$\frac{dC_3}{dt} = k_a C_a (k_{23} C_2 - k_{34} C_3) / D \quad (6.10)$$

$$\frac{dC_4}{dt} = k_a C_a k_{34} C_3 / D \quad (6.11)$$

$$\frac{dC_5}{dt} = 8 k_a C_a k_5 (C_1 + C_2) / D \quad (6.12)$$

where $D = k_a C_a + n k_5 C_1 + (n-1) k_5 C_2 + k_{23} C_2 + k_{34} C_3 + k_{12} C_1$ (6.13)

and n is the stoichiometric coefficient for the formation of "carbon oxides".

No attempt has been made to discriminate between models since it is impossible to distinguish between the S.S.A.M. and Redox mechanisms by kinetic measurements alone. No sequential design of experiments has been used since no parameter estimates have been reported for the ranges of conversions used in this study. Moreover, the adequacy of the model to describe

the reaction over this range of conversions has not been established. If major inadequacies of the models do not become apparent from this initial study, then future experiments can be performed to obtain better parameter estimates in these models. The parameter estimates obtained here would then be useful in establishing the best experiments to be performed for their estimation. This study may also suggest modification or additional effects that need to be included in the model; if these effects can be modelled in different ways, then model discrimination experiments can be performed to evaluate the "best" model to describe them. For those reasons, experiments were conducted according to factorial and partial factorial designs which covered the range of independent variables, temperature, xylene concentation, oxygen concentration and W/Fa_o values to give a wide range of operating conditions around those normally employed in industrial practice.

6.3. Statistical Methods Employed in Parameter Estimation

Hunter (H5) has given an excellent review of the methods available for the estimation of parameter from multi-response data. In this work the method proposed by Box and Draper (B12) has been adopted and this is the only method that will be reviewed here.

Box and Draper have employed Bayes' Theorem to provide a criterion for the "best" parameter estimates given multiple response data from an experiment. Their analysis assumes that

the parameters have a locally uniform prior probability distribution in the region of high likelihood. They show that the best estimates of the parameters, $\hat{\theta}$ are obtained when the determinant

$$|\underset{\sim}{S}| = \left| \sum_{u=1}^{n} (\underset{\sim}{y}_u - \underset{\sim}{\eta}(\underset{\sim}{\xi}_u, \underset{\sim}{\theta}))(\underset{\sim}{y}_u - \underset{\sim}{\eta}(\underset{\sim}{\xi}_u, \underset{\sim}{\theta}))^1 \right| \qquad (6.14)$$

is minimized with respect to the parameters, $\underset{\sim}{\theta}$. In this expression

$$\underset{rx1}{\underset{\sim}{\eta}}(\xi_u, \underset{\sim}{\theta}) = \{\eta_j(\xi_u, \underset{\sim}{\theta})\} \qquad \begin{matrix} u = 1, 2 \ldots n \text{ experiments} \\ j = 1, 2 \ldots r \text{ responses} \end{matrix}$$

is the expected value of the responses assuming that the model is correct. This criterion is equivalent to the well-known minimization of the sum of the squares and the sum of the products of the differences between the observed and predicted responses, properly weighted by the appropriate elements of the inverse of the variance covariance matrix. In the Box-Draper method the true variance-covariance matrix is replaced by its maximum likelihood estimate.

To apply any of these methods for parameter estimation the following assumptions are made:

(i) Each of the responses is normally distributed and has a constant variance-covariance matrix over the entire response surface, and

(ii) Each of the observed responses, y_j, for one experiment is independent of the observed responses for another experiment.

The latter requirement is easily satisfied by experimental design; the former requires analysis as follows.

There are two ways to establish that the variance covariance matrix is constant over the entire response surface. Both rely on a transformation of the observed response, such as:

$$y_j^T = y_j^\lambda \qquad \lambda \neq 0 \tag{6.15}$$

$$y_j^T = \ln y_j \qquad \lambda = 0 \tag{6.16}$$

Each response need not be transformed in the same way.

Box and Cox (B13) have derived a criterion which not only ensures constancy of the variance-covariance matrix but ensures that that the errors are normally distributed. The method requires minimizing the residual sum of squares $S(\underline{\lambda}, \underline{z})$ with respect to the transformation parameters, $\underline{\lambda}$, where in the case of a power transformation

$$z_j = \left\{\frac{y_j^\lambda}{\dot{y}^{\lambda-1}}\right\} \qquad j = 1, 2 \ldots r \qquad \lambda \neq 0 \tag{6.17}$$

and in the case of a logarithmic transformation

$$z_j = \{\dot{y}_j \ln(y_j)\} \qquad j = 1, 2 \ldots r \qquad \lambda = 0 \tag{6.18}$$

where $\dot{y}$ is the geometric mean of the observations. This method thus requires the best estimates of the parameters to be evaluated for each transformation to allow the residual sum

of squares to be evaluated. Since the transformation of each response in the multiresponse case need not be the same, a search for the minimum residual sum of squares over the entire transformation parameter space must be performed. The computational task is therefore quite formidable.

The other method, although less rigorous, is to replicate experiments over the entire range of operating conditions $\underline{x}$. At each of these conditions an estimate of the variance-covariance matrix can be obtained; a pooled estimate of the variances of all the responses can also be determined. The individual and pooled variance-covariance estimates can be tested to determine if they are constant within a given confidence region. If they are not the transformations suggested by Equations (6.16) and (6.17) can be tried until the statistical tests suggest that constancy of the variance-covariance matrix has been achieved. In this study this method has been adopted. However, the treatment is not completely rigorous. The Box-Draper method assumes constancy of the variance-covariance matrix. The transformations have only been tested for constancy of variance.

Box et al. (B14) have recently discussed some of the problems associated with fitting multiresponse models. In particular, they have discussed the problem of having linear dependencies in the data. Such linear dependencies occur when all the responses are not determined independently. For example, one response may be calculated from the other responses and the stoichiometry of the system. Another source of error

is due to the normalization of the data. These practices can lead to considerable differences between the calculated parameters and the "best-fit" parameters.

6.4. Experimental Program

(1.) 902 Catalyst

Experimental techniques used to obtain steady-state data were discussed in detail in Chapter 4. In all, 46 experiments were conducted on this catalyst. The first set was done as a factorial design considering two levels of temperature orthoxylene concentration, oxygen concentration and total gas flow rate. In addition, six experiments were conducted in a random fashion at the centre-point conditions at various times throughout the program in order to monitor the catalyst activity. The 2^4 level factorial design was used to determine the relative magnitudes of the effects of orthoxylene and oxygen concentrations on the rate of orthoxylene oxidation. The results of these experiments are summarized in Table 6.1.

At the completion of the initial 24 experiments it was deemed necessary to conduct a further set of experiments at five different experimental conditions. These were replicated at least four times. These replicates were done in a random fashion. These experiments were performed to establish the constancy of the variances of the responses over the range of experimental conditions and observed responses. The main concern was with the carbon dioxide and phthalic anhydride/phthalide/orthotoluic acid responses, since over some experimental conditions these

Table 6.1. Steady-State SO_2 Reaction Data used in Model Fitting

Experiment Number	Experimental Conditions (Settings)				Exit Concentration gm.moles litre x10^9				Carbon Balance
	Temperature (°C)	Xylene Level %	Oxygen Level %	Total Flow (cc/min.)	O-xylene	OTA	PAA/PI/OTAc	CO/CO_2	
1	350	1.5	20	200	260.5	38.65	3.688	36.45	.934
2	330	1	10	100	198.0	7.943	1.527	14.85	.945
3	330	1	10	300	232.3	2.780	0.1204	3.015	1.000
4	350	1.5	20	200	284.5	28.60	1.007	28.52	.960
5	370	1	10	100	124.8	50.63	7.175	71.94	.937
6	370	1	30	100	42.01	96.63	35.75	215.4	.906
7	370	2	10	300	605.7	25.37	0.5468	32.89	.877
8	370	2	30	100	323.7	148.6	20.96	211.2	.972
9	330	1	30	100	304.3	21.87	1.617	42.22	1.020
10	350	1.5	20	200	256.3	31.50	1.585	34.76	.976
11	370	1	30	300	139.5	67.61	6.876	65.35	.962
12	330	2	10	100	392.4	3.989	0	7.502	.946
13	370	1.5	20	250	232.5	52.65	5.102	54.15	.939
14	350	1.5	20	200	246.1	38.91	4.039	32.8	.874
15	370	2	10	100	288.0	41.55	3.959	71.45	.991
16	370	2	10	100	298.1	46.32	2.443	69.67	1.01
17	330	1	30	300	215.7	12.46	0.3165	14.49	.990
18	370	2	30	300	374.2	75.48	4.607	84.49	.965

(Continued)

Table 6.1 continued

19	330	2	10	300	410.7	2.105	0	13.65	.834
20	350	1.5	20	200	306.8	21.28	0.4320	29.76	.999
21	370	1	10	300	183.2	23.69	0.8930	25.72	.991
22	350	1.5	20	200	279.3	23.82	0.9863	31.14	.976
23	330	2	30	100	363.5	17.49	0	39.42	.966
24	330	2	30	300	477.1	7.418	0	15.13	.992

* Carbon atoms from product analysis/carbon atoms from inlet analysis.

! Any zero concentrations have taken a value of 10^{-7} gm. moles/litre for calculation purposes.

Table 6.2 Steady-State 902 Reaction Data used in Model Fitting and to Evaluate Variance-Covariance Matrix

Replicated Condition	Experiment Number	Experimental Conditions (Settings)				Exit Concentrations gm.mole/litre x10.5				Carbon Balance
		Temperature (°C)	Xylene Level %	Oxygen Level %	Total Flow (cc/min)	O-xylene	OTA	PAA/PI/OTAc	CO/CO_2	
1	25	350	1.5	20	200	273.2	27.62	.3427	33.03	.989
1	26	350	1.5	20	200	286.8	23.88	.3177	30.84	.986
1	35	350	1.5	20	200	309.9	18.06	.1935	27.56	.946
1	39	350	1.5	20	200	292.2	19.73	.2487	32.62	.968
1	43	350	1.5	20	200	289.7	23.49	.2592	40.52	.962
2	27	330	1.5	20	100	311.2	5.673	.2407	21.43	.972
2	28	330	1.5	20	100	308.2	3.586	.2214	13.68	.957
2	30	330	1.5	20	100	315.6	4.852	.2665	17.70	.991
2	31	330	1.5	20	100	301.1	4.155	.2784	20.60	.948
2	33	330	1.5	20	100	320.8	4.741	.2552	18.54	.922
3	38	350	1.5	20	100	297.6	33.01	1.028	58.74	1.01
3	41	350	1.5	20	100	274.3	31.80	1.048	56.54	.991
3	42	350	1.5	20	100	276.1	31.59	.9900	55.51	.942
3	46	350	1.5	20	100	270.4	35.54	1.359	59.56	1.010
4	32	370	1.5	20	100	204.2	72.96	4.421	112.8	.958
4	34	370	1.5	20	100	215.6	72.08	4.582	113.6	.956
4	40	370	1.5	20	100	200.9	72.08	4.582	110.9	.954
4	45	370	1.5	20	100	206.8	70.99	4.256	109.9	.941
5	29	390	1.5	20	100	126.6	99.98	15.85	226.8	.911
5	36	390	1.5	20	100	131.7	117.3	18.60	266.9	.880
5	37	390	1.5	20	100	126.2	112.8	18.39	246.9	.912
5	44	390	1.5	20	100	125.1	106.0	15.48	232.8	.962

responses were quite low and the errors may have been quite different in these situations. The difficulty of accurately measuring these low concentrations has already been discussed. The results of the replicated experiments are presented in Table 6.2.

The variance-covariance matrices were calculated for each of the five data sets in Table 6.2. The pooled variance-covariance matrix was then determined, for the 5 replicated conditions. The computer program for determining the variance-covariance matrices is listed in Appendix I . The variances for the four responses were tested by the method proposed by Bartlett (B15) to detect if there were significant differences between the variances for the different conditions. This testing was done to determine if the variances were essentially constant over the range of conversions studied in the 24 factorial design. The method compares the logarithm of the average variance with the sum of the logarithms of the separate variances. The test assumes the hypothesis

$$H_o: \sigma_1^2 = \sigma_2^2 = \ldots \sigma_n^2 \ldots = \sigma^2.$$

If this hypothesis is correct then the pooled variance

$$S^2 = \frac{1}{\left(\sum_{i=1}^{n} p_i - n\right)} \sum_{i=1}^{n} (p_i - 1)\, S_i^2 \qquad (6.19)$$

(where p_i is the number of replicates in a sample i and n is the number of samples.)

has a χ^2 distribution with a mean of σ^2 and ν degrees of freedom

where $\nu = \sum_{i=1}^{n} \nu_i$. Bartlett showed that

$$\Lambda = -\frac{1}{C} \sum_{i=1}^{n} p_i \ln \left(\frac{S_i^2}{S^2}\right) \qquad (6.20)$$

where $C = 1 + \frac{1}{3(n-1)} \left(\sum_{i=1}^{n} \frac{1}{p_i} - \frac{1}{\sum_{i=1}^{n} p_i} \right)$ (6.21)

has an approximate χ^2 distribution with (n-1) degrees of freedom. If the value of Λ calculated by Equation (6.20) exceeds the value of $\chi^2_{1-\alpha}$ for (n-1) degrees of freedom, the hypothesis that $\sigma_1^2 = \sigma_2^2 = \sigma^2$ is rejected.

In this study we had 5 different replicated conditions. Therefore it was necessary to compare the Λ values for each response with $\chi^2_{1-.05}$. For 4 degrees of freedom ($\chi^2 = 9.49$). The values of Λ were determined for transformations of the power form and the logarithmic transformation given by Equations (6.15) and (6.16) respectively. The exponents used in the power transformation were -1, $\frac{1}{2}$, 1, $\frac{3}{2}$ and 2. It was found that the ortho-xylene response had homogeneity of variance over the range of concentrations studied. However the variances of the other three responses were not constant and so transformations were necessary to produce homogeneity of variance in these cases. For the carbon oxides and orthotolualdehyde responses the best transformation tried was the square root of the response. In the case of the phthalic anhydride/phthalide/orthotoluic acid

Table 6.3 Steady-State TiO_2 Reaction Data used in Model Fitting

Experiment Number	Experimental Conditions (Settings)				Exit Concentrations gm. moles/litre x 10^6					Carbon Balance
	Temperature (^oC)	Xylene Level %	Oxygen Level %	Total Flow (cc/min.)	Xylene	OTA	PI	PAA	CO/CO_2	
6	370	1.5	20	200	204.3	11.55	4.692	66.58	88.77	1.000
7	350	1	30	300	153.8	9.566	4.101	49.50	80.22	.975
8	390	2	30	300	310.3	20.19	5.532	58.16	106.5	.992
9	390	2	10	100	273.5	13.52	5.466	46.08	64.93	.973
10	390	1	30	100	60.32	5.031	5.630	101.9	165.2	1.01
11	390	1	10	300	165.3	8.914	3.916	27.16	26.60	.961
12	350	1	10	100	130.5	6.500	4.811	92.95	109.4	1.03
13	350	2	30	100	226.9	12.65	6.978	144.7	245.9	1.03
14	350	2	10	300	417.1	14.93	5.210	36.49	35.77	1.00

response the logarithmic transformation produced constancy of variance.

(2.) TiO_2 Catalyst

Only a limited experimental program was conducted on the TiO_2 catalyst since it was not suitable for use in the transported bed reactor. The steady-state concentration data that were used to estimate parameters in the model described above are presented in Table 6.3. Since only nine experiments were performed at truly steady-state conditions, the number of experimental conditions covered is small; however, with five observed independent responses for each experiment there are sufficient degrees of freedom to provide reasonable estimates of the eleven parameters in the model. It is expected that more experiments would have to be performed to obtain the minimum confidence region for the parameters from this experimental system.

6.5 Parameter Estimation

(1.) 902 Catalyst

Parameter estimation was carried out on the reaction data for experiments 1 to 46 in Tables 6.1 and 6.2 using the model described by Equations (6.1) through (6.5). Initially, parameters were estimated without transforming the responses; parameters were then estimated using the transformed responses to evaluate the effect of the transformations on the parameter estimates. A problem was encountered in the estimation method due to the fact that a bias was placed in the estimates because

the carbon balances in almost all cases were less than unity. As indicated earlier, the apparent loss of carbon can be attributed to tar formation when using the silica-gel supported catalysts. An immediate solution to this problem would appear to be to divide all responses by the carbon balance ratio so that the carbon balance for all experiments would be unity. However, this type of normalization has been reported by Box et al. (B14) to build a linear dependency into the data which would then result in the Box and Draper estimation procedure converging to nonsensical values. Therefore, it was decided to modify the kinetic model by taking tar formation into account.

Since no model for tar formation can be easily postulated on theoretical grounds it was decided to use the simplest model which could be suggested by the experimental observations. Since the experiments had been performed according to a factorial design, it was very easy to evaluate a linear model assuming the following model

$$f_{T_u} = a\,T_u + b\,C_{Aou} + d\,C_{O_2}u + f\,F_{Tu} + \varepsilon_u \qquad (6.22)$$

where f_{Tu} is the amount of carbon, as tar, obtained from the loss of carbon in experiment u; $T_u, C_{Aou}, C_{O_2}u, F_{Tu}$ are the temperature and inlet concentrations of orthoxylene and oxygen and total flow respectively. The parameters a, b, d and f indicate the effects of the respective experimental conditions. Table 6.4 presents these effects calculated from the carbon balance data in Table 6.1.

Table 6.4. Effects of Independent Variables on Carbon Balance Ratio

Effect Due to	Effect	95% Confidence Interval
Temperature	-0.0262	± 0.0383
Xylene Concentration	-0.0087	± 0.0383
Oxygen Concentration	+0.0144	± 0.0383
Total Flow	+0.0059	± 0.0383

To test if these effects were significant compared with experimental error the 95% confidence intervals were determined for the effects. The confidence intervals were found by estimating the variance for the tar formation from the six centre point experiments in Table 6.1 and the five which are given in Table 6.2. The variance was estimated to be 11.877×10^{-4}. Therefore the 95% confidence intervals for the effects are;

$$\pm \sqrt{\frac{S^2}{4}} \cdot t_{0.95}$$

where $t_{0.95}$ for 10 degrees of freedom = 2.228

∴ The confidence intervals are ± 0.0383. Hence the 95% confidence intervals for all four effects include zero so that the assumption that tar formation is independent of temperature, orthoxylene concentration and oxygen concentration and flow is valid. Therefore tar formation can be described by a zero order rate constant which does not depend on temperature. The simplest model that can be assumed is that the tar formation occurs solely from the cracking of xylene; hence the only

modification necessary to the reaction equations is to incorporate the zero order rate constant in Equation (6.1) which then becomes

$$-\frac{dC_1}{dt} = k_a C_a ((k_1 + k_5)C_1 - k_6)/D \qquad (6.1a)$$

Preliminary Parameter Estimates

Having decided to adopt a model described by Equations (6.1a) through (6.5), it was necessary to obtain preliminary estimates of the pre-exponential factors and activation energies associated with rate constants k_a, k_{12}, k_{23} and k_5 and an estimate of k_6. Reasonable initial estimates of these parameters should minimize the computer time required to evaluate the "best" estimates that can be obtained from the experimental data. Analysis of the experimental design in Table 6.1 shows that the overall rate of conversion of orthoxylene is virtually independent of the inlet concentration of orthoxylene in the range 1 to 2%. However, there is a strong dependency on the inlet oxygen concentration. Therefore for the purposes of preliminary parameter estimates it was assumed that in Equation (2.11) which describes the overall conversion of xylene, that

$n k_r C_r >> k_a C_a$ i.e. $\theta \to 0$

$$r_r = \frac{k_a C_a k_r C_r}{k_a C_a + n k_r C_r} \qquad (2.11)$$

$$r_r = \frac{k_a C_a}{n} \qquad (6.23)$$

That is the rate of conversion of orthoxylene is first order with respect to oxygen and zero order with respect to orthoxylene. (The changing order of reaction with changing experimental conditions for this mechanism has been well described elsewhere (M7). The oxidation of orthoxylene by a single step reaction in a plug flow reactor is given by

$$\frac{W}{F_{ao}} = \int_0^{x_{out}} -\frac{dx}{r_r} = \int_0^{x_{out}} \frac{-dx}{\frac{k_a C_a}{n}} \qquad (6.24)$$

$$\text{But } C_a = C_{ao} - C_{ao}\left(n.x.\frac{Cr_o}{C_{ao}}\right) \qquad (6.25)$$

Equation (6.24) becomes

$$\frac{W}{F_{ao}} = \int_0^{x_{out}} \frac{-dx}{\frac{k_a C_{ao}}{n}\left(1-X\frac{nCr_o}{C_{ao}}\right)} \qquad (6.26)$$

Integrating between $x = 0$ and $x = x_{out}$ gives

$$\frac{W}{F_{ao}} = -\frac{1}{k_a Cr_o}\log\left(1-x_{out}\left(\frac{n\,Cr_o}{C_{ao}}\right)\right) \qquad (6.27)$$

$$k_a = -\frac{F_{ao}}{W\,Cr_o}\log\left(1-x_{out}\left(\frac{n\,Cr_o}{C_{ao}}\right)\right) \qquad (6.28)$$

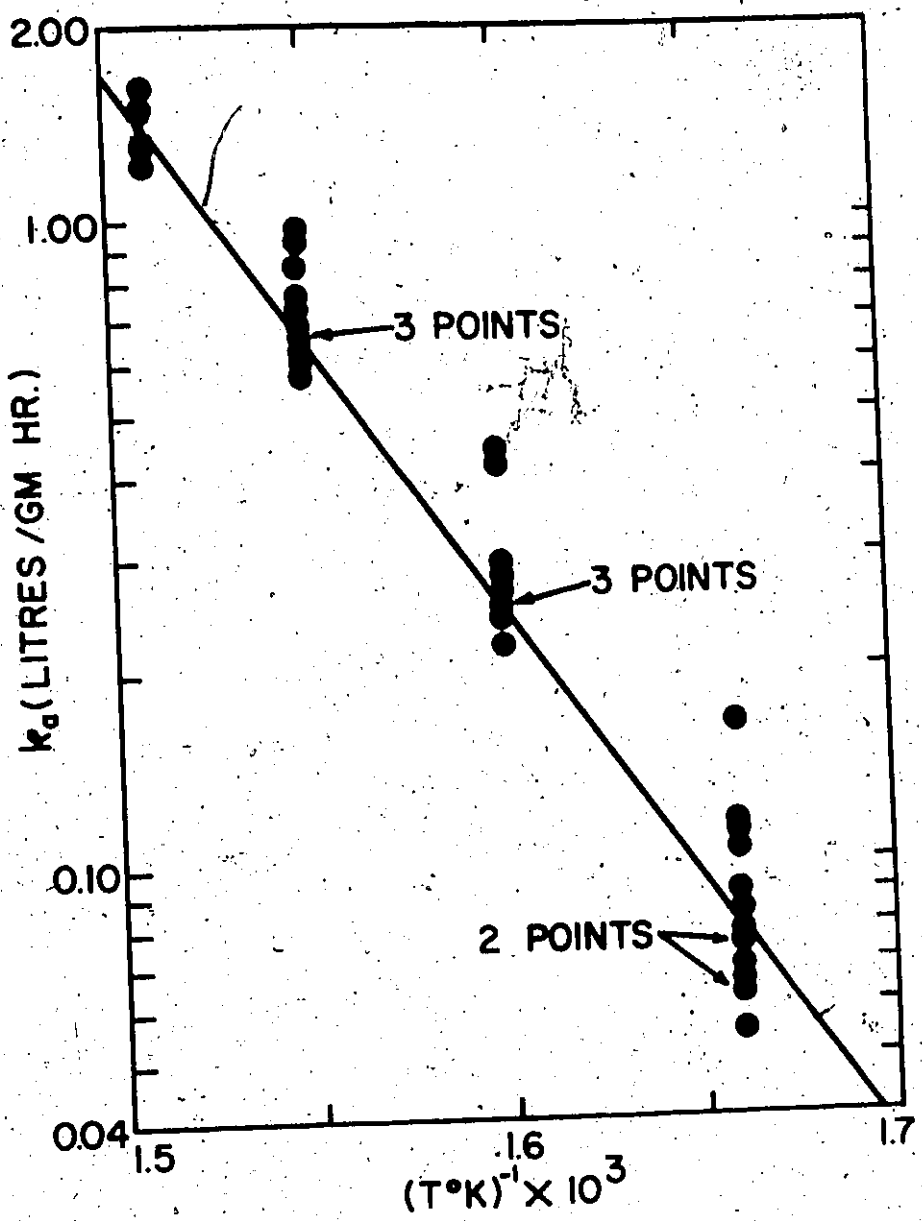

Figure 6.3. Arrhenius Plot of k_a Values.

Values of k_a were obtained directly from Equation (6.28) for the 46 experiments conducted on the 902 catalysts. These constants have been plotted against reciprocal temperature (^{0}K) in Figure 6.3 so that an estimate of E_a could be obtained. The fit was made by eye since the values of K_a and E_a are only used as preliminary extimates. The preliminary estimates of K_a and E_a are 1.0×10^{13} litres/gm.hr and 38,000 cals/gm mole respectively.

In order to obtain preliminary estimates of K_{12}, K_{23}, K_5, E_{12}, E_{23}, and E_5, that is, the pre-exponential factors, and activation energies for the rate constants, the value of k_r obtained from the analysis of the transported bed data in Chapter 7 has been used. In the analysis of the transported bed data it has been assumed that at short contact times $0 \rightarrow 1$ since at contact times of the order of 1/2 second the reaction should not be limited by the oxygen available. The first order rate constants for orthoxylene conversion are plotted against reciprocal temperature in Figure 7.7. From this plot the values of K_r and E_r have been determined to be $5 \times 10^7 \frac{\text{litres}}{\text{gm.hr.}}$ and 16,700 cals/gm. mole respectively. Preliminary estimates of K_{12} and K_5 were determined by proportioning the value K_r according to the selectivities of orthotolualdehyde and carbon oxides observed in the experiments. A similar approach was used to estimate K_{23}.

The preliminary estimate of k_6, the zero-order rate constant for the conversion of orthoxylene to tarry material was obtained by calculating the average carbon balance ratio over the 46 experiments. The mean value was found to be 0.956,

indicating that approximately 4 percent of the xylene fed is converted to tars. At 350°C, the centre point condition, tar formation accounts for around 30 percent of the xylene converted therefore a preliminary value of $k_6 = K_6$ was calculated according to $\frac{1}{2}(k_{12} + k_5)_{350°C} Cr_o$ where Cr_o is typically 4×10^{-4} gm. moles/litre. Therefore a reasonable starting estimate for K_6 appeared to be 1×10^{-2} gm. moles/gm.hr.

Parameters K_{12}, K_{23}, K_5, K_6, K_a, E_{12}, E_{23}, E_5 and E_a were then estimated using the Box-Draper criterion. The determinant indicated in Equation (6.14) was minimized by the Nelder-Meade expanding Simplex optimization routine (N2). The independent responses used in evaluating this determinant were the concentrations orthoxylene, orthotolualdehyde, phthalic anhydride/phthalide/orthotoluic acid and carbon oxides. The Simplex method has been recommended by Box (B16) for the simultaneous estimation of large numbers of parameters. Listings of the computer programs used in the parameter estimation are given in Appendix I. The method is summarized below:

(i) Punched data including reaction conditions of temperature, pressure, pressure drop across the catalyst bed, flows, weight of catalyst and experimental inlet and exit concentrations are obtained from a program that reduces raw data that includes the chromatographic areas from the electronic integrator to concentrations of components as mole functions. The details of this transformation are presented in Chapter 3.

(ii) These data along with the preliminary estimates of the parameters are read into the main program. The Simplex

optimization routine is then called. Normalized parameters are used in the Simplex method. That is, estimates are obtained relative to the initial values which are unity.

(iii) The Simplex routine calls subroutine Object which converts the normalized parameters to the values used in the rate equations. The pre-exponential factors are reparameterized according to the method recommended by Hunter and Atkinson (H6) in order to reduce the extent of correlation between the K's and the E's. In this case the rate constants were reparameterized according to a base temperature of 350°C.

$$\text{Therefore} \qquad K_a = K_a^* \, e^{-\frac{E_a}{R}\left(\frac{1}{T} - \frac{1}{623}\right)} \quad \text{etc.} \qquad (6.29)$$

$$\text{where} \qquad K_a^* = K_a \, e^{-E/623xR} \qquad (6.30)$$

That is, values of K_a^*, K_{12}^* ... K_5^* were estimated instead of K_a, K_{12} ... K_5.

(iv) Object then calls a Merson modification of the Runge-Kutta method to integrate the rate equations numerically.

(v) When all the experimental conditions have been analyzed in this manner, the determinant is evaluated in Subroutine Deter, and the procedure is repeated.

Plots of residuals for all responses are plotted against the independent variables, temperature, orthoxylene and oxygen inlet concentrations.

Parameters estimated by the above method are presented

in Table 6.5.

The effect of the transformation of the responses on the parameter estimates was demonstrated by carrying out this parameter estimation procedure using the transformations indicated in Section 6.4. The corresponding parameters are presented in Table 6.5.

Table 6.5. Rate Parameters for Orthoxylene Oxidation on 902 Catalyst

Parameter	Value	
	Untransformed case	Transformed case
E_a	34,052	35,800
K_a	2.45×10^{11}	9.14×10^{11}
E_{12}	21,990	21,842
K_{12}	5.04×10^{9}	4.26×10^{9}
E_{23}	1,825	2,842
K_{23}	3.82×10^{2}	7.44×10^{2}
E_5	20,814	17,658
K_5	3.05×10^{8}	2.49×10^{8}
K_6	9.13×10^{-3}	8.43×10^{-3}

Residuals are plotted for all four responses against the independent variables temperature, orthoxylene inlet concentration, oxygen inlet concentration and run number in Figures 6.4 to 6.7. In addition, predicted concentrations of orthoxylene, orthotolualdehyde, phthalic anhydride/phthalide/orthotoluic acid and CO/CO_2 are plotted against the measured

In Figures 6.4 to 6.7 the following symbols have been used

- ⊙ O-xylene
- ▽ O-tolualdehyde
- ◇ PAA/PI/OTAc
- △ CO_2/CO

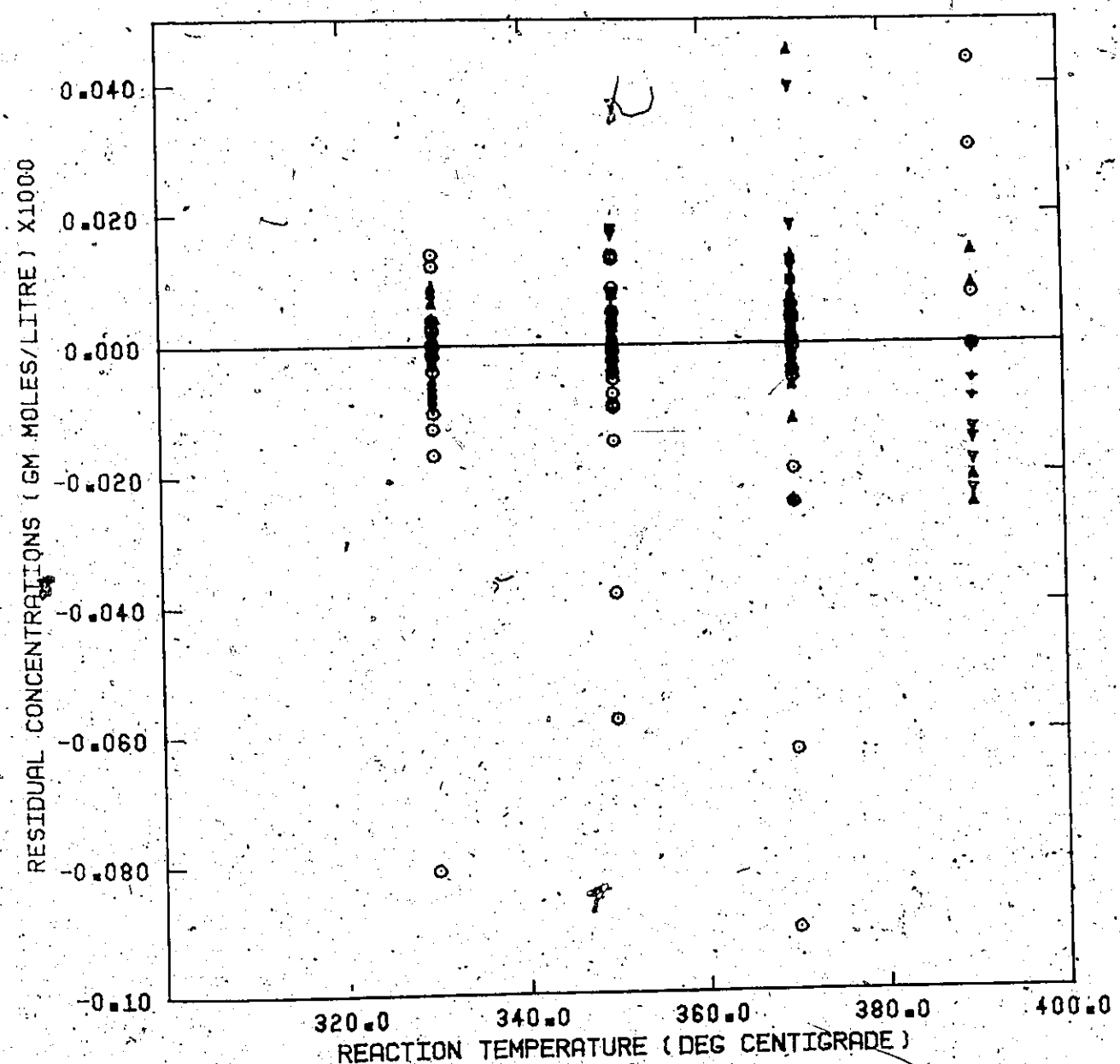

Figure 6.4. Residual Plot - 002 Catalyst.

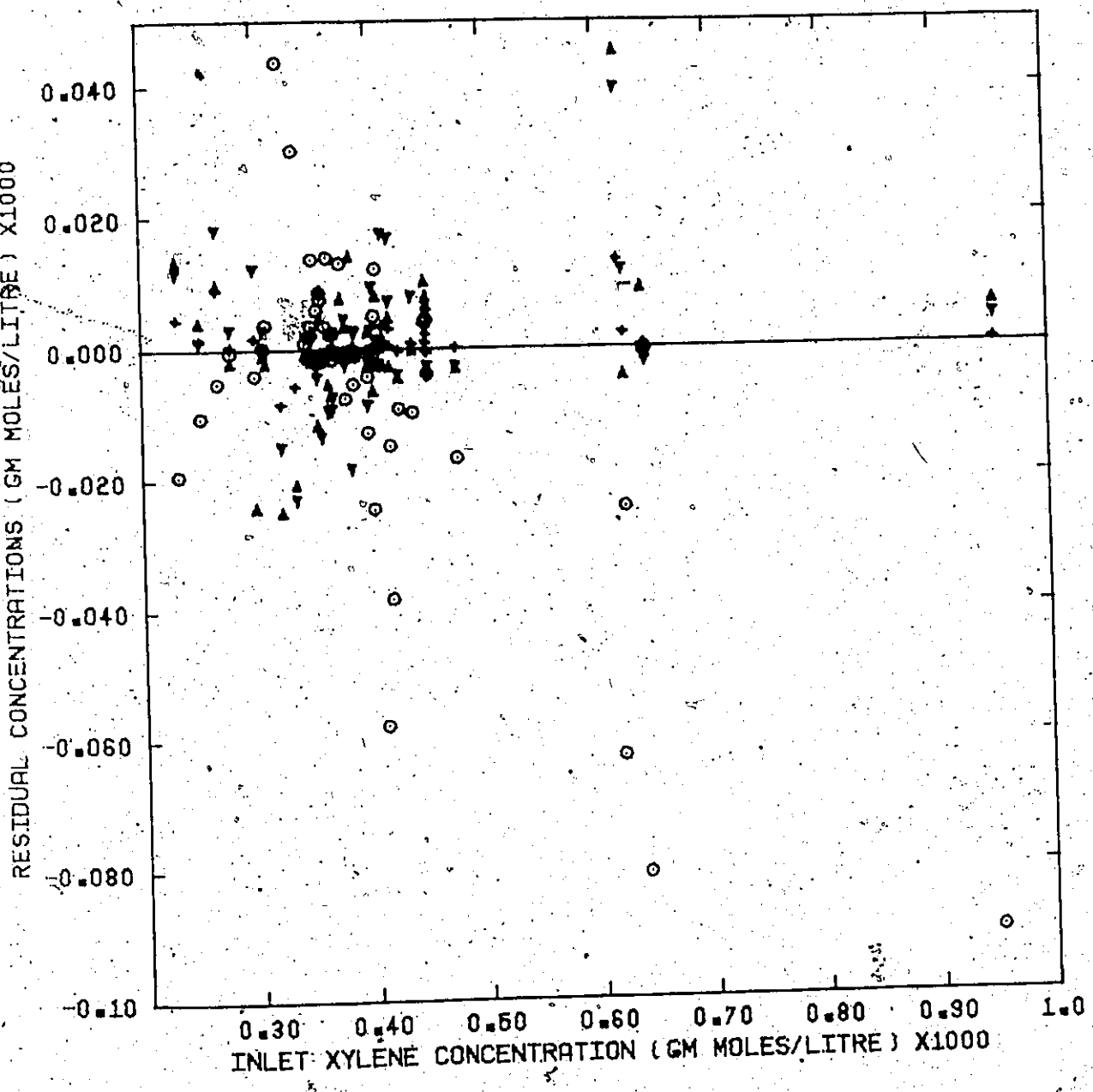

Figure 6.5. Residual Plot - 902 Catalyst.

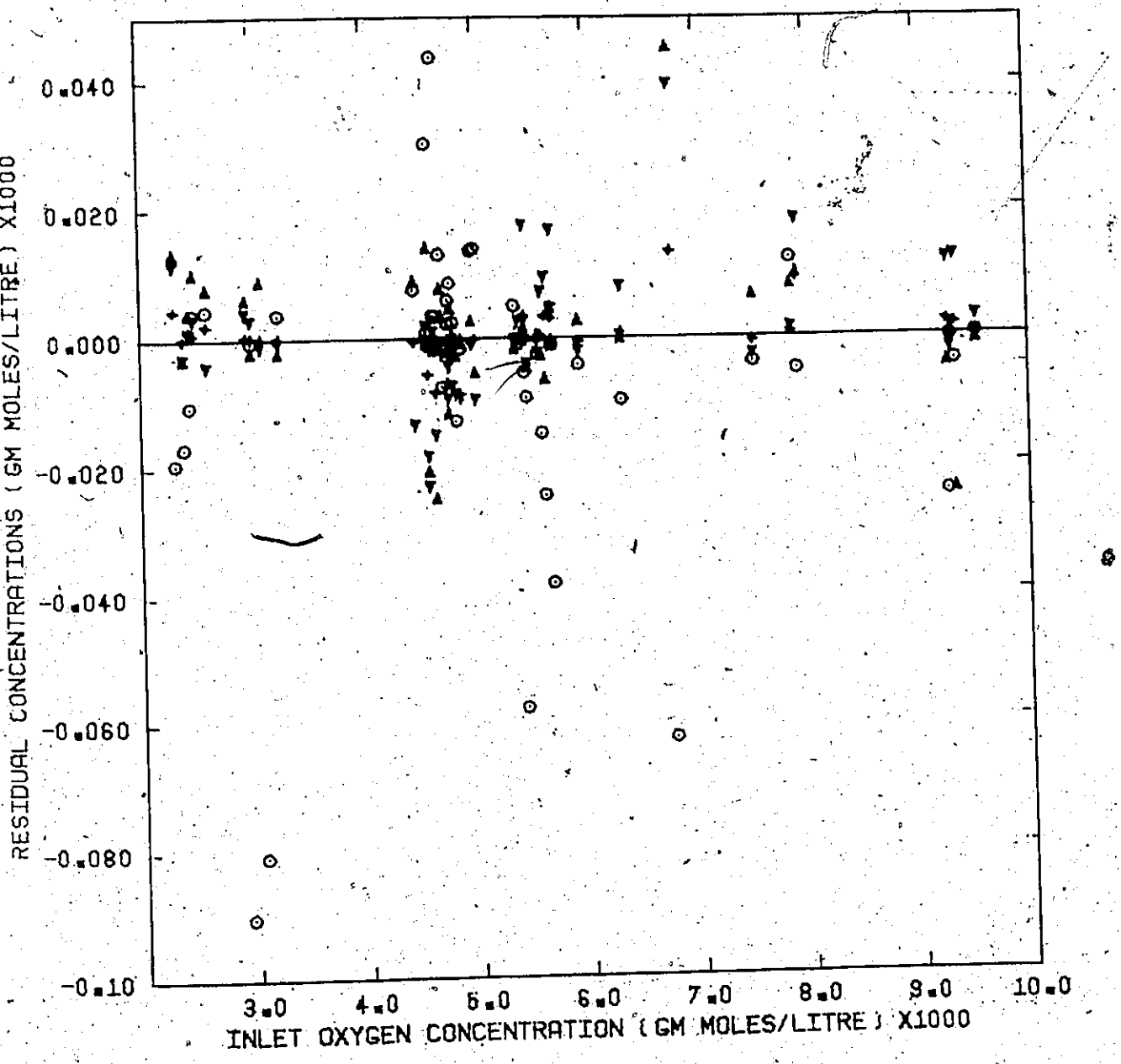

Figure 6.6. Residual Plot - 902 Catalyst.

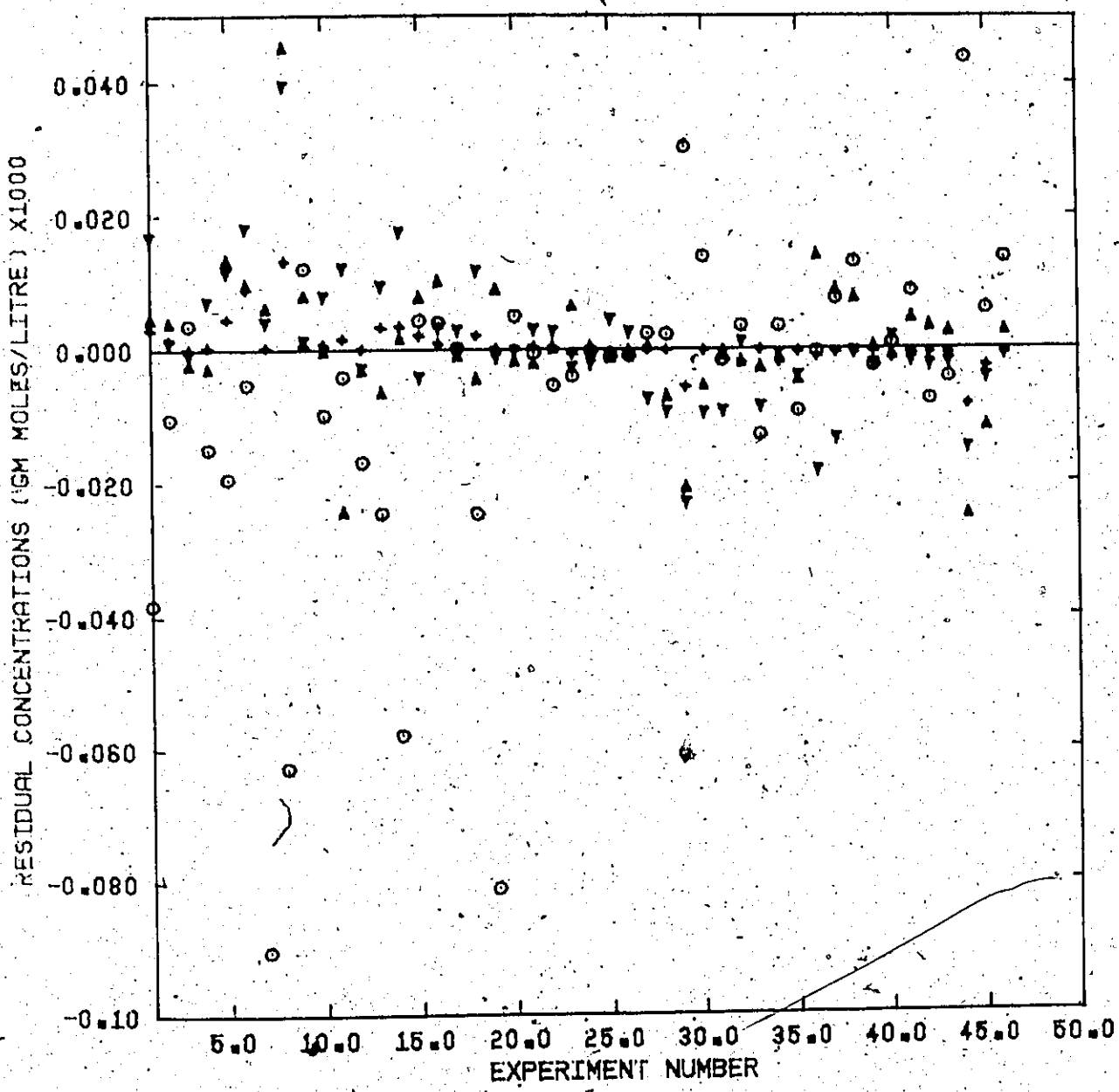

Figure 6.7. Residual Plot - 902 Catalyst.

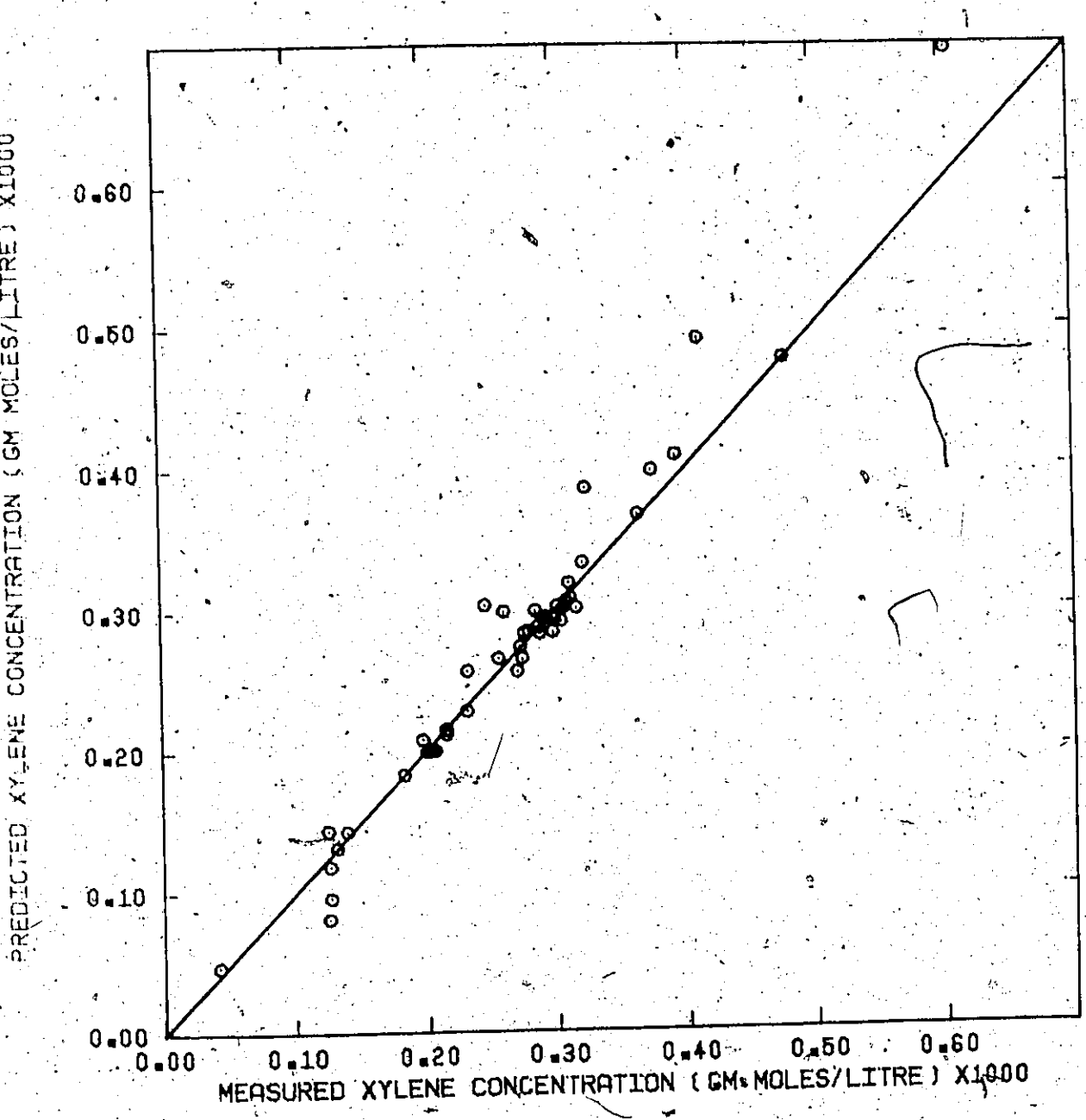

Figure 6.8. Predicted Versus Measured O-xylene Concentrations - 902 Catalyst.

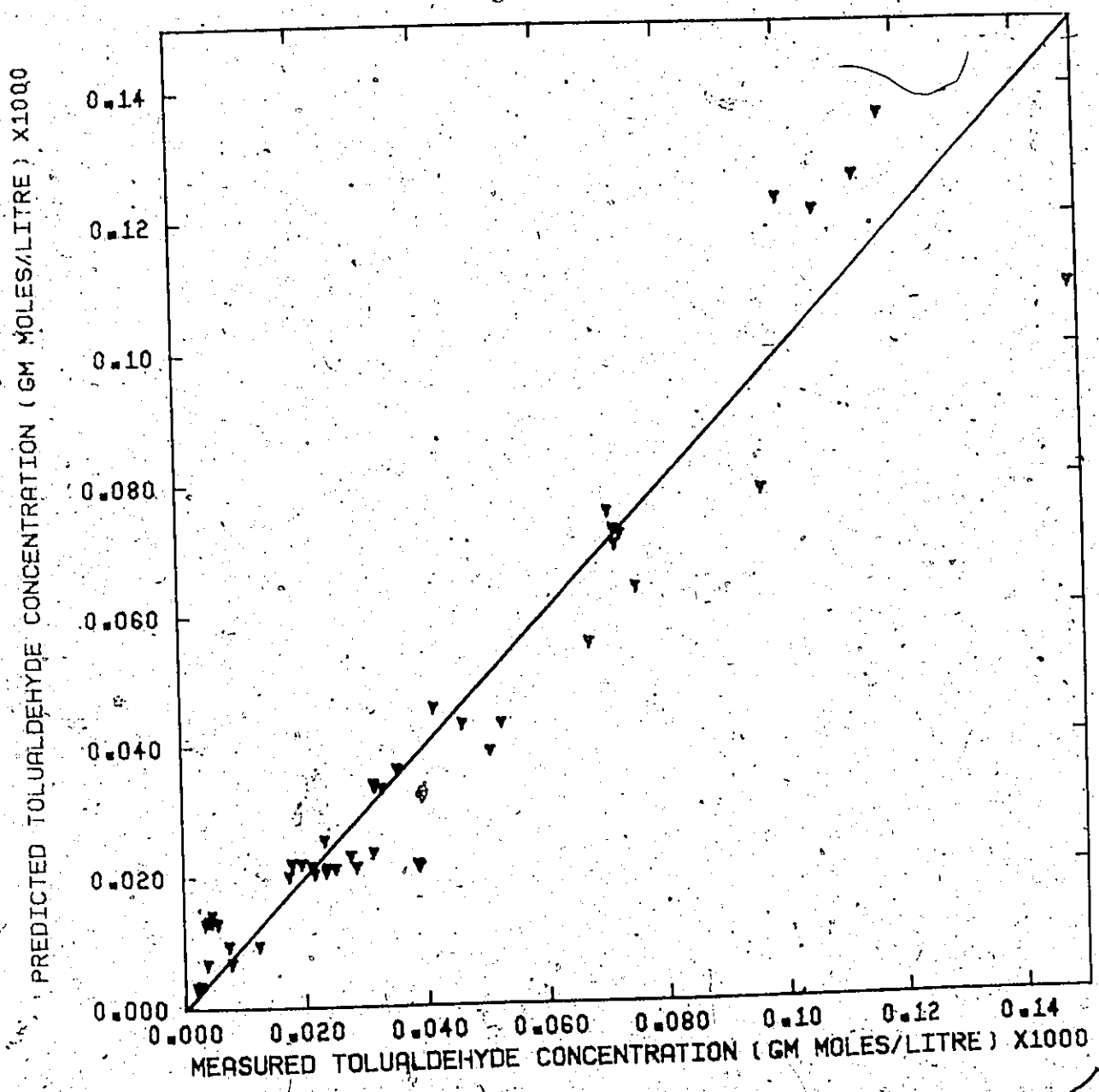

Figure 6.9. Predicted Versus Measured O-tolualdehyde Concentrations - 902 Catalyst.

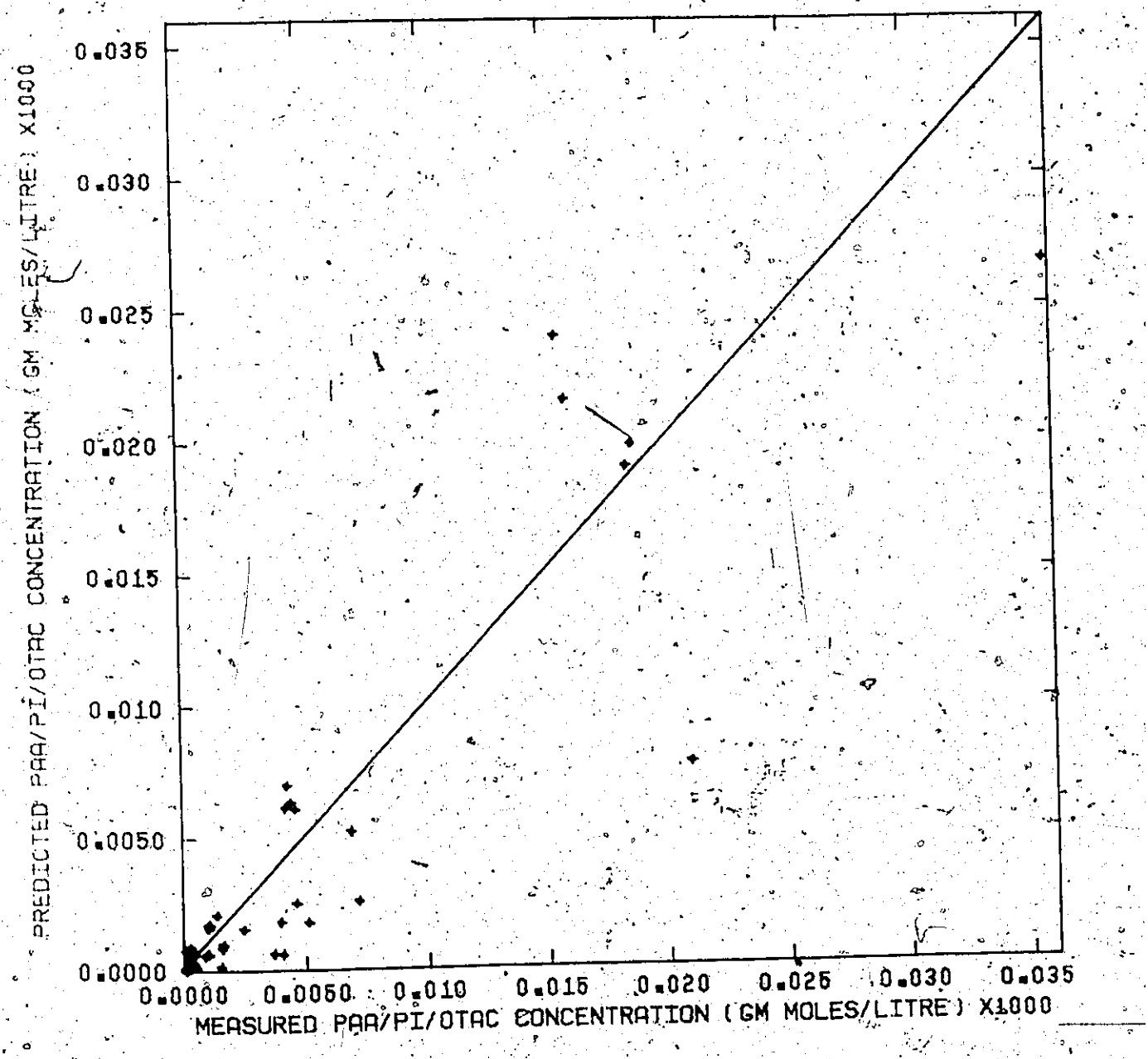

Figure 6.10. Predicted Versus Measured PAA/PI/OTAC Concentrations - 902 Catalyst.

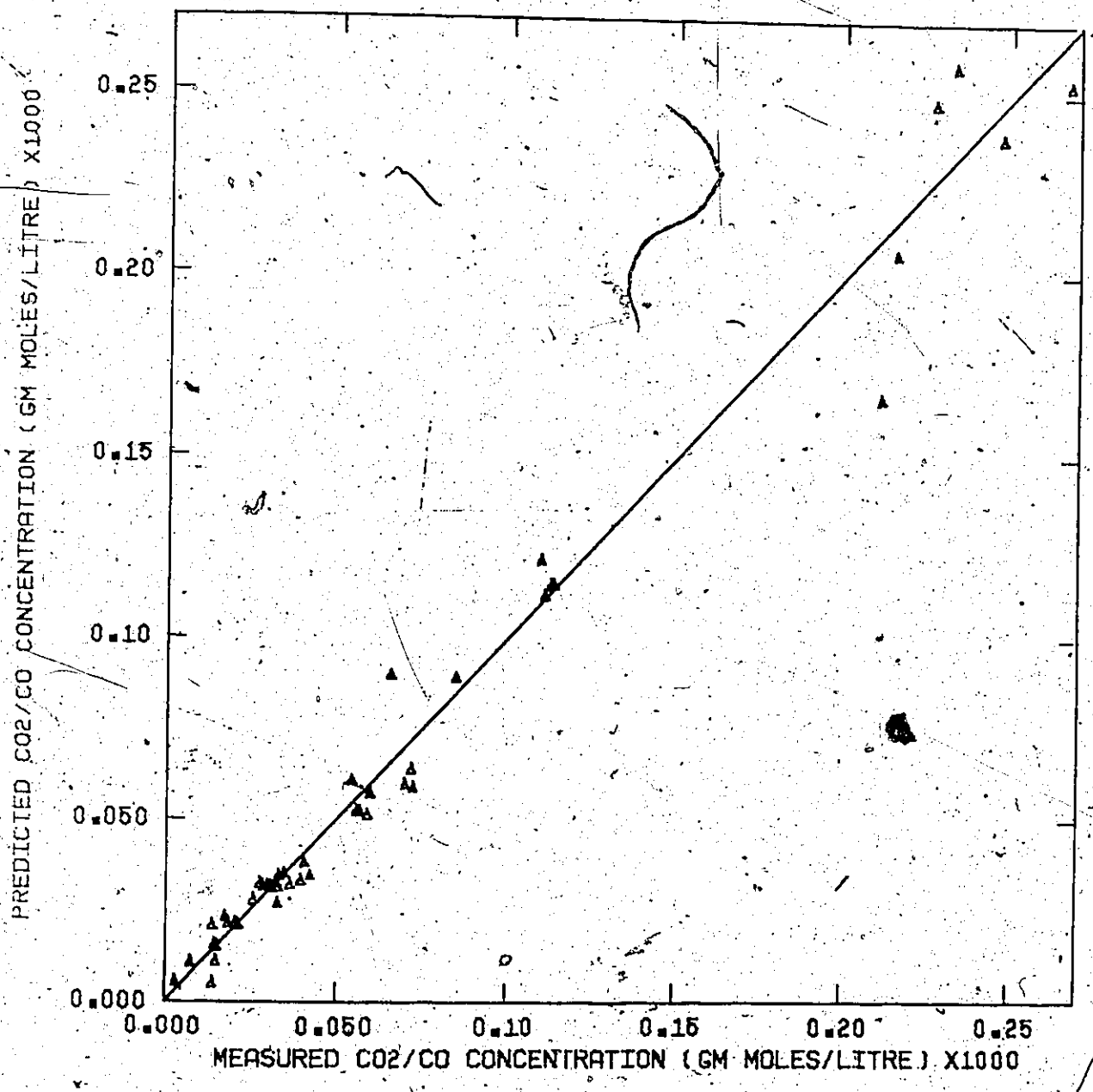

Figure 6.11. Predicted Versus Measured CO_2/CO Concentrations - 902 Catalyst.

values in Figures 6.8 to 6.11. These figures are based on the parameters estimated from the transformed responses.

(2.) TiO_2 Catalyst

It was noted in Chapter 5 that the rates of ortho-xylene conversion appeared to have little, if any, temperature dependence over the range of temperatures studied. This was attributed to a loss of SO_3 from the catalyst. A parameter has been included in the rate equations to account for the loss of activity due to SO_3 loss. This parameter, which we have called the "active site parameter" has been assumed to obey an exponential temperature dependency that takes into account decreased activity from that which would be obtained if no thermal deactivation took place. That is, each Equation (6.8) through (6.12) in the model is multiplied by the fraction of active sites which is given by $\exp\left(\frac{E_s}{R}\left(\frac{1}{T}-\frac{1}{T^*}\right)\right)$ where T^* is the temperature of the centre point experiment ($370^{\circ}C$). Therefore the fraction of active sites is assumed to be unity at that temperature. It should be noted that the use of an active site parameter has been successful in the hydrogenolysis of butane on a nickel catalyst in our laboratory (S13).

The experiments from which data were used to estimate the parameters are summarized in Table 6.3. The calculated rate parameters are presented in Table 6.6. The calculated concentrations of orthoxylene, orthotolualdehyde, phthalide, phthalic anhydride and CO/CO_2 are plotted against the measured values in Figures 6.12 to 6.16. In addition, the residual concentrations are plotted against temperature, experiment number,

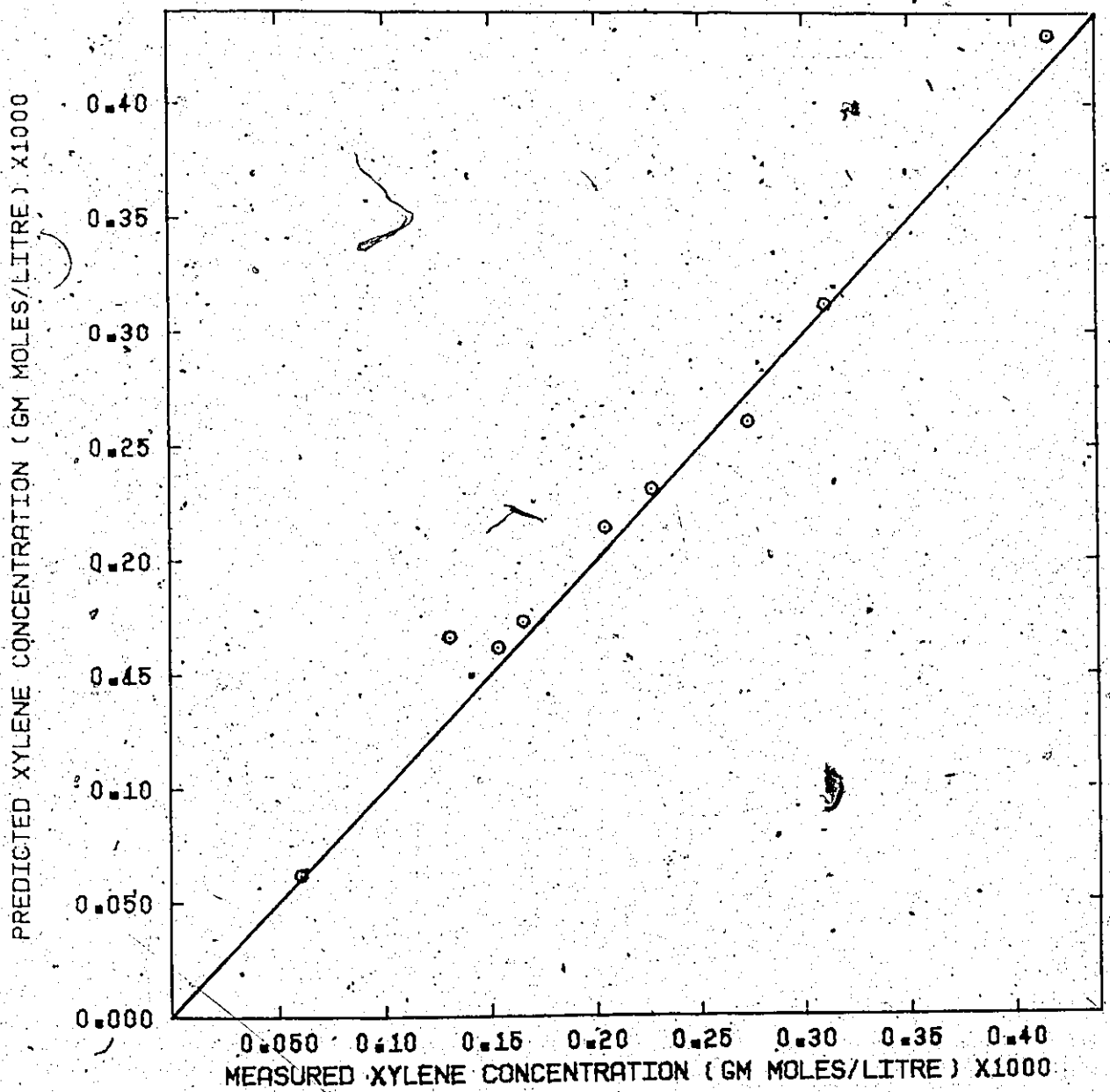

Figure 6.12. Predicted Versus Measured O-xylene Concentrations - TiO_2 Catalyst.

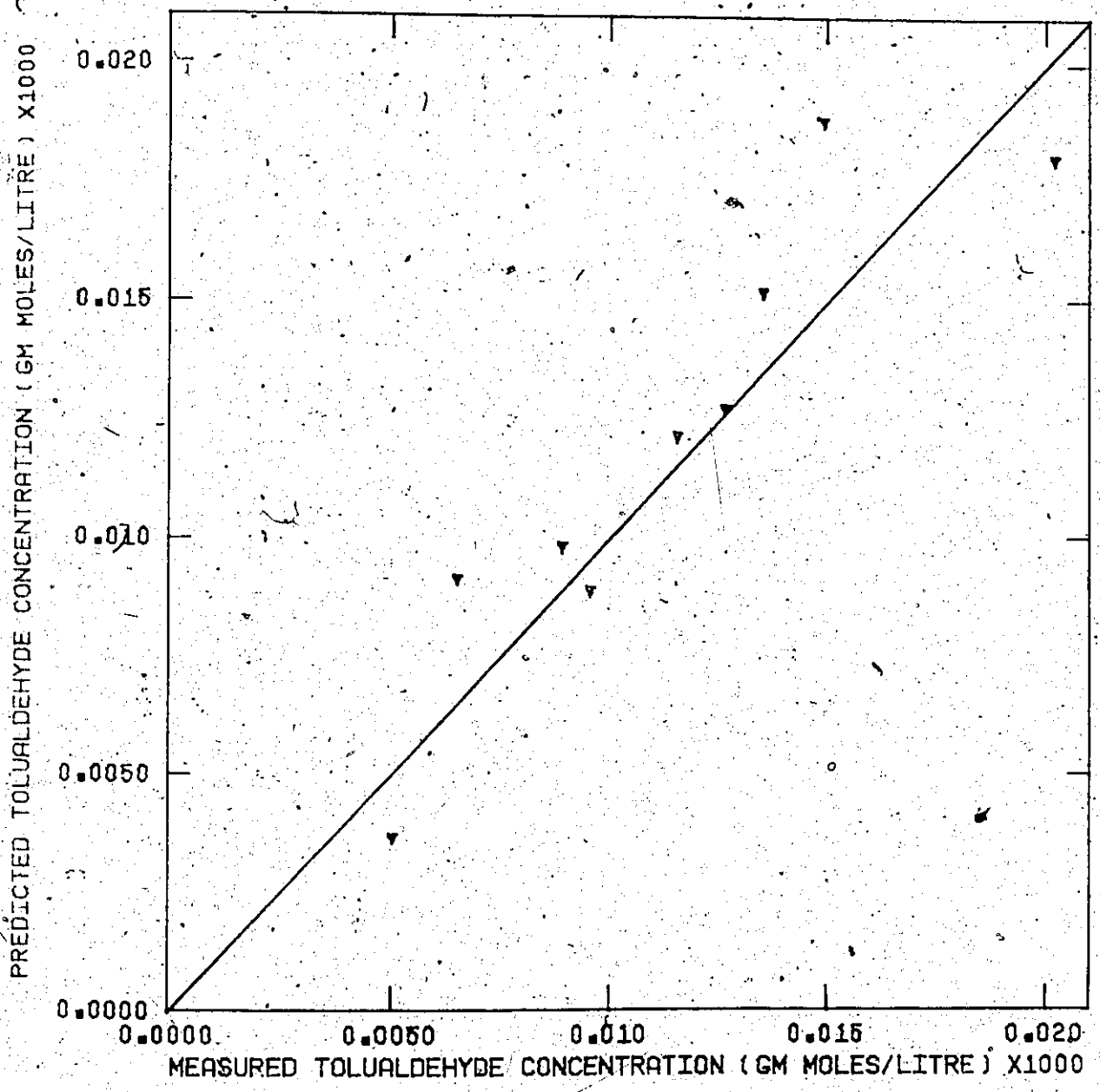

Figure 6.13. Predicted Versus Measured O-tolualdehyde Concentrations - TiO_2 Catalyst.

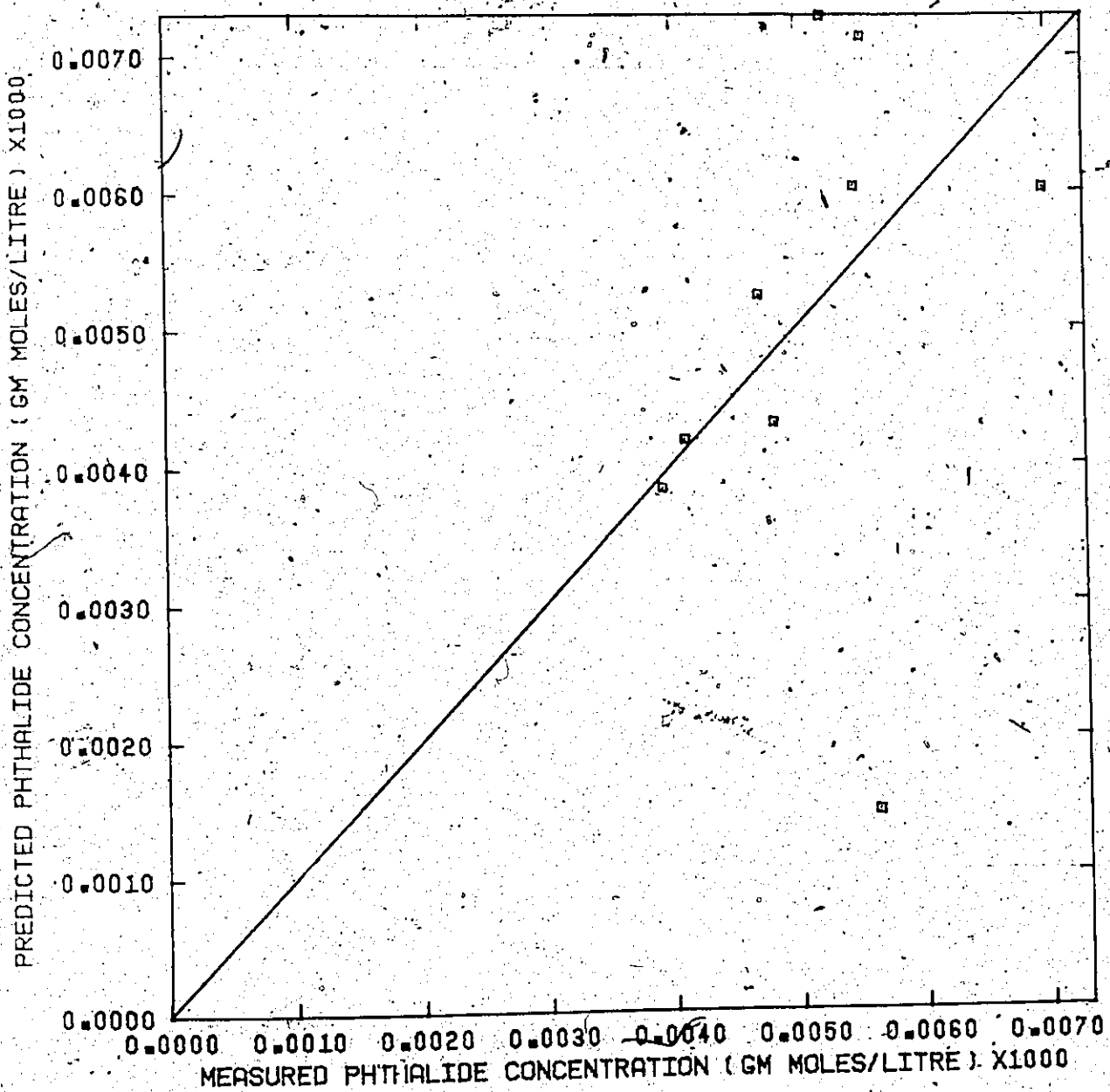

Figure 6.14. Predicted Versus Measured Phthalide Concentrations - TiO_2 Catalyst.

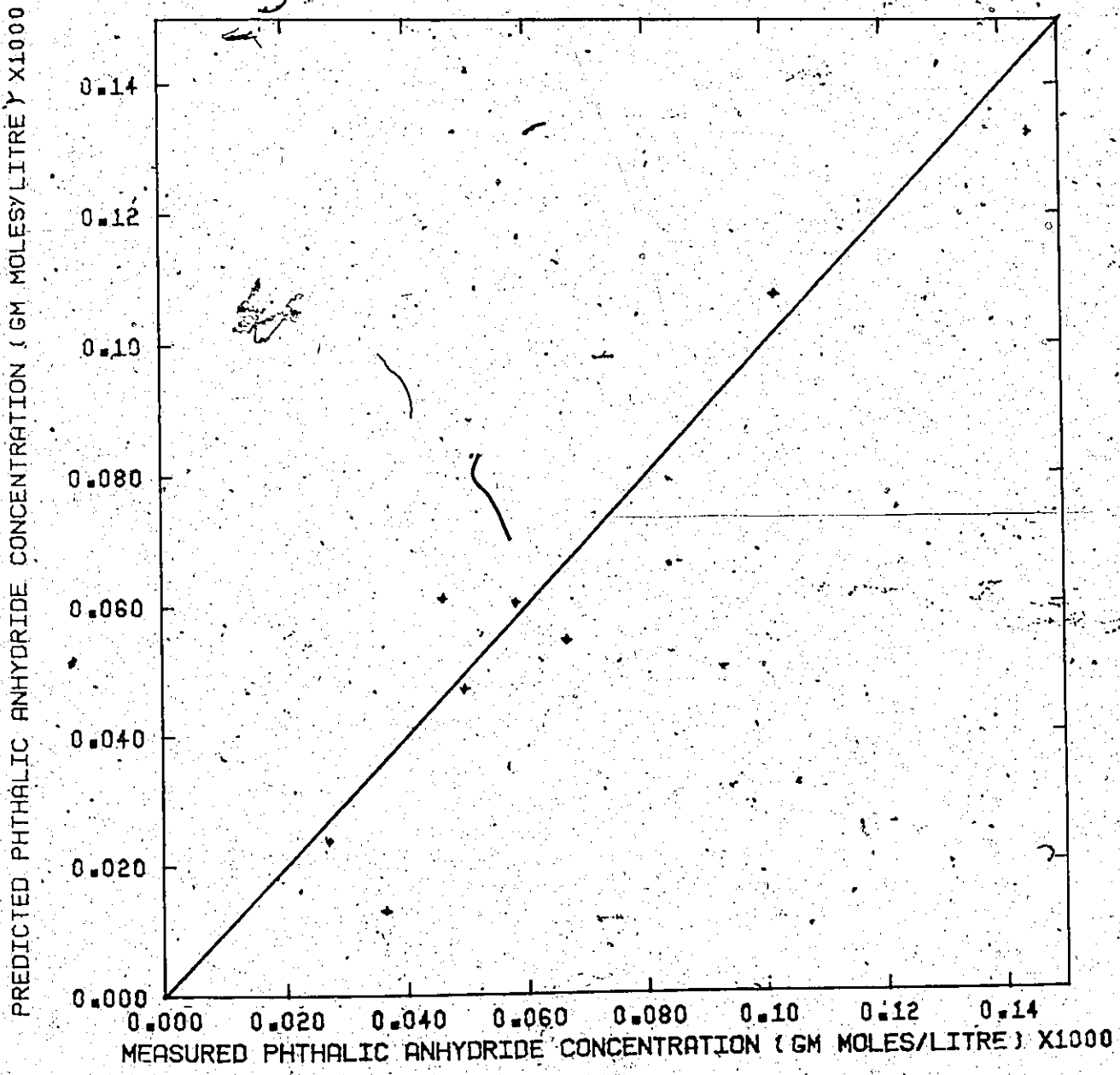

Figure 6.15. Predicted Versus Measured Phthalic Anhydride Concentrations - TiO_2 Catalyst.

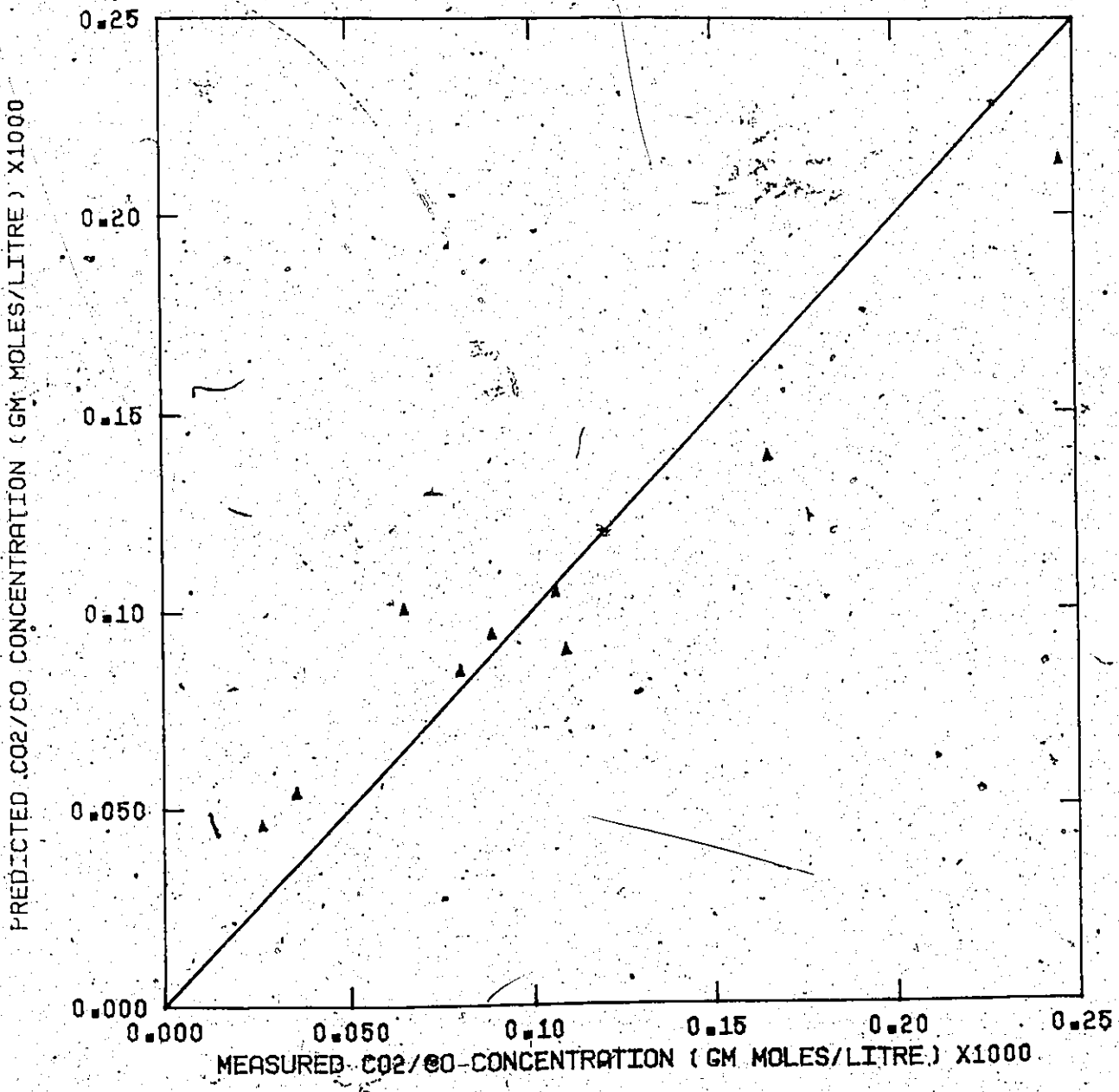

Figure 6.16. Predicted Versus Measured CO_2/CO Concentrations - TiO_2 Catalyst.

In Figures 6.17 to 6.20 the following symbols have been used

- ⊙ O-xylene
- ▽ O-tolualdehyde
- ▣ Phthalide
- ◇ Phthalic anydride
- △ CO_2/CO

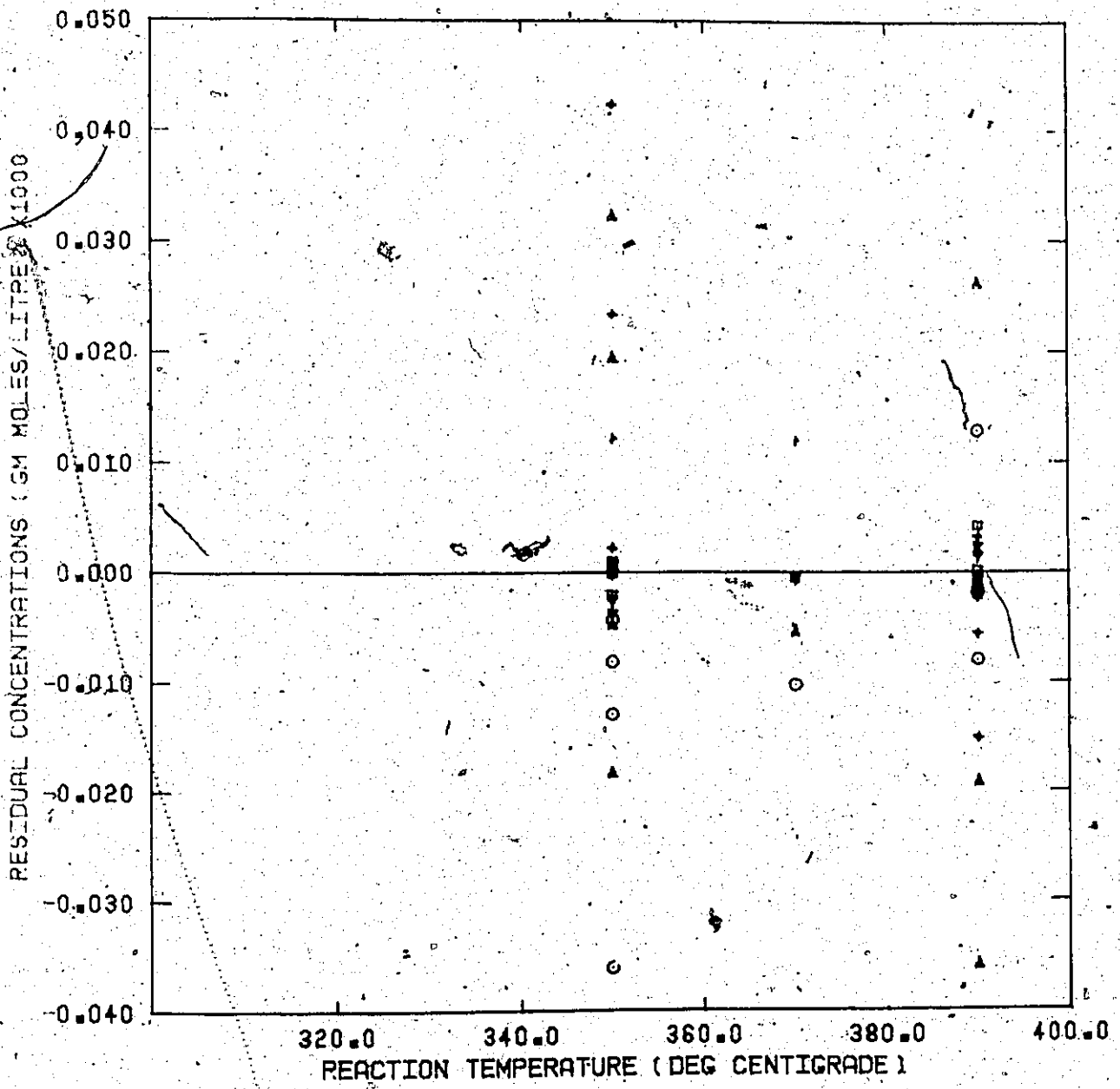

Figure 6.17. Residual Plot - TiO_2 Catalyst.

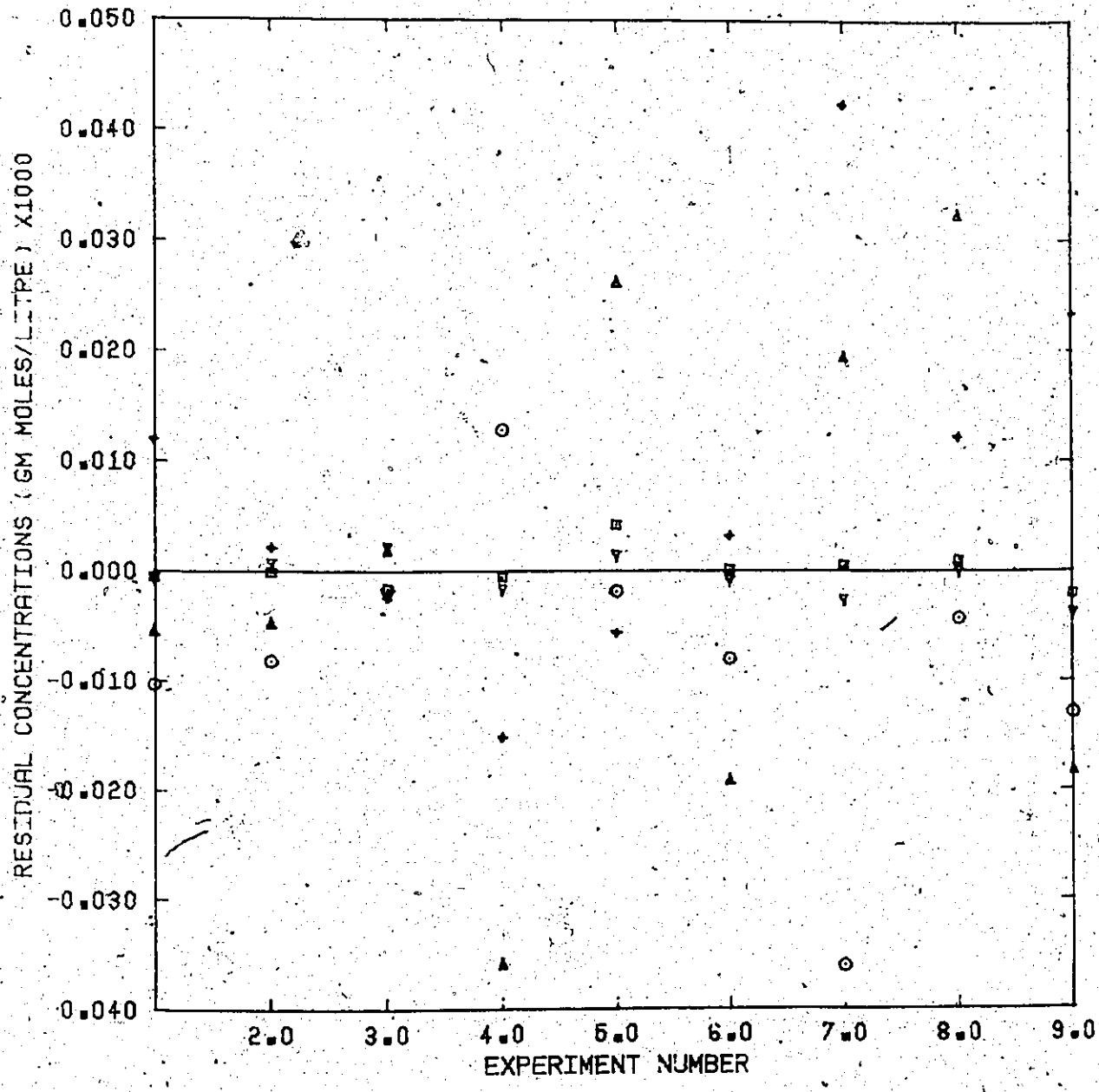

Figure 6.18. Residual Plot - TiO_2 Catalyst.

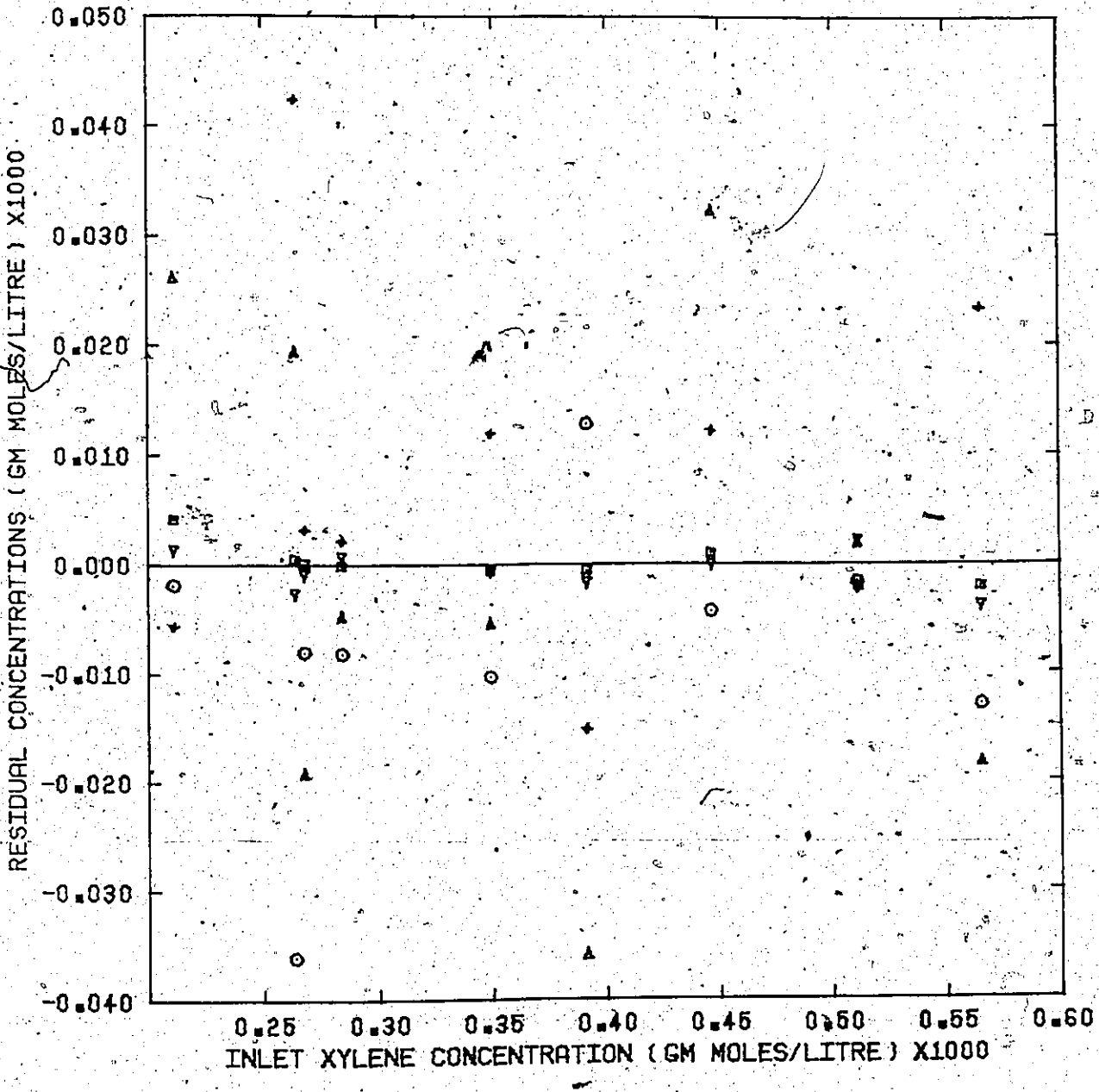

Figure 6.19. Residual Plot - TiO_2 Catalyst.

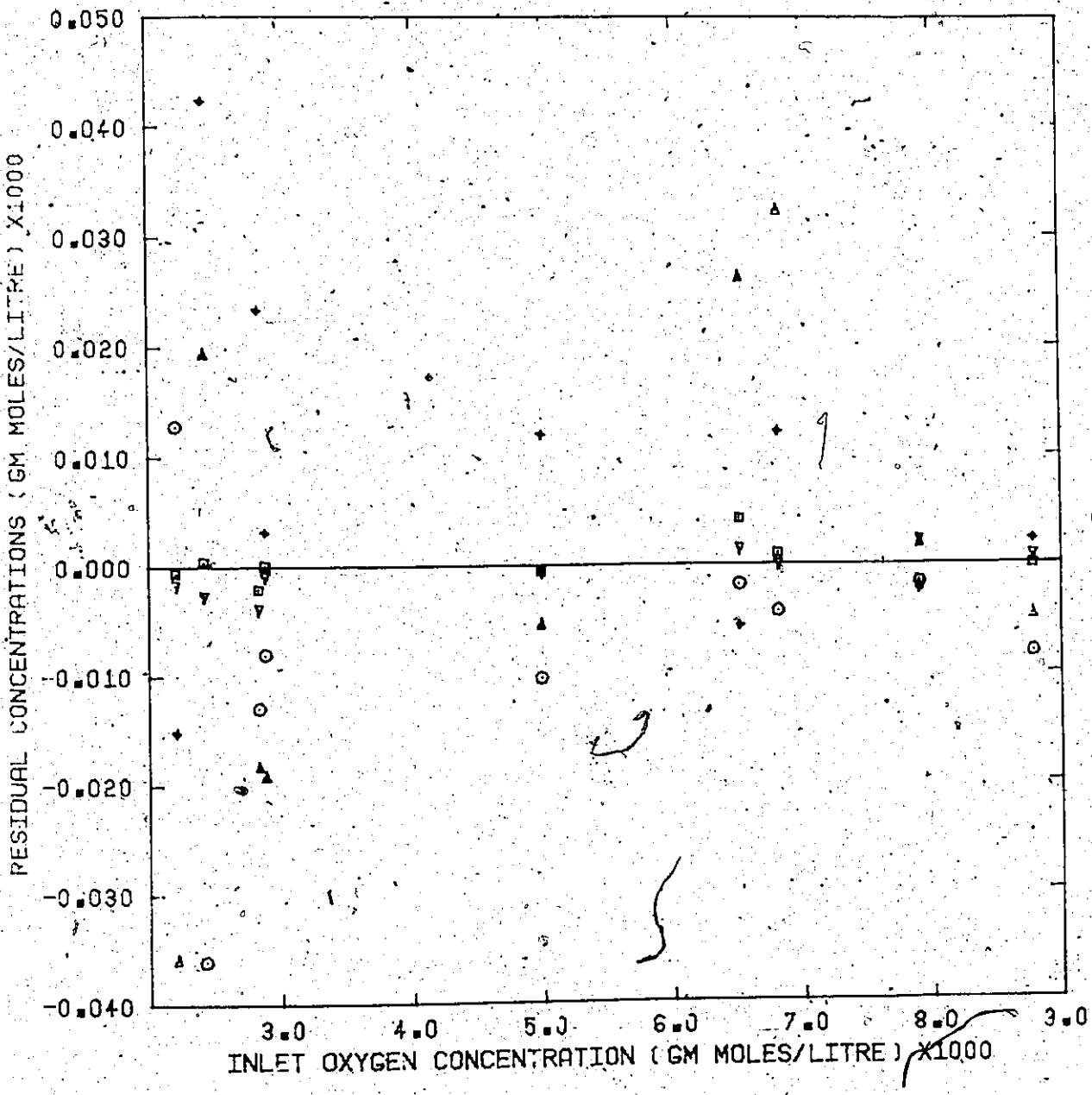

Figure 6.20. Residual Plot - TiO_2 Catalyst.

inlet orthoxylene concentration and inlet oxygen concentration in Figures 6.17 to 6.20. The fraction of active sites corresponding to the E_{as} value of 12,351 cals/gm. mole ^{o}K are 1.85 at 350^{o}C, 1.0 at 370^{o}C and 0.56 at 390^{o}C.

Table 6.6. Reaction Rate Parameters for Orthoxylene Oxidation on Grace TiO_2 Catalyst

E_a	30,848
K_a	6.69×10^{10}
E_{12}	27,307
K_{12}	3.60×10^{10}
E_{23}	26,018
K_{23}	2.44×10^{10}
E_{34}	29,392
K_{34}	8.07×10^{12}
E_5	24,426
K_5	5.87×10^{8}
E_{as}	12,351

6.6. Model Evaluation and Discussion

6.6.1. Discussion on the Transformation Employed

The method of determining the transformation required to make the variances constant in each of the observed responses assumes the errors are normally distributed. Since the Bartlett test which was used to evaluate the homogeneity of variance is very sensitive to departures from normality, this whole scheme

is open to criticism. The Box and Cox method of evaluating the correct transformations assures both homogeneity of the variance-covariance matrix and that the errors on the transformed variables are normally distributed. In their method, the maximum likelihood estimate of the transformation parameters is obtained by minimizing the residual sum of square of $z^{(\lambda)}$

where $$\underset{rx1}{Z_u^{(\lambda)}} = \{Z_{iu}^{(\lambda_i)}\} = \{y_{iu}^{(\lambda_i)} / J_{iu}^{\frac{1}{n}}\} \qquad (6.31)$$

$$\underset{rx1}{\lambda} = \{\lambda_i\} \qquad (6.32)$$

$$i = 1, 2, \ldots r, \quad u = 1, 2 \ldots n$$

and where

$$J_{iu} = J(\lambda_i, y_{iu}) = \prod_{u=1}^{n} \left(\frac{dy_{iu}^{(\lambda_i)}}{dy_{iu}}\right) \qquad (6.33)$$

The residual sum of squares of $\underline{Z}^{(\underline{\lambda})}$ is obtained from:

$$S(\underline{\lambda}, \underline{Z}) = \sum_{u=1}^{n} \sum_{i=1}^{r} \{Z_{iu} - \eta_i^T(\underline{\xi u}, \hat{\theta}^T)\}^2 \qquad (6.34)$$

where η_i^T is the expected value of the response i, transformed in the same way as y_{iu} is transformed to Z_{iu} and $\hat{\theta}^T$ is the best estimates of the parameters obtained with the transformed responses.

The residual sum of squares was evaluated using Equation (6.34) for the transformed responses and was found to be 3.59×10^{-8}. The residual sum of squares was also obtained for the untransformed responses using the appropriate model

parameters; its value was 3.82×10^{-8}. The fact that the residual sum of squares from the transformed system is less than that obtained from the untransformed system suggests at least that the transformations improved the homogeneity of variance and the errors are expected to be more normally distributed. Obviously there is no way of knowing whether the minimum in the residual sum of squares with respect to $\underline{\lambda}$ was obtained. We would suggest, however, that the parameters obtained with the transformed responses are closer to the true parameters than the others. Had the assumed model proved to be adequate, it would have been worthwhile investigating the response surface of $S(\underline{\lambda},\underline{Z})$ in the region of the $\underline{\lambda}$ used, to determine if this was indeed the real minimum. Since, as will be shown below, the model proved inadequate, this was not done.

6.6.2. Evaluation of the Model

In evaluating the adequacy of the assumed models, the following tests should be performed:

(i) Since the kinetic model is based on physical-chemical mechanisms, the values of the parameter estimates should bear some relation to those obtained by other researchers on similar systems. In particular, the activation energies generally should be positive and approximately what have been found for this particular type of reaction. In general, this is true for the results of this study. This point is discussed further in Section 6.6.3.

(ii) The residuals, that is the observed response-minus-the expected value of the response should show no correlation

with the independent variables.

(iii) The residual sum of squares for each response, viz.,

$$\sum_{u=1}^{n} [y_{ui} - \eta_i(\underline{\xi}_u, \underline{\hat{\theta}})]^2$$

divided by the degrees of freedom (nr-p) where p is the number of parameters in the model) should be an estimate of the variance of each of the responses if the model correctly describes the system. To test for lack of fit the mean square lack of fit for each response can be compared, through an appropriate F-test with the mean square pure error determined from replicated experiments. The model will be proven inadequate if the lack of fit mean square is too large compared to the experimental error variance.

In the present case, the residual plots (Figures 6.4 to 6.7 and 6.17 to 6.20) for both catalysts (transformed and untransformed responses) indicate that, in general, the residuals are not appreciably correlated with the independent variables, temperature, inlet orthoxylene concentration and inlet oxygen concentration. A possible exception is a correlation of the orthoxylene residuals with inlet xylene concentration for the 902 catalyst. There does seem to be some correlation of the residuals, however, with run number for the silica-supported catalyst, thus indicating some change in catalyst activity with time. This point is discussed in the next section. Table 6.7 lists the mean square lack of fit for each response obtained from the residual sum of square and the mean square pure error obtained from the replicated experiments. The F-test indicates

that the lack of fit mean squares are too large compared to the estimated experimental error variance and hence the model in its present form is inadequate. This result is expected here since the plots of predicted versus measured responses in Figures 6.8 to 6.11 show considerable deviations from the 45° line. Moreover, the number of experiments which were performed were judged to be inadequate to provide the minimum confidence region for the parameters. Neither was any effort made to perform experiments at the best conditions to evaluate the parameters.

It is emphasized that the main objective of this preliminary study was to uncover gross inadequacies in the mechanism described by the model. The most important consideration therefore is the residual plots and their correlation or lack of it with experimental conditions. A discussion of the model on this basis follows.

Table 6.7. Analysis for Lack of Fit in Model for 902 Catalyst Data

	Degrees of Freedom	O-xylene	O-tolualdhyde	PAA/PI/OTAC	CO/CO_2
SSE	37	2.99×10^{-8}	2.91×10^{-4}	3.66×10^{1}	1.42×10^{-5}
SSPE	17	1.51×10^{-9}	1.24×10^{-5}	3.30×10^{-1}	2.23×10^{-6}
SSLF	20	2.84×10^{-8}	2.79×10^{-4}	3.63×10^{1}	1.20×10^{-5}
MSLF/MSPE	20/17	16.0	19.0	93.4	4.6
$F_{.05,20,17}$	2.23	2.23	2.23	2.23	2.23

6.6.3. Shortcomings of the Model

In general, for most gas-phase reactions catalyzed by solids it is not necessary to model the catalyst behaviour as well as the chemical kinetics since it is generally assumed that the catalyst provides a medium for reaction. However, in the case of the oxidation of hydrocarbons on vanadia catalysts, it is apparent that the state of the catalyst must be modelled. To this end, a rather crude attempt has been made in the case of the TiO_2-supported catalyst to model the catalyst performance by including an active site parameter which accounts for the loss of activity with temperature, probably due to a loss of SO_3 by decomposition of $K_2 S_2 O_7$ in the catalyst. Had this term not been included, unrealistic activation energies of around zero or possibly less than zero would have been obtained had the data been forced to fit the model. Those calculated activation energies would not have been those for the chemical reactions taking place on the catalyst. They would merely be constants which make the data fit the assumed model. It is apparent that precise parameter estimates of chemical reaction parameters can be obtained for oxidation of hydrocarbons on those catalysts only when the catalysts themselves have been adequately modelled.

The prime consideration in modelling catalyst performance is to accurately describe the role of SO_3 in determining the catalyst activity. The approach adopted by Juusola (J4) who assumed activity as a function of time based on a standard activity determined at a specific on-stream time, and the one adopted in this study for the TiO_2 catalysts are rather crude approximations to the catalyst decay problem. In the case

of oxidation on the 902 catalyst no attempt has been made to account for losses in catalyst activity due to SO_3 losses. The result of this is apparent in the plot of residuals against run number in Figure 6.7. The residuals of all responses are correlated with run number. In the case of orthoxylene the predicted concentrations are less than the measured values at the beginning of the series of experiments and are greater at the end. The opposite effect is noted for the reaction products.

The oxidation state of the catalyst also plays an important role in determining the rates of reaction and product distributions. The multiple response models used in this work assume that all hydrocarbon oxidation reactions taking place on the catalyst obey the two-step S.S.A.M. or Redox mechanisms. That is, the rate of oxidation of the hydrocarbon (or oxidized hydrocarbon) to more highly oxidized products is proportional to the number of active sites available for oxidation. The assumption is that one type of active site is available for all reactions and that, following reduction by reaction, these sites are reoxidized by oxygen in the gas phase. This assumption may not be valid. The observation (H3) that a lower oxidation state catalyst increases the rate of oxidation of phthalic anhydride to CO_2, CO and maleic anhydride suggests that sites of lower oxidation state in the catalyst, produced by partial oxidation of the aromatic compound, may be active for total oxidation by oxidation of the aromatic ring. Should such a mechanism be correct, then the aromatic nucleus would be competing with oxygen

from the gas-phase for reaction at these sites. In that case, the rate of oxidation of orthoxylene and orthotolualdehyde would be proportional to $(1-\theta)$ and not to θ as has been assumed previously. Model discrimination studies using data obtained from more accurate kinetic data than obtained here could be used to test the validity of such a model. It is interesting to note that the only oxidation that has not been adequately described by fitting initial rate data to the S.S.A.M. model is that of benzene for which the main products obtained are CO, CO_2 and maleic anhydride. The relatively good fit obtained for the initial rates of oxidation of orthoxylene, toluene and naphthalene in no way negates the proposition that sites of lower oxidation state are responsible for total oxidation, since the analysis to date has lumped all reaction products so that the overall rate of hydrocarbon conversion has been used. The relatively low selectivities to total oxidation products (around 10-20 percent) may not be sufficient to point to inadequacies in the model.

The relative values of the activation energies for the various reaction steps and reoxidation of the catalyst have been presented in Tables 6.5 and 6.6. The activation energies for the reoxidation reaction (E_a) are higher than any of the activation energies for the hydrocarbon oxidation reactions for both catalysts. The value obtained for the 902 catalyst (35.8 K cals/gm. mole ^{o}K) is in agreement with the value 36.3 K cals/gm. mole ^{o}K obtained by Juusola (J4) for the oxidation of orthoxylene on a similar catalyst. The high activation energy for catalyst reoxidation suggests that the order

of reaction with respect to oxygen should be decreasing with increasing temperature. This has been observed elsewhere (J4, H2). The activation energies for carbon oxide formation on both catalysts are less than for most of the partial oxidation steps. This would infer that reaction at higher temperatures should favour partial oxidation over total oxidation. Selectivities presented in Figure 7.6 and selectivities data of other workers (H2, V4) show that the reverse is true. Therefore we can infer that the model we have assumed is inadequate in this respect.

6.7. Ramifications for Future Work

The study described in this chapter has been useful in aiding further work in this department in which it is intended that more adequate models of hydrocarbon oxidations under both steady-state and unsteady-state conditions will be developed. Suitable computer programs for parameter estimation using multiple response data have been developed. In addition, the parameters that have been evaluated and/or the data accumulated in this study may be of some use in designing experiments to discriminate between postulated models.

Further work on the development of suitable reaction models will require accurate control of the orthoxylene concentration in the feed. It is suggested that a syringe pump be used to meter orthoxylene into the feed stream in place of the saturator used in this study. Although the inlet concentration was always measured by gas chromatography, the inability to accurately fix the orthoxylene level prevented true replicate

measurements from being obtained and resulted in an inflated estimate of the variances of the responses. True replicates are necessary for accurate determination of the variance-covariance matrix which is necessary for testing for lack of fit in postulated models.

It is apparent from the foregoing discussion that the role of the catalyst requires considerably more understanding than is currently available. Suggestions for further work in this regard have been given in previous chapters. It is further suggested that naphthalene oxidation may be a preferable reaction to study. The occurrence of fewer intermediates is a distinct advantage. Any attempt to elucidate the reaction mechanism should include the oxidation of intermediate compounds. In the case of naphthalene oxidation, phthalic anhydride and 1,4 naphthaquinone should be oxidized on vanadium catalysts under the same conditions used for naphthalene. A study of the oxidation of benzene over a wider range of conversions than were investigated by Jaswal et al. (J2) would be useful in determining a model to suitable describe the oxidation of the aromatic ring.

6.8. Conclusions

This study has revealed certain weaknesses in reaction models based on the S.S.A.M. or Redox models by obtaining estimates of reaction rate parameters in these models which are applicable over a wide range of conversions on two different vanadia catalysts. Recommendations have been made that will aid in planning future investigations to develop more suitable models.

CHAPTER 7

TRANSPORTED BED REACTOR STUDY

This chapter reports the design, construction and operation of a pilot-plant-scale transported bed reactor. Results of the oxidation of orthoxylene on the Grace 902 catalyst are presented along with data on solids hold-up and pressure drops in the conveying tube. A discussion of the dense-phase conveying regime is made by reference to the theory of Zenz (Z1). Finally, guidelines for experimentation in transported bed reactors are given to aid further studies in these unique gas-solid contacting systems.

7.1. Background

Paetkau (P1) built and operated a transported bed reactor for the oxidation of orthoxylene on an Aero PAA catalyst. However, he experienced several major experimental difficulties. A major weakness was the use of a rotary star valve for solids feeding. Apart from the problem of the valve seizing due to differential expansion at high temperatures, there was also bypassing of the reactant gases through the solids hold tank. Furthermore, the method of chemical analysis was far from complete. Carbon dioxide and carbon monoxide were not measured. Neither the solids flow rate nor the solids hold-up was measured. A simple homogeneous two-phase gas-solids flow model was used to

analyze the chemical reaction data. Despite these shortcomings, the research achieved its goal of demonstrating that hydrocarbon oxidations could be effectively conducted in transported bed reactors. This success was measured by comparing reaction rate data with those obtained by other workers using packed beds of similar catalysts.

Vara Prasad (V3) continued the work of Paetkau using the same apparatus. He experienced the same mechanical difficulties as Paetkau. Most of his effort was directed towards the development of an improved method of chemical analysis. However, he made very little change to the method used by Paetkau. A two sample analysis was used. The reactor effluent first passed to a gas sample valve which introduced a sample to a silicone gum rubber column for analysis of the condensable components. This was an identical procedure to that adopted by Paetkau. Following passage through the valve, the condensable components were removed in a cold-trap, and a gas sample containing oxygen, nitrogen, carbon dioxide and carbon monoxide was collected in a sample bottle. A gas-tight syringe was used to introduce this gas to a molecular sieve 5A column for separation of the fixed gases. The method suffered the disadvantage that there was no way of relating the results of the separate analyses.

Initial work in the current study was concerned with the development of an analytical procedure that could analyze all components from a single sample. Having achieved considerable success in this regard, it was decided to carry out experiments in the transported bed used by Paetkau. Several changes were

made to the rotary star valve in order to overcome the difficulties experienced by him. However, although the valve fed solids freely at temperatures below 200°C, it seized when higher temperatures were used. In addition, the analysis of the gases exiting the reactor was not completely successful, the major difficulties being caused by the ineffectiveness of electrical tracing of the sample lines and the use of a "single shot" sample to determine product composition. As a result of these experiments it was considered necessary to completely redesign the transported bed reactor and the method of product sampling.

7.2. Experimental Apparatus

The preliminary design considerations based on rather meagre information in the literature and the results of the preliminary investigations, suggested the following criteria for a pilot plant unit:

(i) In order to achieve smooth operation characteristics of non-choking gas-solids flow, solid loadings would have to be low, that is, dilute phase transport would prevail and voidage would be greater than 97%. This would mean that very little catalyst would be in contact with the reacting gases.

(ii) Superficial gas velocities would be greater than 20 ft/sec. in order to convey the particles. This coupled with the low solids hold-up suggested that the vertical pipe would have to be fairly long to achieve reasonable contact times.

(iii) In order to achieve near turbulent conditions in the

Figure 7.1. Flowsheet of Transported Bed Apparatus

AB	Air-operated butterfly valve
AN	Air-operated needle valve
AV	Air-operated ball valve
B	Stainless steel bellows
C	Cyclone
CA	Carburetor
CP	Capacitance probe
D	Water overflow
F	Filter
FC	Catalyst fines
FT	Feed tank
G	Sight glass
GG	Filtered sample to gas chromatograph
H	Preheater
HT	Catalyst hold tank
LC	On-off level controller
N	Manually-operated needle valve
O	Orifice
OX	Xylene feed tank
P	Pressure tap
PC	Proportional pressure controller
R	Rotameter
SB	Support beam
SG	Strain gauge weighing device
SO	Sonic orifice
ST	Scrubbing tower
T	Thermocouple
TV	Three way valve
V	Manually-operated ball valve
W	High pressure water
WT	Weighing tank

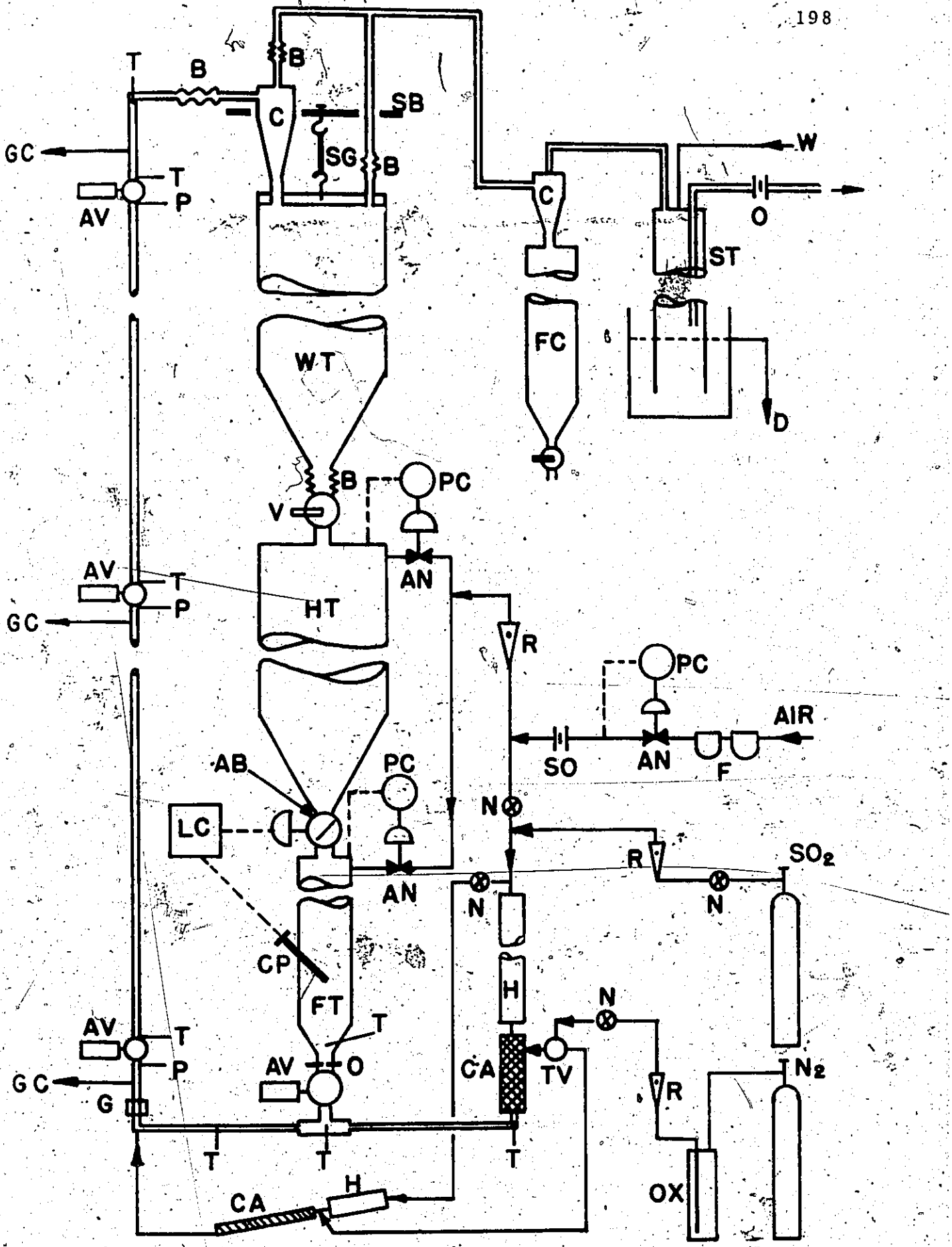
T
B
B
C
SB
SG
B
GC
T
P
AV
W
C
O
ST
FC
D
W.T
B
PC
V
AV
T
P
GC
HT
AN
R
PC
AIR
SO
AN
F
AB
PC
LC
N
R
SO2
AN
N
N
CP
FT
H
N
AV
T
P
GC
G
AV
O
CA
TV
R
N2
T
T
T
H
CA
OX

conveying system to provide some mixing of the gas, the conveying pipe diameter would have to be about 3/4 in.

(iv) In order to achieve full control of the solids flow rate to the system, some form of forced solids feeding would have to be provided.

(v) The solids loading should be high enough to provide a good sink for the heat generated by the reaction and thus control the reaction temperature over the reactor length.

(vi) Solids feed rate and solids hold-up measurements are necessary to evaluate the performance of the reactor.

(vii) Because there is the possibility that there will be fluctuations in the solids flow and imperfect contacting of gas and solids, it is necessary to obtain a sample of the product gases that truly represents the average performance of the reactor.

These criteria were used to design the apparatus described below.

The apparatus is shown diagrammatically in Figure 7.1. More complete details of the various pieces of equipment are given in Appendix H. The circuit consists of a solids hold-tank, a solids feed-control tank, the entry section, the vertical reactor, a cyclone separator and a solids receiver tank. The two upper tanks are 15 in. diameter and 90 in. high. They have 10 thermocouples located at a number of radial and axial positions. The solids feed control tank is 6 in. diameter and 60 in. high and has thermocouples at 5 axial locations. All tanks have conical bottoms designed to minimize the hold-up of solids on their walls. All are heated to any desired temperature by low

voltage-high current Kanthal strip heaters imbedded in Hiloset cement around the tanks. Pressure release valves, set at 15 psig. are connected to each tank to prevent the possibility of tank rupture.

Air is supplied from the 100 psig. mains, filtered and passed through a sonic orifice, the upstream pressure of which is controlled by a proportional controller/pneumatic control valve system. Some of the air is split to provide the driving gas for the solids feed system; the remainder is heated in a steam heater and electrically heated system and then passed through a short horizontal section of pipe. The solids are dropped into the gas in this horizontal pipe. They are conveyed about 8 in. and then transported around a 90° elbow to a vertical 3/4 in. O.D. by 0.68 in I.D. 316 stainless steel tube 27 ft. long. A 90° bend and a 8 in. horizontal section of tubing and expansion bellows connects the reactor to the cyclone separator. The gas leaving the cyclone is conveyed to another cyclone and a spray scrubbing section before it is discharged. In operation, the primary cyclone separated most of the solids so that the solids loss was small during the course of the experimental program.

The solids receiver was equipped with a 2 in. stainless steel ball valve on its bottom so that the solids were collected during a run; the solids could be discharged into the solids hold tank at the end of a run. The system was therefore operated batchwise. A solids inventory of approximately 300 to 350 lb. allowed at least a 10 minute run at the highest solids feed rate. The solids receiver was connected to the solids feed tank

by a 2 in. stainless steel bellows. The solids receiver was held by a yoke arrangement which was connected to a calibrated strain-gauge weigh system. This allowed a continuous weighing of the receiver over the run time. Details of the weighing device and calibrations for the strain gauge are given in Appendix B. The output of the device was continuously recorded throughout the run on a potentiomeric recorder.

A 1/2 in. diameter orifice was inserted at the exit of the solids feed-control tank. The solids level in this tank was controlled by measuring the level of solids by a ceramic capacitance probe (Drexelbrook Eng. Co., Glenside, Pa.) which controlled the open-close operation of a pneumatically operated 2 in. stainless steel butterfly valve on the bottom of the solids hold tank. The air pressure in both of these tanks was controlled by pneumatic control valves on air lines to them. The upstream pressure on these valves was maintained constant by restricting the main air flow to the reactor by a manually controlled needle valve. The system provided excellent control as evidenced by the rate of weight increase of the solids receiver and allowed a fairly wide range of solids feed rates to be achieved.

The orthoxylene was fed as liquid from a nitrogen pressurized feed tank; its flow rate was controlled by a needle valve and metered by a rotameter. A steam-heated exchanger vaporized the orthoxylene just prior to entering the reactor and this vapour was fed through an electrically-heated 1/8 in. tube to mix with the air-catalyst mixture approximately 2 in. after the elbow. Originally, the orthoxylene was vaporized

in a carburetor upstream of the solids addition point but since an appreciable amount of reaction occurred in the horizontal section prior to the vertical reactor, the feed point location was changed. One experiment was conducted in which the ortho-xylene was admitted at a point 7 ft. above the elbow.

Three air-activated, quick shut-off ball valves were installed at 9 in., 158 in. and 281 in. from the 90° bend. Gas samples were removed; pressure was measured by manometers; and temperature was measured by chromel-alumel thermocouples at locations near these valves. Lines to the manometers were filtered with 7 micron stainless steel filter units.

Despite the fact that the hydrocarbon oxidation is highly exothermic, Vara Prasad (V3), using Paetkau's apparatus noted that the temperature at the reactor exit was significantly lower than that at the inlet. In this study additional losses through valves and measuring elements provided extra areas for heat loss. These losses were minimized by attaching a 1 1/8 in. stainless steel tube to each reactor section to provide a sealed air jacket. Two tubular heaters (Chromalox, 230V, 1950 watts) were imbedded in a layer of Thermon heat transfer cement on each section. The two heaters were connected in parallel and were controlled by 110 volt variable transformers. The reactor, preheater tanks and valves were insulated by Johns-Manville Thermobestos insulation and the entire apparatus was clad in aluminium sheeting.

The apparatus used for sampling the reaction gases is shown in Figure 7.2. The gas samples were collected through

Figure 7.2. Gas Sampling Apparatus

B	Ball valve
F	Stainless steel filter in reactor wall
G	Compound gauge
L	Gas sample loop
N	Needle valve
S	Steam tracing (100 psig)
T	Stainless steel sample tanks
V2	Two-way solenoid valve
V3	Three-way solenoid valve

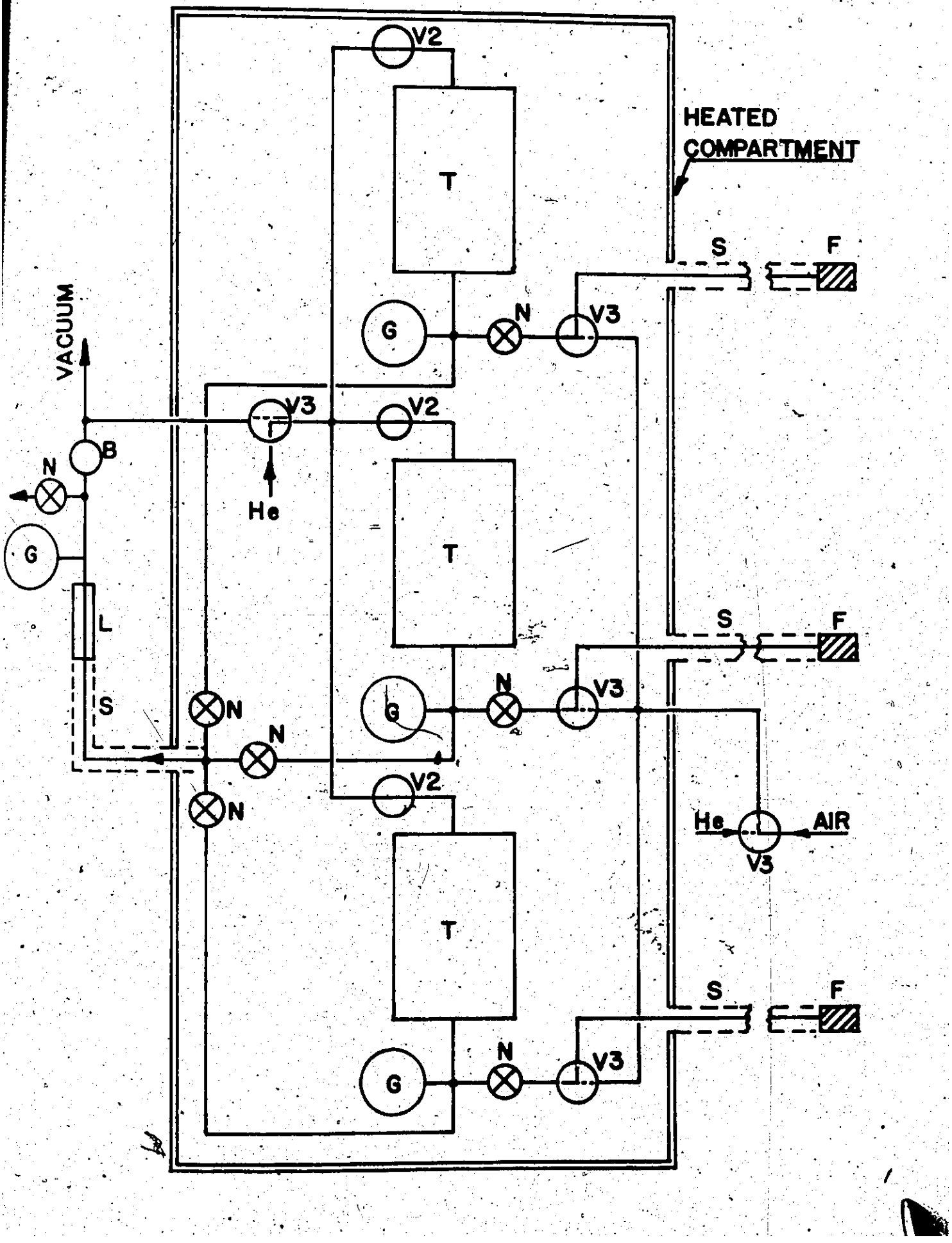
V2
T
HEATED
COMPARTMENT
S
F
VACUUM
G
N
V3
V3
V2
B
N
He
G
T
L
S
S
F
N
N
G
N
V3
N
V2
He
AIR
V3
T
S
F
G
N
V3

porous stainless steel filters (7 micron porosity) into pre-evacuated gas sample bottles (ca. 1000 c.c.). The 1/8 in. O.D stainless steel lines leading to these bottles were steam traced with 100 psig. steam to prevent condensation. All sampling lines and filters were flushed with helium just prior to sampling. The reaction gases were analyzed by drawing samples through the gas sampling valve and then analyzing by the gas chromatographic technique already described. The entire sampling apparatus was maintained at approximately 200°C by enclosing the sample bottles and valves in a heated-compartment, the heat for which was supplied by an air stream which was passed through steam and electrical heaters. The air flow to the sampling system was controlled by a sonic orifice installed in the line from the 100 psig. mains.

Sulphur dioxide was fed to the system to maintain the same concentration level as in the packed bed experiments. Prior to any run, the solids were circulated through the system with air and SO_2 to ensure that the catalyst was fully regenerated.

An orifice on the exit line from the scrubber provided an indication of constant gas flow rate in the reactor and also provided a material balance check on the air flow.

The ball valves used for trapping solids in the reactor were operated by two-way air motors connected to air tanks containing 150 psig air via three-way solenoid valves which had 3/8" orifices. Each tank had a capacity of approximately 7 litres which was more than 20 times the working volume of the air motors. Therefore the valves closed almost instantaneously.

They were reopened manually. These valves and those at the exit of solids weighing tank and the solids feed control tank were supplied by Kamyr of Canada and were equipped with stellite seats and high temperature mica-asbestos packing so that they could be operated at temperatures up to 1200°F if desired. Similarly the butterfly valve used to control the level of catalyst in the feed tank was equipped with high temperature packings. It was supplied by Fisher Governor Co. of Canada Ltd. The air motor was of the air-to-open type with spring operated closure. The air was supplied from a filtered 100 psig. mains via a three-way solenoid valve which was controlled in an on-off mode by the Drexelbrook level controller.

Procedure

At the commencement of a series of experiments, the temperature of the catalyst in the hold tanks was raised by applying voltage to the Kanthal strip heaters attached to the tank walls. In addition, the catalyst was continuously circulated with a hot air/SO_2 mixture to both increase the temperature of the catalyst and to ensure that it was in a highly oxidized state. Between series of experiments the tanks were heated so that the catalyst temperature was maintained at around 200°C. This was necessary because of the large heat capacity of the catalyst inventory and the apparatus.

When the catalyst was at reaction temperature, the solids feed control tank and solids hold tank were pressurized to the levels required to produce a given solids feed rate. The pressure in the hold tank was set at approximately 2 psig.

above that of the feed tank. The air and SO_2 flows were adjusted to the desired values and the temperature of the gas mixture leaving the preheater was adjusted to approximately that of the catalyst by varying the voltage to the strip heaters on the preheater. When all pressures, temperatures and flows were at the desired values, the ball valve immediately below the feed orifice was opened and the solids began to flow. It was noted, from the recorder trace of the strain gauge output, that there was a period of several minutes in which the solids in the reactor built up to their equilibrium level. During the early stages of this unsteady-state period, the pressure gauges showed a marked oscillation but as the solids built up in the reactor, the pressure fluctuations decreased so that, at steady-state operating conditions, they were small (ca. $\pm$ 0.2 psi in 10 psi). Once steady-state solids flow was established, the orthoxylene flow was commenced and adjusted to the desired value.

The gas sample tanks and the lines to the gas sample valve were evacuated and the sample lines to the reactor were continuously purged with helium. The tanks were then partially filled with helium so that they had a vacuum of about 15 inches of mercury. This was done so that the driving force for sampling was not great enough to cause a measurable disturbance in the gas flow to the reactor. When the various pressure measurements for the system had been taken and it was noted that stable feeding of both catalyst and reactant gases had been established, gas samples were taken at three levels in the reactor simultaneously. Sampling was generally started at approximately 6 minutes after

the commencement of the catalyst flow. It took place over a period of approximately one minute.

Immediately after sampling was completed the following procedure was adopted:

(i) The orthoxylene flow was terminated.

(ii) The three, fast acting ball valves were closed simultaneously.

(iii) The ball valve immediately below the feed orifice was closed to prevent solids from building up in the horizontal conveying section.

(iv) The air flow was shut off with a solenoid valve.

(v) The butterfly valve was closed.

(vi) The feed tank, the hold tank and the preheater sections were vented.

All of the above operations were conducted in rapid succession since all were controlled by solenoid valves, the electrical switches for which were mounted on the control panel.

Solid samples trapped between the three ball valves were then collected and weighed. Because of the low terminal settling velocities of the fine, light particles and the possible tendency to adhere to the reactor wall, it was necessary to pass a stream of air down the reactor tube to ensure that all the particles were collected.

The solids which had been collected in the weighing tank during the experiment were then dropped into the solids hold tank and the system was ready to transport the catalyst once again.

Gas samples from the three sample bottles were then analyzed by the gas chromatographic technique described earlier. During the period required for analysis, about 150 minutes, the solid particles were recirculated at least 6 times in order to fully oxidize them in addition to raising or lowering their temperature to that required for the next experiment. In this way it was possible to conduct up to 4 experiments per day.

Temperatures in the reactor, preheater, carburetor, solids tanks and sampling system were monitored continuously throughout the experimental programme with two Honeywell 12 point recorders. Large axial and radial temperature gradients were noted in the bed of catalyst in the solids hold-tank when the catalyst was not circulated frequently throughout the system. However, circulation of catalyst between experiments ensured that variations in reaction temperature, due to variations in solid temperature in the solids hold tank, were never more than $\pm$ 2°C. During the period in which the reaction gases were sampled, variations in reaction temperature, measured by 5 thermocouples located at various points in the reactor, never exceeded $\pm$ 1°C. The large heat capacity of the catalyst relative to the gas ensured that any temperature difference between the air leaving the preheating section and the catalyst flowing from the feed tank was overcome in the horizontal conveying section due to rapid heating or cooling of the gas.

Experimental Conditions

The catalyst used in this study was No. 902 supplied by W. R. Grace and is the same as that employed for most of the

kinetic experiments conducted in the packed bed experiments. The mean particle size and density were determined (Appendix C) to be 126 microns and 0.95 gm./c.c. respectively.

The experimental conditions covered by the series of experiments in which chemical reaction was studied is shown in Table 7.1. Additional experiments to obtain solids hold-up and pressure drop data were conducted at 220°C for solids flow rates between 10.3 and 39.2 lb./min.

TABLE 7.1 Experimental Conditions for the Transported Bed Reactor.

Temperature	233-342°C
Solids Flow rate	29-45 lb./min.
Air Flow rate	2.5-4.5 s.c.f.m.
Orthoxylene Concentrate	1 to 3 mole percent
W/Fa_o	63-350 gm. hr./gm mole

It was demonstrated that no significant homogeneous reaction occurred in the reactor at temperatures in excess of 400°C; neither did homogeneous reaction occur in the sample bottles at their operating temperature of about 200°C.

7.3. Results and Discussion

Solid-Gas Flow Experiments

Zenz and Othmer (Z1) suggest that the flow characteristics of a gas-solids conveying system can be interpreted from pressure drop observations as a function of gas and solids flow

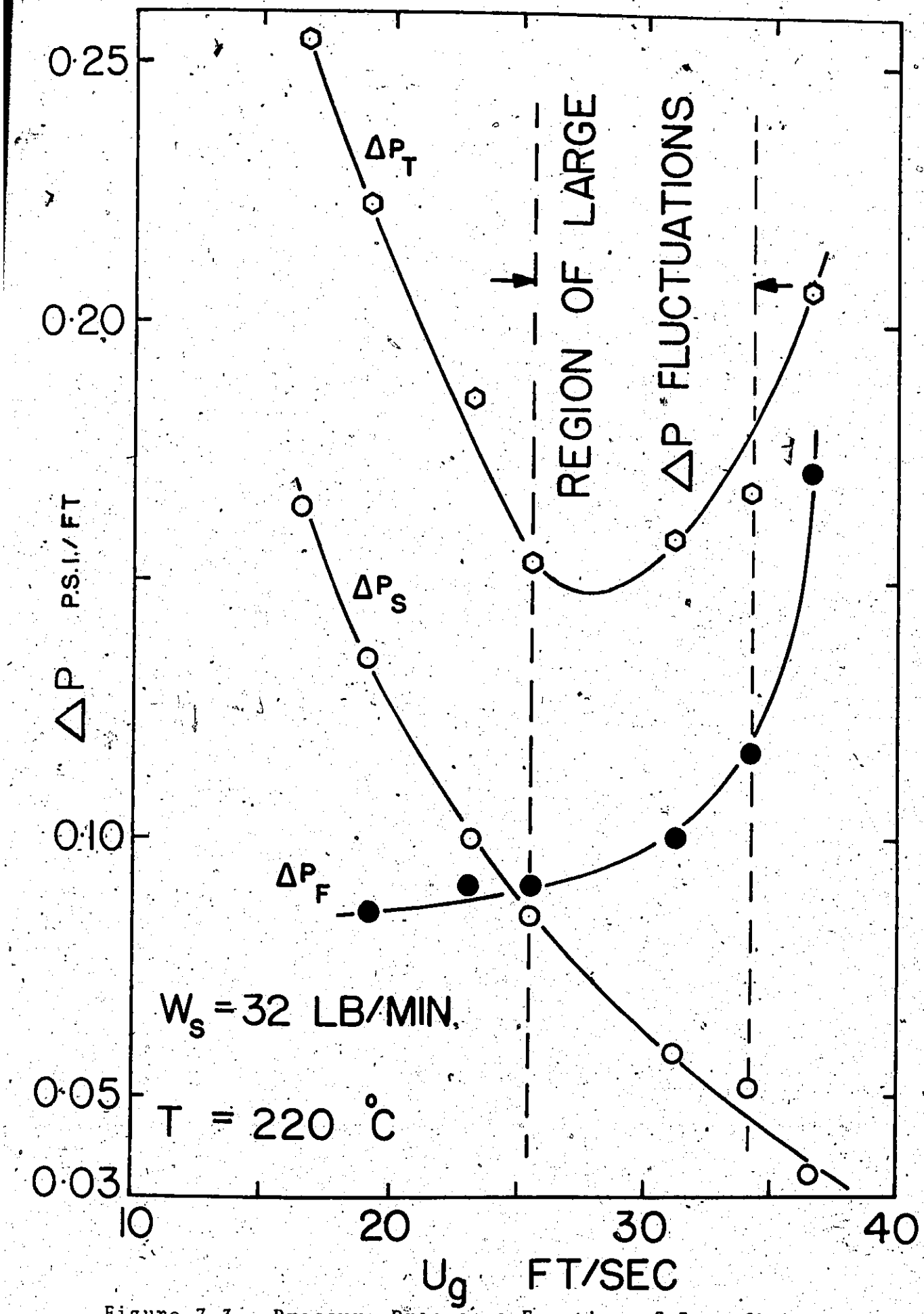

Figure 7.3. Pressure Drop as a Function of Superficial Gas Velocity at Constant Solids Flow Rate.

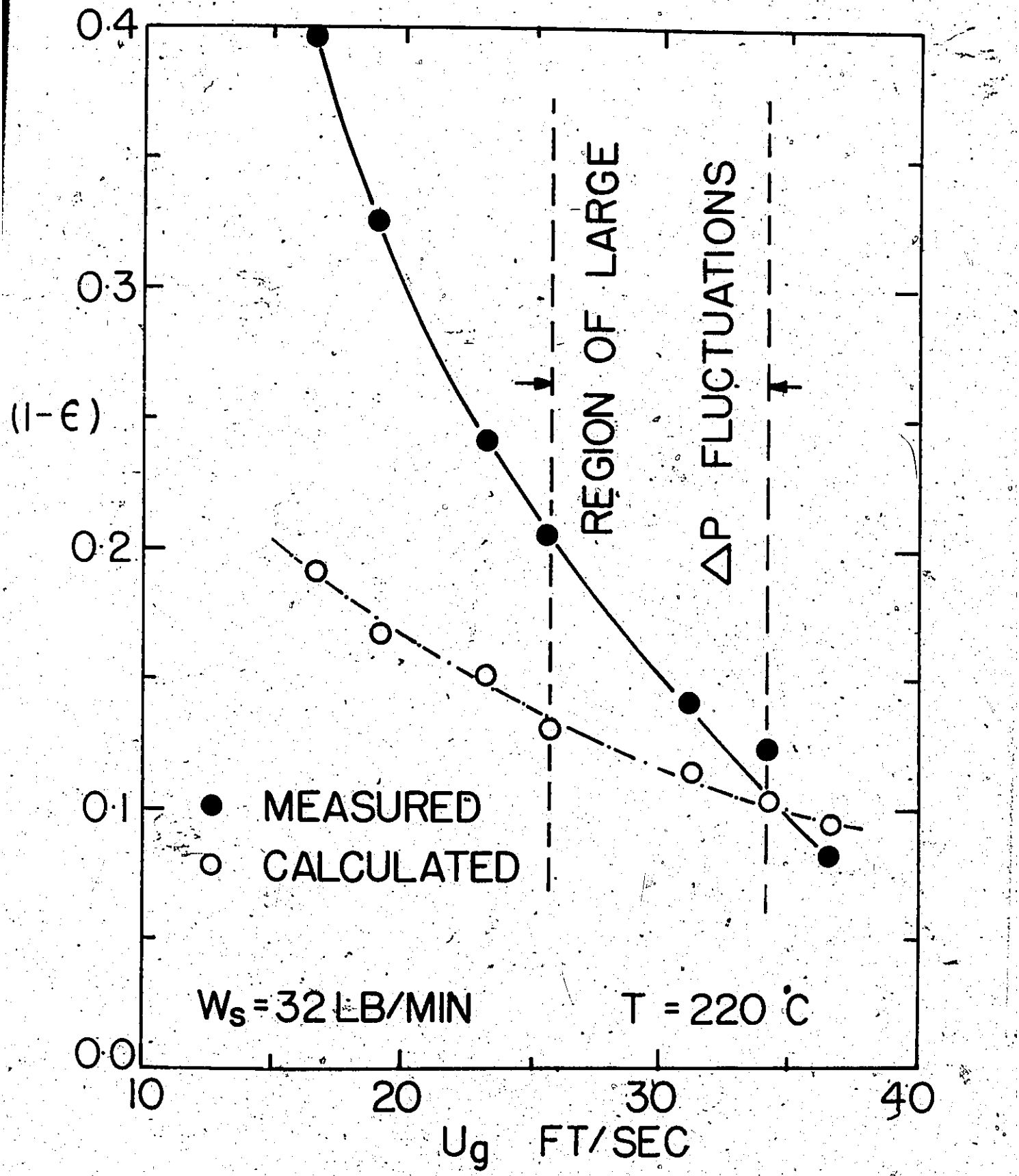

Figure 7.4. Volume Fraction of Solids as a Function of Superficial Gas Velocity at Constant Solids Flow Rate.

rate. This information was obtained from the present system at reaction temperatures. Additional experiments were conducted at 220°C to extend the range of gas flow rates that had been covered by the reaction experiments. These data are summarized in Appendix G. A typical plot of pressure drop as a function of superficial gas velocity for the upper section of the reactor is presented in Figure 7.3. In this case, the solids flow rate was held constant through judicious choice of air pressure in the feed tank and the gas flow was varied. Since the solids hold-up in the 10 ft. section was determined by direct measurement, the static pressure due to the solids-gas mixture could be evaluated. The frictional pressure drop was obtained by difference. The pressure drop behaviour exhibited in Figure 7.3 is similar to that reported by Zenz and Othmer (Z1), but what is not typical is the pressure drop fluctuations recorded over the range of gas flows. At gas flow rates below that where the minimum pressure drop is recorded, the system is expected to be in choked flow and exhibit large pressure fluctuations which are characteristic of slug flow. Such large fluctuations were observed in the region indicated on Figure 7.3, that is near the point of minimum pressure drop; however, at lower gas flow rates, these pressure fluctuations became very small, even less than those observed at the high gas flow rates, and the system exhibited remarkable stability.

Figure 7.4 shows the volume fraction of solids in the tube corresponding to the experiments indicated in Figure 7.3. Those calculated voidages corresponding to homogeneous two-phase flow are also shown for comparison. The region of large pressure

fluctuations is indicated. If it is assumed that the pressure fluctuations are an indication of slug flow, then it would seem that for W_s = 32 lb./min. and below a superficial gas velocity of about 28 ft.sec., the solids-gas suspension flows as a homogeneous mass similar to particulate fluidization but with a solids velocity much less than that of the gas.

The flow phenomena observed in these experiments are very difficult to explain since if the particles are freely suspended and in particulate flow, the drag coefficient on each particle would have to be reduced by several orders of magnitude to achieve such particle-gas slip velocities. At the same time, the voidages are so high that particles must be freely suspended and not moving through the bed as a moving fixed bed as might be expected if the exit line were restricting the flow of particles but not the gas. That is, the system is not behaving like the moving bed process patented by Berg (B4). If, on the other hand, the particles formed concentrated clouds or agglomerates which may break up and reform via the wake mechanism which has been suggested in the literature (Z1) and discussed in some detail in chapter 2, then larger slip velocities could be envisaged since this agglomerate has a terminal velocity determined by its diameter and the dispersed solids density. Figure 7.5 has been extracted from reference (Z2). Our data are included to indicate the slugging limits for extremely fine and light particles in air. All the curves shown in Figure 7.5 were constructed from limited experimentation and it is obvious that any discussion is therefore limited.

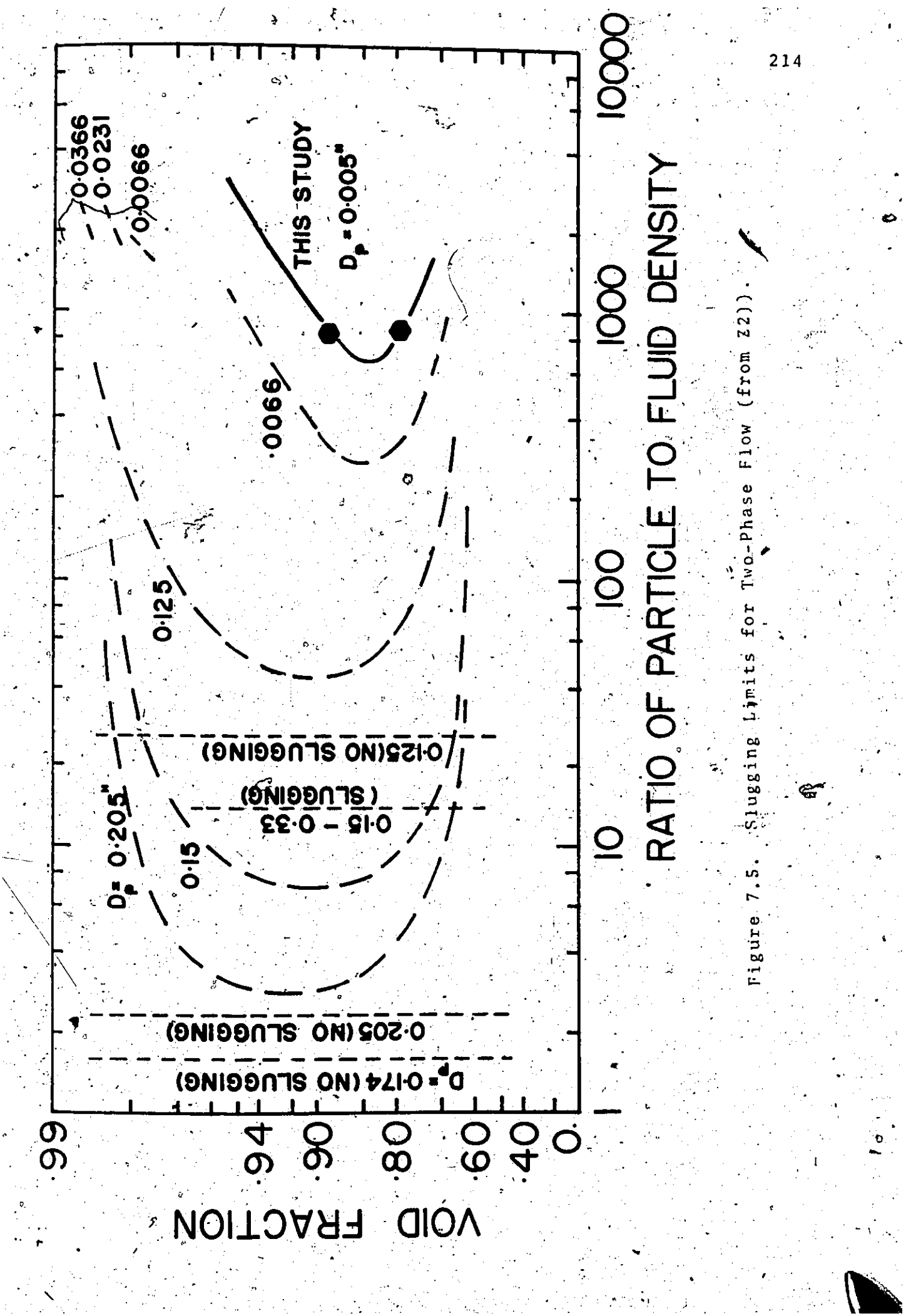

Figure 7.5. Slugging Limits for Two-Phase Flow (from Z2)).

To our knowledge this is the first reporting of this solids-gas behaviour with such high solids-to-gas loadings and for this reason, one can only speculate as to the solids-gas flow behaviour. The question that must be resolved is: How can this solids-gas flow exhibit characteristics of non-slugging flow at gas velocities where slugging would be certain to occur if, as in the normal fluidized bed situation, a batch of solids were contained in this small diameter tube? The answer to this question must relate to the fact that solids are forced into the bottom of the tube. Bubbles of gas may form at the bottom of the tube but two phenomena may occur:

(i) the gas within the emulsion phase may be more than that required for minimum fluidization, that is the gas may not distribute itself between the emulsion and the bubble phases as would be expected in a normal fluidized bed, and

(ii) the high shear rate between the bubbles and gas-solid suspension and between the tube walls may cause the bubbles to break up before they have an opportunity to coalesce to form slugs.

It is well known that slug flow requires considerable distance to establish itself in two-phase systems. The time available in the reactor under the low flow conditions where there may be relatively few bubbles and in which a certain amount of bubble break-up does occur may be too short to form stable bubbles. At the higher gas flows, where slugging does occur, there will be more gas bubbles and hence more coalescence to give rise to larger bubbles and slug flow. At lower solids

loadings there will not be as much shear on the bubbles and this will lead to a faster coalescence rate as well.

These speculations are consistent with the observations during the start up of the system. It was observed that, at the start of the experiment during which time the solids concentration was building up in the tube, there were severe pressure fluctuations characteristic of slug flow. As the pressure drop increased, indicating larger solids hold-up in the reactor, the pressure fluctuations decreased significantly in magnitude so that at steady-state very stable operation was observed. These observations indicate that there was an "envelope" of solids hold-up (or gas voidage) over which slugging occurred and this is consistent with Zenz's speculation as summarized in Figures 2.1 and 7.5. It is obvious that the characterization of this solids-gas flow behaviour requires considerable fundamental research.

The operation of the transported bed reactor was restricted to the high solids fraction region below the onset of large pressure fluctuations. For lack of better information, it has been assumed, in calculating rates of reaction in the following section, that the gas and solids are in intimate contact throughout the reactor length; thus bypassing of gas by bubble formation has been assumed negligible. Obviously this is a weakness in the present analysis and investigation of the solid-gas fluid mechanics should be continued prior to conducting further chemical reaction experiments in the apparatus.

Catalyst losses due to attrition under the operating conditions of this study did not appear to be excessive. Some

fine material was lost initially from the catalyst as supplied. Likewise, erosion of the reactor tube did not seem to occur.

It should be noted that the transported bed apparatus, although primarily designed for conducting chemical reaction experiments, has shown itself to be highly effective for carrying out investigations of solid-gas fluid mechanics. The forced feeding of solids has enabled operation at W_S/W_G ratios in excess of 200. The stability and control of feed rate was excellent. Continuous measurement of solids feed-rate by use of the strain-gauge weighing device is superior to the method generally adopted by other workers who use a valve in the return line from the cyclone to divert the solids for batchwise weighing. The ball valves used for trapping the solids proved to be very effective. However, it would have been desirable to include additional valves at several intermediate points in the reactor so that the variation of solids loading with length of reactor could have been determined. The ability to heat the air and solids from room temperature to around 500°C enables studies to be made at significantly different gas densities.

Several other methods of characterising the solid-gas system were investigated. The use of neutron diagnostics to determine the particle concentration was considered. Preliminary investigations conducted at a beam port in the McMaster Nuclear Reactor showed that the technique was most suited in the dense phase conveying range (0.5 to 0.9 void fraction). The results of the study are presented in Appendix B. The high cost

of a portable neutron source and the safety problems prevented the use of the technique for this study. Nevertheless, the investigation proved useful in showing that the technique can be applied to dense phase conveying in small-tubes, a region in which any of the other radiation attenuation techniques cannot be used. The technique will be invaluable in future studies of the fluid mechanics of two-phase gas-solid flow.

Correlation of capacitance signals using the method proposed by Beck (B6) was considered as a means for measuring the average particle velocity in the conveying section. A capacitance probe was constructed in a length of tube similar to that used in the reactor. However, when a capacitance to e.m.f. transducer that was available in the laboratory proved to be unsuitable it was decided to discontinue this approach because of time and cost involved in the development of suitable units. In addition, we were led to believe that the technique was not as effective as the authors had claimed.

Chemical Reaction in the Transported Bed

In all, twenty experiments were conducted. Because of the large heat capacity of the catalyst load it was not always possible to set the reaction temperature exactly to a desired level. Therefore, no formalized experimental design was adopted. However, a large number of experiments were conducted in the temperature range 295 to 305^{o}C at various times during the experimental program in order to determine if the catalyst activity was constant. The results of these

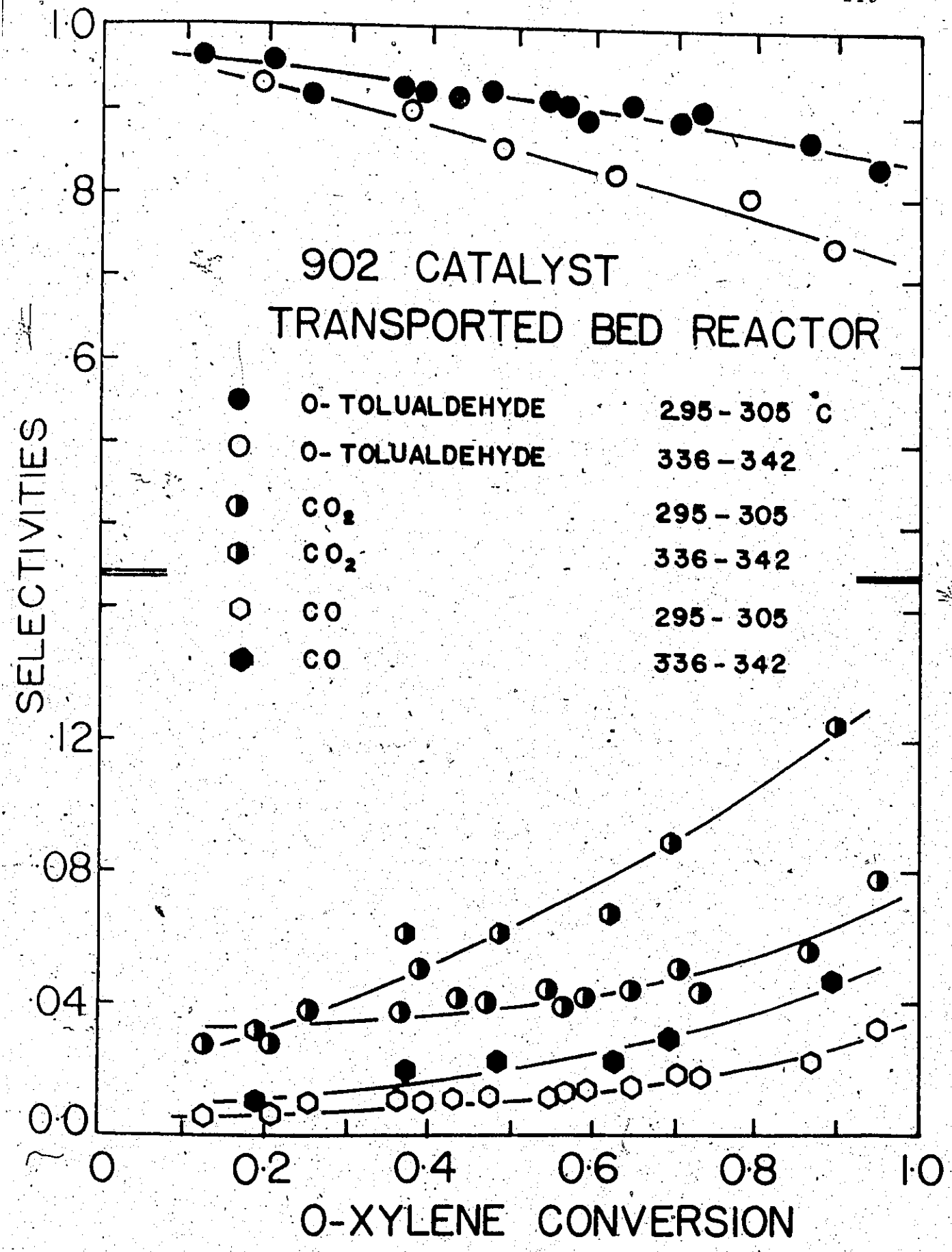

Figure 7.6. Selectivity Data Obtained from Transported Bed Reactor.

experiments are summarized in Table 7.2.

Figure 7.6 shows selectivities obtained at temperatures around 300 and 340°C. In particular, it should be noted that the selectivity to the main partial oxidation product orthotolualdehyde is very high. Industrial reactors rarely exceed 70 percent selectivity as has been noted earlier. The low yields of phthalic anhydride obtained in this study are due to the particular catalyst. It was shown in the fixed bed experiments that silica gel-supported catalysts have poor selectivity for phthalic anhydride production. A silica-supported catalyst was used in this study, since no catalyst with the desired selectivity and fluidization characteristics is available in quantities sufficient for a pilot-plant scale work. In addition to the high selectivity of orthotolualdehyde, it can be seen in Figure 7.6, that the amounts of over-oxidation products, carbon dioxide and carbon monoxide, are doubled by a 40°C change in temperature. The observation that partial oxidation is favoured by reaction at lower temperatures has been noted elsewhere (H2). Therefore oxidation reactions of this type should be conducted at low temperatures to obtain high yields of partial oxidation products. The selectivities for other reaction products including phthalic anhydride, phthalide, maleic anhydride, orthotoluic acid have not been included in Figure 7.6 since they were all present in relatively small concentrations. A peak with almost the same retention time as orthoxylene was noted in some of the chromatograms obtained in the transported bed and unsteady-state fixed bed experiments using the 902 catalyst. This was possibly a small amount of

Run	Experimental Conditions					Mean Voidage Section		Xylene Conversion	Selectivities				
	W/Fa_o	T(°C)	W_s/W_G	W_s(lb/min.)	% Xylene	Top	Bottom	%	OTA	PA	MAA	BZ	
1	64	300	112	36.3	1.66	.87	.84	56.2	91.3	0.4	0.6	3.8	1.4
2	154	302	197	41.2	2.08	.73	.69	87.0	87.6	0.3	1.2	5.6	2.3
3	84	306	142	39.2	1.98	.84	.78	77.5	87.1	0.2	1.4	5.3	1.8
4	78	342	127	35.7	1.96	.83	.80	69.0	79.7	1.4	2.0	9.1	3.0
5	82	305	123	34.8	1.91	.83	.79	65.5	88.8	0.2	0.5	4.5	1.6
6	176	305	114	31.3	0.98	.82	.79	75.6	88.4	0.3	0.8	5.7	1.6
7	94	264	129	35.7	1.98	.79	.76	41.2	95.5	0	0	1.7	0.9
8	97	249	140	39.6	1.94	.79	.75	29.7	92.3	0	0	5.0	0.8
9	85	314	125	34.6	1.97	.83	.77	71.8	89.0	0	0	5.9	2.0
10	146	337	209	39.4	2.82	.68	.64	98.9	58.2	1.8	5.0	20.3	3.5
11	146	300	210	39.0	2.86	.68	.64	95.0	83.3	0.7	1.5	7.8	3.3
12	92	295	160	44.9	1.96	.80	.77	64.9	91.1	0.1	0.4	4.5	1.5
13	353	233	215	39.9	1.75	.53	.47	49.2	90.3	0	0	6.4	2.5
14	126	290	100	30.4	1.11	.84	.81	55.2	91.5	0	0.2	4.6	1.3
15	132	340	112	34.4	1.11	.83	.80	66.9	88.0	0.2	0.6	5.7	1.9
16	109	300	139	39.0	1.96	.78	.71	75.8	90.8	0.3	0.9	4.4	1.8
17	100	333	116	32.6	1.96	.80	.74	79.2	80.9	0.3	2.0	8.0	3.1
18	114	336	90	29.1	1.04	.86	.82	62.6	82.9	0.9	1.7	6.7	2.6
19	115	304	102	32.4	1.06	.86	.82	59.3	89.5	0	0.5	4.2	1.4
20*	82	295	102	32.4	1.06	.91	-	43.4	91.9	0	0.1	4.2	1.0

* Orthoxylene introduced 7 ft. above elbow.

TABLE 7.2. Chemical Reaction Data from Transported Bed Experiments.

p-benzoquinone which has been observed elsewhere (M7, J4).

Analysis of Results

Because of the gas analyses and solids hold-up measurements, it was possible to analyze the reactor in two sections. Gas analysis at the first sample port gave the feed composition for the lower section. The composition of the feed for the upper section was obtained from the mid-reactor samples. The data were analyzed as if they came from two separated reactors. In the analysis which follows only slight differences could be detected between the performance of these two reactors so that the results are presented for the overall reactor. This approach was also adopted because it was felt that the analyses obtained at the first sample port may have been subject to certain errors arising from adsorption and dispersion effects since the sample was taken approximately 2 inches from the point at which orthoxylene was introduced to the catalyst/air stream.

Since the experiments were conducted in a region of solid-gas flow that was not completely defined, it was decided that a simple kinetic model should be adopted. Therefore the data were analyzed on the basis of overall conversion of orthoxylene.

The disappearance of orthoxylene was modelled by a first order reaction, viz.:

$$r_r = k_r c_r \qquad (7.1)$$

that is, assuming $\theta = 1$ in all cases. The values of k_r are plotted against reciprocal absolute temperatures in Figure 7.7.

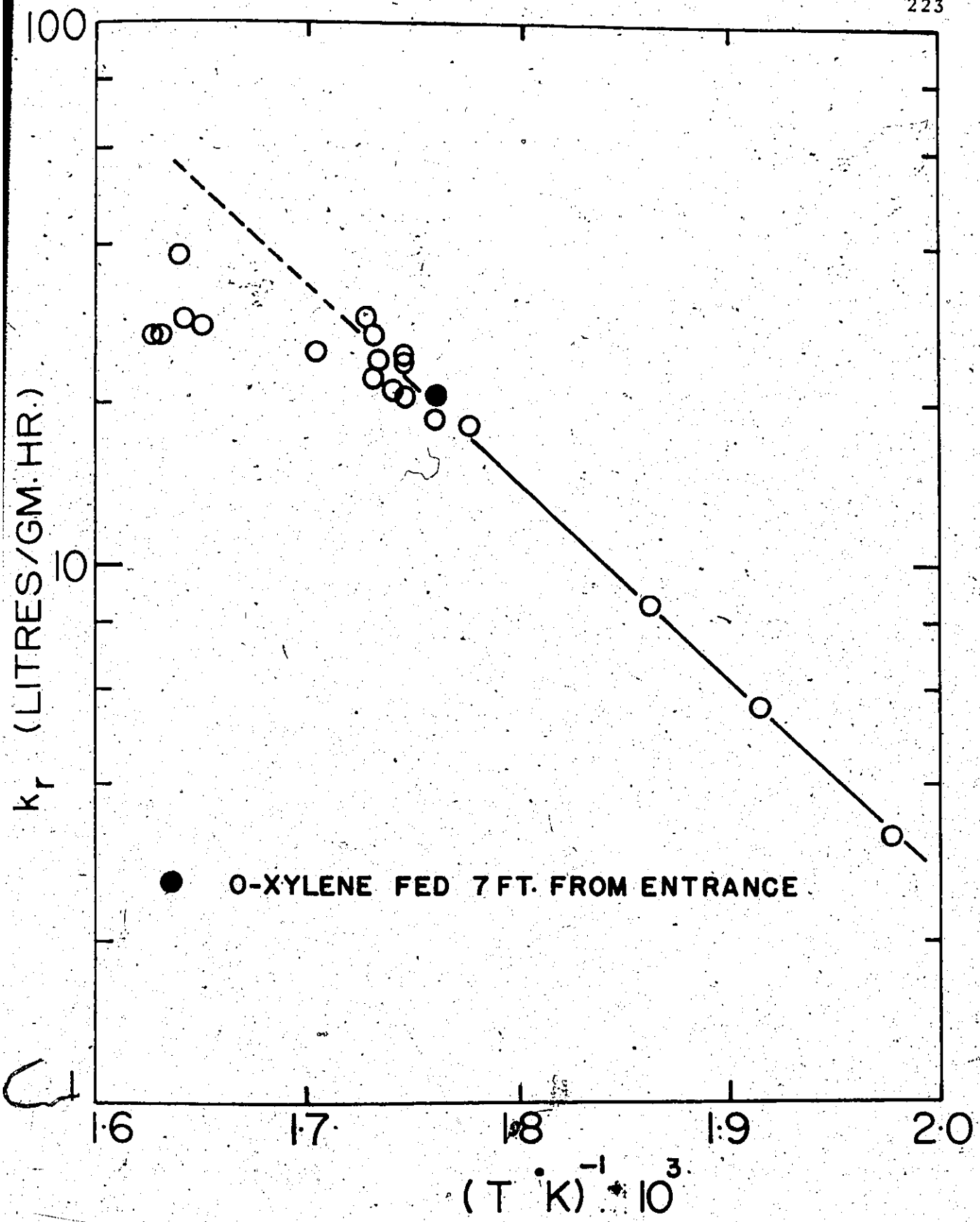

Figure 7.7. Arrhenius Plot of k_r Values.

This plot indicates that an Arrhenius-type temperature dependency is obeyed for temperatures below 300°C. Increasing the reaction temperature above this level produced only small increases in reaction rate except for one experiment where the solids loading in the reactor was quite high.

There are a number of possible explanations for this observed behaviour at higher temperatures:

(i) Mass Transfer Limited Reaction

It is possible that the rate of mass transfer may be limiting the rate of reaction at the higher temperatures. Two observations are important: Firstly, it is shown in Appendix A that mass transfer rates are significantly higher than rates of reaction. Secondly, the sharp discontinuity in Figure 7.7 is inconsistent with mass transfer control. Mass transfer is a temperature dependent process and therefore a slight increase in the tabulated value of k_r would be expected with increased temperature. However, measured reaction rate at 300°C and 340°C were almost identical.

(ii) Loss of Catalyst Activity at the Higher Temperatures

In Chapter 4 it was shown that SO_3 losses from German-type catalysts account for the loss of catalyst activity with time. It might therefore be argued that perhaps the catalyst activity is reduced at higher temperatures through depletion of SO_3. The long term catalyst activity did not change since experiments around 300°C ($\frac{1}{T} = 1.75 \times 10^{-3}$) were carried out following experiments at other temperatures to monitor catalyst

activity. No significant nor systematic variation in these results is observed.

The short-term activity relates to the assumption that $\theta = 1$. If in fact the amount of oxygen consumed per gram of catalyst was more at the higher temperatures than at the lower values, then a decrease in activity might be suggested. Again there is no correlation of the deviation with this ratio. Further substantiation of this is provided by the observation that the reaction rate constants are essentially the same for both sections of the reactor. It might be argued that such an effect may be masked by the fact that less of the catalyst contacts the reaction gases in the lower section because of the reactor length required to disperse the orthoxylene over the entire reactor cross section. It would seem highly improbable that this effect would produce the same effect for all experiments considering the range of variables employed.

The extremely high reaction rates in both the transported bed and the packed bed reactors at short on-stream times suggest that there is the possibility of different types of active oxygen under these conditions, that is, the oxygen in the surface layers of the catalyst lattice and oxygen which is chemisorbed to the catalyst surface. Kakinoki et al. (K4) have shown, by experiments conducted in a B.E.T. apparatus at 400°C, that 2 c.c. of oxygen can be adsorbed on one gram of a similar catalyst. Even more oxygen is expected to be adsorbed at lower temperatures. The regeneration stage in the transported bed not only reoxidizes the catalyst but replenishes the

chemisorbed oxygen as well. The amount of chemisorbed oxygen will be reduced at the higher temperatures and this could explain a reduced activity at high temperatures. This mechanism should, however, produce a gradual change in activity with temperature unless there are different types of chemisorbed oxygen above and below 300°C. Such differences have been detected in other catalyst systems.

(iii) Adsorption of Hydrocarbon on the Catalyst

The reactor model assumes that the rate of adsorption of orthoxylene is instantaneous, that is, it reaches its equilibrium concentration on the catalyst surface within a very short reactor length and hence does not influence the rate of reaction. It is also implicitly assumed that the amount of reactant is small relative to the gas phase. If this were an important effect, there would be a strong correlation of performance with solids hold-up in the reactor; such correlation was not observed. It is also assumed that adsorption is non-selective, that is, the ratio of concentrations of adsorbed species is the same as that in the gas phase.

It is recognized that these adsorption effects could be very important in transported bed reactors, since they differ from normal reactors which contain a fixed catalyst charge which has time to equilibrate with the surrounding gas. This aspect obviously warrants further study. However, this adsorption phenomenon cannot explain the observed variation with temperature.

(iv) Solids-Gas Contacting

In this analysis, the gas and solids are assumed to be intimately mixed. The fluid mechanical behaviour is assumed to be the same under all operating conditions. On the other hand, as the reaction temperature is increased, the fluid velocity must increase for the same mass flow of gas. If, in fact, this increased gas velocity caused a change in the flow behaviour of the solids-gas mixture of just above 300°C and this in turn caused part of the gas to bypass the catalyst, then an apparent loss in reaction rate would be observed. Since operation is close to the apparent slugging regime, this seems to be a logical explanation for the lower reaction rates. The one point which is much higher is at much higher solids loading and lower gas velocity and the flow regime under these conditions may be similar to that at the lower temperatures thus somewhat substantiating this hypothesis.

Thus only when the flow regimes are adequately mapped for this reactor, can an adequate analysis of reactor performance be effected.

It should be noted that the above discussion of the reduced rates observed at temperatures above 300°C is purely speculative. An attempt has been made to highlight the points that must be considered in a more rigorous analysis of this unique type of reactor. Although it is felt that the reduced rates are a result of less efficient gas-solid contacting, it is acknowledged that adsorption effects may also be present. However, their effect is likely to be small.

The temperature range from 233°C to 343°C is much greater than that normally studied in reaction experiments. Therefore one cannot discount the possibility, albeit remote, that a different kinetic mechanism may apply above and below 300°C. It was noted earlier, in Chapter 5 that the catalyst forms different melts at different temperatures. The possibility of a phase change at these temperatures cannot therefore be discounted. It is obvious from the packed bed experimentation that considerable research must be conducted into these catalyst systems.

7.4. Conclusions and Recommendations

Notwithstanding the shortcomings of the analysis of the results, it can be stated without qualification that the transported bed provides a means of obtaining extremely high reaction rates for oxidation reactions involving the catalytic mechanisms associated with the orthoxylene oxidation reaction. Figure 7.8 demonstrates this dramatically; it shows that the reaction rates observed in this system are very much higher than those observed in a fixed bed of the same catalyst. Indeed, extrapolation of the transported bed data to higher temperatures suggests that the reaction rates are even higher than those observed in the packed bed after it is on-stream for only 10 seconds. The advantage of these high reaction rates can be exploited by conducting hydrocarbon oxidations at temperatures lower than those normally used. In this way, higher selectivities to partial oxidation products can be achieved. The industrial

Figure 7.8. Rates of Reaction on 902 Catalyst. Comparison of rates of xylene conversion obtained for different catalysts at .01 atm o-xylene and 0.21 atm oxygen pressures.

A After 10 seconds contact on 902 catalyst in packed bed

B Transported bed data for 902 catalyst.

C Steady-state packed bed data on 902 catalyst.

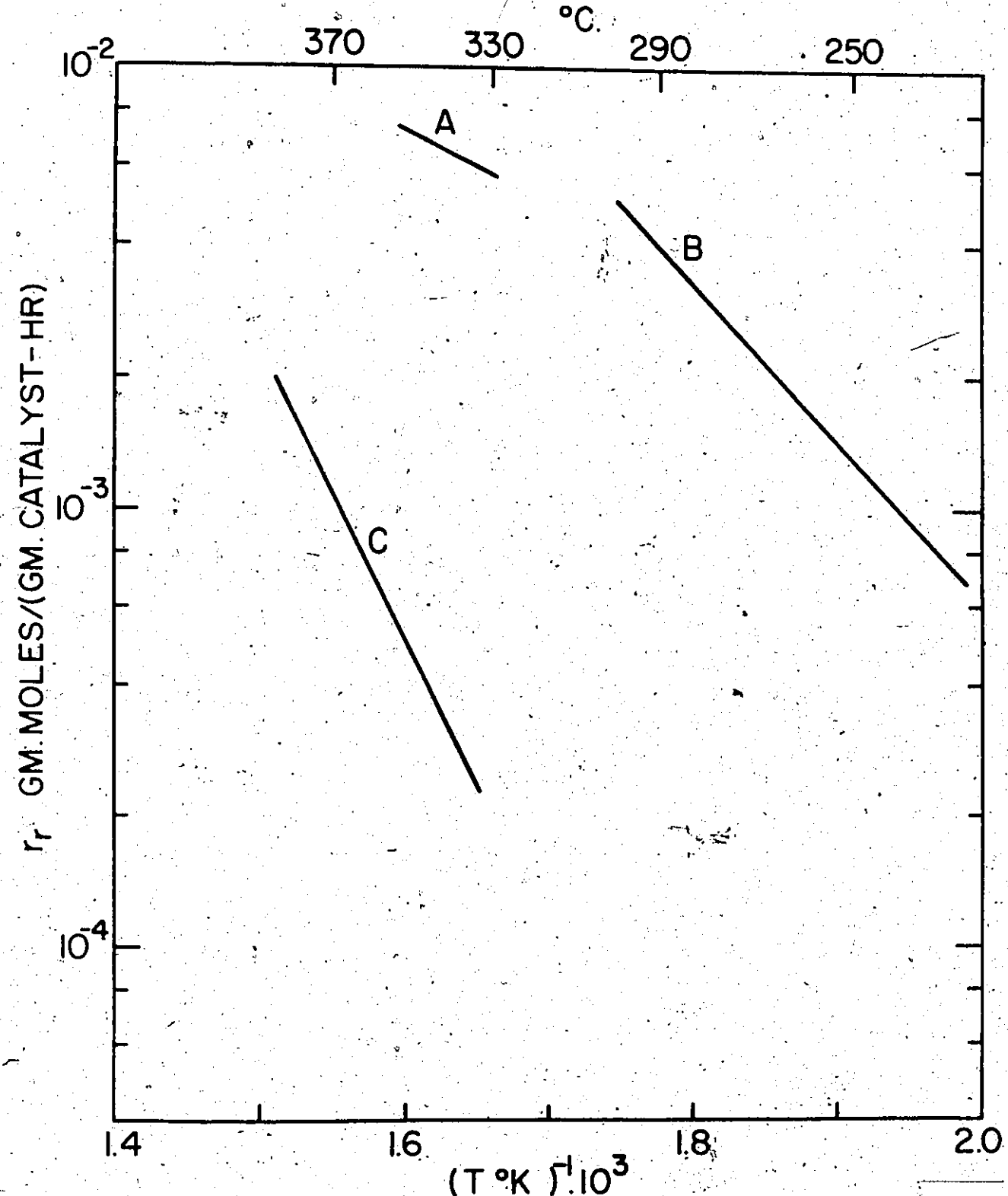
°C
370
330
290
250
10^{-2}
10^{-3}
10^{-4}
A
B
C
r_r GM.MOLES/(GM.CATALYST-HR)
1.4
1.6
1.8
2.0
$(T\,°K)^{-1}.10^3$

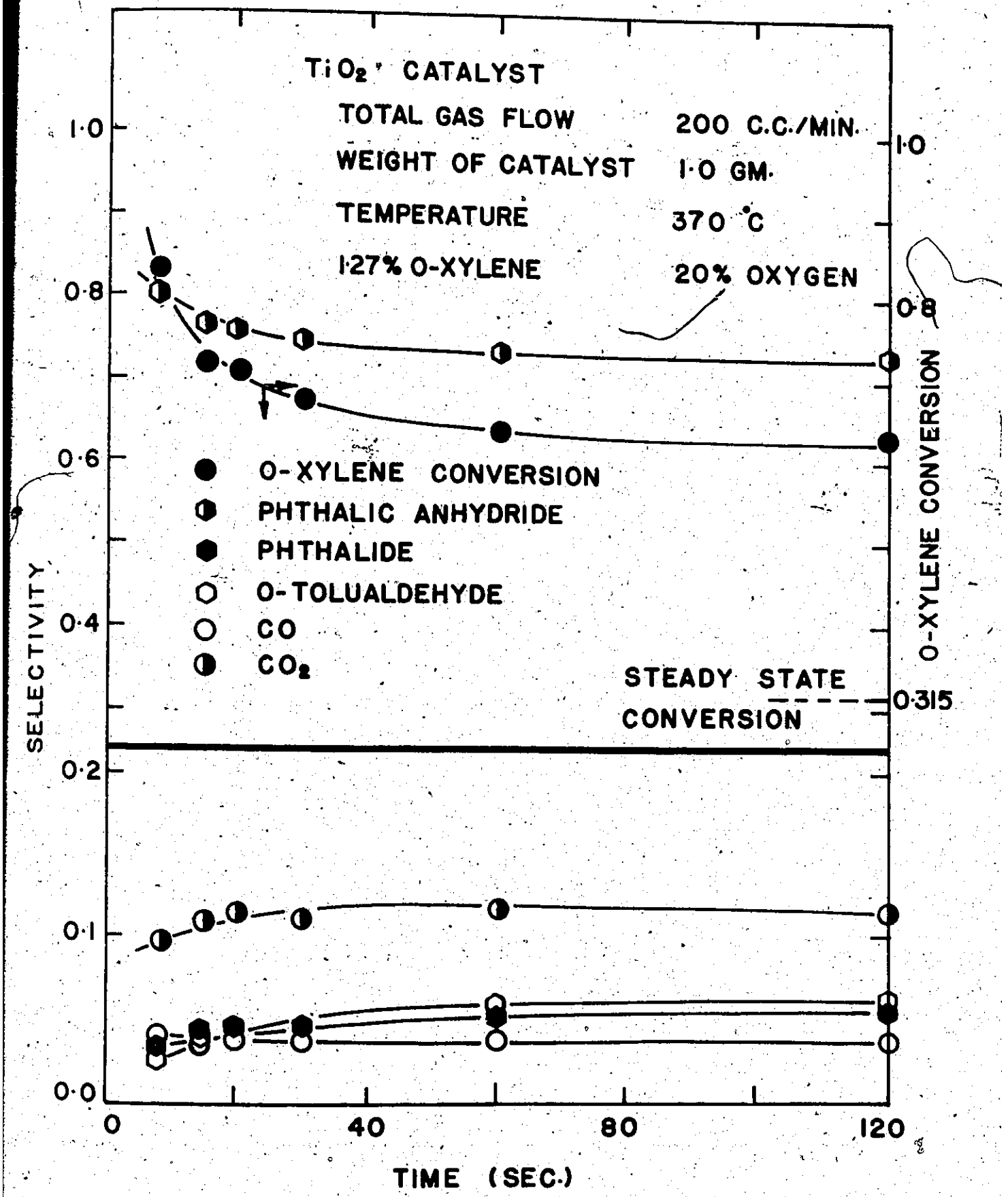

Figure 7.9. Initial Rates and Selectivities on TiO_2-Supported Catalyst.

potential of this situation becomes an economic tradeoff between the saving in feedstocks and the additional costs associated with the more complex equipment and possible catalyst losses.

The major objective of this work was to investigate the potential of transported bed reactors for conducting hydrocarbon oxidations. This objective has been achieved. It was also hoped at the outset of the research that high yields of phthalic anhydride might have been obtained. The packed bed research indicated that this objective could not be met with commercially available fluidization catalysts. However, the potential of the system for phthalic anhydride production is demonstrated by reference to Figure 7.9 which shows the unsteady-state performance of a typical catalyst used for producing phthalic anhydride from orthoxylene. It can be seen that for this catalyst the initial rates are only several times greater than the steady-state value. However, even this increase in rate could result in obtaining the same yield as a fixed bed at a 40°C lower reaction temperature, thereby improving the selectivity to phthalic anhydride. The physical properties of the catalyst must also be considered. It is recognized that although the titania-supported catalyst has excellent selectivity to phthalic anhydride it may not be suitable for use in a transported bed reactor because it may suffer from excessive attrition.

CHAPTER 8

SUMMARY AND CONCLUSIONS

8.1. Summary

The results of this research and the contributions to knowledge can be summarized as follows:

(i) A method of chromatographic analysis of the products of the partial oxidation of orthoxylene from a single sample has been developed. It has been shown to be effective over a wide range of product distributions and conversions.

(ii) This single step analysis has enabled a study to be made of the transient operation of packed beds of vanadia catalysts for the oxidation reaction.

(iii) The importance of sulphur dioxide addition has been discussed in some depth relative to the decay phenomena observed in this and other studies. In particular, the effect of thermal deactivation has been observed.

(iv) The influence of the catalyst-support material in determining reaction selectivities has been investigated by conducting experiments in packed beds of catalysts supported on silica, alumina and titania.

(v) A comprehensive investigation of both the unsteady-state and steady-state performance of a silica-gel-supported catalyst was conducted in an isothermal packed bed reactor.

(vi) Kinetic parameters were estimated for a reaction model involving series and parallel steps using the steady-state

observations of conversion and reaction product concentrations for the silica-supported and titania-supported catalysts.

(vii) A pilot-plant transported bed reactor was designed and constructed. This involved a detailed knowledge of particle flow from bins, vertical pneumatic transport, measurement and control of particle and gas flows, particle-gas separations and gas sampling. In addition, health and pollution hazards had to be considered in the design.

(viii) Pressure-drop and solids hold-up measurements were made over a wide range of gas and particle flows. To the best of the author's knowledge these experiments covered a range of dense-phase pneumatic conveying hitherto unreported for such small, light particles.

(ix) The oxidation of orthoxylene in air was studied in a transported bed reactor over a wide range of temperatures (233 to 342°C) and orthoxylene concentrations (1 to 3 percent).

(x) As a result of the current study, the important factors to be considered in future research involving transported bed reactors have been discussed.

8.2. Recommendations for Future Work

It is apparent as a result of this research that considerable fundamental research has to be conducted in the following areas:

(i) the partial oxidation of aromatic organic compounds on vanadia catalysts including the effect of support and chemical additions to the catalyst.

(ii) dense phase pneumatic conveying,

(iii) further evaluation of the transported bed as a chemical reactor.

Some of the specific research that needs to be initiated on each of these topics is discussed in turn.

1. Oxidation of Aromatic Hydrocarbons on Vanadium Pentoxide Catalysts

(i) Before any further studies of the oxidation of aromatic hydrocarbons are made, it is essential that the role of SO_3 in determining catalyst reactivity and selectivity is better understood. The work of Mizushina et al.(M3) indicates that there is an optimum SO_3 level for a given catalyst. The conclusions researched in that study have been criticized earlier in the text. The value of the work was limited by the fact that most of the experiments were conducted at 100 percent conversion of orthoxylene. A detailed study should therefore be made at lower conversions.

(ii) The role of SO_2 in the feed gas in determining the SO_3 level in the catalyst is not well understood. The fact that one group (K1) has found it necessary to use 50 times the SO_2 level that another group (E2) has used to stabilize catalyst activity suggests that further investigation of this aspect should be conducted. In particular, it would be helpful to determine the extent of SO_2 oxidation under conditions of orthoxylene oxidation. Published data on rates of SO_2 oxidation on vanadia catalysts would suggest that this is small.

(iii) The large differences in temperatures at which melts are thought to occur in the V_2O_5-K_2SO_4-SO_3 system suggests that it would be helpful to construct a phase diagram for this system. In addition, the decomposition of potassium pyrosulphate should be studied since it would aid in determining the role of K_2SO_4 and SO_3 in these systems.

(iv) The major weakness of the research by the Japanese group referred to earlier is that they used reactors in which 100 percent conversion of orthoxylene was obtained. Many of their results were therefore inconclusive. Therefore many of their experiments on the effect of catalyst support material should be conducted in isothermal packed bed reactors operating at less than 100 percent conversion. Additional support materials should be investigated with a view to finding a robust catalyst that is capable of producing high yields of phthalic anhydride in fluidized and transported beds.

(v) For chemical engineers the ultimate aim should be to provide a system of design equations which adequately model the yields and conversions for reaction conditions approximating those used industrially. This cannot be done with the present state of knowledge of these oxidation reactions. When some of the fundamental questions concerning catalyst behaviour have been answered it will be possible to provide a more adequate model to describe the chemical kinetics occurring on these catalysts.

(vi) Work on the S.S.A.M. model as typified by the study of Juusola (J4) should be extended to higher conversions. This could be accomplished by operating in isothermal packed beds

of the type used in the current study. A catalyst capable of producing high yields of phthalic anhydride from both orthoxylene and naphthalene feedstocks should be used. In addition, a detailed study of the oxidation at short contact times may offer further support for the mechanisms of the reactions. The limited unsteady-state data obtained in the current study suggests that extrapolation of conversion and selectivity data to zero time ($\theta = 1$) should be possible for these systems.

II Fluid Mechanics of Dense-Phase Pneumatic Conveying

(i) The hold-up and pressure drop data presented in this thesis were obtained from very few experiments. The effectiveness and accuracy of the experimental methods have been well established in this preliminary investigation. Further experimentation at different solids loadings should now be conducted. The range of gas flows can be extended by using different sized sonic orifices. The flow rates of particles can be changed by using different sized orifices at the exit of the feed tank. In this way it may be possible to map entire slugging regions for particles of a given size.

(ii) Since the apparatus has been shown to be capable of accurately controlling and measuring solids flows, it is suggested that it be used for fundamental studies of dense phase conveying. The two heated reactor sections can be replaced by commercially-available boro silicate glass pipe of the same bore (5/8 in.) so that flow visualization studies can

be made. It is suggested that glass pipe be used in place of polymethyl methacrylate since the latter would suffer considerable scratching due to particle abrasion.

III Transported Bed Reactor Studies Involving Oxidation Reactions on Vanadium Pentoxide Catalysts

(i) The extent to which adsorption effects determine the reactor performance should be investigated. This can be obtained indirectly from carbon balances made on the basis of the xylene and air flows and gas compositions measured at various axial locations. Although the problem of air leakage into the sampling system prevented an accurate determination of a total carbon balance in the current study, the data obtained did indicate that the amount of orthoxylene adsorbed on the catalyst was small compared to that in the gas phase. The use of higher quality valves and fittings should eliminate the difficulties experienced in this study. Additional adsorption studies of the type described by de Lasa and Gau (D1) should also be conducted on silica-gel particles containing no active catalytic agent. Separate adsorption studies using microbalance techniques may also prove useful.

(ii) Although the current study achieved its objective of showing that hydrocarbon oxidations of the orthoxylene type can be successfully carried out in a transported bed reactor, it was somewhat disappointing that more industrially acceptable reaction yields were not obtained. This has been shown to be due to the particular catalyst employed. Since it is unlikely that a suitable orthoxylene oxidation catalyst having the

desired fluidization properties will be available in the short term, it is suggested that future work be concerned with naphthalene oxidation. The 902 catalyst used in this study is successfully used industrially to produce phthalic anhydride from naphthalene in fluidized beds. A new feed system to monitor the flow of molten naphthalene would have to be constructed. The chemical analysis could be accomplished using the gas chromatographic technique described in Chapter 3. Calibration for naphthalene, and 1, 4 naphthaquinone should be the only additional measurements required. Apart from the problem of feeding molten naphthalene it is felt that naphthalene oxidation is a superior reaction to orthoxylene oxidation for investigating the performance of a transported bed reactor. This because the latter reaction involves many isolatable intermediates including ortho-tolualdehyde, ortho-toluic acid and phthalide whereas the former is generally considered to involve only one, namely naphthaquinone. Parameter estimation would be easier in the case of the less complex reaction sequence. Therefore naphthalene oxidation would be superior for a study of the type described by Shaw et al (S12). In such a study the parameters describing the fluid mechanics of a gas-solid contacting system can be estimated from chemical reaction response data for the system if prior estimates of the reaction rate parameters in the reaction model are available from packed bed experiments.

(iii) The oxidation of SO_2 to SO_3 on vanadium pentoxide catalysts is a reaction that may exploit the advantages of a transported bed reactor. It is likely that high initial

rates of reaction similar to those obtained for orthoxylene will apply for SO_2 oxidation. This would permit oxidation of SO_2 at lower temperatures than are normally employed thereby taking advantage of more favourable equilibrium conditions. This method may have some advantage in the removal of SO_2 from gas streams to meet pollution standards.

8.3. Industrial Considerations

(i) The data of this and other studies (M7, J4, H2) indicate that for orthoxylene concentrations between 1 and 3 percent by volume in air, the rate of reaction in a packed bed operating at steady state is almost independent (zero order) of xylene concentration. However, the rate of reaction is found to be highly dependent on the oxygen level for oxygen concentrations in the range 10% to 30%. This indicates that the rate determining step in the oxidation of the hydrocarbon is the rate of re-oxidation of the catalyst. Therefore increased throughput can be achieved in industrial reactors by enriching the air with oxygen. An alternative approach would be to use a catalyst that is always in a highly oxidized state. The transported bed reactor provides this alternative.

(ii) At the time this research project was commenced, orthoxylene was rapidly overtaking naphthalene as the major feedstock for phthalic anhydride manufacture (O1). In fact, in 1968 30% of the phthalic anhydride produced in the U.S. was based on orthoxylene and by the end of 1972 this figure had risen to 55%. During that period increasing amounts of ortho-xylene were produced by superfractionation from mixed xylenes

recovered in petroleum refining whilst coal tar production remained almost constant (02). Coal tar naphthalene is obtained as a by-product of steel making and the constant production level is due to a change in steel making technology in which decreased amounts of coke are required per ton of pig iron. Some petroleum naphthalene is also produced but this is generally more expensive than coal tar naphthalene. The current shortage of oil and interest in coal as a source of synthetic fuels, suggests that coal tar naphthalene may once again become the main feedstock for phthalic anhydride production. Since suitable fluidized oxidation catalysts are available for naphthalene oxidation, it is possible that this work on transported beds may have some industrial potential. The advantage of operating at lower reaction temperatures, thereby decreasing the extent of over-oxidation, would have to be weighed against the increased cost of more complex equipment, possible losses of catalyst by attrition, and erosion of reactor internals.

(iii) Product purification is a major cost factor in phthalic anhydride production. Therefore industrial reactors generally run at 100 percent conversion of orthoxylene or naphthalene. However, excessive residence times should be avoided to prevent further oxidation of the phthalic anhydride produced. Such a condition is difficult to achieve in fluidized beds. However, packed bed and transported bed reactors, because of their near plug flow characteristics for the reactants can achieve close-to 100 percent conversion without excessive over-oxidation. The major impurity in the condensed product stream is maleic

anhydride which is probably mainly produced by over-oxidation of phthalic anhydride. It has been shown by Hughes and Adams (H3) that this reaction occurs at relatively high rates only at high temperatures (in excess of 400°C) and on catalysts having high concentrations of V_2O_4. Therefore operation at low temperatures with highly oxidized catalysts in transported beds should significantly reduce maleic anhydride formation.

The advantages of transported bed reactors for conducting aromatic hydrocarbon oxidations described above are based on limited experimentation in a laboratory packed bed reactor and in a pilot-plant scale transported bed reactor. Further work should be continued on this project to determine if the system does have industrial potential.

One can envisage a typical industrial reactor consisting of a bundle of vertical conveying tubes (approximately 1 inch in bore and 30 to 60 feet high) around which a suitable heat transfer fluid circulates for cooling. Catalyst reoxidation would be accomplished in a separate fluidized bed reactor which might also be used to strip adsorbed products from the spent catalyst.

BIBLIOGRAPHY

A1 Atack, (To British Alizarine Co. Ltd.), British Patent No. 182,843 (1922) in Marek, L. F., Hahn, D. A., "The Catalytic Oxidation of Organic Compounds in the Vapour Phase", The Chemical Catalogue Co. (1932).

A2 Anderson, R. B., Private communication, (McMaster University), 1973.

B1 Bunn, D. P., Gruenke, G. F., Jones, H. B., Luessenhop, D. C., Youngblood, D. J., Chem. Eng. Prog. 65, (6), 88, (1969).

B2 Bhalla, S. K., M.Eng. Thesis, McMaster University, (1967).

B3 Boothroyd, R. G., "Flowing Gas-Solids Suspensions", Chapman and Hall, London, (1971).

B4 Berg, C., U.S. Patents 2,684,868; 2,684,870; 2684,872, (July 27, 1954).

B5 Bulsara, P. U., Zenz, F. A., Eckert, R. A., Ind. Eng. Chem. Process Des. Develop., 3, 348, (1964).

B6 Beck, M. S., Wainwright, N., Powder Technol., 2, 189 (1968/69).

B7 Beck, M. S., Drane, J., Plaskowski, A., Wainwright, N., Powder Technol., 2, 269, (1968/69).

B8 Beck, M. S., Wainwright, N., Control, Jan. 1969, P.52.

B9 Bystrom, A., Wilhelmi, K. A., Brotzen, O., Acta Chem. Scand., 4, 1119 (1950).

B10 Box, G. E. P., Hunter, J. S., Technometrics, 3, 311, (1961).

B11 Ibid, 3, 449, (1961).

B12 Box, G. E. P., Draper, N. R., Biometrika, 52, 355, (1965).

B13 Box, G. E. P., Cox, D. R., J. Roy. Statis. Soc., Series B, 26, 211, (1964).

B14 Box, G. E. P., Hunter, W. G., MacGregor, J. F., Erjavec, J., Technometrcs, 15, 33, (1973).

B15 Bartlett, M. S., J. Roy. Statis. Soc., Suppl., 4, 137, (1937).

B16 Box, M. J., Compt. J., 9, 67, (1966).

B17 Baron, T., Manning, W. R., Johnstone, H. F., Chem. Eng. Prog., 48, 125, (1952).

C1 Capes, C. E., Can. J. Chem. Eng., 49, 182, (1971).

C2 Calderbank, P. H., Caldwell, A. D., First International Symposium on Chemical Reaction Engineering, Washington, D.C., June, 1970.

C3 Calderbank, P. H., Private communication, (May, 1972).

C4 Calderbank, P. H. Watt, G. I. Ellis, S. N., Second International Symposium on Chemical Reaction Engineering, Amsterdam, May, 1972.

C5 Cotton, F. A., Wilkinson, G., "Advanced Inorganic Chemistry - A Comprehensive Text", Second Ed., Interscience, New York, (1966).

D1 de Lhsa, H., Gau, G., Chem. Eng. Sci., 28, 1875, (1973).

D2 Dixon, J. K., Longfield, J. E., in Emmett, P. H., Ed., "Catalysis", Vol. VII, 212-217, Reinhold, New York, (1960).

D3 Duckworth, R. A., Chemical and Process Engineering, 50, (1), 69, (1969).

D4 Downie, J., Shelstad, K. A., Graydon, W. F., Can. J. Chem. Eng., 39, 201, (1961).

D5 Dye, D. E., Journal of Basic Engineering, Transactions of ASME, p. 1025, (Dec., 1965).

E1 Echigoya, E., Yen, S., Morikawa, K., Kagaku Kogaku, 32, 1002, (1969).

F1 Fugate, W. O., U.S. Patent 2,698,330, (1954).

F2 Froment, G. F., Private communication, 1971.

F3 Froment, G. F., Private communication, 1973.

F4 Farbar, L., Morley, M. J., Ind. Eng. Chem., 49, 1143, (1957).

G1 Garrett, L. W., Chem. Eng. Prog., 56 (4), 39, (1960).

G2 Goldberg, A. S., Boothroyd, R. G., Brit. Chem. Eng., 14, 1705, (1969).

G3 Goldberg, A. S. Boothroyd, R. G., Brit. Chem. Eng., 15, 357, (1970).

H1 Hayashi, R., Hudgins, R. R., Graydon, W. F., Can. J. Chem. Eng., 41, 220, (1963).

H2 Herten, J., Froment, G. F., Ind. Eng. Chem. Process Des. Develop., 1, 516, (1968).

H3 Hughes, M. F., Adams, R. T., J. Phys. Chem., 64, 781, (1960).

H4 Hollis, O. L., Anal. Chem., 38, 309, (1966).

H5 Hunter, W. G., Ind. Eng. Chem. Fundamentals, 6, 461, (1967).

H6 Hunter, W. G., Atkinson, A. C., Chem. Eng., 73, No. 12, 159, (1966).

I1 Imamura, H., Tsuzi, J., Yokoogi, M., Radioisotopes, 11, 16, (1962).

J1 Jasimuzzaman, A., Ph.D. Thesis, The University of Alberta, Edmonton, Alberta, Canada, (1972).

J2 Jaswal, I. T., Mann, R. F., Juusola, J. A., Downie, J., Can. J. Chem. Eng., 47, 284, (1969).

J3 Juusola, J. A., Mann, R. F., Downie, J., J. Catalysis, 17, 106 (1970).

J4 Juusola, J. A., Ph.D Thesis, Queen's University, Kingston, Canada, (1971).

J5 Jariwala, S. L., Wakeman, I. B., J. Chromatog. Sci., 8, 612 (1970).

J6 Juusola, J. A., Bacon, D. W., Downie, J., Can. J. Chem. Eng., 50, 796, (1972).

K1 Kakinoki, H., Sahara, N., Kamata, I., Aigami, Y., Shokubar, 4, 113, (1962).

K2 Kunii, D., Levenspiel, O., "Fluidization Engineering," Wiley, New York, (1960).

K3 Klar, R., Australian Patent 167,576, (April 30, 1956).

K4 Kakinoki, H., Mizushina, F., Tanaka, T., Aigami, Y., Suzuki, H., Sekiyu, Gakkai, Shi, 7, (3), 164, (1964).

K5 Keulemans, A. I. M., "Gas Chromatography", Reinhold, New York, (1959).

L1 Levonspiel, O., J. of Catal., 25, 265, (1972).

L2 List, H. L., D. Chem. E. Thesis, Polytechnic Institute of Brooklyn, New York, (1958).

M1 Mertens, E., J. Chem. Phys., 47, 286, (1950).

M2 Moss, R. A., Kelly, A. J., Int. J. Heat Mass Transf., 13, 491, (1970).

M3 Mizushina, F., Tanaka, T., Aigami, Y., Kakinoki, H., Suzuki, H., Sekiyu, Shi, 7, (11), 30, (1964).

M4 Maselli, J. M., Kim, G., (to W. R. Grace and Co.) Canadian Patent No. 873904, (June 22, 1971).

M5 Mars, P., van Krevelen, D. W., Chem. Eng. Sci., (Spec. Suppl.), 3, 41, (1954).

M6 Mann, R. F., Downie, J., Can. J. Chem. Eng., 46, 71, (1969).

M7 Mann, R. F., Ph.D Thesis, Queen's University, Kingston, Canada, (1966).

M8 Mellor, J. W., "A Comprehensive Treatise on Inorganic and Theoretical Chemistry," Vol. 10, pp. 445-46, Longmans, London, 1930.

M9 Mickley, H. S., Trilling, C. A., Ind. Eng. Chem., 41, 1135, (1949).

M10 Mugakami, Y., Bull. Chem. Soc. Japan, 32, 316, (1959).

M11 Mikkelson, L., Davidson, I., Hewlett-Packard Technical Paper No. 45.

N1 Nonnenmacher, H., M. Appl. Andrusson, K. German Patent 1,144,709, assigned to BASF, (March 6, 1963).

N2 Nelder, J. A., Mead, R., Compt. J., 7, 308, (1965).

O1 Ockerbloom, N. E., Hydrocarbon Processing, 50, (9), 162, (1971).

O2 ibid., 50, (12), 101, (1971).

P1 Paetkau, T. R., M.Eng. Thesis, McMaster University, (1966).

P2 Purnell, H., "Gas Chromatography", Wiley, New York, (1962).

R1 Rose, H. E., Barnacle, H. E., The Engineer, 203, 898, (1957).

R2 Ross, G. L., Calderbank, P. H., Chem. Eng. Sci., 26, 2003, (1971).

R3 Riley, H. L., in "Catalysis in Practice", Inst. Chem. Eng., London, 1963.

S1 Soo, S. L., Regalbuto, J. A., Can. J. Chem. Eng., 38, 160, (1960).

S2 Soo, S. L., Trezec, G. J., Ind. Eng. Chem. Fund., 5, 388, (1966).

S3 Suzuki, H., Kakinoki, H., Mizushima, F., Kamata, I., Sekiyu, Gakkai; Shi, 7, (1), 15, (1964).

S4 Simard, G. L., Stoger, J. F., Arnott, R. J., Siegel, L. A., Ind. Eng. Chem., 47, 1424, (1955).

S5 Shelstad, K. A., Downie, J., Graydon, W. F., Can. J. Chem. Eng., 38, 102, (1960).

S6 Spitz, P. H., Hydrocarbon Processing, 47, (11), 162, (1968).

S7 Saffer, A., "Vanadium Catalysis in the Manufacture of Phthalic Anhydride", in "Catalysis in Practice", Inst. Chem. Eng., London, 1963.

S8 Satterfield, C. N., Loftus, J., A.I.Ch.E. Journal, 11, 1103, (1956).

S9 Safar Baezar, M. A., D.Eng. Thesis, Nancy, (1970).

S10 Satterfield, C. N., Loftus, J., J. Phys. Chem., 69, 909, (1965).

S11 Squires, A., Presentation to Panel Discussion on Fluidization Joint Meeting Can.I.Ch.E.-A.I.Ch.E., Vancouver, (Sept., 1973).

S12 Shaw, I. D., Hoffman, T. W., Orlickas, A., Reilly, P. M., Can. J. Chem. Eng., 50, 637, (1972).

S13 Shaw, I. D., Ph.D Thesis, McMaster University, (1974).

S14 Sathyamarayana, D. N., Patel, C. C., J. Inorg. Nucl. Chem., 27, 297, (1965).

T1 Towers, R. R., in Standen, A., (Ed.), "Kirk-Othmer Encyclopedia of Chemical Technology," 2nd ed., vol. 6, p. 114, Interscience Pub., New York, (1965).

T2 The Engineering Equipment Users Association, "Pneumatic Handling of Powdered Materials", Constable, London, (1963).

T3 Themelis, N. J., Gauvin, W. H., Can. J. Chem. Eng., 41, 1, (1963).

T4 Tandy, G. H., J. Appl. Chem., 6, 68, (1956).

T5 Thomas, C. L., "Catalytic Processes and Proven Catalysts", Academic Press, New York, (1970).

U1 Ushakova, V. P., Korneichuk, G. P., Zhigailo, Ya, V., Ukrain. Khim. Zhur., 23, 191, (1957).

V1 Van Zoonon, D., 3rd. Europ. Cong. Chem. Eng., "The Interaction between Fluids and Particles", 1962, A54 (I.Chem.E.: London).

V2 Vrbaski, T., Mathews, W. K., J. Catalysis, 5, 125, (1966).

V3 Vara Prasad, S. S., Post-doctoral Fellowship Report, McMaster University, (1969).

V4 Van Welsenaere, Unpublished data, University of Ghent, Belgium, (1972).

W1 Wenderlein, H., German Patent, 1,112,060, (1961).

Z1 Zenz, F. A., Othmer, D. F., "Fluidization and Fluid-Particle Systems", Reinhold, New York, (1960).

Z2 Zenz, F. A., Petroleum Refiner, 36, (6), 133-42, (1957).

Z3 Zahner, J. C., First International Symposium on Chemical Reaction Engineering, Washington, D.C., June, 1970.

APPENDIX A

ADDITIONAL CALCULATIONS

A.1. Mass Transfer Considerations Transported Bed Reactor

1. External Diffusion Resistance

In a gas/solid catalytic reaction, it is important to know the magnitude of the resistance to diffusion of the gas from the main stream to the catalyst surface. If this resistance is large enough it may control the overall rate of reaction. The approach generally taken is to calculate the concentration difference, or driving force, necessary to transfer reactant through the gas film at a rate equal to the observed reaction rate. If the concentration difference is insignificant compared to the concentration in the main stream, then the diffusion resistance, is negligible.

In the transported bed reactor, diffusion by convection is difficult to estimate because the velocity of the solids relative to the gas varies depending on the W_S/W_G ratio employed. Slip velocities vary from almost zero at low particle concentrations to approximately half the gas velocity at high concentrations (Table G.2.2, Appendix G). Therefore, the worst case, that is, all diffusion is by molecular diffusion, has been assumed. For this limiting case, the Sherwood number approaches 2. That is,

$$N_{SH} = 2 = \frac{k_G \, RT \, d_p}{D} \qquad (A.1)$$

where N_{SH} = Sherwood Number

k_G = Mass transfer coefficient, $\frac{\text{gm.-moles}}{\text{sec. cm}^2\text{. atm.}}$

d_p = particle diameter, cm.

D = molecular diffusion coefficient of the diffusing species, $\text{cm.}^2/\text{sec.}$

R = 82.06 atm. $\text{cm.}^3/\text{gm.-mole, }^\circ\text{K}$

T = $342^\circ\text{C} = 615^\circ\text{K}$ (the highest reaction temperature studied)

The concentration difference will be calculated for the particles of largest size present in significant quantities as they will offer the largest resistance to diffusion.

d_p for largest particles $\approx$ 0.0200 cm. (Figure C.2, Appendix C).

For orthoxylene diffusing in air at 300°C, D = 0.19 $\text{cm.}^2/\text{sec.}$ (J4). Therefore a value of 0.20 $\text{cm.}^2/\text{sec.}$ will be taken for 342°C. Solving equation (A.1) for (k_G),

$$k_G = \frac{2 \times 0.2}{82.06 \times 615 \times .020} = 3.9 \times 10^{-4} \quad \frac{\text{gm.-moles}}{\text{sec. cm.}^2 \text{ atm.}}$$

From Fick's law, the molar flux N is given by

$$N = k_G (C_{AB} - C_{AS}) = 3.9 \times 10^{-4} (C_{AB} - C_{AS}) \quad \frac{\text{gm.-moles}}{\text{sec. cm.}^2}$$

where C_{AB} = concentration of orthoxylene in the main stream, atm.

C_{AS} = concentration of orthoxylene on the catalyst surface, atm.

The molar flux, N, of orthoxylene can be calculated from the reaction rate and the specific surface of the particle:

$$\text{Specific surface of the particle} = \frac{6}{d_p \rho_s} = \frac{6}{0.02 \times 2.1} = 140 \ \frac{\text{cm.}^2}{\text{gm.}}$$

The maximum rate of reaction (Based on first order rate constant from Figure 7.7 and 2 percent xylene in feed)

$$= 1.2 \times 10^{-2} \ \frac{\text{gm.-moles}}{\text{gm. hr.}}$$

$$= 3.3 \times 10^{-6} \ \frac{\text{gm.-moles}}{\text{gm.sec.}}$$

$$\therefore \quad N = \frac{3.3 \times 10^{-6}}{140} = 2.4 \times 10^{-8} \ \text{gm.-moles/sec. cm.}^2$$

$$\therefore \quad C_{AB} - C_{AS} = \frac{2.4 \times 10^{-8}}{3.9 \times 10^{-4}} = 6.2 \times 10^{-5} \ \text{atm.}$$

minimum main stream concentration = 0.01 atm.

It is seen that under the most conservative conditions, the concentration difference required to transfer the reactant to the catalyst surface is less than 1% of the main stream concentration. Therefore, the concentration on the catalyst surface can be considered equal to the main stream concentration and external diffusion resistance can be neglected.

2. Pore Diffusion Resistance

Juusola (J4) has presented theoretical and experimental evaluations of the effects of pore resistance on the reaction rates for catalysts that are similar to the 902 catalyst used in this study. He has calculated the effectiveness factor to be 0.998, thereby indicating that reaction rates are not

influenced by pore diffusion resistance. Experimental results for a 2.5 fold change in particle size indicated no pore diffusion limitations. In this work we have employed particles having a mean diameter of approximately one twentieth of those employed by Jousola. Therefore, it is likely that the effectiveness factor is very close to unity.

A.2 Estimation of the Extent of Homogeneous Reaction in the Transported Bed Reactor

As stated in Chapter 7, negligible homogeneous reaction was observed at temperatures up to 400°C. Since, however, appreciable amounts of blank reaction have been reported elsewhere (M7) it was deemed desirable to confirm our observations by calculating the extent of homogeneous reaction using kinetic parameters obtained elsewhere. Therefore the contribution of homogeneous reaction has been calculated from the first order rate constant reported by Satterfield and Loftus (S10)

$$\ln k = 10.05 - 20{,}000/RT$$

at $T = 615^{\circ}K$

$k = 2.0\ 10^{-3}$ sec.$^{-1}$

The material balance for a plug flow tubular reaction, assuming a first order reaction gives

$$k\tau = \ln \frac{1}{1-X_A} \qquad (A.2)$$

where τ is the space time in the reactor (seconds) and X_A is the conversion of orthoxylene by homogeneous reaction.

The maximum space time used in this study was less than 1 second so we shall assume a value of 1 second for this calculation

$$\therefore \text{ from (A.1)} \qquad X_A = 1 - e^{-k\tau}$$

$$= 1 - e^{-.002}$$

Therefore the extent of homogeneous reaction is negligible under the conditions of this study.

APPENDIX B

CALIBRATIONS

During the course of the research it was necessary to calibrate several pieces of equipment. These calibrations have been included to aid further work on the transported bed reactor.

B.1. Sonic Nozzle Calibrations

During startup, the pressure drop across the transported bed increases from the empty tube pressure drop (order of inches of water) to the steady-state value (order of 10 psi). Therefore some flow control must be employed so that the total gas flow remains constant regardless of changes in downstream pressure. Dye (D5) has evaluated the performance of a small-sized, critical flow meter assembly and has found it suitable to control flows of the order of those employed in this study. Therefore this method of flow control was adopted in the current study instead of using the more conventional method involving a differential pressure cell and pressure controller to maintain a constant pressure drop across an orifice.

In a sonic nozzle, the flow rate is proportional to the pressure before the nozzle and to the cross-sectional area of the nozzle throat, provided that the pressure ratio across the throat is maintained in excess of the critical ratio. For air, the critical ratio is approximately 1.9. Thus to maintain a constant air flow all that is necessary is to have some means of accurately controlling the pressure before the nozzle. In this study a Honeywell proportional pressure controller and a Research

Control Valve pneumatic control valve were used to maintain the constant upstream pressure.

The nozzle assembly was designed so that nozzles of different bores could be readily interchanged so that a large range of flows could be achieved. The nozzles were machined from brass according to ASME specifications[1] and were highly polished.

The flow through the nozzle can be calculated from the real gas law. When air is employed, the mass flowrate is given by

$$W_G = 0.533\ C_V\ A\ \frac{P_1}{\sqrt{T}}\ .\ 3600 \qquad (B.1)$$

where W_G is the mass flowrate of air in pounds/hr.

C_V is the discharge coefficient for the sonic nozzle.

A is the cross-sectional area of the nozzle throat (in^2).

P_1 is the pressure upstream of the nozzle (p.s.i.a.).

T is the temperature of the air (^oR).

The nozzles employed in this study were calibrated using a wet test meter (Precision Scientific Co., Chicago, U.S.A.). The calibrations are shown in Figure B.1.

This method of flow control has proven itself to be inexpensive and reliable. It is highly recommended for other studies.

---

1. "Fluid Meters, Their Theory and Application", The American Society of Mechanical Engineers Research Committee on Fluid Meters, Fifth Edition, Published by ASME, New York (1950).

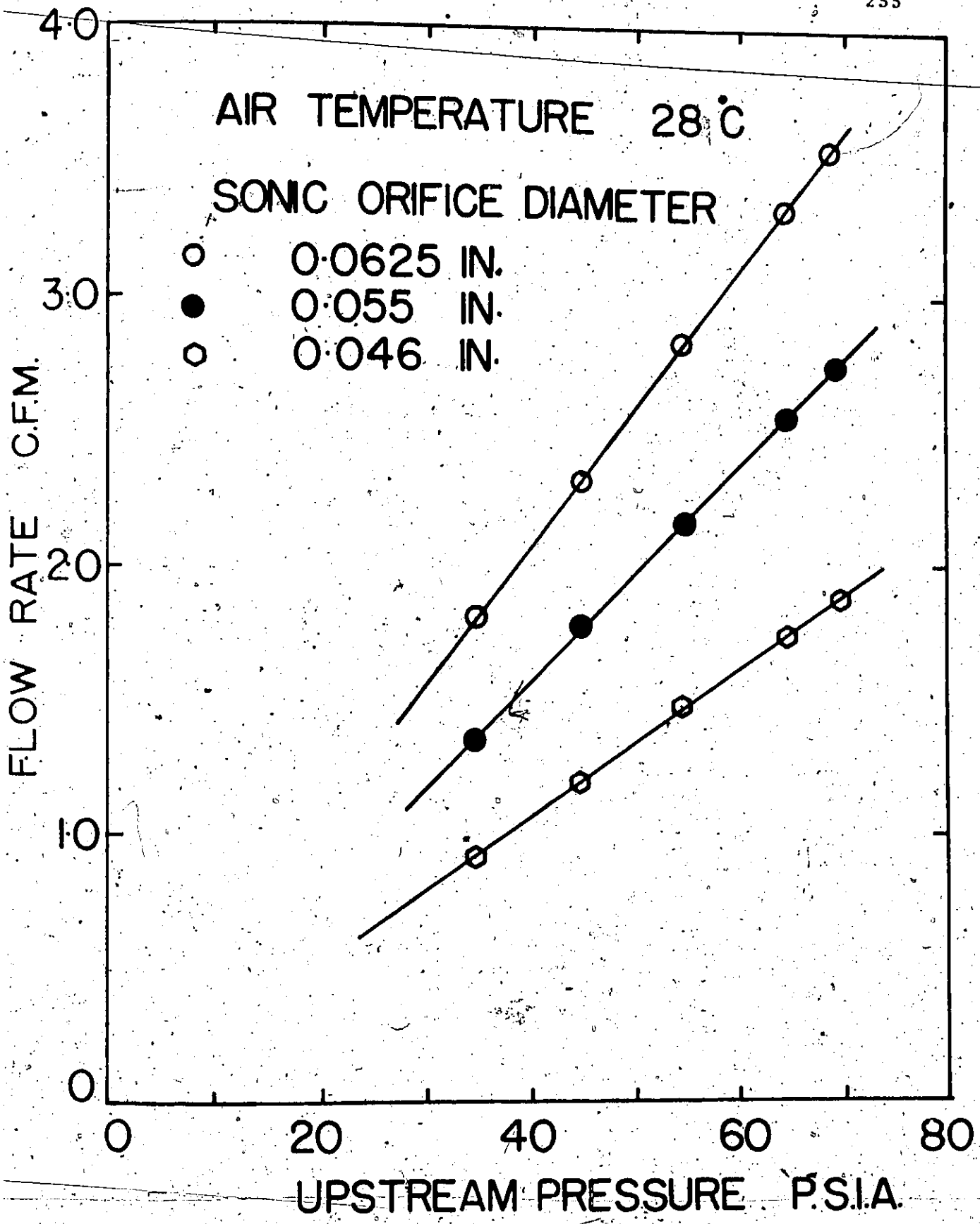

Figure B.1. Sonic Nozzle Calibrations.

B.2. Calibration of Straingauge Weighing Device

The straingauge and the associated transducer converter were manufactured by S.E. Laboratories, Feltham, Middlesex, England. The straingauge was attached to a machined metal bar which supported the weighing tank. This assembly was calibrated before being used in this study by applying different loads to the cell. This calibration is shown in Figure B.2.

The weighing tank was not freely suspended but was connected to the reactor, the solids hold tank, and the exit line by flexible stainless steel couplings. Therefore it was necessary to calibrate the straingauge under operating conditions by adding lead bricks to the weighing tank. A typical calibration made during the reaction experiments is presented in Figure B.2.

It was felt that different solids temperatures might produce different characteristics in the bellows and so frequent checks were made on the calibration. However, it was found that the calibration was constant over the range of temperatures from 200°C to 350°C. Large changes in the zero reading occurred throughout the experimental programme, probably due to changes in the metal bar. However the calibration in millivolts per pound remained unchanged. Cooling water was circulated through 1/8 inch copper coils surrounding the straingauge in order to prevent a breakdown of the cement which was used to attach the gauge to the metal bar.

This continuous method for measuring solids flow rates has been shown to be highly effective. It is recommended for use in similar pneumatic transported studies. The stainless

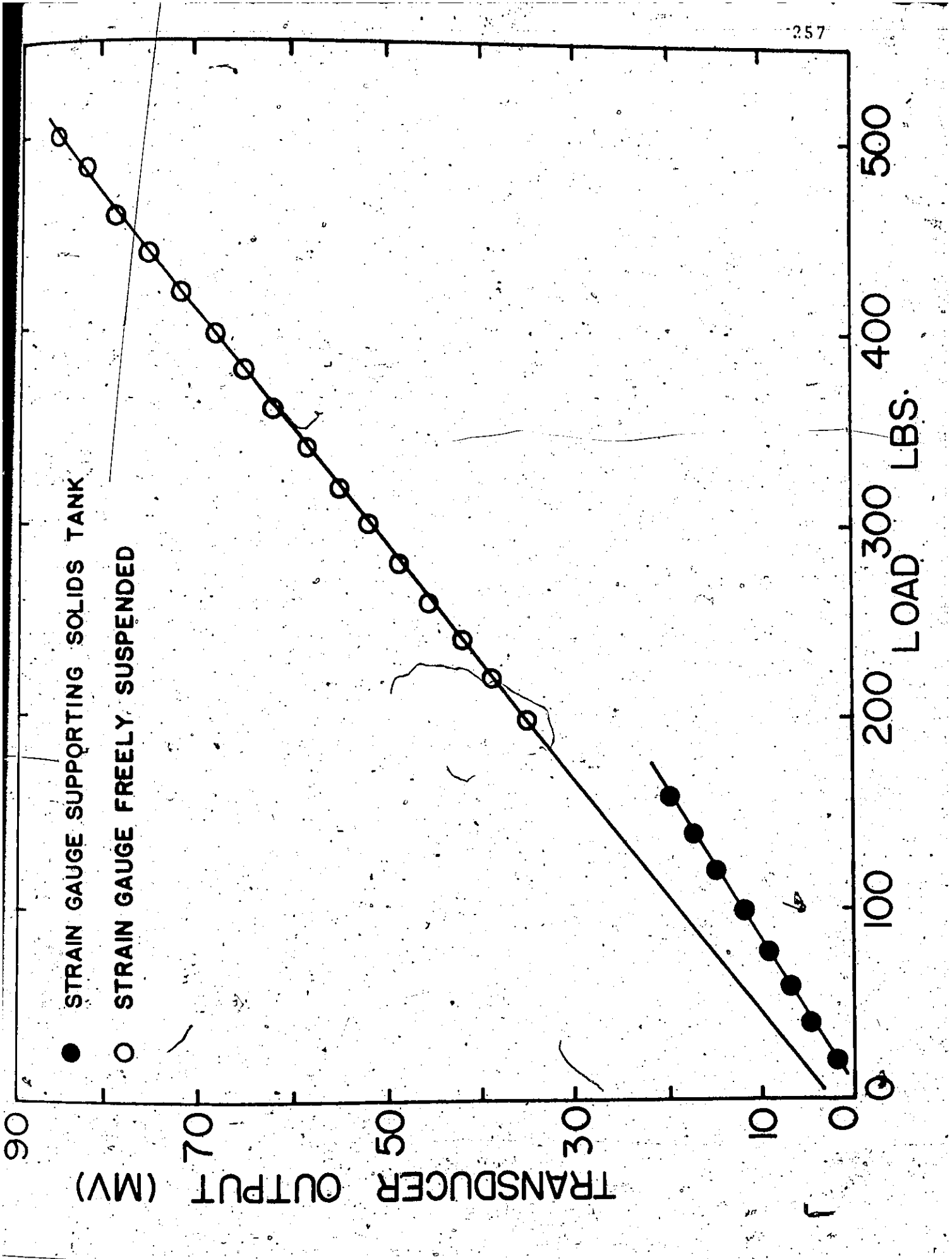

Figure B.2. Strain Gauge Calibration.

steel bellows provided less support than was anticipated; the response in mv/lb. for the strain-gauge supporting the tank was 80 percent of the response obtained when it was freely suspended.

B.3. Void Fraction Measurement by Neutron Diagnostics

The measurement of void fractions in the transported bed reactor by neutron diagnostics was considered early in the research programme. To test the applicability of the method, tests were conducted at a beam port of the McMaster University Nuclear Reactor. Particle concentrations of the order of those that would be encountered in a 3/4 inch reaction tube were simulated by forming packed beds of catalyst particles which were contained between two aluminium plates. Measurements were made on six samples. In addition, the count-rate was obtained for the condition in which no catalyst was contained between the plates. The results of the study are shown in Figure B.3. The catalyst used in this investigation was the Aero PAA catalyst obtained from American Cyanamid.

The method has been shown to be excellent for measuring voidages for dense phase conveying in tubes of the order of 3/4" to 2 inches, a range that is generally not suited to measurement by stronger or weaker forms of radiation (see Chapter 2). However, the high cost of portable neutron sources and a height limitation caused by the position of the beam port in the nuclear reactor prevent its use for two-phase gas-solid flow studies at this time. The price of portable neutron sources is steadily being reduced and it is likely that the method will have widespread use for these studies in future years.

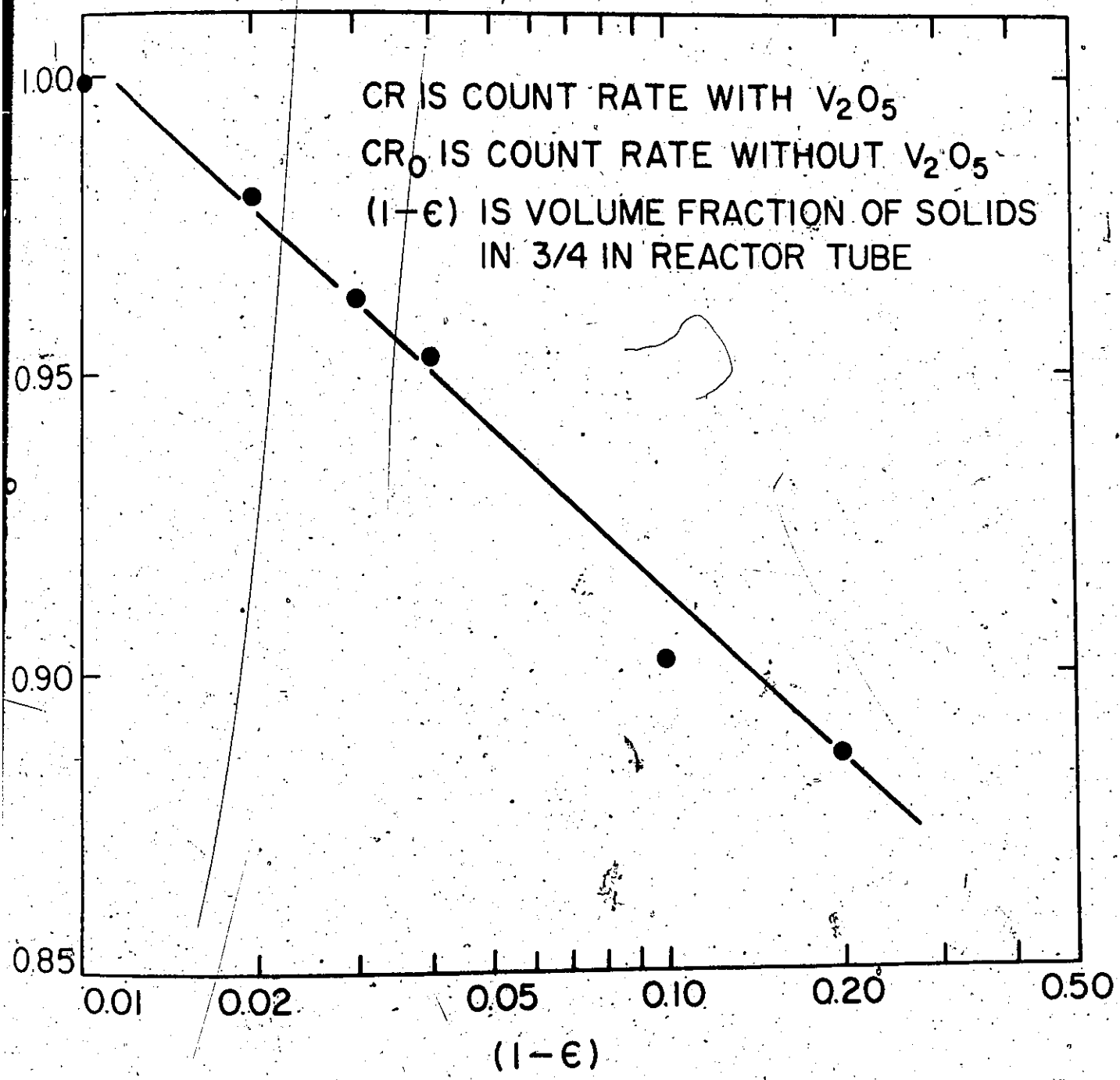

Figure B. 3. Void Fraction Determination by Neutron Diagnostics.

APPENDIX C

CATALYST PREPARATION AND CHARACTERIZATION

C.1 Catalyst Preparation

The catalyst prepared in this laboratory was shown in Chapter 5 to have poor selectivity for partial oxidation of orthoxylene. This was not unexpected since the catalyst was not promoted with $K_2S_2O_7$. The method of preparation is presented here, however, since it may be useful as a step in the preparation of suitable promoted catalysts.

Many metal oxide catalysts are prepared by impregnating the catalyst support with a suitable salt of the metal, generally the nitrate, and heating the resultant preparation at elevated temperatures to decompose the salt to the oxide. In this case the support material selected was chromatographic grade silica gel (Chromatographic Specialties Ltd.) and the salt selected was an oxalate complex. Cotton and Wilkinson (C5) suggest that an oxalate complex $[(NH_4)_2\ VO(C_2O_4)_2]\cdot 2H_2O$ is easily obtained by boiling ammonium vanadate with ammonium oxalate. However, a simpler method has since been reported by Sathyamarayana and Patel (S14) who have shown that an oxalate is formed by adding V_2O_5 to boiling oxalic acid in water in the mole ratio of V to oxalic acid of 2:3, according to the following reactions

$$V_2O_5 + H_2C_2O_4 \rightarrow 2VO_2 + H_2O + 2CO_2 \qquad (C.1)$$

$$2VO_2 + 2H_2C_2O_4 \rightarrow 2VOC_2O_4 + 2H_2O \qquad (C.2)$$

The latter method was adopted in this study.

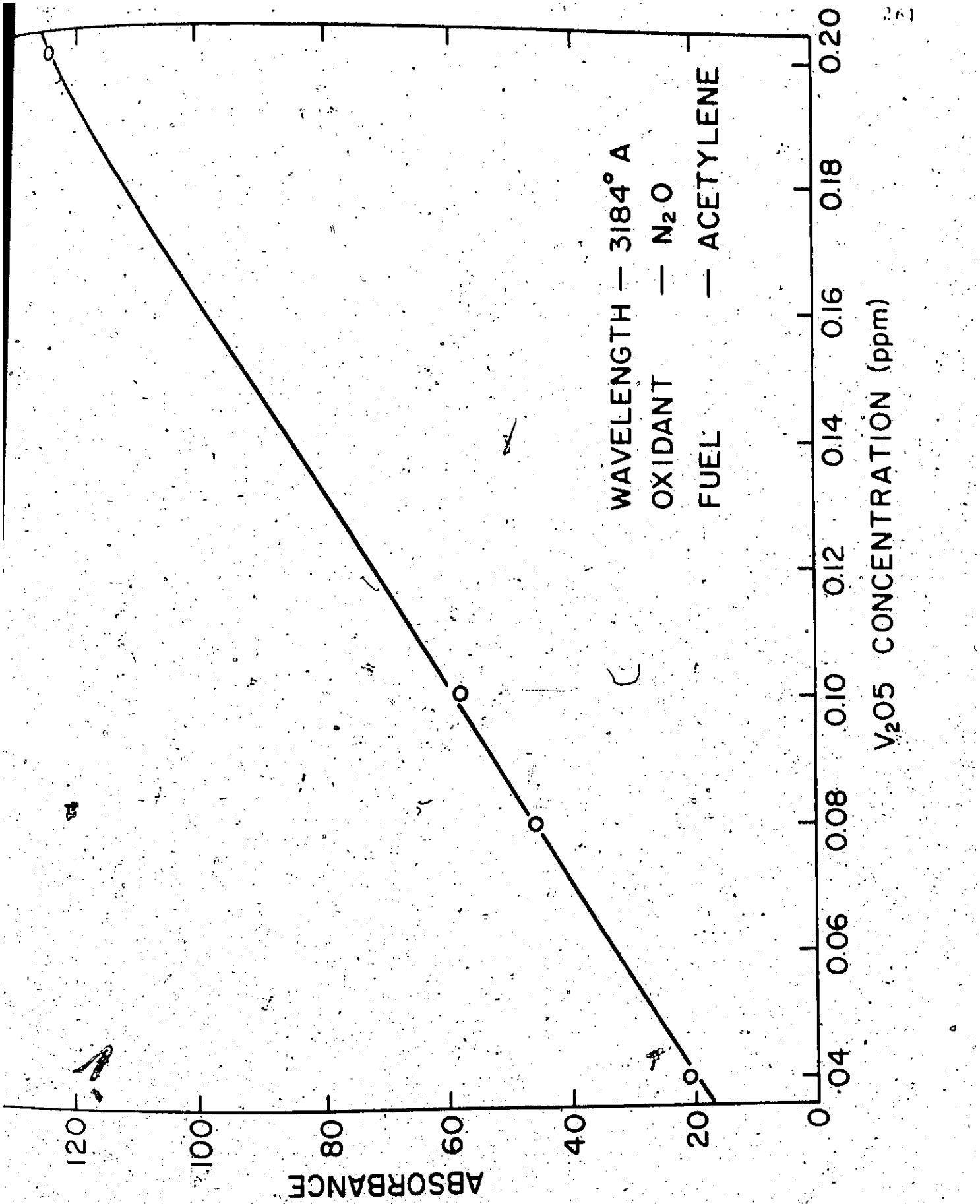

Figure C.1. Calibration of Atomic Absorption Apparatus.

The catalyst was prepared by gently stirring the silica gel into a solution of the oxalate that was prepared in the above. The amount of solution and solid used was such that the addition of the total silica gel produced a thick paste; thereby ensuring uniformity of impregnation of the support with the oxalate. This blue-coloured material was then placed on a tray in a muffle furnace and heated at a temperature of 400°C for 24 hours. The resultant catalyst was bright orange in colour, indicative of V_2O_5 formation.

C.2 A Method to Measure the Vanadium Content of Vanadia Catalysts

It was considered desirable to find a method of measuring the vanadium content of catalysts of the type used in this study. The method of oxalate preparation proposed by Sathyamayana and Patel (S14) is ideal in this application since the catalyst can be added to a boiling solution of oxalic acid and water and the oxalate is formed according to reactions C.1 and C.2 above. Atomic absorption spectroscopy can then be used to determine the vanadium content of the resultant oxalate solution when it has been suitably diluted. Figure C.1 shows a calibration curve obtained for vanadium, expressed as vanadium pentoxide, according to the above procedure. This technique may prove of some use in determining the vanadium content of catalyst preparations.

C.3 Screen Analysis of Catalyst Used in Transported Bed Reactor

The catalyst used in the transported bed was screened to determine the mean particle diameter. This size is important

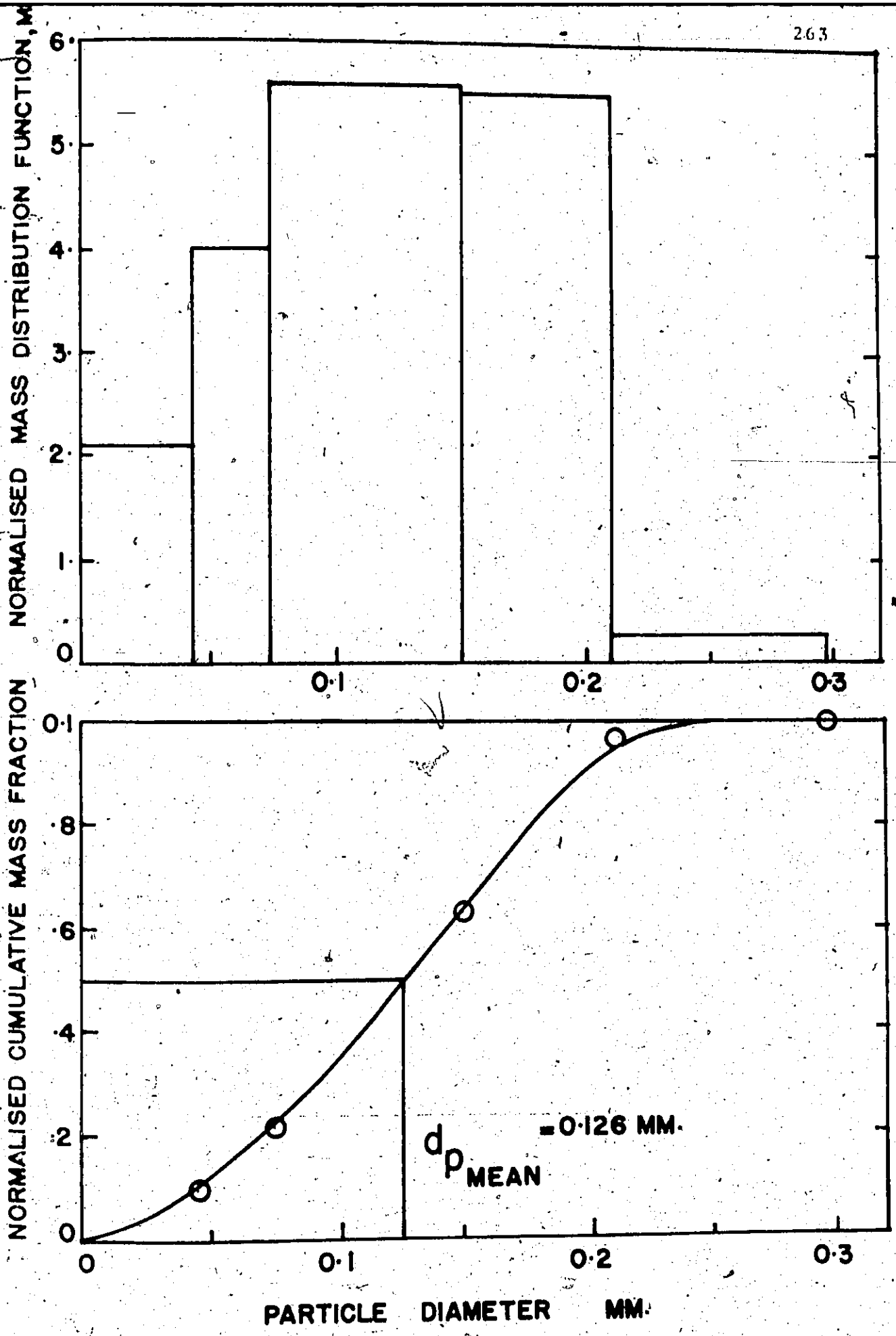

Figure C.2. Screen Analysis of Catalyst Particles.

for two-phase flow calculations. The results of the analysis are shown in Figure C.2. The data presented here were obtained at the end of the current series of experiments so that will be useful for future work that will be done in this system.

C.4 Particle Density Measurements

In order to do the two-phase flow calculations presented in Chapter 7, it was necessary to know the "free fall" particle density, that is, the mean density of the particle taking into account both the solid material and the gas contained within the pores. Catalyst manufacturers generally specify either the skeletal density or the bulk density of the particles. In the case of highly porous catalysts the "free fall" density is greatly different from the skeletal density. The W. R. Grace 902 catalyst is reported to have a bulk density of approximately 0.6 gm./cc. Therefore the "free fall" density should be approximately unity. A method, based on the mercury porosimeter (Micromeritics Instrument Corporation), was used to determine this value more accurately. The method and calculation is described below.

(i) A glass cell of the porosimeter is weighed.

(ii) The cell is evacuated and mercury flows into the cell until it is filled. The count number (indicating the level of mercury in the constant bore tube of the cell) is noted.

(iii) The cell is weighed to determine the weight of mercury contained in the cell.

(iv) The cell is cleaned, dried and reweighed.

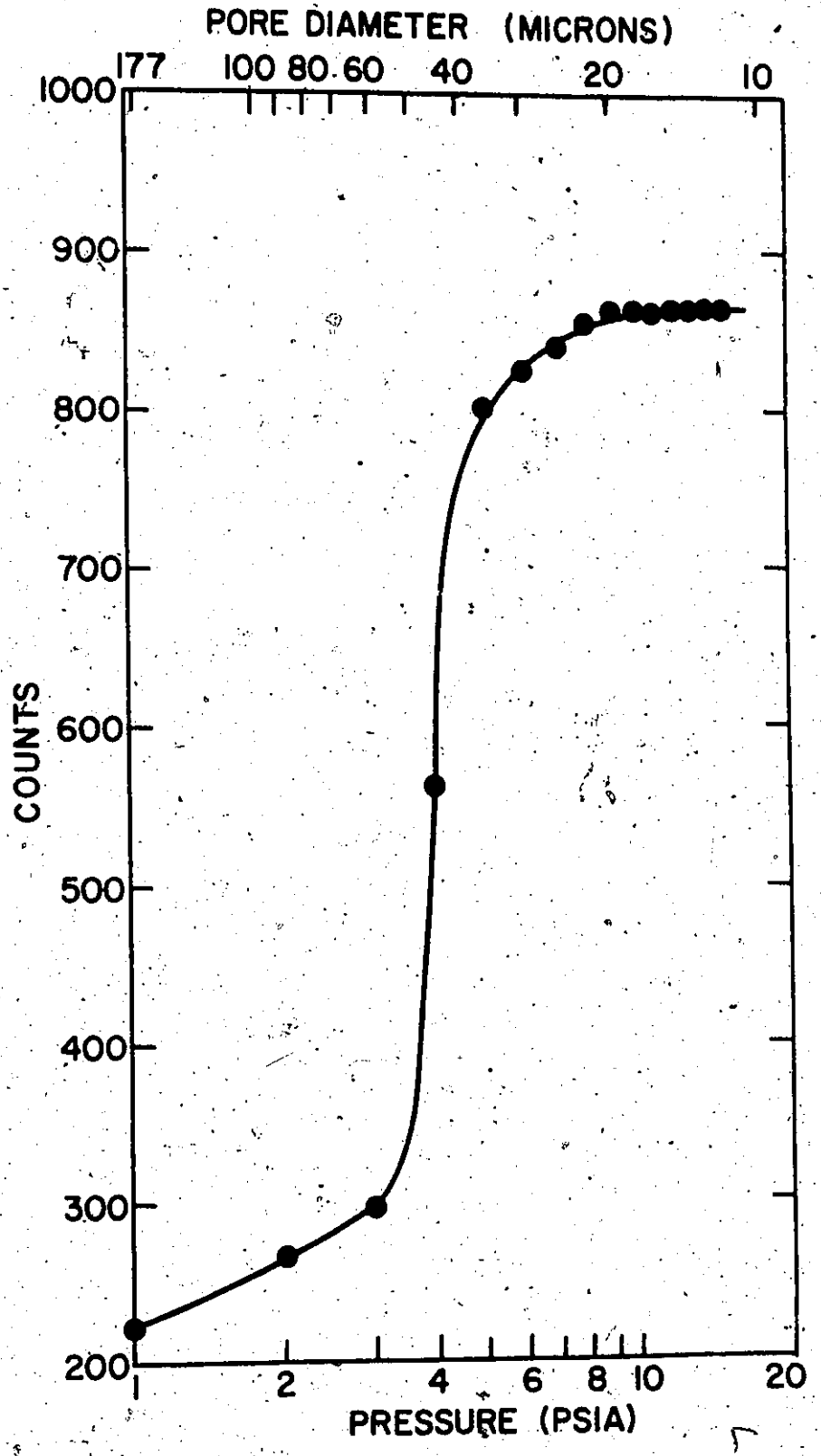

Figure C.3. Particle Density Measurement Using Mercury Porosimeter.

(v) A weighed, dry sample of catalyst is placed in the cell.

(vi) The cell is evacuated and mercury flows into the cell.

(vii) The pressure in the mercury reservoir is increased to force mercury into the voidages between the particles. The count number is noted as the pressure is increased in 1 psi increments. A constant count number with increased pressure indicates that the voidages have been filled with mercury.

(viii) The cell is reweighed to determine the mass of mercury present.

(ix) The density of the particle was determined from the above data as follows

W^B_{Hg} = 344.80 gm. C^B = 127 V^B_{Hg} = 25.35 cc.

W^T_{Hg} = 292.24 gm. C^T = 868 V^T_{Hg} = 21.49 cc.

W^T_S = 3.16 gm.

where W^T_{Hg} is the weight of mercury in the blank test, W^T_{Hg} is the weight of mercury in the sample test, C^B and C^T are the count rates and W^T_S is the weight of catalyst used in the analysis.

$$\Delta V = (868-127) \times 0.000748 \left(\frac{c.c.}{count}\right) \leftarrow \text{cell factor}$$

$$= 0.554 \text{ c.c.}$$

$$V^T_{S+Hg} = 25.35-0.554 = 24.80 \text{ c.c.}$$

$$V_S = 24.80-21.49 = 3.31 \text{ c.c.}$$

$$\rho_S = \frac{3.16}{3.31} = 0.955 \frac{gm.}{c.c.}$$

Figure C.3 shows the porosimeter data obtained. The abrupt change in count rate at around 4 p.s.i.a. pressure

indicates a high concentration of voidages having equivalent diameters of around 50 microns. This size would be typical of the voidages in packed beds of particles having diameters of between 150 and 200 microns, the size used in this test. It should be noted that air was used to pressurize the mercury. Hydraulic oil is normally employed when determining pore size distributions for catalysts.

This method of density determination will prove useful for fluid mechanics studies in fluidized and transported beds. Since this application is not reported in the instruction manual for the porosimeter, it has been discussed in detail here.

The author wishes to thank Dr. R. Hemrajani for his help in devising the method and conducting the measurements.

APPENDIX D

SAFETY CONSIDERATIONS WHEN HANDLING VANADIA CATALYSTS

The dangers of handling fluidized oxidation catalysts of the 902, 906 and Aero PAA types used in this study are two fold due to the presence of two toxic agents, silica and vanadium pentoxide, in these catalysts. The effect of inhalation of fine particles of silica into the lungs is well known; it results in silicosis. Inhalation of vanadium pentoxide dust or fumes is also harmful. Therefore considerable care should be taken when handling this type of catalyst. Also one should be mindful of the possibility of leaks in the flow system of a pilot-plant-scale reactor and of the precautions necessary to prevent toxic levels of catalyst from leaving by vent lines in these systems. In this study we have taken steps to minimize these hazards by the following means:

(i) Pressure release valves were installed at three locations in the system so that there was little danger of a tank rupturing and spilling catalyst into the laboratory. These valves were set at 15 psig which was considerably lower than the pressure (30 psig) at which the solids hold tanks were tested. The lines from the pressure release valves were vented through a series of furnace filters to trap any fine particles that might have been entrained in air leaving the tanks.

(ii) Fine particles not separated by the two cyclones in the venting system were removed by scrubbing in a water spray. In this way the silica particles settled in a catchment section

at the bottom of the scrubbing tower and the soluble catalyst constituents, V_2O_5, K_2SO_4 and SO_3, were washed away.

Charging and emptying the system of its load of approximately 350 pounds of catalyst could have caused exposure to toxic levels of both silica and vanadia. However, the following precautions were taken at those times and when sampling solids held up in the reactor sections.

(i) A respirator (Willson No. 1009) was worn at all times when handling large quantities of catalyst. This type of respirator is recommended for protection against very toxic hazards of dusts, mists, fumes and smokes.

(ii) Care was taken to wash any parts of the body not covered by clothing immediately after exposure to the catalyst.

(iii) Clothes were washed following handling of large quantities of catalyst.

Detailed information on the effects of exposure to vanadium pentoxide dusts was obtained from the Environmental Health Services Branch of the Ontario Department of Health. A comprehensive review of the literature was obtained. This information is summarized below.

The initial reaction to acute exposures to vanadium pentoxide is irritation to the respiratory system including mucous membrane of the nose with resulting nose bleeds, and more severe irritation up to pneumonia. Except in extreme cases recovery would be expected. Chronic lesions would not be expected.

The American Conference of Governmental Industrial Hygienists (ACGIH) have set a Threshold Limit Value (TLV) of 0.5 mg/cu.m. for vanadium pentoxide dust. A TLV is a time weighted exposure that can be tolerated 8 hours a day, 40 hours a week for a working lifetime. Apparently it is being considered that the 0.5 mg/cu.m. be considered a ceiling level which should never be exceeded. However, very short exposures as high as 100 mg/cu.m. may not cause definable symptoms.

APPENDIX E

THE EFFECT OF USING HELIUM AS THE DILUENT GAS

At the request of Dr. P. Silveston of the University of Waterloo, Waterloo, Ontario, an experiment was conducted in which helium replaced nitrogen as the diluent gas. His research group has carried out investigations of the oxidation of SO_2 and CO on vanadium pentoxide. They have found as did Baron et al., (B17) that the molecular weight of the diluent gas has a profound effect on the reaction rate and the activation energy for the oxidation of SO_2. Baron et al. found that the reaction rate was higher and the activation energy lower, the higher the molecular weight of the inert gas. This effect is such that the rate of reaction using helium can be as little as one-tenth of the value using nitrogen. Silveston's group has made similar observations. However, they have found no inert gas effect when CO is oxidized.

In this investigation helium was used as diluent in a single experiment conducted at the centre point condition for the original 902 catalyst. The results of these experiments are presented in Figure 4.9. They are enlarged upon in Table E.1 below.

It can be seen from the results in Figure 4.9 and Table E.1 that there is no significant difference between the result of the experiment using helium and those using nitrogen. It would appear that any difference is well within experimental error. This was not a major part of the research program so the

study was terminated after this one experiment had indicated that the inert gas effect did not apply to orthoxylene oxidation on a vanadia catalyst.

The following reaction conditions were employed for these experiments.

Temperature:	370°C
Total Flow:	250 cc/min.
Oxygen Level:	20%
Xylene Level:	1.4%
Weight of Catalyst:	1.0 grams

Table E.1. Influence of Diluent Gas on Conversion and Selectivities

Experiment	Diluent	Xylene Conversion	SELECTIVITIES					
			OTA	PT	PAA	OTAc	CO_2	CO
1	N_2	.404	.738	.049	.061	.003	.114	.037
4	N_2	.428	.742	.050	.064	.003	.106	.036
10	N_2	.421	.730	.050	.066	.004	.113	.038
12	N_2	.425	.734	.048	.061	.004	.114	.039
13	H_e	.405	.743	.051	.059	0	.110	.037

APPENDIX F

DEVELOPMENT OF REACTION EQUATIONS FOR STEADY-STATE MODELS

The reaction equations series-parallel reaction schemes presented in Chapter 6 for the oxidation of ortho-xylene on the 902 and TiO_2 catalysts were developed as follows:

1. 902 Catalyst

The reaction scheme is shown in Figure 6.1. The rate of disappearance of orthoxylene is given by

$$-\frac{dC_1}{dt} = (k_{12} + k_5)\, C_1\, \theta \qquad (F.1)$$

The rate of formation of orthotolualdehyde is given by

$$\frac{dC_2}{dt} = (k_{12}\, C_1 - k_5\, C_2 - k_{23}\, C_2)\, \theta \qquad (F.2)$$

The rate of formation of PAA/PI/OTAc is given by

$$\frac{dC_3}{dt} = k_{23}\, C_2\, \theta \qquad (F.3)$$

The rate of formation of CO/CO_2 is given by

$$\frac{dC_5}{dt} = 8(k_5\, C_1 + k_5\, C_2)\, \theta \qquad (F.4)$$

The rate of oxidation of the catalyst is given by

$$r_a = k_a\, C_a\, (1-\theta) \qquad (F.5)$$

The rate of oxygen usage can also be obtained from the rates of hydrocarbon oxidation through the stoichiometric coefficients.

The rates of the oxygen reactions are as follows:

For orthoxylene to orthotolualdehyde 1 mole of oxygen is consumed per mole of orthotolualdehyde formed.

$$r_{a1} = k_{12} C_1 \theta \qquad (F.6)$$

For orthoxylene to CO/CO_2 n moles of oxygen are consumed per mole of orthoxylene reacted. Where n is the stoichiometric coefficient defined in Chapter 6.

$$r_{a2} = n k_5 C_1 \theta \qquad (F.7)$$

For orthotolualdehyde to CO/CO_2 n-1 moles of oxygen are consumed per mole of orthotolualdehyde reacted.

$$r_{a3} = (n-1) k_5 C_2 \theta \qquad (F.8)$$

For orthotolualdehyde to PAA/PI/OTAc n_{23} moles of oxygen are consumed per mole of orthotolualdehyde reacted.

$$r_{a4} = n_{23} k_{23} C_2 \theta \qquad (F.9)$$

Overall rate of oxygen reaction is then

$$r_a = r_{a1} + r_{a2} + r_{a3} + r_{a4} = ((k_{12} + nk_5) C_1 + (n_{23} k_{23} + (n-1) k_5) C_2) \theta \qquad (F.10)$$

Equating (F.10) and (F.5) for steady-state conditions gives

$$\theta = \frac{k_a C_a}{k_a C_a + k_{12} C_1 + nk_5 C_1 + n_{23} k_{23} C_2 + (n-1) k_5 C_2} \qquad (F.11)$$

Substitution in Equations (F.1) through (F.4) gives Equations (6.1) through (6.5) in Chapter 6.

2. TiO_2 Catalyst

The reaction scheme is shown in Figure 6.2. Through a similar development to that given above we can write the rate of disappearance of orthoxylene and the rates of formation of orthotolualdehyde, phthalide, phthalic anhydride and carbon oxides as follows.

$$-\frac{dC_1}{dt} = (k_{12} + k_5)\, C_1\, \theta \qquad (F.12)$$

$$\frac{dC_2}{dt} = (k_{12}\, C_1 - k_5\, C_2 - k_{23}\, C_2)\, \theta \qquad (F.13)$$

$$\frac{dC_3}{dt} = (k_{23}\, C_2 - k_{34}\, C_3)\, \theta \qquad (F.14)$$

$$\frac{dC_4}{dt} = k_{34}\, C_3\, \theta \qquad (F.15)$$

$$\frac{dC_5}{dt} = 8\,(k_5\, C_1 + k_5\, C_2)\, \theta \qquad (F.16)$$

The rates of oxygen consumption for the formation of ortho-tolualdehyde from orthoxylene, CO/CO_2 for orthoxylene, CO/CO_2 from orthotolualdehyde, phthalide from orthotolualdehyde, and phthalic anhydride from phthalide are as follows.

$$r_{a1} = k_{12}\, C_1\, \theta \qquad (F.17)$$

$$r_{a2} = n\, k_5\, C_1\, \theta \qquad (F.18)$$

$$r_{a3} = (n-1)\, k_5\, C_2\, \theta \qquad (F.19)$$

$$r_{a4} = k_{23}\, C_2\, \theta \qquad (F.20)$$

$$r_{a5} = k_{34}\, C_3\, \theta \qquad (F.21)$$

Therefore overall rate of oxygen usage is given by

$$r_a = (k_{12} C_f + n k_5 C_1 + (n-1) k_5 C_2 + k_{23} C_2 + k_{34} C_3) \theta \quad (F.22)$$

The rate of reoxidation of the reduced catalyst sites is given by

$$r_a = k_a C_a (1-\theta) \quad (F-23)$$

Equating Equations (F.22) and (F.23) leads to

$$\theta = \frac{k_a C_a}{k_a C_a + k_{12} C_1 + n k_5 C_1 + k_{23} C_2 + k_{34} C_3 + (n-1) k_5 C_2} \quad (F-24)$$

Substitution for θ in Equations (F.12) through (F.16) leads to the system of reaction Equations (6.8) through in Chapter 6.13.

APPENDIX G

EXPERIMENTAL RESULTS

This appendix contains data that have been divided into two main sections, namely, the packed bed results and the transported bed results.

G.1. Results of Packed Bed Experimentation

The following tables list the experimental conditions used, and the product compositions measured for the packed bed experimentation on 4 of the catalysts investigated. These data are for two of the silica-supported catalysts, the original 902 and the 902 used in the transported bed study, and the two titania-supported catalysts, the von Heyden WO and the W. R. Grace TiO_2/Sb_2O_3 catalyst.

The data for each catalyst and for each type of experiment on a particular catalyst have been listed according to run number, i.e., the order in which they were performed. To simplify the presentation the following column headings have been adopted. The coding system is as follows:

1. Run number
2. Temperature of reaction
3. Total gas flow at inlet conditions (litres/second)
4. Inlet orthoxylene concentration (gm. moles/litre)
5. Inlet orthoxylene concentration (gm. moles/litre)
6. Inlet pressure (mm. Hg)
7. Pressure drop across reactor (mm Hg)
8a. Carbon balance ratio (carbon atoms out/carbon atoms in)
   - steady-state experiments

8b. Time on-stream following reoxidation (seconds) - unsteady-state experiments

9. Exit orthoxylene concentration (gm. moles/litre)

10. Exit orthotolualdehyde concentration (gm. moles/litre)

11. Exit phthalide concentration (gm. moles/litre)

12. Exit phthalic anhydride concentration (gm. moles/litre)

13. Exit carbon dioxide concentration (gm. moles/litre)

14. Exit carbon monoxide concentration (gm. moles/litre)

15a. Exit orthotoluic acid concentration (gm. moles/litre
- SiO_2-supported catalysts

15b. Exit maleic anhydride concentration (gm. moles/litre)
- TiO_2-supported catalysts.

Table G.1.1 - Inlet Conditions for Experiments Conducted on 902 Catalyst used in Transported Bed Study. (These conditions apply to compositions in Tables 6.1, 6.2 and G.1.2.)

	2	3	4	5	6	7	8
1	3.50E+02	4.93E-03	4.16E-04	5.60E-03	1.07E+03	2.20E+02	9.77E-01
2	3.50E+02	2.88E-03	2.31E-04	3.42E-03	9.10E+02	1.06E+02	9.09E-01
3	3.50E+02	6.43E-03	5.06E-04	7.49E-03	1.08E+03	2.30E+02	1.03E+00
4	3.50E+02	4.94E-03	4.16E-04	5.59E-03	1.07E+03	2.20E+02	1.00E+00
5	3.70E+02	2.93E-03	2.31E-04	2.30E-03	9.14E+02	1.06E+02	9.80E-01
6	3.70E+02	2.54E-03	2.66E-04	7.90E-03	1.07E+03	1.74E+02	9.47E-01
7	3.70E+02	6.85E-03	9.52E-04	2.93E-03	1.21E+03	2.93E+02	9.17E-01
8	3.70E+02	2.97E-03	6.20E-04	6.70E-03	9.39E+02	1.20E+02	1.02E+00
9	3.30E+02	2.57E-03	4.05E-04	7.84E-03	1.00E+03	6.93E+02	1.07E+00
10	3.50E+02	4.20E-03	4.37E-04	6.91E-03	1.23E+03	3.84E+02	1.02E+00
11	3.70E+02	6.43E-03	2.99E-04	9.33E-03	1.27E+03	2.93E+02	1.01E+00
12	3.30E+02	2.85E-03	4.76E-04	2.38E-03	9.05E+02	1.06E+02	9.90E-01
13	3.70E+02	6.01E-03	4.02E-04	5.62E-03	1.14E+03	2.42E+02	9.83E-01
14	3.50E+02	4.98E-03	4.11E-04	5.43E-03	1.08E+03	1.94E+02	9.14E-01
15	3.70E+02	2.56E-03	4.49E-04	2.59E-03	1.03E+03	2.30E+02	1.04E+00
16	3.70E+02	2.69E-03	4.48E-04	2.47E-03	1.02E+03	2.18E+02	1.00E+00
17	3.30E+02	6.41E-03	3.05E-04	9.53E-03	1.16E+03	2.60E+02	1.04E+00
18	3.70E+02	6.60E-03	6.24E-04	9.20E-03	1.40E+03	2.71E+02	1.01E+00
19	3.30E+02	6.62E-03	6.40E-04	3.07E-03	1.17E+03	2.64E+02	8.72E-01
20	3.50E+02	4.93E-03	4.03E-04	5.34E-03	1.05E+03	1.82E+02	1.04E+00
21	3.70E+02	6.74E-03	2.78E-04	2.98E-03	1.21E+03	2.80E+02	1.04E+00
22	3.50E+02	5.05E-03	3.85E-04	5.43E-03	1.05E+03	1.89E+02	1.02E+00
23	3.30E+02	2.88E-03	4.50E-04	7.50E-03	9.16E+02	1.00E+02	1.01E+00
24	3.30E+02	6.57E-03	6.48E-04	9.29E-03	1.20E+03	2.82E+02	1.04E+00
25	3.50E+02	4.75E-03	3.77E-04	5.68E-03	1.09E+03	1.97E+02	1.03E+00
26	3.50E+02	5.00E-03	3.87E-04	5.38E-03	1.05E+03	1.83E+02	1.03E+00
27	3.30E+02	2.96E-03	3.67E-04	4.79E-03	8.95E+02	8.80E+01	1.02E+00
28	3.30E+02	2.94E-03	3.65E-04	4.74E-03	8.90E+02	9.00E+01	1.00E+00
29	3.90E+02	3.10E-03	3.34E-04	4.57E-03	9.40E+02	1.05E+02	9.53E-01
30	3.30E+02	2.78E-03	3.63E-04	4.99E-03	9.33E+02	9.40E+01	1.04E+00
31	3.30E+02	2.87E-03	3.66E-04	4.86E-03	9.11E+02	1.01E+02	9.92E-01
32	3.70E+02	3.01E-03	3.48E-04	4.62E-03	9.24E+02	1.05E+02	1.00E+00
33	3.30E+02	2.90E-03	3.97E-04	4.82E-03	9.09E+02	9.50E+01	9.65E-01
34	3.70E+02	3.04E-03	3.60E-04	4.63E-03	9.28E+02	1.03E+02	1.00E+00
35	3.50E+02	4.94E-03	4.24E-04	5.45E-03	1.06E+03	1.83E+02	9.89E-01
36	3.90E+02	3.05E-03	3.83E-04	4.57E-03	9.35E+02	1.02E+02	9.21E-01
37	3.90E+02	3.13E-03	3.56E-04	4.45E-03	9.10E+02	1.04E+02	9.54E-01
38	3.50E+02	2.93E-03	3.74E-04	4.68E-03	9.13E+02	9.40E+01	1.06E+00
39	3.50E+02	4.82E-03	4.07E-04	5.50E-03	1.08E+03	2.13E+02	1.01E+00
40	3.70E+02	3.00E-03	3.43E-04	4.50E-03	9.11E+02	9.90E+01	9.98E-01
41	3.50E+02	2.92E-03	3.56E-04	4.79E-03	9.29E+02	9.90E+01	1.04E+00
42	3.50E+02	2.85E-03	3.78E-04	4.70E-03	9.21E+02	1.03E+02	9.85E-01
43	3.50E+02	4.58E-03	3.98E-04	5.93E-03	1.15E+03	1.90E+02	1.01E+00
44	3.90E+02	3.00E-03	3.21E-04	4.63E-03	9.[illegible]E+02	1.05E+02	1.01E+00
45	3.70E+02	2.94E-03	3.53E-04	4.75E-03	9.59E+02	1.05E+02	9.84E-01
46	3.50E+02	2.79E-03	3.50E-04	4.96E-03	9.68E+02	9.90E+01	1.05E+00

Product Compositions

Sb	9	10	11	12	13	14	15a	
[illegible]	4.74E-06	1.39E-04	3.1[illegible]E+05	2.59E-05	2.21E-04	7.32E-05	7.15E-05	
1.50E+01	8.74E-06	1.52E-04	3.27E-05	2.28E-05	2.10E-04	6.97E-05	1.05E-04	
[illegible]	[illegible]	[illegible]	[illegible]	[illegible]	[illegible]	[illegible]	[illegible]	
[illegible]	[illegible]	[illegible]	[illegible]	[illegible]	[illegible]	[illegible]	[illegible]	1
[illegible]	[illegible]	[illegible]	[illegible]	[illegible]	[illegible]	[illegible]	[illegible]	
1.20E+02	2.55E-04	5.55E-05	4.62E-07	8.53E-07	4.71E-05	1.55E-05	5.10E-06	
[illegible]	2.65E-04	3.90E-05	1.21E-07	4.10E-07	4.04E-05	1.22E-05	5.46E-06	
[illegible]	2.60E-04	3.86E-05	1.85E-07	3.23E-07	2.90E-05	9.56E-06	4.52E-06	
[illegible]	2.08E-05	7.07E-05	2.12E-05	1.80E-05	1.09E-04	3.74E-05	1.92E-05	
2.00E+01	6.56E-06	1.01E-04	1.81E-05	1.05E-05	9.10E-05	3.09E-05	2.09E-05	2
[illegible]	9.74E-05	6.99E-05	2.36E-06	1.87E-06	5.00E-05	1.60E-05	1.19E-05	
[illegible]	1.67E-04	1.71E-05	1.93E-07	4.02E-07	2.74E-05	8.20E-06	1.70E-06	
5.00E+02	1.92E-04	5.51E-06	0.	0.	1.70E-05	4.93E-06	2.17E-06	
[illegible]	1.99E-04	6.41E-06	0.	0.	1.44E-05	2.80E-06	2.80E-06	
[illegible]	3.26E-05	1.16E-04	9.19E-06	5.78E-06	4.50E-05	2.00E-05	1.59E-05	
[illegible]	4.84E-05	1.07E-04	[illegible]	[illegible]	3.70E-05	[illegible]	[illegible]	
1.50E+01	1.33E-04	5.98E-05	1.09E-06	1.11E-06	2.42E-05	9.39E-06	6.37E-06	
2.00E+01	1.41E-04	5.36E-05	1.03E-06	1.10E-06	2.57E-05	9.03E-06	3.89E-06	
3.00E+01	1.42E-04	2.53E-05	2.69E-07	3.84E-07	1.36E-05	5.47E-06	1.70E-06	
[illegible]	1.61E-04	2.57E-05	1.03E-07	2.30E-07	8.93E-06	5.01E-06	1.27E-06	
9.00E+01	2.15E-04	6.77E-06	0.	0.	5.92E-06	2.81E-06	7.22E-07	
1.20E+02	2.23E-04	3.06E-06	0.	0.	3.11E-06	2.19E-06	1.32E-06	
[illegible]	2.30E-04	1.65E-06	0.	0.	2.09E-06	8.92E-07	5.07E-07	3
[illegible]	2.57E-06	1.17E-04	2.92E-05	2.91E-05	2.36E-04	7.73E-05	5.35E-05	
[illegible]	2.81E-06	1.49E-04	3.12E-05	2.20E-05	2.13E-04	6.93E-05	8.48E-05	
1.50E+01	2.62E-05	1.60E-04	2.35E-05	1.49E-05	1.81E-04	5.87E-05	7.77E-05	
[illegible]	7.34E-05	1.53E-04	7.17E-06	6.10E-06	1.15E-04	3.91E-05	4.03E-05	4
6.00E+01	1.87E-04	8.40E-05	1.50E-06	1.86E-06	6.37E-05	2.06E-05	1.27E-05	
[illegible]	2.41E-04	4.47E-05	3.92E-07	7.15E-07	4.30E-05	1.35E-05	3.24E-06	
[illegible]	2.63E-04	3.32E-05	1.30E-07	4.17E-07	3.79E-05	1.11E-05	2.56E-06	
[illegible]	2.82E-04	2.82E-05	0.	2.42E-07	2.31E-05	7.05E-06	2.78E-06	
1.00E+01	0.	2.42E-05	1.99E-05	4.17E-05	3.51E-04	1.09E-04	5.35E-05	
1.50E+01	0.	2.07E-05	1.84E-05	4.68E-05	3.20E-04	1.05E-04	5.50E-05	
2.00E+01	0.	5.00E-05	2.54E-05	3.29E-05	2.79E-04	8.73E-05	4.55E-05	5
[illegible]	1.31E-05	8.54E-05	1.39E-05	1.41E-05	1.78E-04	5.67E-05	4.44E-05	
[illegible]	6.37E-05	8.01E-05	5.47E-06	5.14E-06	1.00E-04	3.34E-05	1.73E-05	
[illegible]	1.01E-04	5.90E-05	3.63E-06	2.86E-06	7.68E-05	2.35E-05	1.32E-05	
[illegible]	1.21E-04	5.23E-05	1.70E-06	1.87E-06	5.85E-05	1.85E-05	8.06E-06	
1.00E+01	0.	1.00E-05	9.05E-06	4.57E-05	3.52E-04	1.18E-04	4.98E-05	
1.50E+01	0.	1.79E-05	1.68E-05	5.30E-05	3.83E-04	1.25E-04	6.00E-05	
2.00E+01	0.	3.02E-05	1.87E-05	5.05E-05	3.96E-04	1.23E-04	6.40E-05	
3.00E+01	0.	4.11E-05	2.42E-05	4.44E-05	3.53E-04	1.13E-04	6.19E-05	
6.00E+01	7.20E-07	6.21E-05	2.27E-05	3.35E-05	3.02E-04	9.79E-05	5.15E-05	6
1.20E+02	1.42E-06	7.51E-05	2.09E-05	2.59E-05	2.59E-04	8.36E-05	3.91E-05	
[illegible]	1.26E-05	9.07E-05	2.19E-05	1.92E-05	2.23E-04	7.05E-05	2.68E-05	
[illegible]	4.09E-05	9.89E-05	1.03E-05	1.06E-05	1.66E-04	5.38E-05	3.02E-05	
5.50E+00	1.73E-05	2.03E-04	3.01E-05	3.39E-05	3.62E-04	1.20E-04	1.00E-04	
8.00E+00	3.64E-05	2.32E-04	3.01E-05	2.84E-05	3.25E-04	1.12E-04	9.72E-05	
1.00E+01	6.37E-05	2.34E-04	2.67E-05	2.09E-05	2.86E-04	9.44E-05	1.05E-04	
1.50E+01	2.00E-04	2.14E-04	1.02E-05	7.88E-06	1.78E-04	6.33E-05	5.84E-05	7
3.00E+01	3.95E-04	9.97E-05	2.01E-06	2.20E-06	8.00E-05	2.67E-05	6.42E-06	
6.00E+01	4.30E-04	4.82E-05	3.00E-07	6.64E-07	4.12E-05	1.50E-05	0.	
1.20E+02	4.94E-04	3.61E-05	5.10E-07	2.20E-07	3.83E-05	1.24E-05	6.80E-07	

8b	9	10	11	12	13	14	15a	
[illegible]E+01	0.	4.70E-05	8.07E-06	6.91E-05	6.10E-04	2.51E-04	1.02E-04	
[illegible]E+01	1.60E-05	2.00E-04	5.63E-05	7.18E-05	7.01E-04	2.46E-04	1.70E-04	
[illegible]	[illegible]	2.95E-0[illegible]	[illegible]	[illegible]	[illegible]	[illegible]	[illegible]	
[illegible]E+01	1.98E+04	2.16E-04	1.21E-05	1.17E-05	2.69E-04	8.92E-05	5.98E-05	8
[illegible]	2.71E-04	2.50E-04	[illegible]	5.95E-06	1.20E-04	6.07E-05	2.34E-05	
[illegible]	[illegible]	[illegible]	[illegible]	[illegible]	[illegible]	5.38E-05	[illegible]	
[illegible]	[illegible]	[illegible]	[illegible]	[illegible]	[illegible]	[illegible]	[illegible]	
		[illegible]	[illegible]	6.59E-06	2.47E-04	7.00E-05	2.45E-05	
		1.61E-05	0.		2.42E-04	6.94E-05	1.19E-05	
[illegible]	0.	9.87E-05	4.46E-07	1.00E-05	[illegible]	2.05E-05	5.90E-06	9
[illegible]	0.	[illegible]	[illegible]	1.16E-05	9.09E-05	2.65E-05	7.70E-06	
[illegible]E+01	1.73E-04	7.70E-05	7.07E-07	6.54E-07	5.62E-05	1.59E-05	1.09E-06	
[illegible]E+02	2.16E-04	1.76E-05	7.50E-07	3.66E-07	5.97E-05	6.90E-06	[illegible]	
[illegible]E+03	2.79E-04	1.91E-05	0.	2.41E-05	2.45E-04	7.40E-05	4.67E-05	
[illegible]E+01	1.16E-05	1.63E-04	4.07E-05	2.71E-05	2.45E-05	7.24E-05	1.15E-06	10
[illegible]E+01	1.22E-04	7.78E-05	3.32E-06	5.72E-06	7.40E-05	1.29E-05	1.02E-06	
[illegible]E+02	2.57E-04	2.69E-05	1.00E-07	5.42E-07	4.20E-05	6.79E-06	2.09E-06	
[illegible]E+03	2.69E-04	3.09E-05	1.95E-07	4.71E-07	5.10E-05	6.08E-05	3.12E-05	
[illegible]E+01	5.56E-06	1.00E-04	1.01E-05	1.06E-05	1.04E-04	5.18E-05	3.09E-05	
[illegible]	1.[illegible]E-05	1.07E-04	1.3[illegible]E-05	1.[illegible]E-05	1.50E-04	5.08E-05	2.95E-05	
[illegible]E+01	2.44E-05	1.11E-04	1.09E-05	1.08E-05	1.62E-04	3.95E-05	2.20E-05	11
[illegible]E+01	4.83E-05	1.12E-04	7.29E-06	6.00E-06	1.10E-04	3.16E-05	1.56E-05	
[illegible]E+01	7.66E-05	1.03E-04	4.79E-06	4.49E-06	9.06E-05	2.16E-05	1.14E-05	
[illegible]E+02	1.07E-04	8.67E-05	2.96E-06	2.92E-06	7.41E-05	1.85E-05	9.92E-06	
[illegible]E+02	1.33E-04	7.09E-05	1.78E-06	1.86E-06	4.20E-05	4.16E-05	1.09E-05	
[illegible]E+03	1.55E-04	1.51E-04	5.79E-06	1.19E-05	1.40E-04	7.12E-06	7.20E-07	
[illegible]E+01	1.51E-05	1.51E-04	5.62E-07	6.42E-07	2.05E-05	5.77E-06	1.90E-06	
[illegible]E+01	3.04E-04	1.56E-05		2.16E-07	1.00E-05	5.77E-06	7.71E-07	12
[illegible]E+02	3.72E-04	5.37E-06	0.	0.	6.82E-06	3.95E-06	6.09E-07	
[illegible]E+02	3.80E-04	1.54E-06	0.	0.	1.00E-05	3.04E-06	0.	
[illegible]E+02	4.05E-04	1.92E-06	0.		7.15E-06	1.09E-06		
[illegible]E+03	3.85E-04	3.71E-06	1.67E-07	0.	1.57E-04	4.75E-05	1.05E-05	
[illegible]E+01	6.92E-05	1.44E-04	7.59E-06	7.11E-06	7.69E-05	2.00E-05	7.77E-06	
[illegible]E+01	1.69E-04	9.63E-05	2.63E-06	2.79E-06	5.79E-05	2.11E-05	6.14E-06	13
[illegible]E+02	1.95E-04	4.61E-05	1.76E-06	3.90E-06	7.57E-06	4.05E-05	9.08E-06	
[illegible]E+02	2.19E-04	7.42E-05	3.49E-07	6.20E-06	7.08E-05	2.76E-05	1.51E-05	
[illegible]E+01	1.56E-04	6.95E-05	2.95E-06	5.00E-06	2.75E-05	1.06E-05	5.02E-06	
[illegible]E+03	2.67E-04	4.07E-05	8.57E-07	3.25E-06	2.90E-05	9.65E-06	4.50E-06	14
[illegible]E+03	2.52E-04	4.04E-05	6.03E-07	7.97E-07	5.70E-05	1.65E-05	5.40E-06	15
[illegible]E+02	2.79E-04	4.15E-05	9.54E-07	1.00E-06	1.40E-04	5.76E-07	1.55E-07	
		1.02E-07	0.	6.44E-06	3.92E-04	1.14E-04	3.76E-05	
[illegible]E+01	0.	1.02E-04	2.03E-07	2.02E-05	1.90E-04	5.12E-05	2.11E-05	
3.00E+01	6.95E-06	1.30E-04	3.21E-06	1.10E-05	8.92E-04	2.70E-05	1.04E-06	16
6.00E+01	1.50E-04	6.39E-05	3.15E-06	1.77E-06	7.73E-05	2.19E-05	1.06E-06	
1.20E+02	2.42E-04	4.80E-05	1.39E-06	1.25E-06	5.74E-05	1.91E-05	1.29E-06	
3.60E+02	2.86E-04	4.41E-05	6.41E-07	9.67E-07	1.18E-04	3.07E-05	1.07E-05	
3.00E+03	2.80E-04	1.30E-04	1.41E-05	1.03E-05	4.55E-05	1.07E-05	5.74E-06	
1.50E+01	1.57E-05	4.40E-05	6.76E-07	9.67E-07	5.54E-05	6.00E-06	2.00E-06	17
6.00E+01	1.62E-04	1.61E-05	1.22E-07	4.17E-07	1.51E-05	2.29E-06	7.00E-07	
1.20E+02	1.95E-04	1.21E-05	0.	0.	2.51E-04	6.06E-05	2.76E-05	
3.60E+03	1.83E-04	2.24E-04	1.22E-05	1.16E-05	1.55E-04	5.12E-05	1.81E-05	
1.50E+01	9.80E-05	1.77E-04	5.24E-06	5.49E-06	1.10E-04	5.04E-05	1.14E-05	
3.00E+01	2.08E-04	1.28E-04	2.54E-06	3.16E-06	9.45E-05	3.17E-05	1.01E-05	18
6.00E+01	2.83E-04	1.10E-04	1.82E-06	2.35E-06	8.29E-05	2.70E-05	6.60E-06	
1.20E+02	3.10E-04	9.52E-05	1.22E-06	1.08E-06	6.90E-05	2.15E-05	5.07E-07	
3.00E+02	3.56E-04	7.97E-05	6.60E-07	1.14E-06				
3.00E+03	3.56E-04							

8b	9	10	11	12	13	14	15a	
1.50E+01	3.97E-04	4.99E-05	0.	0.	3.41E-05	9.49E-06	2.17E-06	
3.00E+01	4.54E-04	1.13E-05	0.	0.	1.50E-05	3.55E-06	1.18E-06	
6.00E+01	4.77E-04	3.84E-06	0.	0.	1.10E-05	1.97E-06	6.58E-07	19
3.00E+02	4.85E-04	1.03E-06	0.	0.	2.52E-05	0.	0.	
3.60E+03	2.99E-04	2.16E-05	0.	0.	2.58E-05	5.68E-06	1.09E-06	20
1.50E+01	2.30E-05	1.10E-04	1.43E-05	1.03E-05	1.38E-04	4.67E-05	1.30E-05	
3.00E+01	6.25E-05	9.74E-05	3.48E-06	3.93E-06	8.10E-05	2.66E-05	1.05E-05	
6.00E+01	1.28E-04	5.87E-05	1.35E-06	1.50E-06	4.47E-05	1.49E-05	6.90E-06	
1.20E+02	1.02E-04	3.62E-05	4.66E-07	5.09E-07	3.07E-05	9.06E-06	3.68E-06	21
3.00E+02	1.79E-04	3.13E-05	2.50E-07	5.01E-06	2.80E-05	8.16E-06	2.69E-06	
3.00E+03	1.82E-04	2.42E-05	0.	0.	1.97E-05	5.82E-06	2.46E-06	
2.40E+03	2.75E-04	2.45E-05	0.	0.	2.91E-05	7.24E-06	2.50E-06	22
1.50E+01	2.53E-04	4.78E-04	0.	1.93E-05	2.96E-05	2.76E-04	5.01E-05	
3.00E+01	1.85E-04	8.04E-05	0.	2.16E-06	9.14E-05	2.72E-05	1.66E-05	
6.00E+01	2.97E-04	3.52E-05	0.	1.01E-06	8.92E-05	1.87E-05	1.15E-05	23
1.20E+02	3.32E-04	1.92E-05	0.	3.08E-07	6.78E-05	1.04E-05	1.17E-05	
3.00E+02	3.52E-04	1.10E-05	0.	0.	5.57E-05	1.24E-05	1.10E-05	
3.60E+03	3.45E-04	1.42E-05	0.	0.	3.71E-05	6.35E-06	0.	
1.50E+01	2.37E-04	1.43E-04	5.53E-07	3.00E-06	9.33E-05	2.90E-05	6.66E-06	
3.00E+01	4.11E-04	3.80E-05	0.	2.86E-07	4.26E-05	1.08E-05	3.05E-06	24
6.00E+01	4.45E-04	1.52E-05	0.	0.	2.74E-05	7.33E-06	2.11E-06	
3.00E+02	4.67E-04	7.71E-06	0.	0.	5.80E-06	4.13E-06	0.	
3.00E+01	1.05E-04	1.34E-04	7.04E-06	5.55E-06	1.21E-04	4.05E-05	2.32E-05	
3.00E+01	7.71E-05	1.50E-04	2.54E-06	6.26E-06	1.10E-04	3.90E-05	2.50E-05	25
3.00E+01	2.92E-05	1.49E-04	5.51E-06	1.35E-05	1.57E-04	5.00E-05	2.73E-05	
3.00E+01	7.81E-05	9.96E-05	5.73E-07	8.43E-06	1.32E-04	5.96E-05	1.42E-05	
3.00E+01	0.	9.62E-05	1.77E-05	4.19E-05	4.80E-04	1.57E-04	6.42E-05	
3.60E+03	3.16E-04	4.65E-06	0.	2.67E-07	1.40E-05	3.15E-06	0.	
3.00E+01	5.28E-05	1.46E-04	1.04E-05	9.79E-06	1.42E-04	4.32E-05	4.04E-05	
3.00E+01	0.	1.31E-04	2.67E-05	2.05E-05	3.21E-04	1.00E-04	1.05E-04	
3.00E+01	0.	1.50E-04	2.99E-05	1.60E-05	1.97E-04	5.94E-05	6.05E-05	
3.00E+01	0.	1.34E-04	2.67E-05	2.57E-05	3.53E-04	1.05E-04	8.00E-05	
3.00E+01	7.29E-05	1.57E-04	6.71E-06	6.10E-06	1.27E-04	4.12E-05	4.67E-05	
3.00E+01	0.	1.10E-04	2.37E-05	3.35E-05	4.14E-04	1.40E-04	9.07E-05	
3.00E+01	0.	9.71E-05	1.96E-05	3.31E-05	4.10E-04	1.44E-04	9.00E-05	
3.00E+01	0.	1.17E-04	1.14E-05	2.75E-05	2.87E-04	9.02E-05	5.22E-05	
3.00E+01	7.29E-05	1.51E-04	3.66E-06	7.01E-06	1.25E-04	4.06E-05	3.00E-05	
3.00E+01	0.	8.81E-05	1.42E-05	2.02E-05	2.20E-04	7.02E-05	4.71E-05	
3.00E+01	0.	9.97E-05	1.07E-05	2.49E-05	2.04E-04	6.32E-05	5.05E-05	
3.00E+01	0.	1.25E-04	2.09E-05	2.74E-05	2.20E-04	6.32E-05	3.33E-05	
3.00E+01	1.28E-04	1.42E-04	3.42E-06	5.15E-06	1.10E-04	3.75E-05	2.01E-05	
3.00E+01	0.	6.16E-05	0.	2.92E-05	4.12E-04	1.43E-04	9.90E-05	
3.00E+01	0.	1.06E-04	3.36E-04	3.01E-05	4.87E-04	1.00E-04	2.06E-04	4(
3.00E+01	0.	5.02E-04	1.43E-04	9.63E-05	9.30E-04	2.99E-04		

Table V.1.3. Results of experiments conducted on [illegible] 902 Catalyst at Steady-State Conditions and after 30 Secons On-stream

Inlet Conditions	2	3	4	5	6	7	8a
1	3.70E+02	7.66E-03	3.09E-04	4.40E-03	9.11E+02	1.51E+02	1.03E+00
2	3.90E+02	1.14E-02	2.10E-04	2.40E-03	9.11E+02	2.37E+02	1.00E+00
3	3.90E+02	1.14E-02	4.47E-04	7.14E-03	1.01E+03	2.50E+02	1.00E+00
4	3.70E+02	7.63E-03	3.12E-04	4.43E-03	9.11E+02	1.51E+02	1.02E+00
5	3.50E+02	3.34E-03	1.85E-04	2.05E-03	8.19E+02	5.95E+01	1.03E+00
6	3.50E+02	3.30E-03	3.77E-04	6.19E-03	8.19E+02	9.60E+01	1.03E+00
7	3.50E+02	1.11E-02	4.01E-04	4.50E-03	8.19E+02	2.19E+02	1.09E+02
8	3.90E+02	3.50E-03	1.67E-04	2.04E-03	8.20E+02	6.00E+01	1.09E+02
9	3.90E+02	1.09E-02	2.31E-04	7.50E-03	9.08E+02	2.47E+02	1.03E+00
10	3.70E+02	7.61E-03	3.23E-04	4.40E-03	9.09E+02	1.49E+02	1.01E+00
11	3.90E+02	3.53E-03	3.47E-04	2.05E-03	8.20E+02	6.00E+01	1.07E+00
12	3.70E+02	7.59E-03	3.16E-04	4.51E-03	9.08E+02	1.48E+02	1.05E+00
13	3.70E+02	7.59E-03	3.10E-04	4.51E-03	9.08E+02	1.48E+02	1.01E+00

Product Compositions at Steady-State Conditions

1	9	10	11	12	13	14	15a
1	1.50E-04	7.53E-05	4.93E-06	8.27E-06	9.27E-05	2.96E-05	1.77E-07
2	8.99E-05	4.81E-05	3.53E-06	5.04E-06	7.42E-05	2.49E-05	2.15E-07
3	1.27E-04	1.34E-04	1.15E-05	1.86E-05	2.58E-04	9.11E-05	3.39E-06
4	1.44E-04	8.01E-05	5.56E-06	8.91E-06	9.19E-05	3.07E-05	1.04E-06
5	1.13E-04	5.69E-05	5.50E-06	4.90E-06	5.44E-05	1.60E-05	8.03E-07
6	1.80E-04	1.11E-04	8.10E-06	1.14E-05	1.64E-04	5.25E-05	1.80E-06
7	3.47E-04	1.95E-05	0.	8.80E-07	2.10E-05	4.91E-06	4.60E-07
8	1.67E-05	4.54E-06	0.	7.21E-05	4.93E-04	1.70E-04	5.47E-07
9	1.15E-04	4.82E-05	1.95E-06	2.01E-06	3.57E-05	1.17E-05	0.
10	1.91E-04	7.99E-05	5.49E-06	1.10E-06	9.67E-05	3.50E-05	1.36E-06
11	1.63E-04	8.07E-05	1.00E-05	2.17E-05	2.60E-04	9.29E-05	6.05E-06
12	1.49E-04	8.07E-05	5.25E-06	8.75E-06	1.01E-04	3.42E-05	1.29E-06
13	1.52E-04	7.69E-05	5.23E-06	8.10E-06	9.09E-05	3.07E-05	0.

Product Compositions after 30 Seconds Reaction

1	9	10	11	12	13	14	15a
2	3.03E-05	6.81E-05	9.01E-06	1.46E-05	1.97E-04	6.61E-05	1.16E-05
3	8.54E-05	1.50E-04	1.77E-05	2.97E-05	3.84E-04	1.34E-04	1.90E-05
4	3.05E-05	1.20E-04	2.15E-05	2.71E-05	2.81E-04	9.52E-05	1.99E-05
5	1.20E-05	2.31E-05	0.	5.93E-05	2.58E-04	8.41E-05	1.71E-05
6	2.56E-05	7.14E-05	4.24E-05	9.05E-05	4.04E-04	1.34E-04	3.44E-05
7	3.16E-04	4.31E-05	2.39E-07	3.34E-05	2.71E-05	1.35E-05	8.12E-07
8	8.47E-06	7.47E-07	0.	6.56E-05	4.88E-04	1.73E-04	3.00E-05
9	1.99E-06	1.03E-04	1.25E-05	9.50E-06	1.01E-04	3.58E-05	4.31E-06
10	1.46E-05	1.21E-04	2.26E-05	2.81E-05	2.73E-04	9.52E-05	3.42E-05
11	1.32E-05	4.21E-05	1.61E-05	8.20E-05	7.00E-04	2.62E-04	6.07E-05

Table G.1.4. Steady-state Reaction Data on W. R. Grace TiO_2-supported Catalyst

Inlet Conditions

1	2	3	4	5	6	7	8a
1	3.70E+02	5.48E-03	3.19E-04	7.11E-03	1.01E+03	1.44E+02	1.00E+00
2	3.50E+02	2.96E-03	2.18E-04	2.43E-03	8.87E+02	7.20E+01	1.07E+00
3	3.50E+02	3.09E-03	4.10E-04	7.13E-03	8.91E+02	7.40E+01	1.06E+00
4	3.70E+02	5.40E-03	3.39E-04	5.04E-03	1.02E+03	1.40E+02	1.07E+00
5	3.50E+02	6.97E-03	5.47E-04	2.98E-03	1.13E+03	2.04E+02	1.07E+00
6	3.70E+02	5.45E-03	3.49E-04	4.99E-03	1.01E+03	1.40E+02	1.05E+00
7	3.50E+02	6.92E-03	2.84E-04	8.77E-03	1.14E+03	2.04E+02	1.02E+00
8	3.90E+02	7.66E-03	5.11E-04	7.90E-03	1.15E+03	2.25E+02	1.04E+00
9	3.90E+02	3.22E-03	3.91E-04	2.21E-03	8.92E+02	8.00E+01	1.02E+00
10	3.90E+02	3.21E-03	2.11E-04	6.52E-03	8.96E+02	8.00E+01	1.05E+00
11	3.90E+02	7.44E-03	2.67E-04	2.88E-03	1.16E+03	2.19E+02	1.01E+00
12	3.50E+02	3.04E-03	2.63E-04	2.42E-03	8.87E+02	7.20E+01	1.07E+00
13	3.50E+02	3.03E-03	4.46E-04	6.81E-03	8.89E+02	7.20E+01	1.08E+00
14	3.50E+02	7.17E-03	5.05E-04	2.05E-03	1.13E+03	1.78E+02	1.05E+00
15	3.70E+02	5.40E-03	4.13E-04	5.19E-03	1.02E+03	1.43E+02	1.03E+00
16	3.90E+02	5.51E-03	3.62E-04	5.02E-03	1.02E+03	1.44E+02	1.06E+00
17	4.00E+02	5.59E-03	3.70E-04	4.94E-03	1.02E+03	1.44E+02	9.42E-01
18	3.80E+02	5.43E-03	3.81E-04	5.09E-03	1.02E+03	1.44E+02	9.74E-01

Product Compositions

1	9	10	11	12	13	14	15b
1	1.64E-04	1.12E-05	5.12E-06	7.03E-05	7.40E-05	2.45E-05	0.
2	8.75E-05	5.61E-06	4.64E-06	9.22E-05	8.96E-05	2.70E-05	0.
3	1.74E-04	1.21E-05	8.11E-06	1.57E-04	2.11E-04	6.26E-05	0.
4	1.94E-04	1.18E-05	6.10E-06	7.50E-05	7.25E-05	2.22E-05	0.
5	3.77E-04	1.72E-05	7.59E-06	4.91E-05	5.65E-05	1.31E-05	0.
6	2.04E-04	1.16E-05	4.69E-06	6.66E-05	6.96E-05	1.90E-05	0.
7	1.54E-04	9.57E-06	4.10E-06	4.95E-05	5.98E-05	2.04E-05	0.
8	3.10E-04	2.02E-05	5.53E-06	5.82E-05	8.32E-05	2.33E-05	0.
9	2.73E-04	1.35E-05	5.47E-06	4.61E-05	5.54E-05	1.15E-05	0.
10	6.03E-05	5.03E-06	5.63E-06	1.02E-04	1.42E-04	4.21E-05	0.
11	1.65E-04	8.91E-06	3.92E-06	2.72E-05	2.04E-05	6.21E-06	0.
12	1.30E-04	6.50E-06	4.81E-06	9.30E-05	6.39E-05	2.56E-05	0.
13	2.27E-04	1.27E-05	6.98E-06	1.42E-04	1.93E-04	5.26E-05	0.
14	4.17E-04	1.49E-05	5.21E-06	5.65E-05	2.79E-05	7.86E-06	0.
15	2.55E-04	1.30E-05	5.80E-06	6.57E-05	6.43E-05	2.04E-05	0.
16	2.25E-04	1.38E-05	6.98E-06	6.03E-05	6.17E-05	1.76E-05	0.
17	1.98E-04	1.47E-05	4.67E-06	5.27E-05	6.19E-05	2.13E-05	0.
18	2.53E-04	1.25E-05	4.34E-06	2.96E-05	3.26E-05	7.66E-06	0.

Table G.1.5.--Results of Unsteady-State Experiments Conducted on W. R. Grace TiO_2-supported Catalyst.

1	2	3	4	5	6	7
	Inlet Conditions					
1	3.70E+02	5.40E-03	3.19E-04	4.99E-03	1.01E+03	1.40E+02
2	3.70E+02	5.40E-03	3.40E-04	4.99E-03	1.01E+03	1.40E+02
3	3.70E+02	5.48E-03	3.19E-04	5.11E-03	1.01E+03	1.44E+02
4	3.70E+02	5.40E-03	3.39E-04	5.04E-03	1.02E+03	1.40E+02

8a	9	10	11	12	13	14	15b	
1.02E+01	5.20E-05	6.89E-06	6.49E-06	1.28E-04	1.88E-04	5.90E-05	0.	
2.52E+01	7.84E-05	8.03E-06	7.06E-06	1.44E-04	1.82E-04	5.80E-05	0.	
2.02E+01	8.68E-05	8.36E-06	8.07E-06	1.41E-04	1.72E-04	5.57E-05	0.	
2.70E+03	1.41E-04	1.14E-05	7.80E-06	1.13E-04	1.40E-04	4.07E-05	0.	
6.50E+03	1.89E-04	1.26E-05	5.80E-06	8.31E-05	9.72E-05	2.92E-05	0.	
1.02E+04	1.91E-04	1.18E-05	5.41E-06	7.70E-05	7.72E-05	2.40E-05	0.	1
1.30E+04	2.12E-04	1.27E-05	4.02E-06	6.44E-05	6.48E-05	1.95E-05	0.	
1.64E+04	2.08E-04	1.17E-05	5.34E-06	6.73E-05	6.61E-05	1.92E-05	0.	
1.88E+04	2.08E-04	1.22E-05	4.02E-06	6.30E-05	6.51E-05	1.94E-05	0.	
2.02E+04	2.12E-04	1.24E-05	5.68E-06	6.76E-05	7.08E-05	1.91E-05	0.	
2.07E+04	1.09E-04	1.07E-05	4.34E-06	6.15E-05	6.49E-05	1.75E-05	0.	
5.06E+03	1.62E-04	1.19E-05	7.89E-06	9.20E-05	1.01E-04	3.15E-05	0.	2
1.02E+04	1.77E-04	1.14E-05	5.02E-06	7.95E-05	8.20E-05	2.60E-05	0.	

8.00E+00	3.89E-05	5.41E-06	6.52E-06	1.63E-04	1.58E-04	6.02E-05	4.06E-06
1.00E+01	5.32E-05	6.34E-06	7.15E-06	1.59E-04	1.62E-04	5.68E-05	3.30E-06
1.50E+01	7.43E-05	7.67E-06	7.10E-06	1.41E-04	1.61E-04	5.20E-05	3.91E-06
2.00E+01	7.51E-05	7.79E-06	8.66E-06	1.36E-04	1.70E-04	5.26E-05	0.
3.00E+01	8.54E-05	8.61E-06	8.60E-06	1.21E-04	1.55E-04	5.21E-05	3.05E-06
5.00E+01	1.02E-04	9.59E-06	8.26E-06	1.10E-04	1.40E-04	4.76E-05	0.
1.20E+02	1.02E-04	9.51E-06	8.44E-06	1.10E-04	1.42E-04	4.73E-05	0.
3.00E+02	1.02E-04	9.52E-06	7.42E-06	1.17E-04	1.35E-04	4.51E-05	0.
6.00E+02	1.09E-04	9.78E-06	7.65E-06	1.12E-04	1.34E-04	4.39E-05	0.
8.24E+03	1.28E-04	1.10E-05	7.31E-06	1.01E-04	1.15E-04	3.73E-05	0.
5.70E+03	1.43E-04	1.10E-05	6.39E-06	9.11E-05	1.05E-04	3.21E-05	0.
8.40E+03	1.49E-04	1.12E-05	6.23E-06	8.55E-05	1.01E-04	2.97E-05	0.
1.06E+04	1.57E-04	1.14E-05	6.02E-06	7.99E-05	9.70E-05	2.76E-05	0.
1.89E+04	1.65E-04	1.11E-05	5.73E-06	7.40E-05	8.29E-05	2.30E-05	0.
2.16E+04	1.64E-04	1.12E-05	5.12E-06	7.03E-05	7.40E-05	2.24E-05	0.

1.50E+01	6.60E-05	6.21E-06	8.66E-06	1.62E-04	1.91E-04	6.09E-05	0.
4.00E+01	7.92E-05	8.15E-06	7.85E-06	1.42E-04	1.69E-04	6.00E-05	0.
2.70E+03	1.30E-05	1.12E-05	9.31E-06	1.24E-04	1.50E-04	4.09E-05	0.
5.26E+03	1.48E-04	1.15E-05	7.84E-06	1.01E-04	1.10E-04	3.55E-05	0.
1.06E+04	1.70E-04	1.30E-05	7.06E-06	9.23E-05	9.63E-05	2.69E-05	0.
1.50E+04	1.74E-04	1.26E-05	5.92E-06	8.31E-05	9.07E-05	2.74E-05	0.
1.92E+04	1.80E-04	1.25E-05	6.95E-06	8.39E-05	8.63E-05	2.53E-05	0.
2.18E+04	1.84E-04	1.18E-05	6.37E-06	7.99E-05	8.29E-05	2.48E-05	0.
2.46E+04	1.86E-04	1.19E-05	7.34E-06	8.17E-05	8.14E-05	2.48E-05	0.
3.18E+04	1.93E-04	1.21E-05	6.63E-06	7.84E-05	7.04E-05	2.26E-05	0.
3.48E+04	1.94E-04	1.18E-05	6.10E-06	7.50E-05	7.25E-05	2.22E-05	0.
3.77E+04	1.89E-04	1.08E-05	6.31E-06	7.60E-05	7.74E-05	2.14E-05	0.

4

Table G.1.6. Experiments Conducted on W. R. Grace TiO_2-supported Catalyst using no Oxygen in Feed.

1	2	3	4	5	6	7
1	3.90E+02	3.11E-03	2.18E-04	0.	1.90E+02	9.00E+01

8b	9	10	11	12	13	14	15a
1.00E+01	0.	0.	0.	1.55E-04	1.57E-04	6.74E-05	0.
2.20E+01	0.	6.35E-07	0.	1.44E-04	1.14E-04	4.75E-05	0.
3.60E+01	2.15E-05	2.60E-06	2.36E-06	1.41E-04	9.22E-05	3.40E-05	0.
4.80E+01	2.59E-05	2.95E-06	4.00E-06	1.27E-04	8.12E-05	2.78E-05	0.
5.80E+01	8.47E-05	5.95E-06	4.79E-06	9.49E-05	4.30E-05	1.04E-05	0.
7.20E+01	8.86E-05	5.47E-06	4.30E-06	8.24E-05	3.49E-05	7.04E-06	0.
8.70E+01	1.07E-04	5.89E-06	4.08E-06	7.41E-05	2.90E-05	4.97E-06	0.
1.00E+02	1.39E-04	7.70E-06	5.22E-06	5.21E-05	1.99E-05	1.44E-06	0.
1.50E+02	1.93E-04	8.86E-06	1.02E-06	2.36E-05	5.19E-06	8.14E-07	0.
2.00E+02	2.01E-04	8.04E-06	1.40E-06	1.16E-05	0.	0.	0.

Table G.1.7. Experiments on W. R. Grace TiO_2-supported Catalyst in which the Reoxidation of the Catalyst was Investigated.

1	2	3	4	5	6	7
1	3.90E+02	7.62E-03	5.11E-04	7.96E-03	1.15E+03	2.25E+02

8b	9	10	11	12	13	14	15a
3.00E+00	1.99E-05	6.92E-06	8.68E-06	2.25E-04	2.94E-04	1.25E-04	0.
4.80E+00	7.05E-05	1.36E-05	1.40E-05	2.35E-04	2.93E-04	1.11E-04	0.
5.00E+00	8.01E-05	1.23E-05	1.23E-05	2.41E-04	3.02E-04	1.14E-04	0.
1.50E+01	1.05E-04	1.40E-05	1.41E-05	2.25E-04	3.10E-04	1.13E-04	0.
2.90E+01	1.09E-04	1.44E-05	1.32E-05	2.25E-04	3.06E-04	1.12E-04	0.
6.00E+01	1.35E-04	1.80E-05	1.41E-05	1.92E-04	2.40E-04	8.39E-05	0.
1.20E+02	1.68E-04	1.92E-05	1.30E-05	1.04E-04	2.30E-04	8.48E-05	0.
2.70E+03	2.64E-04	2.14E-05	9.43E-06	9.14E-05	1.40E-04	3.83E-05	0.
2.55E+04	3.18E-04	2.13E-05	7.53E-06	6.18E-05	8.46E-05	2.31E-05	0.
4.26E+04	3.11E-04	1.86E-05	1.65E-05	6.11E-05	7.23E-05	2.24E-05	0.
7.92E+04	3.10E-04	2.02E-05	5.53E-06	5.82E-05	8.32E-05	2.33E-05	0.
5.00E+00	1.71E-04	1.98E-05	1.73E-05	1.64E-04	2.35E-04	7.27E-05	0.
4.00E+00	1.20E-04	1.66E-05	1.44E-05	2.01E-04	2.69E-04	9.28E-05	0.
5.00E+00	9.65E-05	1.58E-05	1.20E-05	2.23E-04	2.77E-04	9.87E-05	0.
5.00E+00	4.30E-05	1.05E-05	1.01E-05	2.47E-04	4.35E-04	1.63E-04	0.
5.00E+00	7.45E-05	1.39E-05	1.31E-05	2.37E-04	2.64E-04	1.12E-04	0.

Table G.1.8 Steady-State Experiments on von Heyden "WO" Catalyst.

1	2	3	4	5	6	7	8
1	3.50E+02	5.69E-03	3.45E-04	6.54E-03	1.65E+03	3.59E+02	9.44E-01
	[illegible]	2.69E-03	2.36E-04	4.70E-03	9.17E+02	1.24E+02	9.81E-01
	[illegible]	4.07E-03	2.42E-04	6.00E-03	1.10E+03	1.99E+02	9.94E-01
4	3.30E+02	4.29E-03	2.80E-04	5.77E-03	1.00E+03	2.31E+02	9.97E-01
5	3.30E+02	2.51E-03	2.37E-04	4.94E-03	9.17E+02	1.24E+02	9.65E-01
6	3.30E+02	1.37E-03	2.12E-04	4.83E-03	8.30E+02	6.00E+01	1.02E+00
7	3.71E+02	4.40E-03	2.41E-04	5.45E-03	1.10E+03	2.53E+02	1.13E+00
8	3.71E+02	5.84E-03	3.23E-04	6.33E-03	1.26E+03	3.77E+02	1.05E+00
9	3.71E+02	2.54E-03	2.31E-04	4.83E-03	9.38E+02	1.31E+02	1.09E+00
10	3.80E+02	2.58E-03	2.28E-04	4.70E-03	9.38E+02	1.31E+02	1.08E+00
11	3.91E+02	2.62E-03	2.24E-04	4.66E-03	9.38E+02	1.31E+02	1.11E+00
12	4.00E+02	2.66E-03	2.22E-04	4.62E-03	9.38E+02	1.31E+02	1.12E+00
13	4.10E+02	1.42E-02	4.14E-05	8.63E-04	9.38E+02	1.31E+02	1.10E+00
14	4.20E+02	2.74E-03	2.15E-04	4.48E-03	9.38E+02	1.31E+02	1.09E+00
15	4.31E+02	2.78E-03	2.12E-04	4.42E-03	9.38E+02	1.31E+02	1.10E+00
16	4.40E+02	2.82E-03	2.09E-04	4.36E-03	9.38E+02	1.31E+02	1.08E+00
17	4.50E+02	2.85E-03	2.06E-04	4.30E-03	9.38E+02	1.31E+02	1.10E+00
18	4.60E+02	2.89E-03	2.03E-04	4.24E-03	9.38E+02	1.31E+02	1.09E+00
19	3.50E+02	4.45E-03	3.94E-01	5.51E+00	1.11E+03	2.31E+02	9.78E-01
20	3.50E+02	4.45E-03	3.94E-01	5.51E+00	1.11E+03	2.31E+02	1.00E+00
21	3.50E+02	4.45E-03	3.94E-01	5.51E+00	1.11E+03	2.31E+02	9.85E-01
22	3.50E+02	4.45E-03	3.94E-01	5.51E+00	1.11E+03	2.31E+02	9.82E-01
23	3.50E+02	4.45E-03	3.91E-01	5.51E+00	1.11E+03	2.31E+02	9.74E-01
24	3.50E+02	4.45E-03	3.94E-01	5.51E+00	1.11E+03	2.31E+02	1.00E+00

1	9	10	11	12	13	14	15b
1	1.63E-04	1.06E-05	8.50E-06	3.27E-05	1.02E-04	3.31E-05	0.
2	1.53E-05	2.21E-06	2.15E-06	1.27E-04	2.98E-04	9.78E-05	0.
3	9.56E-05	8.40E-06	7.40E-06	7.35E-05	1.70E-04	6.00E-05	0.
4	1.96E-04	4.80E-06	2.14E-06	5.26E-06	7.30E-05	1.45E-05	0.
5	1.52E-04	6.70E-06	3.29E-06	1.71E-05	8.48E-05	3.99E-05	0.
6	6.21E-05	4.26E-06	5.19E-06	8.29E-05	2.63E-04	1.02E-05	0.
7	1.63E-05	4.00E-06	2.22E-06	1.27E-04	3.18E-04	1.04E-04	3.27E-06
8	8.04E-05	9.91E-06	1.05E-05	9.12E-05	2.76E-04	7.61E-05	1.82E-06
9	0.	0.	0.	1.46E-04	3.66E-04	1.21E-04	5.63E-06
10	0.	0.	0.	1.43E-04	3.78E-04	1.30E-04	9.01E-06
11	0.	0.	0.	1.43E-04	3.86E-04	1.26E-04	1.07E-05
12	0.	0.	0.	1.42E-04	3.73E-04	1.27E-04	8.72E-06
13	0.	0.	0.	7.88E-06	2.17E-05	7.63E-06	5.58E-07
14	0.	0.	0.	1.26E-04	4.04E-04	1.40E-04	9.10E-06
15	0.	0.	0.	1.17E-04	4.48E-04	1.53E-04	8.28E-06
16	0.	0.	0.	1.06E-04	4.86E-04	1.65E-04	7.04E-06
17	0.	0.	0.	9.98E-05	5.29E-05	1.78E-04	6.73E-06
18	0.	0.	0.	8.40E-05	6.[illegible]E-04	1.91E-04	4.69E-06
19	2.25E-01	1.61E-02	8.19E-03	3.34E-02	1.09E-01	4.43E-02	0.
20	2.24E-01	1.66E-02	1.05E-01	3.94E-02	1.14E-01	4.05E-02	0.
21	2.22E-01	1.64E-02	8.32E-03	3.82E-02	1.18E-01	4.56E-02	0.
22	2.22E-01	1.68E-02	6.82E-03	3.93E-02	1.09E-01	4.53E-02	0.
23	2.19E-01	1.68E-02	7.36E-03	3.94E-02	1.14E-01	4.24E-02	0.
24	2.20E-01	1.66E-02	9.64E-03	3.78E-02	1.33E-01	4.37E-02	0.

G.2. Results of Transported Bed Experimentation

Tables G.2.1 and G.2.2 list the results of studies made of the fluid mechanical properties under conditions with and without chemical reaction respectively. The coding used in these tables is as follows:

1. Run number
2. W_S/W_G (mass flow rate of catalyst/mass flow rate of air)
3. Temperature
4. W_S = mass flow rate of catalyst (pounds/minute)
5. Air flow (cubic feet per minute)
6. Catalyst trapped in bottom section (grams)
7. Catalyst trapped in top section (grams)
8. Average gas velocity bottom section (ft./sec.)
9. Average gas velocity top section (ft./sec.)
10. Average particle velocity bottom section (ft./sec.)
11. Average particle velocity top section (ft./sec.)
12. Average slip velocity bottom section (ft./sec.)
13. Average slip velocity top section (ft./sec.)
14. Void fraction in bottom section
15. Void fraction in top section
16. Void fraction in bottom section calculated on the assumption of zero slip velocity
17. Void fraction in top section calculated on the assumption of zero slip velocity
18. Superficial gas velocity bottom section (ft./sec.)
19. Superficial gas velocity top section (ft./sec.)
20. Pressure drop in bottom section (p.s.i. per ft.)

21. Pressure drop in top section (p.s.i. per ft.)

22. Pressure drop in bottom section due to catalyst mass (p.s.i. per ft.)

23. Pressure drop in top section due to catalyst mass (p.s.i./ft.)

24. Pressure drop in bottom section due to friction (p.s.i/ft.)

25. Pressure drop in top section due to friction (p.s.i./ft.)

Table G.2.1. Fluid Mechanics Data for Experiments With Chemical Reaction

1	2	3	4	5	6	7
1	1.12E+02	3.00E+02	3.63E+01	4.42E+00	1.35E+02	9.43E+01
2	1.97E+02	3.02E+02	4.12E+01	2.85E+00	2.65E+02	1.96E+02
3	1.42E+02	3.06E+02	3.92E+01	3.78E+00	1.91E+02	1.19E+02
4	1.27E+02	3.42E+02	3.57E+01	3.83E+00	1.69E+02	1.21E+02
5	1.23E+02	3.05E+02	3.48E+01	3.80E+00	1.76E+02	1.25E+02
6	1.14E+02	3.05E+02	3.13E+01	3.74E+00	1.82E+02	1.34E+02
7	1.29E+02	2.64E+02	3.57E+01	3.78E+00	2.01E+02	1.49E+02
8	1.40E+02	2.49E+02	3.96E+01	3.86E+00	2.10E+02	1.50E+02
9	1.25E+02	3.14E+02	3.40E+01	3.76E+00	1.91E+02	1.22E+02
10	2.09E+02	3.37E+02	3.94E+01	2.57E+00	3.08E+02	2.34E+02
11	2.10E+02	3.00E+02	3.90E+01	2.53E+00	3.08E+02	2.34E+02
12	1.60E+02	2.95E+02	4.49E+01	3.83E+00	1.95E+02	1.45E+02
13	2.15E+02	2.33E+02	3.99E+01	2.53E+00	4.53E+02	3.39E+02
14	1.00E+02	2.90E+02	3.04E+01	4.13E+00	1.63E+02	1.19E+02
15	1.12E+02	3.40E+02	3.44E+01	4.17E+00	1.73E+02	1.22E+02
16	1.39E+02	3.00E+02	3.90E+01	3.83E+00	2.40E+02	1.59E+02
17	1.16E+02	3.33E+02	3.26E+01	3.83E+00	2.26E+02	1.46E+02
18	8.98E+01	3.36E+02	2.91E+01	4.42E+00	1.52E+02	1.02E+02
19	1.02E+02	3.04E+02	3.24E+01	4.35E+00	1.53E+02	1.04E+02
20	1.02E+02	2.95E+02	3.24E+01	4.35E+00	1.17E+02	

1	8	9	10	11	12	13
1	4.40E+01	5.13E+01	2.54E+01	3.38E+01	1.86E+01	1.75E+01
2	3.52E+01	4.16E+01	1.47E+01	1.85E+01	2.05E+01	2.31E+01
3	4.14E+01	4.73E+01	1.94E+01	2.88E+01	2.20E+01	1.84E+01
4	4.31E+01	5.10E+01	2.00E+01	2.59E+01	2.32E+01	2.51E+01
5	4.13E+01	4.86E+01	1.87E+01	2.44E+01	2.26E+01	2.42E+01
6	4.03E+01	4.79E+01	1.62E+01	2.05E+01	2.41E+01	2.74E+01
7	3.90E+01	4.61E+01	1.67E+01	2.11E+01	2.23E+01	2.50E+01
8	3.92E+01	4.58E+01	1.78E+01	2.32E+01	2.14E+01	2.26E+01
9	4.20E+01	4.81E+01	1.71E+01	2.48E+01	2.48E+01	2.33E+01
10	3.64E+01	4.33E+01	1.21E+01	1.48E+01	2.43E+01	2.85E+01
11	3.37E+01	4.01E+01	1.19E+01	1.46E+01	2.17E+01	2.54E+01
12	4.14E+01	4.91E+01	2.18E+01	2.72E+01	1.96E+01	2.19E+01
13	4.05E+01	4.50E+01	8.32E+00	1.03E+01	3.21E+01	3.47E+01
14	4.21E+01	4.97E+01	1.76E+01	2.25E+01	2.45E+01	2.72E+01
15	4.69E+01	5.49E+01	1.87E+01	2.46E+01	2.82E+01	3.02E+01
16	4.52E+01	5.07E+01	1.50E+01	2.15E+01	3.02E+01	2.92E+01
17	4.63E+01	5.29E+01	1.36E+01	1.95E+01	3.27E+01	3.30E+01
18	4.78E+01	5.56E+01	1.80E+01	2.49E+01	2.98E+01	3.07E+01
19	4.47E+01	5.21E+01	1.99E+01	2.72E+01	2.48E+01	2.49E+01
20	4.64E+01		2.60E+01		2.04E+01	

	14	15	16	17	18	19
1	8.41E-01	8.70E-01	9.02E-01	9.10E-01	3.70E+01	4.49E+01
2	6.90E-01	7.29E-01	8.42E-01	8.59E-01	2.43E+01	3.04E+01
3	7.76E-01	8.35E-01	8.81E-01	8.92E-01	3.21E+01	3.95E+01
4	8.02E-01	8.33E-01	8.93E-01	9.00E-01	3.40E+01	4.25E+01
5	7.94E-01	8.27E-01	8.95E-01	9.05E-01	3.28E+01	4.02E+01
6	7.87E-01	8.15E-01	9.02E-01	9.11E-01	3.17E+01	3.90E+01
7	7.64E-01	7.95E-01	8.83E-01	8.94E-01	2.98E+01	3.66E+01
8	7.54E-01	7.93E-01	8.71E-01	8.83E-01	2.96E+01	3.63E+01
9	7.76E-01	8.31E-01	8.95E-01	9.05E-01	3.20E+01	4.00E+01
10	6.39E-01	6.76E-01	8.42E-01	8.60E-01	2.33E+01	2.93E+01
11	6.39E-01	6.76E-01	8.33E-01	8.51E-01	2.15E+01	2.71E+01
12	7.72E-01	7.99E-01	8.65E-01	8.78E-01	3.19E+01	3.92E+01
13	4.70E-01	5.31E-01	8.12E-01	8.32E-01	1.90E+01	2.39E+01
14	8.09E-01	8.36E-01	9.10E-01	9.18E-01	3.40E+01	4.15E+01
15	7.97E-01	8.31E-01	9.05E-01	9.16E-01	3.74E+01	4.56E+01
16	7.12E-01	7.80E-01	8.82E-01	8.93E-01	3.22E+01	3.96E+01
17	7.36E-01	7.97E-01	9.04E-01	9.14E-01	3.41E+01	4.19E+01
18	8.22E-01	8.58E-01	9.24E-01	9.31E-01	3.93E+01	4.77E+01
19	8.20E-01	8.56E-01	9.11E-01	9.19E-01	3.67E+01	4.46E+01
20	8.62E-01		9.18E-01		4.00E+01	

	20	21	22	23	24	25
1	1.81E-01	1.53E-01	6.56E-02	5.40E-02	1.15E-01	9.86E-02
2	2.24E-01	2.20E-01	1.28E-01	1.12E-01	9.59E-02	1.08E-01
3	2.01E-01	1.91E-01	9.25E-02	6.83E-02	1.08E-01	1.22E-01
4	2.01E-01	1.91E-01	8.19E-02	6.92E-02	1.19E-01	1.22E-01
5	2.01E-01	1.91E-01	8.53E-02	7.15E-02	1.15E-01	1.19E-01
6	2.01E-01	1.93E-01	8.82E-02	7.67E-02	1.12E-01	1.18E-01
7	2.01E-01	1.91E-01	9.76E-02	8.50E-02	1.03E-01	1.06E-01
8	2.01E-01	1.87E-01	1.02E-01	8.58E-02	9.89E-02	1.01E-01
9	2.01E-01	1.91E-01	9.25E-02	6.99E-02	1.08E-01	1.21E-01
10	2.32E-01	2.29E-01	1.49E-01	1.34E-01	8.27E-02	9.50E-02
11	2.32E-01	2.33E-01	1.49E-01	1.34E-01	8.27E-02	9.92E-02
12	2.01E-01	1.91E-01	9.46E-02	8.30E-02	1.06E-01	1.06E-01
13	2.32E-01	2.33E-01	2.19E-01	1.94E-01	1.27E-02	3.91E-02
14	1.89E-01	1.82E-01	7.92E-02	6.79E-02	1.10E-01	1.14E-01
15	1.89E-01	1.78E-01	8.40E-02	7.00E-02	1.05E-01	1.08E-01
16	2.01E-01	1.91E-01	1.19E-01	9.09E-02	8.15E-02	9.99E-02
17	2.01E-01	1.91E-01	1.09E-01	8.38E-02	9.11E-02	1.07E-01
18	1.81E-01	1.74E-01	7.39E-02	5.84E-02	1.07E-01	1.15E-01
19	1.85E-01	1.74E-01	7.44E-02	5.97E-02	1.11E-01	1.14E-01
20	1.61E-01		5.69E-02		1.04E-01	

Table G.2.2. Fluid Mechanics Data for Experiments without Chemical Reaction

1	2	3	4	5	6	7
1	1.49E+02	2.20E+02	3.20E+01	2.93E+00	2.04E+02	1.31E+02
2	1.80E+02	2.20E+02	3.40E+01	2.56E+00	2.41E+02	1.54E+02
3	2.11E+02	2.20E+02	3.17E+01	2.05E+00	2.99E+02	2.08E+02
4	2.48E+02	2.20E+02	3.24E+01	1.78E+00	3.57E+02	2.53E+02
5	9.36E+01	2.20E+02	2.47E+01	5.60E+00	1.24E+02	7.42E+01
6	6.59E+01	2.20E+02	2.10E+01	4.35E+00	9.24E+01	4.88E+01
7	5.00E+01	2.20E+02	1.82E+01	4.97E+00	6.93E+01	2.99E+01
8	2.47E+01	2.20E+02	1.03E+01	5.68E+00	3.49E+01	1.29E+01
9	9.96E+01	2.20E+02	3.21E+01	4.40E+00	1.33E+02	7.92E+01
10	1.17E+02	2.20E+02	3.32E+01	3.88E+00	1.54E+02	9.05E+01
11	1.48E+02	2.20E+02	3.73E+01	3.45E+00	1.74E+02	1.08E+02
12	1.62E+02	2.20E+02	3.59E+01	3.02E+00	2.20E+02	1.35E+02
13	1.04E+02	2.20E+02	3.00E+01	3.94E+00	1.22E+02	6.67E+01
14	8.68E+01	2.20E+02	2.80E+01	4.40E+00	1.27E+02	8.25E+01
15	7.28E+01	2.20E+02	2.89E+01	5.42E+00	9.78E+01	5.19E+01
16	9.87E+01	2.20E+02	3.92E+01	5.42E+00	1.41E+02	8.20E+01
17	9.37E+01	2.20E+02	3.72E+01	5.42E+00	1.29E+02	7.34E+01
18	7.91E+01	2.20E+02	3.14E+01	5.42E+00	1.03E+02	5.32E+01

1	8	9	10	11	12	13
1	2.83E+01	3.24E+01	1.47E+01	1.89E+01	1.36E+01	1.34E+01
2	2.66E+01	3.06E+01	1.33E+01	1.71E+01	1.34E+01	1.35E+01
3	2.37E+01	2.84E+01	9.95E+00	1.18E+01	1.38E+01	1.65E+01
4	2.28E+01	2.75E+01	8.50E+00	9.93E+00	1.43E+01	1.76E+01
5	3.07E+01	3.49E+01	1.86E+01	2.58E+01	1.21E+01	9.06E+00
6	3.45E+01	3.86E+01	2.13E+01	3.34E+01	1.32E+01	5.28E+00
7	3.72E+01	4.11E+01	2.46E+01	4.72E+01	1.26E+01	-6.07E+00
8	3.87E+01	4.26E+01	2.77E+01	6.19E+01	1.10E+01	-1.93E+01
9	3.41E+01	3.90E+01	2.26E+01	3.14E+01	1.15E+01	7.58E+00
10	3.20E+01	3.65E+01	2.02E+01	2.84E+01	1.18E+01	7.85E+00
11	2.90E+01	3.36E+01	2.01E+01	2.68E+01	8.92E+00	6.71E+00
12	2.78E+01	3.19E+01	1.53E+01	2.06E+01	1.25E+01	1.13E+01
13	3.11E+01	3.52E+01	2.30E+01	3.49E+01	8.15E+00	3.29E-01
14	3.39E+01	3.75E+01	2.07E+01	3.47E+01	1.31E+01	2.73E+00
15	3.54E+01	4.04E+01	2.77E+01	4.32E+01	7.07E+00	-2.77E+00
16	3.58E+01	4.04E+01	2.60E+01	3.71E+01	9.84E+00	3.39E+00
17	3.58E+01	4.03E+01	2.71E+01	3.93E+01	8.74E+00	1.03E+00
18	3.52E+01	4.00E+01	2.86E+01	4.57E+01	6.60E+00	-5.79E+00

1	14	15	16	17	18	19
1	7.59E-01	7.95E-01	8.36E-01	8.69E-01	2.15E+01	2.57E+01
2	7.16E-01	7.59E-01	8.35E-01	8.49E-01	1.91E+01	2.32E+01
3	6.48E-01	6.75E-01	8.14E-01	8.33E-01	1.54E+01	1.91E+01
4	5.78E-01	6.04E-01	7.86E-01	8.09E-01	1.32E+01	1.66E+01
5	8.53E-01	8.84E-01	9.08E-01	9.11E-01	2.92E+01	3.38E+01
6	8.91E-01	9.24E-01	9.30E-01	9.33E-01	3.07E+01	3.57E+01
7	9.18E-01	9.53E-01	9.44E-01	9.47E-01	3.42E+01	3.92E+01
8	9.59E-01	9.80E-01	9.70E-01	9.71E-01	3.71E+01	4.18E+01
9	8.43E-01	8.76E-01	8.90E-01	8.98E-01	2.87E+01	3.42E+01
10	8.18E-01	8.58E-01	8.77E-01	8.86E-01	2.[illegible]E+01	3.11E+01
11	7.95E-01	8.31E-01	8.48E-01	8.60E-01	2.51E+01	2.79E+01
12	7.40E-01	7.88E-01	8.38E-01	8.52E-01	2.06E+01	2.52E+01
13	8.55E-01	8.96E-01	8.89E-01	8.97E-01	2.66E+01	3.15E+01
14	8.51E-01	9.02E-01	9.03E-01	9.09E-01	2.88E+01	3.38E+01
15	8.85E-01	9.19E-01	9.07E-01	9.14E-01	3.13E+01	3.71E+01
16	8.53E-01	8.72E-01	8.73E-01	8.81E-01	2.99E+01	3.53E+01
17	8.48E-01	8.85E-01	8.81E-01	8.88E-01	3.04E+01	3.57E+01
18	8.78E-01	9.17E-01	8.99E-01	9.06E-01	3.09E+01	3.66E+01

1	20	21	22	23	24	25
1	1.71E-01	1.54E-01	9.96E-02	8.48E-02	7.09E-02	6.87E-02
2	1.94E-01	1.86E-01	1.17E-01	9.99E-02	7.68E-02	8.50E-02
3	2.24E-01	2.25E-01	1.46E-01	1.35E-01	7.82E-02	9.09E-02
4	2.46E-01	2.54E-01	1.79E-01	1.64E-01	7.13E-02	9.04E-02
5	1.49E-01	1.06E-01	6.06E-02	4.81E-02	8.81E-02	5.75E-02
6	1.15E-01	1.06E-01	4.51E-02	3.10E-02	6.99E-02	7.39E-02
7	1.03E-01	7.20E-02	3.30E-02	1.94E-02	6.93E-02	5.20E-02
8	8.13E-02	2.88E-02	1.70E-02	8.35E-03	6.42E-02	2.04E-02
9	1.71E-01	1.68E-01	6.51E-02	5.13E-02	1.05E-01	1.17E-01
10	1.69E-01	1.58E-01	7.53E-02	5.66E-02	9.32E-02	9.97E-02
11	1.88E-01	2.04E-01	8.49E-02	6.98E-02	1.03E-01	1.34E-01
12	2.02E-01	2.25E-01	1.06E-01	8.70E-02	9.40E-02	1.30E-01
13	1.71E-01	1.34E-01	8.90E-02	4.32E-02	1.11E-01	9.11E-02
14	1.51E-01	1.30E-01	8.19E-02	4.05E-02	8.88E-02	8.90E-02
15	1.59E-01	2.13E-01	4.70E-02	5.36E-02	1.11E-01	1.80E-01
16	1.98E-01	1.63E-01	6.90E-02	5.31E-02	1.29E-01	1.10E-01
17	1.82E-01	1.49E-01	6.29E-02	4.75E-02	1.20E-01	1.01E-01
18	1.71E-01	2.06E-01	5.03E-02	3.45E-02	1.20E-01	1.72E-01

Table G.2.3. lists the results of the chemical reaction studies conducted in the transported bed reactor. The coding used in this table is as follows:

1. Run number
2. Temperature of reaction (^{o}C)
3. Overall W/F_{Ao} value (gm. cat. hr./gm. mole xylene)
4. Inlet xylene mole fraction
5. First order rate constant (litres/gm. hr) - result for bottom section of reactor
6. First order rate constant (litres/gm. hr.) - result from top section of reactor
7. Fractional conversion of orthoxylene
8. Selectivity for orthotolualdehyde formation
9. Selectivity for phthalic anhydride formation
10. Selectivity for phthalide formation
11. Selectivity for carbon dioxide formation
12. Selectivity for carbon monoxide formation
13. Selectivity for orthotoluic acid formation

Inlet Conditions

	2	3	4	5	6
1	3.06E+02	6.36E+01	1.66E-02	2.23E+01	2.46E+01
2	3.02E+02	1.54E+02	2.08E-02	2.03E+01	2.09E+01
3	3.06E+02	8.35E+01	1.98E-02	2.27E+01	2.93E+01
4	3.42E+02	7.81E+01	1.96E-02	2.44E+01	2.85E+01
5	3.85E+02	8.22E+01	1.91E-02	2.09E+01	2.10E+01
6	3.05E+02	1.76E+02	9.80E-03	2.59E+01	2.69E+01
7	2.64E+02	9.43E+01	1.98E-02	7.13E+00	8.59E+00
8	2.49E+02	9.69E+01	1.94E-02	4.02E+00	5.48E+00
9	3.14E+02	8.49E+01	1.97E-02	2.32E+01	2.49E+01
10	3.37E+02	1.46E+02	2.82E-02	3.19E+01	3.02E+01
11	3.00E+02	1.48E+02	2.86E-02	1.87E+01	2.38E+01
12	2.95E+02	9.16E+01	1.96E-02	1.90E+01	1.80E+01
13	2.33E+02	3.53E+02	1.75E-02	2.44E+00	3.19E+00
14	2.90E+02	1.26E+02	1.11E-02	1.87E+01	1.83E+01
15	3.40E+02	1.32E+02	1.11E-02	2.73E+01	2.61E+01
16	3.00E+02	1.09E+02	1.96E-02	1.98E+01	2.02E+01
17	3.33E+02	1.00E+02	1.96E-02	2.83E+01	2.72E+01
18	3.36E+02	1.14E+02	1.04E-02	3.18E+01	2.84E+01
19	3.04E+02	1.15E+02	1.06E-02	2.92E+01	2.39E+01
20	2.95E+02	8.19E+01	1.06E-02	2.05E+01	

Product Composition at Bottom Sample Port

	7	8	9	10	11	12	13
1	9.69E-02	9.36E-01	0.	0.	2.92E-02	8.10E-03	2.71E-02
2	2.58E-01	9.19E-01	1.31E-03	0.	3.84E-02	1.24E-02	2.87E-02
3	2.04E-01	9.33E-01	3.94E-03	0.	3.19E-02	1.15E-02	1.98E-02
4	7.42E-02	7.14E-01	0.	0.	2.12E-01	6.04E-02	7.39E-03
5	1.39E-01	9.38E-01	1.14E-02	0.	2.49E-02	9.30E-03	1.63E-02
6	2.66E-01	9.01E-01	2.01E-02	0.	4.55E-02	9.90E-03	2.40E-02
7	5.50E-02	9.52E-01	0.	0.	4.76E-02	0.	0.
8	4.85E-02	9.41E-01	0.	0.	5.92E-02	0.	0.
9	1.60E-01	9.06E-01	0.	0.	7.27E-02	1.61E-02	5.39E-03
10	2.22E-01	7.51E-01	9.90E-03	0.	1.89E-01	5.32E-02	7.13E-03
11	2.28E-01	9.08E-01	0.	0.	4.58E-02	1.54E-02	2.05E-02
12	1.14E-01	9.40E-01	0.	0.	4.46E-02	7.77E-03	7.91E-03
13	7.15E-02	9.41E-01	0.	0.	5.88E-02	0.	0.
14	1.25E-01	9.66E-01	0.	0.	2.69E-02	7.51E-03	0.
15	1.96E-01	9.35E-01	0.	0.	3.07E-02	1.16E-02	2.23E-02
16	2.16E-01	9.83E-01	2.98E-03	0.	1.01E-02	1.89E-03	2.53E-03
17	3.15E-01	8.76E-01	1.72E-03	0.	5.76E-02	2.14E-02	4.29E-02
18	3.78E-01	9.00E-01	8.17E-03	0.	6.17E-02	1.91E-02	1.10E-02
19	1.91E-01	9.47E-01	1.39E-03	0.	2.76E-02	8.73E-03	1.48E-02
20	2.08E-01	9.55E-01	0.	0.	2.69E-02	7.38E-03	8.31E-03

1	7	8	9	10	11	12	13
1	[illegible]	[illegible]	1.9[illegible]	0.	[illegible]	[illegible]	[illegible]
2	7.02E-01	8.97E-01	5.15E-03	1.73E-03	5.15E-02	1.94E-02	2.97E-02
3	5.28E-01	9.05E-01	4.29E-03	5.37E-03	4.10E-02	1.51E-02	2.86E-02
4	4.85E-01	8.56E-01	9.00E-03	8.35E-03	6.27E-02	2.39E-02	4.09E-02
5	4.63E-01	9.14E-01	6.36E-03	2.29E-03	3.67E-02	1.42E-02	2.69E-02
6	5.62E-01	9.25E-01	0.	0.	4.64E-02	1.44E-02	1.[illegible]E-02
7	2.35E-01	9.62E-01	0.	0.	1.66E-02	9.47E-03	1.10E-02
8	[illegible]	[illegible]	[illegible]	0.	[illegible]	[illegible]	[illegible]
9	[illegible]	[illegible]	[illegible]	[illegible]	[illegible]	[illegible]	[illegible]
10	9.00E-01	7.37E-01	3.51E-04	8.95E-03	1.49E-01	4.72E-02	4.73E-02
11	7.66E-01	8.92E-01	2.66E-03	1.13E-03	5.91E-02	2.92E-02	2.00E-02
12	4.76E-01	9.26E-01	0.	0.	4.07E-02	1.31E-02	2.04E-02
13	2.71E-01	8.89E-01	0.	0.	5.74E-02	2.31E-02	3.09E-02
14	3.93E-01	9.23E-01	0.	0.	5.11E-02	1.14E-02	1.40E-02
15	5.10E-01	9.09E-01	1.66E-03	0.	4.70E-02	1.66E-02	2.57E-02
16	5.69E-01	9.06E-01	4.04E-03	4.23E-03	5.96E-02	1.96E-02	2.81E-02
17	6.49E-01	8.50E-01	1.15E-02	5.41E-03	8.69E-02	2.97E-02	4.07E-02
18	4.98E-01	8.43E-01	1.37E-02	8.92E-03	8.92E-02	2.35E-02	4.50E-02
19	[illegible]	[illegible]	0.	0.	1.91E-02	1.20E-02	1.36E-02
20	4.34E-01	9.19E-01	1.37E-03	0.	4.21E-02	1.04E-02	2.75E-02

Composition at Top Sample Port

1	7	8	9	10	11	12	13
1	9.62E-01	9.15E-01	6.13E-03	3.51E-03	3.81E-02	1.39E-02	2.92E-02
2	8.70E-01	8.76E-01	1.17E-02	5.00E-03	5.04E-02	2.43E-02	2.65E-02
3	7.75E-01	8.71E-01	1.39E-02	9.20E-03	9.28E-02	3.81E-02	3.49E-02
4	6.90E-01	7.97E-01	2.03E-02	1.69E-02	9.00E-02	3.05E-02	4.79E-02
5	6.55E-01	8.86E-01	4.86E-03	1.77E-03	4.50E-02	1.37E-02	4.51E-02
6	7.56E-01	8.84E-01	7.81E-03	2.69E-03	5.73E-02	1.63E-02	3.21E-02
7	4.12E-01	9.55E-01	0.	0.	1.72E-02	9.47E-03	1.85E-02
8	2.97E-01	9.23E-01	0.	0.	5.01E-02	7.10E-03	1.94E-02
9	7.18E-01	8.90E-01	0.	0.	5.87E-02	2.00E-02	3.12E-02
10	9.89E-01	9.02E-01	9.02E-02	1.70E-02	2.03E-01	1.30E-02	1.39E-02
11	9.50E-01	8.33E-01	1.52E-02	8.59E-03	7.19E-02	3.30E-02	3.30E-02
12	6.49E-01	9.11E-01	4.05E-03	9.00E-04	4.32E-02	1.52E-02	2.54E-02
13	4.92E-01	9.03E-01	0.	0.	6.42E-02	2.51E-02	8.04E-03
14	5.52E-01	9.15E-01	2.41E-03	0.	4.50E-02	1.20E-02	2.45E-02
15	6.69E-01	8.80E-01	6.26E-03	1.91E-03	5.70E-02	1.90E-02	3.58E-02
16	7.38E-01	9.08E-01	8.57E-03	2.61E-03	4.40E-02	1.77E-02	1.90E-02
17	7.92E-01	8.09E-01	1.98E-02	8.40E-03	8.00E-02	3.09E-02	5.22E-02
18	6.26E-01	8.29E-01	1.69E-02	9.48E-03	8.68E-02	2.57E-02	5.25E-02
19	5.93E-01	8.99E-01	4.12E-03	0.	4.25E-02	1.57E-02	4.44E-02

APPENDIX II

EQUIPMENT SPECIFICATIONS

II.1. Transported Bed Reactor

The major components in the transported bed apparatus are listed below.

Valves

2, 3 and 4-way Solenoid Valves

Type: Asco Red-Hat solenoid valves

Manufacturer: Asco Electric Limited

Air Control Valves (3)

Manufacturer: Research Controls Inc.

Material: 316 stainless steel

Range: 3-15 psig

Action: Air to open

Solids Control Butterfly Valve

Manufacturer: Fisher Governor Company

Material: 316 stainless steel

Size: 2 inch

Range: 6-30 psig

Action: Air to open

Upper temperature limit: 900°F (continuous operation)

Solids Trapping Valves

Manufacturer: Kamyr Valves Inc.

Material: 316 stainless steel

Size: 5/8 inch

Range: 0-150 psig

Action: 2-way air cylinder - air to close - open manually

Seal: Stellite

Packing: Asbestos

Upper temperature limit: 1000°F (continuous operation)

Ball Valve on Feed Tank

Manufacturer: Kamyr Valves Inc.

Material: 316 stainless steel

Size: 2 inch

Range: 0-150 psia

Action: 2-way air cylinder - air to open/air to close - via 4-way solenoid valve

Seat: Stellite

Packing: Asbestos

Upper temperature limit: 1000°F (continuous operation)

Ball Valve on Weighing Tank

As above except manually operated

Pressure Relief Valve

Manufacturer: Crane Co.

Model: No. 2551 brass pop safety valve

Size: 1/2 inch

Orthoxylene Control Valve

Manufacturer: Millaflow Corp.

Type: Diaphragm

Model: No. 41100000

Controllers

Air Pressure Controllers (Proportional Control)

Manufacturer: Minneapolis Honeywell

1. Pressure upstream of sonic orifice

Model: No. PP97A1076 2

Range: 10-300 psig

2. Pressure in solids hold tank

Model: No. PP97A1043 2

Range: 2-50 psig

3. Pressure in solids feed tank

Model: No. PP97A1035 1

Range: 0-15 psig

Level Controller

Manufacturer: Drexelbrook Engineering Co.

Model: 406-1

Action: High level fail safe - on-off control

Features: Delayed operation following increase in level

Measuring element: Ceramic capacitance probe - maximum temperature rating 1000°F

Strain Gauge Weighing Device

Manufacturer: S.E. Laboratories (Engineering) Ltd.

Transducer Converter: Model SE 905/2/1

Recording Instruments: Keithley 160 Digital multimeter

Sargent Model DSRG Recorder

II.2. Gas Chromatographic Technique

Gas Chromatograph

Manufacturer: Varian Aerograph

Model: 1520

Features: Matrix Temperature Programmer.

Detector: Thermal Conductivity

Modifications: Replaced carrier gas flow controller with 2 model NRS Flow Controllers (Brooks Instrument Division, Emerson Electric Company)

Integrator

Manufacturer: Hewlett-Packard

Model: 3370B

Recorder

Manufacturer: Minneapolis Honeywell

Model: Electronic 19

Gas Sample Valves

Manufacturer: Carle Instrument Inc.

Type: Micro-Volume Switching Valve with Zero-Dead Volume

Catalogue No.: 2014

II.3. Chemicals

Liquid and Solid Components

1. Orthoxylene

(a). For analytical work:

Matheson, Coleman and Bell

Cat. No.: XX17

Grade: Chromatographic quality purity: 99 + %

(b). Reactor grade:

Eastman organic Chemicals Ltd.

Grade: Highest purity

Melting point: (-25°C) - (-23°C)

2. Malcic Anhydride

Matheson, Coleman and Bell

Cat. No.: MX 113

Purity: 53-55°C (M.P.)

3. Orthotolualdehyde

Matheson, Coleman and Bell

Cat. No.: TX 720

Purity: practical grade

4. Acetone

J. T. Baker and Co.

Cat. No.: A 137

Purity: chromatographic

5. Phthalic anhydride

J. T. Baker and Co.

Cat. No.: 0272

Purity: Analytical

6. p-Benzoquinone

Fisher Scientific Co.

Cat. No. Q36

Purity: Purified Lab. grade

7. Orthotoluic acid

Fisher Scientific Co.

Cat. No.: 1646

Purity: Analytical

8. Phthalide

Fisher Scientific Co.

Cat. No.: 17827

Purity: Lab. grade

2. Gases

The gases used were commercial grade unless otherwise stated.

1. Helium: Canadian Liquid Air Limited
2. High Purity Nitrogen: Canadian Liquid Air Limited
3. Oxygen: Canadian Liquid Air Limited
4. Carbon Dioxide: Canadian Liquid Air Limited
5. Carbon Monoxide: Matheson of Canada Limited
6. Sulphur Dioxide: Matheson of Canada Limited
7. Carbon Dioxide (5.06%), Carbon Monoxide (1.00%), Nitrogen (93.94%) - certified standard: Matheson of Canada Limited
8. Sulphur Dioxide (0.5%), Nitrogen (99.5%) - calibrated standard: Matheson of Canada.

APPENDIX I

LISTINGS OF COMPUTER PROGRAMS

This section contains listings of computer programs that were written in Fortran IV to perform calculations on data from the packed bed experiments. A brief description of each program follows:

Program 1

This program takes run data such as chromatogram areas, gas flows, pressure drops, etc. from the packed bed experiments and converts them into inlet and exit stream compositons. The calculated compositions and the reaction conditions are punched for use in the parameter estimation program.

Program 2

This program estimates common parameters from multi-response data using the Box-Draper Criterion.

Program 3

This program calculates the variance-covariance matrix from concentration data obtained from replicated experiments. In addition, the Bartlett test is conducted to determine if there is constancy of variance for each of the individual responses.

```
C     TO CONVERT RAW DATA FROM EXPERIMENTAL INLET AND OUTLET
C     ANALYSES AND TO PUNCH DATA FOR PARAMETER ESTIMATION AND
C     SEQUENTIAL EXPERIMENTAL DESIGN PROGRAMS
C     ****************************************************************
C     ****************************************************************
C     ***PHTHALIC ANHYDRIDE REACTOR MODEL***
C     ****************************************************************
C     ****************************************************************
C     LANGMUIR STATE ADSORPTION MODEL
C     ****************************************************************
C     NOMENCLATURE
C     ****************************************************************
C
C     T - ABSOLUTE TEMP.(K)
C     TOX - TEMPERATURE OF OXYLENE SATURATOR (DEG C)
C     FO2 - FLOWRATE OF OXYGEN C.C./MIN.
C     FN2 - FLOW RATE OF NITROGEN, CC./MIN.
C     TA - TOX+273.2
C     P - ABSOLUTE PRESSURE AT WHICH FO2,FN2 ARE MEASURED,MM. HG.
C     TA - TEMPERATURE AT WHICH FO2,FN2 ARE MEASURED
C     N - EXPERIMENT RUN NUMBER
C     A,B, - CONSTANTS IN OXLYENE VAPOUR PRESSURE CORRELATION
C     POX - VAPOUR PRESSURE OXYLENE
C     O2,N2,OX - FLOWRATES IN MOLES/MIN.
C     YO2,YN2,YOX - MOLE FRACTIONS
C     TA,P - TEMP(C), ABSOLUTE PRESSURE AT REACTOR INLET
C     COX,CO2,CN2 - CONCENTRATIONS OF COMPONENTS (GM.MOLES/LITRE)
C     C - CONCENTRATIONS IN MERSON (GM.MOLES/LITRE)
C     FR - MOLE FRACTION OF EXIT
C     YE - EXPERIMENTAL EXIT CONCENTRATION (GM.MOLE/LITRE)
C     A1 - AREA OF INLET ANALYSIS
C     AO - AREA OF OUTLET ANALYSIS
C     RM - RELATIVE RESPONSE
C     RA - RATIO
C     1,2,3,4,5,6,7,8,9 - OX,OTA,PI,PA,CO2,O2,N2,H2O,CO,RESPECTIVELY
C     ****************************************************************
C     TO IS MAA FOR TIO2 - SUPPORTED CATALYST
C     TO IS OTAC FOR SIO2 - SUPPORTED CATALYST
C     W - WEIGHT OF CATALYST, GRAMS
C     DELP - PRESSURE DROP ACROSS REACTOR, MM. HG.
C     PT - TOTAL ABSOLUTE PRESSURE IN REACTOR, MM. HG.
C     XN IS STOICHIOMETRIC COEFFICIENT FOR CARBON OXIDE FORMATION
C     XN1 IS SPARE STOICHIOMETRIC COEFFICIENT
C     XN2 IS STOICHIOMETRIC COEFFICIENT FOR PT/PAA FORMATION
C     MODIFY THIS EXPRESSION ACCORDINGLY IF OTHER COMPOUNDS ARE TO BE LUMPED
C     ****************************************************************
C     ****************************************************************
      DIMENSION Y(10)
      DIMENSION ARRAY(25,25)
      DIMENSION RM(10),AI(10),AO(10),RA(10),YE(10),FR(10)
C     ****************************************************************
C
      REAL NN,N2
      REAL NN1,NN2
```

```
C  RELATIVE MOLAR RESPONSES FOR ALL COMPONENTS
   DATA(RM(ID,I=1,10)/3.04,3.19,3.28,3.34,1.27,.97(,1.,.5,1.06,1.0/
C  NSETS IS THE NUMBER OF DIFFERENT REACTION CONDITIONS
   READ(5,997)NSETS
   DO 5000 KKK=1,NSETS
C  ***************************************************************
C  ZERO STORAGE ARRAY - ARRAY(I,J)
   DO11 I=1,25
   DO 11 J=1,25
   ARRAY(I,J)=0.
11 CONTINUE
C  ***************************************************************
   READ(5,997) KRUN
   READ(5,800)TAMB,PAMB,TOX,FO2,FN2,TR,PR,DELP,W
   READ(5,800)AI(1),AI(6),AI(7)
C  READ ANALYSIS DATA
C  CALCULATE CONCENTRATIONS AND VOLUMETRIC FLOWRATE INTO REACTOR.
C  FLOWS IN MOLES/UNIT TIME
   TA=TAMB+273.2
   DEN=22400.*TA*760./(273.2*PAMB)
   O2=FO2/DEN
   N2=FN2/DEN
C  REACTOR EXPERIMENTAL CONDITIONS
   GRADP = DELP/W
   PT=PR
C  CALCULATE MOLE FRACTION OF O-XYLENE
   RA(1)=(AI(1)/AI(7))*(RM(7)/RM(1))
   RA(6)=(AI(6)/AI(7))*(RM(7)/RM(6))
   YOX=RA(1)/(1.+RA(1)+RA(6))
   RAA=RA(1)
   RAD=RA(6)
   OX=(O2+N2)*YOX/(1.-YOX)
   T=TR+273.2
   FGAS=(O2+N2+OX)*22400.*T*760./(273.2*PR)
C  CALCULATE CONCENTRATIONS IN REACTOR IN MOLES/CC.
   COX=OX/FGAS
   CO2=O2/FGAS
   CN2=N2/FGAS
C  ***************************************************************
   WRITE(6,998)KRUN
   WRITE(6,988) TOX,FO2,FN2,TAMB,PAMB,FGAS
   WRITE(6,996 ) TR,PR,W,DELP
                 ******************
   FAO=OX*60.
```

```
AO=R/FAO

NDA IS THE NUMBER OF EXIT ANALYSES CONDUCTED AT EACH EXPERIMENTAL COND
READ(5,997)NDA
DO 800 III=1,NDA
READ(5,800)(AO(I),I=1,10)
CALCULATE EXPERIMENTAL EXIT CONCENTRATION
DO 1 I=1,7
1 RA(I)=(AO(I)/AO(7))*(RM(7)/RM(I))
RA(9)=(AO(9)/AO(7))*(RM(7)/RM(9))
RA(10)=(AO(10)/AO(7))*(RM(7)/RM(10))
CALCULATE WATER RESPONSE
                    ********************
RA(8)=RA(2)+RA(3)*2.+RA(4)*3.+(RA(5)+RA(9))*5./8.+RA(10)*1.5
                    ********************
CALCULATE OXYGEN RESPONSE
                    ********************
RAC=RA(2)*1.0+RA(3)*2.+RA(4)*3.+RA(5)*10.5/8.+RA(9)*6.5/8.+RA(10)*
11.5
                    ********************
CALCULATE OVERALL STOICHIOMETRIC COEFFICIENT,
CSN=(RAD-RA(6))/(RAA-RA(1))

CALCULATE OXYGEN BALANCE (STOICHIOMETRIC O2 OUT - MEASURED O2 OUT
OB=(RAD-RAC)/RA(6)
COO=(RAD-RA(6))/RAC

CALCULATE STIOCHIOMETRIC NUMBER FOR CARBON OXIDES FORMED
NN=((RA(5)*10.5)+(RA(9)*6.5))/(RA(5)+RA(9))
NN1=1.
CALCULATE STOIGHIOMETRIC COEFFICIENT FOR PAA +PI FORMATION ******
NN2=(RA(3)+RA(4)*2.)/(RA(3)+RA(4))

CARBON BALANCE

RAB=RA(1)+RA(2)+RA(3)+RA(4)+(RA(5)+RA(9))/8.+RA(10)/2.
CBR=RAB/RAA

CALCULATE CONVERSION AND SELECTIVITIES
CONV=RAB-RA(1)
YIELD=CONV/RAB
SOTA=RA(2)/CONV
SPI =RA(3)/CONV
SPAA=RA(4)/CONV
SCO2=RA(5)/(CONV*8.)
SCO =RA(9)/(CONV*8.)
SMA =RA(10)/(CONV*2.)
SUM=0.0

DO 820 I=1,10
820 SUM=SUM+RA(I)
POUT=PR-DELP
CONS=273.2*POUT/(22.400*760.*T)
DO 803 I=1,10
FR(I)=RA(I)/SUM
```

```
      Y(I)=FR(I)*CONS
C     CONCENTRATIONS FOR INTEGRATION
C     CONCENTRATIONS IN GM-MOLES/LITRE
      FGAS=FGAS*1.0E-03
      WRITE(6,975) VPOX,YOX
      Y(1)=COX*1.0E03
      Y(2)=0.
      Y(3)=0.
      Y(4)=0.
      Y(5)=0.
      Y(6)=CO2*1.0E03
      Y(7)=CN2*1.0E03
      Y(8)=0.
      Y(9)=0.
      Y(10)=0.
C     GAS FLOW RATE (LITRES / SEC)
      FGAS=FGAS/60.
      WRITE(6,976) Y(1),Y(6),Y(7)
      DO 5 I=1,9
      ARRAY(I,J)=Y(I)
5     CONTINUE
      DO 6 K=10,18
      II=K-9
      ARRAY(K,J)=YE(II)
6     CONTINUE
C     ADD CO AND CO2 CONCENTRATIONS FOR USE IN PARAMETER ESTIMATION
      ARRAY(14,J)=ARRAY(14,J)+ARRAY(18,J)
      ARRAY(19,J)=T
      ARRAY(20,J)=DELP
      ARRAY(21,J)=W
      ARRAY(22,J)=PT
      ARRAY(23,J)=FGAS
      ARRAY(24,J)=GRADP
      WRITE(6,222)
      WRITE(6,231)
      WRITE(6,811)YIELD,SUTA,SPI,SPAA,SCO2,SCO,SMA
      WRITE(6,226)WFAO
      WRITE(6,812), CBR
      WRITE(6,223)
      WRITE(6,999)OB,NN,CSN,COU
      WRITE(6,810)
      WRITE(6,230)
      WRITE(6,811)(YE(I),I=1,10)
      WRITE(6,224)
      WRITE(6,230)
      WRITE(6,811)(FR(I),I=1,10)
      WRITE(6,232)
      WRITE(6,233)(ARRAY(I,J),I=1,24)
      RRATE=YIELD/WFAO
      WRITE(6,261) RRATE
C     PUNCH DATA FOR PARAMETER ESTIMATION AND EXPERIMENTAL DESIGN PROGRAMS
      WRITE(7,234) KRUN,NN,NN1,NN2
      WRITE(7,233) (ARRAY(I,J),I=1,24)
4     CONTINUE
```

```
    2 CONTINUE
    3 CONTINUE
  200 CONTINUE
  201 FORMAT(I2)
  888 FORMAT(1H1,20X,*RUN NUMBER* I3//)
  999 FORMAT(* TEMPERATURE OF O-XYLENE SATURATOR = * F6.1 * DEG.C.*//
     1 * OXYGEN    FLOWRATE = *  F6.2 * CC/MIN.*/
     2 * NITROGEN FLOWRATE = * F6.2 * CC/MIN.*//
     3 * AMBIENT TEMPERATURE = * F6.1 * DEG.C.*/
     4 * AMBIENT PRESSURE = * F7.1 * MM.HG.*//
     5 * TOTAL FLOWRATE AT REACTOR,TEMPERATURE AND PRESSURE = *F7.2
     6 * CC/MIN *)
  998 FORMAT(* REACTOR TEMPERATURE = * F8.2 * DEG.C.*/
     1 * REACTOR PRESSURE = * F8.2 * MM.HG.*/
     2 * WEIGHT OF CATALYST = * F8.2 /
     3 * PRESSURE DROP ACROSS REACTOR = * F6.1 * MM.HG.*/)
  997 FORMAT(/ * VAPOUR PRESSURE OF O-XYLENE = * F5.2 * MM.HG.* /
     1 * MOLE FRACTION OF O-XYLENE = * F7.5 /)
     2 FORMAT(* INLET CONCENTRATION O*/ 10X *O-XYLENE = * E9.3 * GM.MOLE/
     1CC.*  / 10X *OXYGEN  = * E9.3 * GM.MOLE/CC.* / 10X
     2 *NITROGEN = * E9.3 * GM.MOLE/CC.*/)
  996 FORMAT(* EXPERIMENTAL EXIT CONCENTRATION (GM.MOLES/LITRE) */)
  995 FORMAT(8X,*OX*,10X,*OTA*,11X,*PI*,11X,*PA*,10X,*CO2*,11X,*O2*,11X,
     1*N2*,10X,*H2O*,11X,*CO*,11X,*MA*)
  231 FORMAT(8XT*OX*,10X,*OTA*,11X,*PI*,11X,*PA*,6X,*CO2*,11X,*CO*,11X,*
     1MA*)
  232 FORMAT(/,* ARRAY(I,J)---DATA FOR ESTIMATION AND DESIGN PROGRAMS*/)
  233 FORMAT(8E10.4)
  234 FORMAT(I3,5X,3F8.4)
  666 FORMAT(5F15.5)
  810 FORMAT(10F8.0)
  811 FORMAT(10E13.3)
  222 FORMAT(1X,*CONVERSION AND SELECTIVITIES*)
  223 FORMAT(1X,*OXYGEN BALANCES*)
  224 FORMAT(1X,*EXPERIMENTAL EXIT MOLE FRACTIONS*)
  905 FORMAT(5E15.5)
  812 FORMAT(/* CARBON BALANCE RATIO = * E10.3 /)
  907 FORMAT(/,20X,* NUMBER OF PARAMETERS * I3)
  909 FORMAT(1H1,20X,* NUMBER OF EXPERIMENTS *I3//)
  226 FORMAT(1X,*WEIGHT =*,F8.3)
  261 FORMAT(1X,* RATE OF XYLENE CONVERSION =*,E10.4,1X,*GMMOLE/GMHR*)
    7 CALL EXIT
      END
```

```
      PROGRAM 2
C     THIS PROGRAM CALCULATES KINETIC PARAMETERS BY BOX - DRAPER METHOD
C     THE FOLLOWING SUBROUTINES ARE USED
C*************     SUBROUTINES*************
C     SIMPLX
C     OBJECT
C     MERSON
C     DERIVS
C     DATGET
C     ----------     ---------     ---------     ---------     ------
C*******
C*******FOUR INDEPENDANT RESPONSES  -  OX,OTA,PA,CO2
      COMMON/STOC/NN1,NN2
      COMMON/PARA1/KAI,KR12I,KR23I,KR5I,EA,E12,E23,E5
      COMMON/CONST/NN,R,NEX,NP,NC
      COMMON/STRAY/ARRAY
      COMMON/REPAR/TBASE
      COMMON/PARA6/FFI

      DIMENSION ARRAY(25,50),XX(11)
      DIMENSION RKO(5)
C     **********  CURRENT ESTIMATES OF PARAMETERS ********
      REAL KAI,KR12I,KR23I,KR5I,NN
      REAL NN1,NN2
C     ******      CONSTANTS      *********
C     NR ---RESPONSES
      NR=4
C     TBASE IS TEMPERATURE USED FOR REPARAMETERIZATION BY HUNTER/ATKINSON
C     METHOD
      TBASE=350.
      R=-1.9872
C     NP NUMBER OF PARAMETERS
      NP=9
C     NMAX MAXIMUM NUMBER OF MINIMIZATIONS OF DETERMINANT CRITERION
      NMAX=100

C
C     READ INITIAL PARAMETER ESTIMATES
C     NOTE THAT INITIAL ESTIMATES OF PRE EXPONENTIAL FACTORS ARE ALREADY
C     REPARAMETERIZED BY HUNTER/ATKINSON METHOD
      READ(5,103) KAI,KR12I,KR23I,KR5I
      READ(5,106)EA,E12,E23,E5
      READ(5,103)FFI
C     **********      READ IN EXPERIMENTAL DATA      **********
      READ(5,101)NEX
      DO 10 J=1,NEX
      READ(5,102) KRUN,NN,NN1,NN2
      READ(5,103) (ARRAY(I,J),I=1,24)
      WRITE(6,105) KRUN
      WRITE(6,104)
      WRITE(6,103) (ARRAY(I,J),I=1,24)
   10 CONTINUE
      WRITE(6,994)
      WRITE(6,993) KAI,EA,KR12I,E12,KR23I,E23,KR5I,E5
C     NORMALISE PARAMETERS **********************************

C     NORMALIZE INITIAL PARAMETER ESTIMATES
```

```
      DO 11 I=1,NP
      XX(I)=1.
   11 CONTINUE

      TBASE=TBASE+273.2
C     CONVERT INITIAL ESTIMATES OF REPARAMETERIZED PRE EXPONENTIAL FACTORS FOR
C     PRINTING ACTUAL VALUES
      RKO(1)=KR1I*EXP(E1/(TBASE*R))
      RKO(2)=KR12I*EXP(E12/(TBASE*R))
      RKO(3)=KR23I*EXP(E23/(TBASE*R))
      RKO(4)=KR5I*EXP(E5/(TBASE*R))
      WRITE(6,1000)(RKO(L),L=1,NR)
      R=1.9872
      CALL OPTIMISATION ROUTINE
      CALL SIMPLX(NP,NMAX,XX)

C     **********    FORMAT STATEMENTS    ******
  101 FORMAT(I3)
  102 FORMAT(I3,5X,3F8.4)
  103 FORMAT(8E10.4)
  104 FORMAT(2X,* EXPERIMENTAL DATA - ARRAY(I,J) *)
  105 FORMAT(2X,* RUN NUMBER = *,I3)
  106 FORMAT(8F10.0)
  994 FORMAT(/21X, *FREQUENCY FACTORS* 6X *ACTIVATION ENERGIES */ )
  993 FORMAT(* ADSORPTION* 10X,E13.4,10X,F12.0 /
     1 * OXYLENE - OTA* 7X,E13.4,10X,F12.0 /,
     2 * OTA-PAR*14X,E13.4,F22.0/
     4 * ORGANICS - CO2*6X,E13.4,F22.0/)
 1000 FORMAT(1X,5E15.4)
      STOP
      END
```

```
      SUBROUTINE SIMPLX(NP,AAA,XX)
C     SIMPLEX METHOD OF OPTIMIZATION (NELDER AND MEAD MODIFICATION)
C
C     PROGRAM IS BASED ON ALGORITHM SHOWN IN COMPUTER J.,VOL.7,308 (1965)
C     AND ON EXISTING PROGRAMS
C
      DIMENSION U(12),PHI(11),X(11,12),PHIH(11),PHIS(11),PHIL(11),
     1 PHIO(11),PHIR(11),PHIC(11),PHIE(11)
      DIMENSION XX(11)
C     ----------
C     X(I,J)  I NO.OF PARAMETERS  J=1  INITIAL CALCULATION POINT
C     EPS   ERROR TOLERANCE
C     NMAX  MAX. NUMBER OF FUNCTION EVALUATIONS
C     K  NUMBER OF INDEPENDENT VARIABLES IN OBJECTIVE FUNCTION
C     ALPHA BETA GAMMA  REFLECTION CONTRACTION EXPANSION COEFFICIENTS
      ALPHA=1.0
      BETA=0.5
      GAMMA=2.0
      EPS=1.0E-08
      DELTX=0.1
      K=NP
C
      KK=K+1
      NCOUNT=0
C     VARIABLE INDICATING SIMPLEX METHOD HAS STOPPED
C     CONVER=0. (NOT STOPPED),CONVER=1. (STOPPED)
      CONVER=0.
      UH=US=UL=0.
C
C     AS ONLY ONE INITIAL ESTIMATE IS READ FOR EACH PARAMETER THE OTHER
C     POINTS IN THE SIMPLEX ARE SET UP BY INCREMENTING THESE ESTIMATES AS
C     FOLLOWS ----------
C     VARIABLES XX(I) ARE NORMALISED WITH RESPECT TO INITIAL VALUES
      DO 100 I=1,K
      X(I,1)=XX(I)
  100 CONTINUE
C     ----------
      DO 3 J=2,KK
      DO 1 I=1,K
    1 X(I,J)=X(I,1)
    3 X(J-1,J)=X(J-1,1)+DELTX
C     ----------
C     EVALUATE FUNCTION INITIALLY AT K+1 FEASIBLE POINTS
C
    2 DO 6 J=1,KK
      DO 4 I=1,K
      PHI(I)=X(I,J)
    4 CONTINUE
      NCOUNT=NCOUNT+1
      CALL OBJECT(PHI ,SUM,NCOUNT)
      IF(NCOUNT.GE.NMAX) GO TO 48
      IF(CONVER.EQ.1.) GO TO 48
    6 U(J)=SUM
      GO TO 8
    8 CONTINUE
C     FIND RELATIVE ORDER OF FUNCTION VALUES
      UH=U(1)
      JH=1
      DO 10 J=2,KK
```

```
      IF(U(J).LT.UH)GO TO 10
      UH=U(J)
      JH=J
   10 CONTINUE
      UL=U(1)
      JL=1
      DO 12 J=2,KK
      IF(U(J).GT.UL) GO TO 12
      UL=U(J)
      JL=J
   12 CONTINUE
      US=UL
      DO 14 J=1,KK
      IF(J.EQ.JH)GO TO 14
      IF(U(J).LE.US)GO TO 14
      US=U(J)
      JS=J
   14 CONTINUE
      OBTAIN THE CORRESPONDING INDEPENDENT VARIABLES
      DO 16 I=1,K
      PHIH(I)=X(I,JH)
      PHIS(I)=X(I,JS)
   16 PHIL(I)=X(I,JL)
      WRITE(6,17)NCOUNT,UH,US,UL,(PHIL(I),I=1,K)
   17 FORMAT(1X,*NO*,I4,*FUNCT. H S L*,3E12.4,*LOW VAR*,10F7.4)
      IF(NCOUNT.GE.NMAX)GO TO 48
      IF(CONVER.EQ.1.)GO TO 48
      CALCULATE THE CENTROID
      DO 20 I=1,K
      SUM=0.
      DO 18 J=1,KK
      IF(J.EQ.JH)GO TO 18
      SUM=SUM+X(I,J)
   18 CONTINUE
   20 PHIO(I)=SUM/(FLOAT(K))
      REFLECTION
      DO 21 I=1,K
      PHIR(I)=P+IO(I)+ALPHA*(PHIO(I)-PHIH(I))
      IF(PHIR(I).LE.0.05) PHIR(I)=0.05
   21 CONTINUE
      NCOUNT=NCOUNT+1
      CALL OBJECT(PHIR, UR,NCOUNT)
      WRITE(6,19)
   19 FORMAT(1X,*REFLECTION*)
      IF((US.GE.UR).AND.(UR.GE.UL))GO TO 28
      IF(UR.LT.UL)GO TO 32
      IF((UH.GT.UR).AND.(UR.GT.US))GO TO 40
      CONTRACTION  (I.E. UR.GT.UH)
   23 DO 24 I=1,K
      PHIC(I)=PHIO(I)+BETA*(PHIH(I)-PHIO(I))
      IF(PHIC(I).LE.0.05) PHIC(I)=0.05
   24 CONTINUE
      NCOUNT=NCOUNT+1
      CALL OBJECT(PHIC, UC,NCOUNT)
      SUCCESSFUL CONTRACTION
      WRITE(6,25)
   25 FORMAT(1X,*CONTRACTION*)
```

```
      IF(UR.LT.UL)GO TO 44
      SHRINKING (I.E. CONTRACTION UNSUCCESSFUL)
      DO 26 J=1,KK
      IF(J.EQ.JL)GO TO 26
      DO 29 I=1,K
      X(I,J)=.5*(X(I,J)+PHIL(I))
   29 CONTINUE
   26 CONTINUE
      NCOUNT=1
      WRITE(6,27)
   27 FORMAT(1X,*SHRINKING*)
      GO TO 2
C     REPLACE PHIH BY PHIR AND RESTART
    8 DO 30 I=1,K
   30 X(I,JH)=PHIR(I)
      U(JH)=UR
      GO TO 8
C     EXPANSION  (I.E. UR.LT.UL)
   32 DO 34 I=1,K
      PHIE(I)=PHIU(I)+GAMMA*(PHIR(I)-PHIU(I))
      IF(PHIE(I).LE.0.05) PHIE(I)=0.05
   34 CONTINUE
      NCOUNT=NCOUNT+1
      CALL OBJECT(PHIE, UE,NCOUNT)
      WRITE(6,35)
   35 FORMAT(1X,*EXPANSION*)
      IF(UE.LT.UL)GO TO 36
      UNSUCCESSFUL EXPANSION
      GO TO 28
C     SUCCESSFUL EXPANSION (REPLACE PHIH BY PHIE)
   36 DO 38 I=1,K
   38 X(I,JH)=PHIE(I)
      U(JH)=UE
      GO TO 8
C     REPLACE PHIH BY PHIR AND CONTRACT
   40 DO 42 I=1,K
      X(I,JH)=PHIR(I)
   42 PHIH(I)=PHIR(I)
      U(JH)=UH=UR
      GO TO 23
C     SUCCESSFUL CONTRACTION
   44 DO 46 I=1,K
   46 X(I,JH)=PHIC(I)
      U(JH)=UC
      GO TO 8
   48 CONTINUE
      RETURN
      END
```

```
      SUBROUTINE OBJECT (XXX,SUM,NCOUNT)
C     THE FUNCTION OF THIS SUBROUTINE IS TO SET UP THE DETERMINANT FOR
C     MINIMIZATION
      COMMON/REPAR/TBASE
      COMMON/PARA6/FFI
      COMMON/PARA5/FF
      COMMON/REPAY
      COMMON/STRAY/ARRAY
      COMMON/STOC/NN1,NN2
      COMMON/PARA1/KAI,KR12I,KR23I,KR5I,EA,E12,E23,E5
      COMMON/PARA2/KA,KR12,KR23,KR5
      COMMON/CONST/NN,R,NEX,NP,NC
      COMMON/MER/T,DELP,W,PT,GRADP
      COMMON/DER/FGAS
      COMMON/ERROR/ERR
      DIMENSION ARRAY(25,50)
      DIMENSIONA(144)
      DIMENSIONY(10)
      DIMENSION XXX(11)
      DIMENSION RES(5,50)
      DIMENSION Z(4)
      DIMENSION YCAL(5,50)
      DIMENSION RSS(5)
      DIMENSION SSR(5)
      DIMENSION ZZ(5,50),ZZP(5,50),GM(5),GMP(5)
      DIMENSION ARRA(25,50),YY(4)
      REAL KAI,KR12I,KR23I,KR5I,KA,KR12,KR23,KR5,NN,N2
      REAL NN1,NN2
      DO 8888 LM=1,5
      SSR(LM)=0.
      RSS(LM)=0.
8888  CONTINUE
      DO 25 I=1,50
      DO25J=1,5
      RES(J,I)=0.
      ZZ(J,I)=0.
      ZZP(J,I)=0.
      GMP(J)=0.
      GM(J)=0.
25    CONTINUE
      NMAX=100
      NR=4
      DO 4 I=1,25
      A(I)=0.
4     CONTINUE
      DO 3 I=1,NP
      XXX(I)=ABS(XXX(I))
3     CONTINUE
      *** ***M    ****   ***   ***   ***   ***V  ***   ***   ****  ****   **
C
C     SET UP ACTUAL PARAMETER VALUES FROM NORMALIZED VALUES OBTAINED FROM
C     SIMPLX SUBROUTINE
      RKA=KAI*XXX(1)
      RK12=KR12I*XXX(3)
      RK23=KR23I*XXX(5)
      RK5=KR5I*XXX(7)
      FF=FFI*XXX(9)
```

```
      EAC=EA*XXX(2)
      E12C=E12*XXX(4)
      E23C=E23*XXX(6)
      E5C=E5*XXX(8)
C
C     ***   ****   ****   ***   ***   ***   ***V  ***   ***   ****   ****   **
      WRITE(6,777)
  777 FORMAT(' ',21X,'FREQUENCY FACTORS AND ACTIVATION ENERGIES',//)
      WRITE(6,776)RKA,EAC,RK12,E12C,RK23,E23C,RK5,E5C
  776 FORMAT(' ADSORPTION* 10X,E13.4,10X,F12.0 /
     1 * OXYLENE - OTA*7X,E13.4,10X,F12.0 /
     2 * OTA-PI*14X,E13.4,F22.0/
     4 * ORGANICS - CO2*6X,E13.4,F22.0/)
      WRITE(6,501)FF
  501 FORMAT(' TAR FORMATION RATE CONSTANT = ',E15.4)
C
      DO 201 J=1,NEX
      DO 2 I=1,9
      Y(I)=ARRAY(I,J)
    2 CONTINUE
      T=ARRAY(19,J)
      DELP=ARRAY(20,J)
      W=ARRAY(21,J)
      PT=ARRAY(22,J)
      FGAS=ARRAY(23,J)
      GRADP=ARRAY(24,J)
C      CALCULATE RATE CONSTANTS FROM PRE - EXPONENTIAL FACTORS AND
C     ACTIVATION ENERGIES
C     ****REPARAMETERIZE BY HUNTER - ATKINSON METHOD
      TSTAR=(TBASE-T)/(TBASE*T)
      RT=TSTAR/R
      KA=RKA*EXP(EAC*RT)
      KR12=RK12*EXP(E12C*RT)
      KR23=RK23*EXP(E23C*RT)
      KR5=RK5*EXP(E5C*RT)
C-----------------------------------------------------------------------
C     ***   ****   ****   ***   ***   ***   ***V  ***   ***   ****   ****   **
C     SET UP TOLERANCES,STEP LENGTH,BOUNDARY CONDITIONS ETC.FOR INTEGRATION
C
      X=0.
      DX=.005
      TOLKM=1.0E-08
      DXMIN=0.0001
      N=4
      DELX=W
CC
      CALL MERSON(X,DELX,DX,DXMIN,TOLKM,N)
C     ***   ****   ****   ***   ***   ***   ***V  ***   ***   ****   ****   **
C      TRANSFORM RESPONSES TO CALCULATE DETERMINANT
      ARRA(10,J)=ARRAY(10,J)
      ARRA(11,J)=SQRT(ARRAY(11,J))
      ARRA(12,J)=ALOG(ARRAY(12,J))
      ARRA(13,J)=SQRT(ARRAY(13,J))
      DO 601 LLL=1,NR
      YY(1)=Y(1)
      YY(2)=SQRT(Y(2))
      YY(3)=ALOG(Y(3))
```

```
      YY(4)=SQRT(Y(4))
      YCAL(LLL,J)=Y(LLL)
  201 CONTINUE
C     ***   ***M    ****   ***   ***   ***   ***V  ***   ***   ****  ****   **
      KK=0
      DO 201 JJ=1,NR
      II=JJ+9
C     *****  ******  *****  *****  *****  *****  *****
C     CALCULATE RESIDUALS
      RES(JJ,J)=ARRAY(II,J)-Y(JJ)
C     CALCULATE RESIDUAL SUM OF SQUARES FOR EACH RESPONSE
      SSR(JJ)=SSR(JJ)+RES(JJ,J)*RES(JJ,J)
      DO 201 K=1,NR
      III=K+9
      KK=KK+1
      B=(ARRAY(II,J)-YY(JJ))*(ARRAY(III,J)-YY(K))
      B=B*100000000.
      A(KK)=B+A(KK)
  201 CONTINUE
C     CALCULATE RESIDUAL SUM OF SQUARES
      SSR(5)=SSR(1)+SSR(2)+SSR(3)+SSR(4)
      WRITE(6,9995)
 9995 FORMAT(10X,*THE RESIDUAL SUMS OF SQUARES OF TRANSFORMED RESPONSE*)
      WRITE(6,9997)SSR(1),SSR(2),SSR(3),SSR(4),SSR(5)
      DO 5555 J=1,NEX
      GM(1)=1.
C     CALCULATE GEOMETRIC MEAN FOR ALL RESPONSES
      GM(2)=GM(2)+ALOG(ARRAY(11,J))
      GM(3)=GM(3)-ALOG(ARRAY(12,J))
      GM(4)=GM(4)+ALOG(ARRAY(13,J))
      GMP(1)=1.
      GMP(2)=GMP(2)+ALOG(YCAL(2,J))
      GMP(3)=GMP(3)-ALOG(YCAL(3,J))
      GMP(4)=GMP(4)+ALOG(YCAL(4,J))
 5555 CONTINUE
      DO 4444 I=1,NR
      GM(I)=GM(I)/NEX
      GMP(I)=GMP(I)/NEX
      GM(I)=EXP(GM(I))
      GMP(I)=EXP(GMP(I))
 4444 CONTINUE
C     ***   ****   ****   ***   ***   ***   ***V  ***   ***   ****  ****   **
C     CALCULATE ZEDS - REQUIRED FOR CALCULATING RES SUM SQUARES OF TRANSFORMED
C     RESPONSES - BOX - COX TRANSFORMATION PAPER
C     ***   ***M   ****   ***   ***   ***   ***V  ***   ***   ****  ****   **
      DO 7777 J=1,NEX
      ZZP(1,J)=YCAL(1,J)
      ZZ(1,J)=ARRAY(10,J)
      ZZP(2,J)=2.*(SQRT(YCAL(2,J))   )*SQRT(GMP(2))
      ZZ(2,J)=2.*(SQRT(ARRAY(11,J))  )*SQRT(GM(2))
      ZZP(4,J)=2.*(SQRT(YCAL(4,J))   )*SQRT(GMP(4))
      ZZ(4,J)=2.*(SQRT(ARRAY(13,J))  )*SQRT(GM(4))
      ZZP(3,J)=ALOG(YCAL(3,J))/GMP(3)
      ZZ(3,J)=ALOG(ARRAY(12,J))/GM(3)
 7777 CONTINUE
      DO 6666 J=1,NEX
      DO 6666 I=1,NR
```

```
      RSS(I)=RSS(I)+(ZZ(I,J)-ZZP(I,J))*(ZZ(I,J)-ZZP(I,J))
  666 CONTINUE
      RSS(5)=RSS(1)+RSS(2)+RSS(3)+RSS(4)
      WRITE(6,9999)
 9999 FORMAT(10X, * THE RESIDUAL SUM OF SQUARES FOR ALL COMPONENTS *)
      WRITE(6,9997) RSS(1),RSS(2),RSS(3),RSS(4),RSS(5)
      FORMAT(10X, *RSS(1) = *,E15.5, *RSS(2) = *,E15.5,
     1 *RSS(3) = *,E15.5, *RSS(4) = *,E15.5, *TOTAL = *,E15.5)
      IF(NCOUNT.LT.NMAX) GO TO 20
C     PLOT RESIDUALS ON LAST ITERATION
      DO 21 J=1,NEX
      D1=RES(1,J)
      D2=RES(2,J)
      D3=RES(3,J)
      D4=RES(4,J)
      E=ARRAY(19,J)
      CALL PLOTPT(D1,E,1)
      CALL PLOTPT(D2,E,2)
      CALL PLOTPT(D3,E,3)
      CALL PLOTPT(D4,E,4)
   21 CONTINUE
      CALL OUTPLT
      DO 22 J=1,NEX
      D1=RES(1,J)
      D2=RES(2,J)
      D3=RES(3,J)
      D4=RES(4,J)
      E=ARRAY(1,J)
      CALL PLOTPT(D1,E,1)
      CALL PLOTPT(D2,E,2)
      CALL PLOTPT(D3,E,3)
      CALL PLOTPT(D4,E,4)
   22 CONTINUE
      CALL OUTPLT
      DO 23 J=1,NEX
      D1=RES(1,J)
      D2=RES(2,J)
      D3=RES(3,J)
      D4=RES(4,J)
      E=ARRAY(6,J)
      CALL PLOTPT(D1,E,1)
      CALL PLOTPT(D2,E,2)
      CALL PLOTPT(D3,E,3)
      CALL PLOTPT(D4,E,4)
   23 CONTINUE
      CALL OUTPLT
   20 CONTINUE
      N=4
C
C
C     EVALUATE DETERMINANT
      CALL DETER(A,D,N)
C
      WRITE(6,301)D,NCOUNT
      SUM=D
```

TIGHT BINDING

```
[illegible] FORMAT(1X,5E15.4)
[illegible] FORMAT(///,1X,*DETERMINANT*,E20.6,10X,*N=*,I3)
      FORMAT(///,*CONCENTRATION [illegible] (G.MOLES/CC.)*//
     1 * DISTANCE* 57X *CARBON* [illegible] )
    2 FORMAT(13X *O-XYLENE* 8X *OTA* 7X *PHTHALIDE* 3X *PHTH.ANHYD.* 4X
     1 *DIOXIDE* 7X *OXYGEN* 5X *NITROGEN* 7X *WATER* 4X *PRESSURE* 4X
     [illegible] *//)
[illegible] FORMAT(F6.3,3X,8E13.3,F9.1,E13.3)
      RETURN
      END
```

```
      SUBROUTINE HERSON(X,DELX,DX,DXMIN,TOLKM,N)
C     INTEGRATE FROM X TO (X+DELX)
C     DX IS ESTIMATE FOR INTEGRATION STEP NECESSARY
C     DXMIN IS MINIMUM STEP LENGTH TO BE PERMITTED
C     TOLKM IS REQUIRED ACCURACY
C     N IS NUMBER OF DEPENDENT VARIABLES
C     CONTROL TRANSFERRED TO FIRST LABEL IF INTEGRATION FAILS, X AND Y(I)
C     THEN CONTAIN NEW VALUES
C     DX AND Y(I) THEN CONTAIN MOST RECENT CORRECT VALUES
C     IN EITHER CASE, DX CONTAINS CURRENT STEP LENGTH
      COMMON/PARA2/KA,KR12,KR23,KR5
      COMMON/PARA1/KA1,KR121,KR231,KR51,EA,E12,E23,E5
      COMMON/STOC/NN1,NN2
      COMMON/DEP/Y
      COMMON/GRAD/DY
      COMMON/CONST/NN,R,NEX,NP,NC
      COMMON/DER/FGAS
      COMMON/NER/T,DELP,W,PT,GRADP
      COMMON/ERROR/ERR
      COMMON/REPAR/TBASE
      DIMENSION Y(10),YOLD(10),FK(5,10),DY(10)
      REAL KA1,KR121,KR231,KR51,KA,KR12,KR23,KR5,NN,N2
      REAL NN1,NN2

      ISW=0
      XMAX=W
      TOLA=5.*TOLKM
      FINTS=DELX/DX+0.5
      TOLB=TOLA/32.
      INTS=FINTS
      IF(INTS.LT.1)INTS=1
      DX=DELX/INTS
      FMULT=DX/3.
      GO TO 4
C     ERROR CHECK
    1 IF(ERR.GT.TOLA) GO TO 20
      IF(ERR.LT.TOLB) GO TO 21
C     INTEGRATION SATISFACTORY, CALCULATE NEW POINTS
C     ----------------------------------------------------------------
C     ***** THE NEXT 17 CARDS ARE NOT PART OF THE STANDARD HERSON *******
C     ***** THEY CALCULATE THE VOLUME CHANGE DUE TO REACTION ***************
    3 DO 2 I=1,N
    2 Y(I)=YOLD(I)+0.5*FK(1,I)+2.0*FK(4,I)+0.5*FK(5,I)
C     OXYGEN BALANCE--OXYGEN TO CO2 AND H2O
      Y(6)=YOLD(6)-(Y(2)-YOLD(2))-(Y(3)-YOLD(3))*2.5-(Y(4)-YOLD(4))*1.31
C     WATER PRODUCED FROM ALL REACTIONS
      Y(8)=YOLD(8)+(Y(2)-YOLD(2))+(Y(3)-YOLD(3))*2.5+(Y(4)-YOLD(4))*.625
C     CORRECT CONCENTRATIONS FOR INCREASED FLOW AND DECREASED PRESSURE
      PTN=PT-GRADP*DX
      YOLD(7)=Y(7)
      VOLPLUS=0.
      DO 200 KK=1,8
  200 VOLPLUS=VOLPLUS+FGAS*(Y(KK)-YOLD(KK))
      VMOLE=22.400*760.*T/(273.2*PTN)
      VOLPLUS=VOLPLUS*VMOLE
      FGASN=(FGAS*PT/PTN)+VOLPLUS
```

```
...=FOAS/FOASN
      DO 210 KK=1,8
  210 Y(KK)=Y(KK)*RATIO
      ...=FOASN
      PT=PTN
      IF(ISW.LT.1) GO TO 101
      ...
      IF(...GT.A-DX) GO TO 100
      DX=XMAX-X
      ISW=1
  100 CONTINUE
      IF(INTS.EQ.1) RETURN
    6 INTS=INTS-1
      PRESERVE CURRENT VALUES
    4 XOLD=X
      IN THE NORMAL RUNGE KUTTA MERSON THE 8 WOULD BE REPLACED BY N
      DO 5 I=1,8
    5 YOLD(I)=Y(I)
      ...STEP ADJUSTMENT IF DX IS LAST STEP
      IF (ISW.EQ.1) GO TO 510
      IHALF=0
      GO TO 9
      ERROR EXCESSIVE, HALVE STEP
   20 DX=0.5*DX
      IF(DX.LT.DXMIN) GO TO 19
      INTS=INTS+INTS
      IHALF=1
      GO TO 8
      STEP LENGTH TOO SMALL, INTEGRATION FAILS
   19 X=XOLD
      DO 23 I=1,8
   23 Y(I)=YOLD(I)
      RETURN
      ERROR SMALL, STEP LENGTH MAY BE INCREASED IF POSSIBLE
      CHECK IF STEP PREVIOUSLY HALVED (PREVENTS CYCLING)
   21 IF(IHALF.EQ.1) GO TO 3
      CHECK IF INTS EVEN
      IDOUBLE=INTS/2
      IF((IDOUBLE*2).EQ.INTS) GO TO 22
      NOT POSSIBLE, INTS ODD
      GO TO 3
      DOUBLE STEP LENGTH
   22 INTS=IDOUBLE
      DX=2.*DX
      GO BACK TO LAST POINT, AND INTEGRATE WITH NEW DX
    8 FMULT=DX/3.
      DO 7 I=1,8
    7 Y(I)=YOLD(I)
      X=XOLD
  510 CONTINUE
      MAIN INTEGRATION PROCESS STARTS HERE ****
C     ADVANCE X BY DX
    9 CALL DERIVS(X,N)
      DO 18 IS=1,5
      GO TO (31,30,32,33,30),IS
   31 X=X+FMULT
```

```
      GO TO 30
   2  X=XOLD+DX
      [illegible] Y(I)
      DO 10 I=1,N
      FK(IS,I)=FMULT*DY(I)
      GO TO (11,12,13,14,10),IS
      PREDICTOR AT (X+DX/3.)
  11  Y(I)=YOLD(I)+FK(1,I)
      GO TO 10
      [illegible] (X+DX/2.)
  12  Y(I)=YOLD(I)+0.5*(FK(1,I)+FK(2,I))
      GO TO 10
      ADVANCE TO (X+DX/2.)
  13  Y(I)=YOLD(I)+0.375*FK(1,I)+1.125*FK(3,I)
      GO TO 10
      ADVANCE TO (X+DX)
  14  Y(I)=YOLD(I)+1.5*FK(1,I)-4.5*FK(3,I)+6.0*FK(4,I)
  10  CONTINUE
      IF(IS.EQ.5) GO TO 16
      EVALUATE DERIVATIVES
      CALL DERIVS(X,N)
      GO TO 18
      ON LAST INTEGRATION, EVALUATE ERROR
  16  ERR=0.0
      DO 17 I=1,N
      EI=ABS(FK(1,I)-4.5*FK(3,I)+4.0*FK(4,I)-0.5*FK(5,I))
      IF(ERR.LT.EI) ERR=EI
  17  CONTINUE
  18  CONTINUE
      GO TO 1
      END
```

```
      SUBROUTINE DERIVS(X,Y)
      COMMON/GRAD/DY
      COMMON/PARA1/KA1,KR12I,KR23I,KR5I,EA,E12,E23,E5
      COMMON/PARA2/KA,KR12,KR23,KR5
      COMMON/DEP/Y
      COMMON/DER/FGAS
      COMMON/CONST/NN,R,NEX,NP,NC
      COMMON/PARA5/FF
      COMMON/STOC/NN1,NN2
      DIMENSION Y(10),DY(10)
      REAL NN1,NN2
      REAL KA1,KR12I,KR23I,KR5I,KA,KR12,KR23,KR5,NN,N2
      ****THIS SUBROUTINE CALCALATES THE RATES OF ALL REACTIONS AT EACH STEP DU

*** V IS RECIPROCAL GAS FLOW (HOURS / LITRE) ********
      V=1./(FGAS*3600.)
      DEN=KA*Y(6)+(KR12*NN1+KR5*NN)*Y(1)+(KR23*NN2+KR5*(NN-1.))*Y(2)
      DY(1)=-V*((KR12+KR5)*Y(1)+FF)*KA*Y(6)/DEN
      DY(2)=V*(KR12*Y(1)-(KR23+KR5)*Y(2))*KA*Y(6)/DEN
      DY(3)=V*KR23*Y(2)*KA*Y(6)/DEN
      DY(4)=8.*V*KR5*(Y(1)+Y(2))*KA*Y(6)/DEN

      RETURN
      END
```

```
      SUBROUTINE DETER(A,D,N)
      DIMENSION A(144),L(12),M(12)
      DETERMINANT PART OF MASTER PROGRAM MINV
C
C
C       DESCRIPTION OF PARAMETERS
C          A - INPUT MATRIX, DESTROYED IN COMPUTATION AND REPLACED BY
C              RESULTANT INVERSE.
C          N - ORDER OF MATRIX A
C          D - RESULTANT DETERMINANT
C          M - WORK VECTOR OF LENGTH N
C          L - WORK VECTOR OF LENGTH N
C       METHOD
C          THE STANDARD GAUSS-JORDAN METHOD IS USED. THE DETERMINANT
C          IS ALSO CALCULATED. A DETERMINANT OF ZERO INDICATES THAT
C          THE MATRIX IS SINGULAR
C
C          SEARCH FOR LARGEST ELEMENT
C
      D=1.0
      NK=-N
      DO 80 K=1,N
      NK=NK+N
      L(K)=K
      M(K)=K
      KK=NK+K
      BIGA=A(KK)
      DO 20 J=K,N
      IZ=N*(J-1)
      DO 20 I=K,N
      IJ=IZ+I
   10 IF( ABS(BIGA)- ABS(A(IJ))) 15,20,20
   15 BIGA=A(IJ)
      L(K)=I
      M(K)=J
   20 CONTINUE
C
C          INTERCHANGE ROWS.
C
      J=L(K)
      IF(J-K) 35,35,25
   25 KI=K-N
      DO 30 I=1,N
      KI=KI+N
      HOLD=-A(KI)
      JI=KI-K+J
      A(KI)=A(JI)
   30 A(JI) =HOLD
C          INTERCHANGE COLUMNS
C
   35 I=M(K)
      IF(I-K) 45,45,38
   38 JP=N*(I-1)
      DO 40 J=1,N
      JK=NK+J
      JI=JP+J
      HOLD=-A(JK)
      A(JK)=A(JI)
   40 A(JI) =HOLD
```

```
      DIVIDE COLUMN BY MINUS PIVOT (VALUE OF PIVOT ELEMENT IS
     1CONTAINED IN BIGA)

   45 IF(BIGA) 48,46,48
   46 D=0.0
      RETURN
   48 DO 55 I=1,N
      IF(I-K) 50,55,50
   50 IK=NK+I
      A(IK)=A(IK)/(-BIGA)
   55 CONTINUE

C
C     REDUCE MATRIX
C
      DO 65 I=1,N
      IK=NK+I
      IJ=I-N
      DO 65 J=1,N
      IJ=IJ+N
      IF(I-K) 60,65,60
   60 IF(J-K) 62,65,62
   62 KJ=IJ-I+K
      A(IJ)=A(IK)*A(KJ)+A(IJ)
   65 CONTINUE
C
C     DIVIDE ROW BY PIVOT
      KJ=K-N
      DO 75 J=1,N
      KJ=KJ+N
      IF(J-K) 70,75,70
   70 A(KJ)=A(KJ)/BIGA
   75 CONTINUE
C        PRODUCT OF PIVOTS
C
      D=D*BIGA
C
C        REPLACE PIVOT BY RECIPROCAL
C
      A(KK)=1.0/BIGA
   80 CONTINUE
      RETURN
      END
```

```
PROGRAM 3
C  THIS PROGRAM CALCULATES VARIANCE - COVARIANCE MATRICES FROM MULTI -RESPONS
C  DATA
C  IN ADDITION BARTLETTS TEST IS USED TOINVESTIGATE HOMOGENEITY OF VARIANCE
      DIMENSION S(20,5),Y(20,5),YAVE(5),YE(10),CV(5,5)
      DIMENSION SSPE(5),SSMPE(5)
      DIMENSION VAR(5,5),DEL(5),P(10)
C  4 INDEPENDENT RESPONSES FOR ANALYSIS
C  MAXIMUM OF 10 DIFFERENT EXPERIMENTAL CONDITIONS
C  MAXIMUM OF 20 REPLICATED EXPERIMENTS AT EACH DIFFERENT CONDITION
C  S(I,J) IS VAR - COVAR MATRIX FOR EACH EXPERIMENTAL CONDITION
C  SSPE(J) IS SUM OF SQUARES PURE ERROR
C  SSMPE IS MEANS SQUARE PURE ERROR
C  PVAR(J) IS POOLED VARIANCES FOR EACH RESPONSE
C  CV(I,J) IS POOLED VAR - COVAR MATRIX
C  DEL(J) IS VALUE TO COMPARE WITH CHI - SQUARE IN BARTLETTS TEST
C  DF IS NUMBER OF DEGREES OF FREEDOM FOR CALCULATING POOLED
C  VARIANCES - COVARIANCES ETC.
C  C IS VALUE IN CALCULATING DEL(J) FOR BARTLETTS TEST.
C
C    ZERO MATRICES
      DO 30 J=1,5
      YAVE(J)=0.
      PVAR(J)=0.
      DEL(J)=0.
      P(J)=0.
      DO 15 L=1,5
   15 CV(L,J)=0.
      DO 10 I=1,20
      Y(I,J)=0.
   10 S(I,J)=0.
      DO 20 N=1,10
      VAR(N,J)=0.
   20 CONTINUE
   30 CONTINUE
C     READ NO. OF REPLICATED EXPERIMENTS,REPEAT FOR EACH
      READ(5,1) NEXCON
      WRITE(6,1) NEXCON
      DO 1000 NNN=1,NEXCON
C     READ IN EXPERIMENTAL DATA FOR ONE EXPERIMENTAL CONDITION
      READ(5,1) NREPL
      WRITE(6,1) NREPL
      P(NNN)=NREPL
      DO 40 N=1,NREPL
      READ(5,2)(YE(I),I=1,4)
      WRITE(6,4)(YE(I),I=1,4)
C     TRANSFORM VARIABLES                    FOR BARTLETTS TEST
C     FOR EACH EXPERIMENTAL CONDITION
C     ********      *****                    *******      *****
      Y(N,1)=YE(1)**1.5
      Y(N,2)=YE(2)**1.5
      Y(N,3)=YE(3)**1.5
      Y(N,4)=YE(4)**1.5
   40 CONTINUE
C     CALCULATE AVERAGE RESPONSES
      DO 50 J=1,4
      YAVE(J)=0.
```

```
      DO 60 N=1,NREPL
      YAVE(J)=Y(N,J)+YAVE(J)
      S(N,J)=0.
   60 CONTINUE
      YAVE(J)=YAVE(J)/NREPL
   70 CONTINUE
C     CALCULATE SELECTIVE ERROR(I,J) - VARIANCE-COVARIANCE MATRIX
      DO 70 KJI=1,NREPL
      DO 80 K=1,4
      DO 90 J=1,4
      A=Y(KJI,J)
      B=YAVE(J)
      D=Y(KJI,K)
      E=YAVE(K)
      S(K,J)=S(K,J)+(A-B)*(D-E)
   90 CONTINUE
   80 CONTINUE
   70 CONTINUE
      DO 100 J=1,4
      DO 110 I=1,4
      CV(I,J)=CV(I,J)+S(I,J)
      S(I,J)=S(I,J)/(NREPL-1)
  110 CONTINUE
C     STORE VARIANCES FOR EACH COMPONENT AND EACH EXPERIMENTAL CONDITION
      VAR(NNN,J)=S(J,J)
      CALCULATE POOLED VARIANCES
      PVAR(J)=PVAR(J)+(P(NNN)-1.)*VAR(NNN,J)
  100 CONTINUE
C      REPEAT FOR ALL EXPERIMENTAL CONDITIONS
      WRITE(6,5)
      WRITE(6,4)((S(I,J),I=1,4),J=1,4)
 1000 CONTINUE
      SUN=0.
      SUM=0.
      DA=NEXCON
      DO 200 K=1,NEXCON
      SUM=SUM+1./P(K)
      SUN=SUN+P(K)
  200 CONTINUE
      DF=SUN-DA
      C=1.+(SUM-(1./SUN))/(3.*(DA-1.))
      DO 170 J=1,4
      SSPE(J)=CV(J,J)
      SSMPE(J)=SSPE(J)/DF
      PVAR(J)=PVAR(J)/DF
  170 CONTINUE
C     BARTELETTS TEST FOR HOMOGENEITY OF VARIANCE
      DO 140 I=1,NEXCON
      DO 150 J=1,4
      DEL(J)=DEL(J)+(P(I)*ALOG(VAR(I,J)/PVAR(J)))
  150 CONTINUE
  140 CONTINUE
C      AVERAGE THE VARIANCE COVARIANCE MATRIX
      DO 120 I=1,4
      DO 130 J=1,4
      CV(I,J)=CV(I,J)/DF
  130 CONTINUE
```

```
      CONTINUE
      WRITE(6,3)
      WRITE(6,4) ((CV(I,J),I=1,4),J=1,4)
      DO 160 J=1,4
      DEL(J)=-DEL(J)/C
  160 CONTINUE
      WRITE(6,5)
      WRITE(6,4)(DEL(J),J=1,4)
      WRITE(6,4)(PVAR(J),J=1,4)
      WRITE(6,4) (SSPE(J),J=1,4)
      WRITE(6,4)(SSMPE(J),J=1,4)
      WRITE(6,4)((VAR(I,J),I=1,4),J=1,5)
    1 FORMAT(I3)
    2 FORMAT(8E10.4)
    3 FORMAT(15X,* THE VARIANCE - COVARIANCE MATRIX FOLLOWS *)
    4 FORMAT(10X,5E16.4)
    5 FORMAT(15X,* VAR-COVAR MATRIX FOR EXPT.,N *)
    6 FORMAT(15X,* DEL FOR COMPARISON WITH CHI - SQUARED FOLLOWS *)
      STOP
      END
```